UNIVERSIDADE FEDERAL DO CEARÁ
CENTRO DE CIÊNCIAS
DEPARTAMENTO DE QUÍMICA ORGÂNICA E INORGÂNICA
PROGRAMA DE PÓS-GRADUAÇÃO EM QUÍMICA

DEBORA BEZERRA DE SOUSA

ESTUDOS METABOLÔMICOS DE COMPOSTOS ORGÂNICOS VOLÁTEIS (COVs) ASSOCIADOS À RESISTÊNCIA DE CLONES DE CAJUEIRO TIPO ANÃO PRECOCE FRENTE AO ATAQUE DE DIFERENTES FITOPATÓGENOS

FORTALEZA
2022

DEBORA BEZERRA DE SOUSA

ESTUDOS METABOLÔMICOS DE COMPOSTOS ORGÂNICOS VOLÁTEIS (COVs) ASSOCIADOS À RESISTÊNCIA DE CLONES DE CAJUEIRO TIPO ANÃO PRECOCE FRENTE AO ATAQUE DE DIFERENTES FITOPATÓGENOS

Tese apresentada ao Programa de Pós-Graduação em Química da Universidade Federal do Ceará, como parte dos requisitos para a obtenção do título de Doutora em Química. Área de concentração: Química Orgânica.

Orientador: Profa. Dra. Mary Anne Sousa Lima.
Coorientador: Pesquisador Dr. Guilherme Julião Zocolo.

FORTALEZA
2022

Dados Internacionais de Catalogação na Publicação
Universidade Federal do Ceará
Biblioteca Universitária
Gerada automaticamente pelo módulo Catalog, mediante os dados fornecidos pelo(a) autor(a)

S696e Sousa, Debora Bezerra de.
Estudos metabolômicos de compostos orgânicos voláteis (COVs) associados à resistência de clones de cajueiro tipo anão precoce frente ao ataque de diferentes fitopatógenos / Debora Bezerra de Sousa. – 2022.
223 f. : il. color.

Tese (doutorado) – Universidade Federal do Ceará, Centro de Ciências, Programa de Pós-Graduação em Bioquímica , Fortaleza, 2022.
Orientação: Profa. Dra. Mary Anne Sousa Lima.
Coorientação: Prof. Dr. Guilherme Julião Zocolo .

1. Resistência . 2. Mofo preto. 3. Antracnose. 4. Oídio. 5. Biomarcadores.. I. Título.

CDD 572

DEBORA BEZERRA DE SOUSA

ESTUDOS METABOLÔMICOS DE COMPOSTOS ORGÂNICOS VOLÁTEIS (COVs) ASSOCIADOS À RESISTÊNCIA DE CLONES DE CAJUEIRO TIPO ANÃO PRECOCE FRENTE AO ATAQUE DE DIFERENTES FITOPATÓGENOS

Tese apresentada ao Programa de Pós-Graduação em Química da Universidade Federal do Ceará, como parte dos requisitos para a obtenção do título de Doutora em Química. Área de concentração: Química Orgânica.

Aprovada em: 15/07/2022.

BANCA EXAMINADORA

_____
Prof. Dra. Mary Anne Sousa Lima (Orientadora)
Universidade Federal do Ceará (UFC)

_____
Prof. Dr. Guilherme Julião Zocolo (Coorientador)
Empresa Brasileira de Pesquisa Agropecuária (Embrapa)

_____
Profa. Dra. Dávila de Souza Zampieri
Universidade Federal do Ceará (UFC)

_____
Prof. Dr. Edy Sousa de Brito
Empresa Brasileira de Pesquisa Agropecuária (Embrapa)

_____
Prof. Dr. Fernando Batista da Costa
Universidade de São Paulo (USP)

_____
Profa. Dra. Tigressa Helena Soares Rodrigues
Universidade Estadual Vale do Acaraú – UVA

Aos meus pais, José Albino (*in memorian*) e Antonia Bezerra. É tudo por vocês e para vocês!
À Natureza, por tudo que nos oferece e por ter fornecido a mim a matéria prima para a realização deste estudo.

AGRADECIMENTOS

À mãe Natureza por sua grandiosa generosidade em nos oferecer tudo o que precisamos para viver. Por fornecer a mim as plantas objeto desse estudo e permitir a sua realização. Ainda há coisas incríveis a serem descobertas!

À São Francisco de Assis pela minha saúde e de meus familiares e por toda força concedida a mim diariamente. A caminhada é árdua, mas com a ajuda do Senhor, tenho conseguido alcançar grandes conquistas.

Aos meus pais, José Albino (*in memorian*) e Antonia Bezerra por todo amor, carinho, pela paciência e por sempre acreditarem em mim. Por me ensinarem os valores da vida, incentivarem meus estudos e vibrarem a cada conquista. Cada luta é por vocês e cada conquista é, antes de tudo, para vocês. Ofereço-lhes meu amor incondicional e lhes serei eternamente grata por tudo. Vocês são a maior razão da minha existência!

À professora e orientadora Mary Anne Sousa Lima pela orientação acadêmica. Pelos ensinamentos e conselhos, além das conversas e palavras de incentivo. Uma profissional com a qual aprendi muito em todos esses anos de pós-graduação!

Ao orientador Dr Guilherme Julião Zocolo pelos grandes ensinamentos não apenas no nível acadêmico, mas também na esfera pessoal. Sem dúvidas, um exemplo de pessoa e de profissional a ser seguido. Pela orientação, por sua educação e disponibilidade em todos os momentos. Pela paciência durante todo esse percurso, pelo incentivo e por sempre acreditar em nosso trabalho, não medindo esforços para a sua realização. Por ter confiado a mim a responsabilidade de executar um projeto tão bonito, complexo e grandioso.

À CAPES pela concessão da bolsa e fomento à pesquisa.

À Universidade Federal do Ceará e ao Programa de Pós-Graduação em Química pela oportunidade.

Aos professores do PPGQuim da UFC por todo o conhecimento compartilhado durante as disciplinas. Sou grata por terem contribuído de maneira ímpar com aminha formação acadêmica e pessoal.

À Embrapa Agroindústria Tropical por conceder a mim a oportunidade de executar este projeto e oferecer as dependências da unidade para a realização de todas as etapas deste estudo.

Aos pesquisadores do Laboratório de Fitopatologia da Embrapa Dr Marlon Vagner Valentin e Luiz Augusto Lopes Serrano pelas contribuições neste trabalho e por colaborarem com a realização deste estudo no Campo Experimental da Embrapa em Pacajus.

A todos os funcionários e estagiários do Campo Experimental da Embrapa em Pacajus pela receptividade, pelo apoio e orientações.

Às analistas do Laboratório Multiusuário de Química de Produtos Naturais – LMQPN da Embrapa, Dra. Tigressa Helena e Dra. Lorena Mara pelo apoio, suporte nas análises de CG-EM realizadas e por todos os ensinamentos.

Aos professores Jair Mafezoli, Edy Sousa de Brito e Gisele Simone Lopes por terem fornecido valiosas contribuições no exame de qualificação.

Aos professores da banca examinadora por terem aceitado o convite e pelas contribuições.

Aos amigos de laboratório da UFC, cuja amizade levo para a vida: Thaizy Martins, Matheus Areal, João Evangelista, Marília Mota, Davi Dantas e Maria Vieira pelas conversas, amizade, companheirismo, incentivo e por fazerem com que cada dia de trabalho no laboratório fosse mais agradável.

Aos colegas de LMQPN que contribuíram com a realização deste trabalho, ensinando-me as técnicas de laboratório e a teoria básica necessária para a compreensão dos estudos. Meu agradecimento especial à Dra. Gisele Silvestre da Silva pela paciência, pelos ensinamentos e pelo incentivo. Sem dúvidas, uma profissional exemplar que auxilia a todos a sua volta e a quem externo meus sinceros agradecimentos.

Às amigas fiéis Mel e Sol pela amizade, carinho e amor com que sempre me recebem a cada volta para casa e por tornarem meus dias mais felizes.

Ao meu grande amigo e parceiro Rodrigo Bonfim por toda paciência, carinho, amor e respeito. Por acreditar em mim e me incentivar em todos os momentos. Por me acompanhar

nessa caminhada e me fazer acreditar que podemos conquistar o que quisermos, basta não desistirmos!

A todos que contribuíram direta ou indiretamente para a concretização deste trabalho e me acompanharam durante esta jornada, meus sinceros agradecimentos.

Muito obrigada!

“A persistência é o caminho do êxito.” (Charles Chaplin)

"Em algum lugar, alguma coisa incrível está esperando para ser descoberta.” (Carl Sagan)

RESUMO

O mofo preto, a antracnose e o oídio, causadas pelos fitopatógenos *Pilgeriella anacardii* Arx & Müller, *Colletotrichum gloeosporioides* e *Pseudoidium anacardii* (F. Noack) U. Braun & R.T. A. Cook respectivamente, são algumas das mais importantes doenças fúngicas que se alastram com facilidade pelos pomares da cultura do cajueiro (*Anacardium occidentale*). No entanto, alguns clones de cajueiro tipo anão precoce apresentam diferentes respostas em relação à resistência e suscetibilidade ao ataque destes fitopatógenos, sendo os mecanismos para esse comportamento ainda não esclarecidos. Neste trabalho, o perfil de compostos orgânicos voláteis (COVs) emitidos pelas folhas e castanhas de quatro tipos de clones de cajueiro anão precoce ('CCP76', 'BRS226', 'BRS189' e 'BRS265') com diferentes níveis de resistência e suscetibilidade às doenças mencionadas, foi investigado ao longo dos meses de março a dezembro de 2019, por cromatografia gasosa acoplada à espectrometria de massas (CG-EM). Os resultados obtidos permitiram identificar um total de 116 COVs oriundos das folhas e 40 COVs das castanhas, caracterizados como terpenos, álcoois, ésteres, aldeídos, cetonas e hidrocarbonetos. A partir destes dados, a construção de gráficos de análise multivariada (HCA, PLS-DA e OPLS-DA) mostraram diferenças significativas entre o perfil dos COVs dos clones resistentes, em relação aos suscetíveis aos fitopatógenos. Nestas análises foi possível verificar que compostos como 3-hexen-1-ol, (*Z*)-2-hexen-1-ol, (*E*)-2-hexen-1-ol, 1-hexanol, α-pineno, β-mirceno, salicilato de metila e α-copaeno podem contribuir para a maior resistência dos clones 'BRS226' e 'BRS265' em relação ao mofo preto, enquanto que os compostos (*E*)-2-hexenal, (*E*)-3-hexen-1-ol, α-terpineno, γ-terpineno, β-pineno, observados nos clones 'CCP76', 'BRS226' e 'BRS189', estão relacionado à resistência à antracnose. Os compostos isovalerato de etila, tiglato de etila, hexanoato de etila, 3-metil-pentanoato de etila, α-pineno, β-pineno foram identificados nas castanhas de caju como os compostos que possivelmente contribuem para a maior resistência dos clones 'CCP76', 'BRS226' e 'BRS265' em relação ao oídio. Estes resultados corroboram os dados da literatura que sugerem os COVs como agentes de biocontrole na prevenção de pragas agrícolas.

Palavras-chave: Resistência; suscetibilidade; mofo preto; antracnose; oídio; CG-EM; análises quimiométricas; biomarcadores.

ABSTRACT

Black mold, anthracnose, and powdery mildew are caused by the phytopathogens *Pilgeriella anacardia* Arx & Müller, *Colletotrichum gloeosporioides and Pseudoidium anacardii* (F. Noack) U. Braun & R.T. A. Cook respectively, being the most important fungal diseases that spread easily in cashew orchards (*Anacardium occidentale*). However, some early dwarf cashew clones show different responses in relation to resistance and susceptibility to the attack of these phytopathogens, with the mechanisms for this behavior not yet been clarified. In this work, the profile of volatile organic compounds (VOCs) emitted by the leaves and cashew nuts of four types of early dwarf cashew clones ('CCP76', 'BRS226', 'BRS189', and 'BRS265') with different levels of resistance and susceptibility to the aforementioned diseases was investigated from March to December 2019 by GC-MS. The results obtained allowed the identification of a total of 116 VOCs from leaves and 40 VOCs from cashew nuts, characterized as terpenes, alcohols, esters, aldehydes, ketones, and hydrocarbons. From these data, the construction of multivariate analysis graphs (HCA, PLS-DA, and OPLS-DA) showed significant differences between the VOCs profile of resistant clones, in relation to those susceptible to phytopathogens. In these analyzes it was possible to verify that compounds such as 3-hexen-1-ol, (*Z*)-2-hexen-1-ol, (*E*)-2-hexen-1-ol, 1-hexanol, α-pinene, β- myrcene, methyl salicylate, and α-copaene may contribute to the greater resistance of clones 'BRS226' and 'BRS265' in relation to black mold, while compounds (*E*)-2-hexenal, (*E*)-3-hexen-1-ol, α-terpinene, γ-terpinene, β-pinene, observed in clones 'CCP76', 'BRS226' and 'BRS189', are related to anthracnose resistance. The compounds ethyl isovalerate, ethyl tiglate, ethyl hexanoate, ethyl 3-methyl-pentanoate, α-pinene, β-pinene were identified in cashew nuts as the compounds that possibly contribute to the greater resistance of 'CCP76', 'BRS226', and 'BRS265' clones in relation to powdery mildew. These results corroborate the data in the literature that suggest VOCs as biocontrol agents in phytopathogens prevention.

Keywords: Resistance; susceptibility; black mold; anthracnose; powdery mildew; GC-MS; chemometric analyses; biomarkers.

LISTA DE FIGURAS

LISTA DE TABELAS

LISTA DE ABREVIATURAS E SIGLAS

ACC	Amêndoa da castanha de caju
CG-EM	Cromatografia Gasosa acoplada à Espectrometria de Massas
COVs	Compostos Orgânicos Voláteis
DMAPP	difosfato de dimetilalila
DVB/CAR/PDMS	divinilbenzeno/carboxeno/polidimetilsiloxano
GLVs	*Green Leaf Volatiles*
GPP	geranil pirofosfato
HCA	*Hierarchical Cluster Analysis*
HPL	hidroperóxido liase
IBGE	Instituto Brasileiro de Geografia e Estatística
IPP	difosfato de isopentenila
LCC	Líquido da castanha de caju
LOX	lipoxigenase
MEP	metileritritol fosfato
OPLS-DA	*Orthogonal Projections to Latent Structures Discriminant Analysis*
PLS-DA	*Partial Least Squares-Discriminant Analysis*
PCA	*Principal Component Analysis*
PCs	*Principal components*
SAR	resistência sistêmica adquirida
SPME	*solid phase microextraction*
TPP	tiamina difosfato
VIP	*Variable Importance in the Projection*

SUMÁRIO

1. INTRODUÇÃO

Anacardium occidentale, mais conhecida como cajueiro, é uma planta originária do Nordeste brasileiro e, do ponto de vista econômico, é considerada a espécie mais importante dentre as 20 espécies do gênero. Essa espécie se adapta muito bem às regiões de clima temperado, subtropical e tropical, favorecendo o seu cultivo nos estados do Ceará e Piauí, que são responsáveis por mais de 90% da produção de caju no Brasil (LEITE et al., 2016; SALEHI et al., 2019).

O cultivo do cajueiro tem importância significativa para muitos países, como Vietnã, Costa do Marfim, Nigéria, Gana, Índia além do Brasil tendo em vista a possibilidade de exploração tanto do fruto como dos chamados coprodutos que agregam importante valor econômico ao agronegócio desta frutífera (OLIVEIRA et al., 2019). Além disso, a riqueza de metabólitos secundários biossintetizados pelas plantas do gênero *Anacardium* é amplamente relatada na literatura, uma vez que são atribuídas atividades larvicida, antimicrobiana, anti-inflamatória e antioxidante a diversas partes da planta, como folhas, caule, fruto e pseudofruto (LEITE et al., 2016).

Devido ao interesse econômico, a implantação de pomares constituídos por clones de cajueiro tipo anão precoce vem sendo há muito tempo efetuada no Brasil, pois favorece a uniformidade nas características consideradas relevantes para o comércio do caju. Além disso, proporciona ao produtor efetuar a colheita manual, poda, aplicação de defensivos agrícolas de modo mais eficiente somado à ocorrência da propagação vegetativa dos clones, fatos que representam um progresso no cultivo do cajueiro. Porém, devido à redução na variabilidade genética, os pomares constituídos por esses clones estão mais susceptíveis a doenças (CARDOSO et al., 1999).

O mofo preto, a antracnose e o oídio são algumas das mais importantes doenças que atingem a cultura do caju, sendo causadas pelos fungos *Pilgeriella anacardii* Arx & Müller, *Colletotrichum gloeosporioides* e *Pseudoidium anacardii* (F. Noack) U. Braun & R.T. A. Cook, respectivamente. A ocorrência de epidemias severas dessas fitopatologias é relatada, sobretudo, na região Nordeste do Brasil, comprometendo anualmente o rendimento dos pomares (FREIRE et al., 2002). Para o manejo dessas doenças, muitas vezes é indicado o uso de fungicidas, porém, além das questões ambientais, muitos produtores não o fazem por motivos econômicos (FREIRE et al., 2002).

O ataque constante de variados tipos de micro-organismos patogênicos (ALLWOOD et al., 2011) induz nas plantas a manifestação de um fator de proteção por

intermédio de mecanismos que envolvem a fortificação da parede celular, além da biossíntese de metabólitos que podem apresentar atividade antimicrobiana (MHLONGO et al., 2018). Estudos genômicos e transcriptômicos são realizados com frequência a fim de identificar os mecanismos genéticos relacionados às interações planta-patógeno, porém, os estudos metabolômicos são menos frequentes na literatura (CASTRO-MORETTI et al., 2020).

A fisiologia das plantas sofre importantes alterações quando esses organismos estão submetidos às interações com micro-organismos, sejam essas interações benéficas ou não. Em virtude disso, os estudos metabolômicos se caracterizam como uma importante ferramenta para a investigação das modificações que ocorrem no hospedeiro durante essas interações. Esse é um campo de estudo em desenvolvimento e de grande importância, sobretudo, para a produção agrícola, de modo que as investigações realizadas podem contribuir significativamente para a melhoria na produção de alimentos (ALLWOOD et al., 2011; CHEN; MA; CHEN, 2019)

Em condições naturais, as plantas são submetidas constantemente ao ataque de patógenos, sobretudo micro-organismos. No entanto, diversos mecanismos de defesa são ativados para que elas consigam se proteger dessas agressões culminando no desenvolvimento de resistência a esses agressores (ALLWOOD et al., 2011). Entende-se como resistência a capacidade que um organismo desenvolve de evitar ou atrasar a penetração do patógeno em suas estruturas, levando ao comprometimento do desenvolvimento do processo de infecção (PINTO, 2016). O processo de infecção leva à liberação de moléculas pelos patógenos que são reconhecidas pelo hospedeiro e ativam mecanismos de biossíntese de moléculas cujo objetivo é minimizar os danos causados pelo agressor, porém, os mecanismos que regem essa resistência são complexos e ainda pouco elucidados (GUPTA et al., 2015).

Os compostos orgânicos voláteis (COVs) são emitidos pelas plantas em situações variadas e consistem em metabólitos secundários de caráter, em sua maioria, lipofílico, com baixos ponto de ebulição e massa molecular, além de apresentarem elevada pressão de vapor em condições naturais (LUBES; GOODARZI, 2017). A literatura reporta que os COVs apresentam funções variadas como antibacteriana, antifúngica, antioxidante, ativadores na expressão ou silenciamento de genes, reprodução vegetal entre outras. Logo, estes compostos possuem importante papel mediador na relação entre plantas e patógenos (LÓPEZ-GRESA et al., 2017; VIVALDO et al., 2017), e a sua emissão pelas plantas tem relação direta com o ecossistema no qual encontram-se inseridas (CALO et al., 2015).

Alguns COVs emitidos por plantas apresentam atividade antimicrobiana devido à presença de várias classes de compostos, como terpenos, álcoois, ácidos, ésteres, aldeídos, cetonas, aminas, entre outros (CALO et al., 2015). Um dos mecanismos de ação é a capacidade

de penetração nas células dos micro-organismos através da membrana celular e causar inibição nas propriedades funcionais das células (BAJPAI; BAEK; KANG, 2012). As interações entre os compostos constituintes dos óleos voláteis podem potencializar os efeitos antimicrobianos dos compostos quando analisados individualmente, logo, os metabólitos voláteis podem ser, em conjunto, responsáveis pelo efeito antimicrobiano dos óleos voláteis de uma planta, o que é conhecido como efeito sinérgico (RUSSO et al., 2015; DOS SANTOS et al., 2019).

Os estudos de metabolômica relacionados aos fungos e às plantas são bastante explorados e apresentam vários avanços ao longo dos anos, porém, os estudos voltados para as interações entre fungos e plantas, sobretudo as interações de fitopatógenos com seus hospedeiros, ainda é um campo pouco investigado (CHEN; MA; CHEN, 2019). Os estudos dessas interações entre plantas e patógenos é bastante complexo e pode levar a um amplo conjunto de resultados difíceis de serem interpretados. Assim, o emprego de ferramentas como métodos de análise não supervisionados, como PCA (do inglês *principal component analysis*) e HCA (do inglês *hierarchical cluster analysis*), além de métodos supervisionados, como PLS-DA (do inglês *partial least squares discriminant analysis*) e OPLS-DA (do inglês *partial least squares orthogonal discriminant analysis*) é bastante útil para auxiliar na identificação de diferenças em grandes grupos de amostras (CHEN; MA; CHEN, 2019).

Sabe-se que os COVs constituem importantes moléculas relacionadas ao mecanismo de defesa das plantas, assim, a identificação e comparação do perfil de COVs aliada ao uso de ferramentas quimiométricas proporcionam métodos robustos que permitem a identificação de candidatos a biomarcadores. Tendo em vista que o cultivo de *A. occidentale* contribui significativamente para a economia do país, sobretudo da região Nordeste, e que os pomares são acometidos por doenças que comprometem a produção de caju, o objetivo principal deste projeto visa à investigação química de clones de cajueiro anão precoce resistentes e suscetíveis às doenças mofo preto, antracnose e oídio, e à identificação de quais compostos orgânicos voláteis podem estar envolvidos no mecanismo de defesa das plantas resistentes comparadas às plantas suscetíveis.

Os resultados obtidos poderão contribuir para o conhecimento do comportamento das plantas de cajueiro, do ponto de vista químico, levando para a sociedade os conhecimentos adquiridos com o intuito de auxiliar na melhoria do cultivo da espécie e possibilitando estudos futuros de desenvolvimento de produtos defensivos agrícolas e menos agressivos à base de produtos naturais. Este estudo é inédito na literatura para cajueiros tipo anão precoce.

Dentro desse contexto, foi investigado o perfil de metabólitos voláteis emitidos pelas folhas e castanhas de quatro clones de cajueiro tipo anão precoce (‘CCP76’, ‘BRS226’,

‘BRS189’ e ‘BRS265’), que apresentam diferentes respostas de resistência e susceptibilidade aos fitopatógenos *Pilgeriella anacardii* Arx & Müller, *Colletotrichum gloeosporioides* e *Pseudoidium anacardii* (F. Noack) U. Braun & R.T. A. Cook. As análises foram realizadas ao longo dos meses de infestação e não-infestação, no período de março a dezembro de 2019, por meio da análise dos COVs por cromatografia gasosa acoplada à espectrometria de massas (CG-EM) (LUBES; GOODARZI, 2017). As ferramentas quimiométricas permitiram o tratamento dos dados visando à identificação de candidatos a biomarcadores de resistência para as doenças mencionadas (CHEN; MA; CHEN, 2019).

2. OBJETIVOS

Realizar estudos metabolômicos, por meio da investigação dos compostos orgânicos voláteis (COVs) de folhas e castanhas de clones de cajueiro tipo anão precoce, empregando a técnica de cromatografia gasosa acoplada à espectrometria de massas (CG-EM) visando à identificação, com o auxílio de ferramentas quimiométricas, dos metabólitos que podem contribuir para a maior resistência de determinados clones às doenças mofo preto, antracnose e oídio.

2.1 Objetivos específicos

- Identificar os COVs oriundos de folhas e castanhas dos clones de cajueiro anão precoce ‘CCP76’, ‘BRS 226’, ‘BRS 189’ e ‘BRS 265’ de acordo com a incidência e declínio das doenças mofo preto, antracnose e oídio no campo;
- Comparar o perfil de COVs das folhas dos referidos clones ao longo do período de incidência e declínio da doença mofo preto (de março até julho de 2019) para identificar, com o uso de ferramentas quimiométricas, quais compostos podem estar envolvidos no mecanismo de defesa dos clones resistentes a essa doença;
- Comparar o perfil de COVs das folhas dos referidos clones ao longo do período de incidência e declínio da doença antracnose (de julho até dezembro de 2019) para identificar, por meio do emprego de ferramentas quimiométricas, quais compostos podem estar envolvidos no mecanismo de defesa dos clones resistentes a essa doença;
- Comparar o perfil de COVs das castanhas dos referidos clones no mês de outubro, ocorrência da doença oídio, para identificar, empregando ferramentas quimiométricas, quais compostos podem estar envolvidos no mecanismo de defesa dessas estruturas das plantas dos clones resistentes a essa doença;
- Sugerir quais moléculas de COVs são possíveis candidatas a biomarcadores de resistência às doenças mofo preto, antracnose e oídio oriundas das análises de folhas e castanhas dos clones de cajueiro anão precoce ‘CCP76’, ‘BRS 226’, ‘BRS 189’ e ‘BRS 265’.

3. REVISÃO DE LITERATURA

3.1 *Anacardium occidentale*: o cajueiro

Anacardium occidentale, popularmente conhecida como cajueiro (Figura 1A), é uma planta pertencente à família Anacardiaceae, que é composta por arbustos e árvores subtropicais e tropicais de onde são conhecidos 77 gêneros e mais de 700 espécies. A literatura reporta que o cajueiro é originário da América do Sul, destacando o Brasil como centro de sua origem (PAIVA; CRISÓSTOMO; BARROS, 2003; SALEHI et al., 2019), de modo que os colonizadores portugueses quando aqui chegaram já o encontraram amplamente distribuído pelo litoral nordestino, compondo a paisagem de dunas, praias e restingas. Anos mais tarde, verificou-se a presença de outras espécies de cajueiro se desenvolvendo espontaneamente nos biomas Amazônia, Cerrado e Caatinga (SERRANO; OLIVEIRA, 2013). Já foram identificadas 21 espécies de cajueiro e, destas, apenas 3 não são encontradas em território brasileiro: *A. Excelsum*, distribuída no Norte da América do Sul e América Central; *A. rhinocarpus* DC, encontrada no Panamá, Venezuela e território colombiano; *A. encardium* Noronha, oriunda da Malásia (PAIVA; CRISÓSTOMO; BARROS, 2003).

Figura 1 – *Anacardium occidentale*: A) Planta; B) Flores; C) Pedúnculo e fruto (castanha de caju); e sua taxonomia apresentada ao lado.

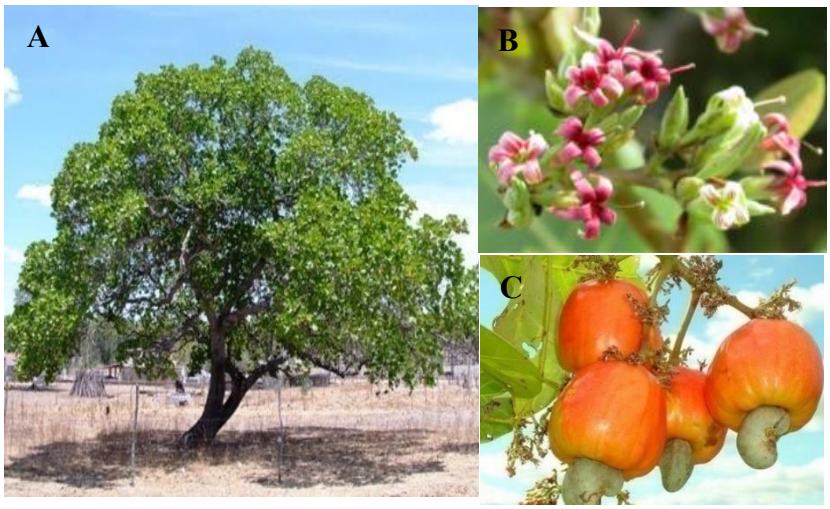

Reino: Plantae
Divisão: Magnoliophyta
Classe: Magnoliopsida
Ordem: Sapindales
Família: Anacardiaceae
Género: *Anacardium*
Espécie: *A. occidentale*

Fonte: Elaborada pela autora (2022).

A. occidentale trata-se de uma planta perene[1] de ramificação próxima ao solo, com folhas simples que medem de 10 a 20 cm de comprimento por 6 a 12 cm de largura, com raízes bem desenvolvidas, podendo superar os 10 m de profundidade (BARROS, 2022).

O caju, cujo nome tem origem tupi e significa "fruto amarelo" ou "fruta amarela de chifre" é tido para muitos como o fruto do cajueiro, porém, trata-se do conjunto entre o pseudofruto (pedúnculo) e a castanha (fruto verdadeiro), com este sendo um aquênio reniforme[2] de coloração marrom-acinzentada formado pelo pericarpo e amêndoa. O pericarpo consiste na casca da castanha e tem em sua constituição três camadas: epicarpo, de elevada resistência é a camada mais externa da castanha, representando cerca de 70% do peso total da mesma; mesocarpo consiste na camada intermediária cujo aspecto é esponjoso contendo alvéolos que são preenchidos pelo líquido da castanha de caju (LCC), um líquido inflamável e cáustico; e o endocarpo, camada mais interna que possui função de proteger a amêndoa (FIGURA 2) (SERRANO; OLIVEIRA, 2013).

Figura 2 - Caju: pseudofruto e fruto verdadeiro.

Fonte: Elaborada pela autora (2022).

O pseudofruto representa 90% do peso total do caju e consiste na sua parte comestível *in natura*, sendo amplamente utilizado na indústria alimentícia e rico em ácidos orgânicos, carboidratos, vitaminas e sais minerais. Já da castanha, são extraídos a amêndoa da castanha do caju (ACC), rica em gorduras, fósforo, ferro, proteínas e carboidratos, além do líquido da castanha do caju (LCC), importante matéria-prima para a fabricação de vernizes, tintas, plásticos, lubrificantes e inseticidas (BARRETTO et al., 2014; OLIVEIRA et al., 2019).

[1] Em botânica, vegetação perene é aquela que dá frutos em estações específicas e mantém, pelo menos, parte da sua estrutura aérea todos os anos. Uma planta perene pode florescer todos os anos ou em ciclos de dois em dois anos, com folhagem permanente.

[2] Aquênio reniforme trata-se de um fruto simples, seco, em forma de rim, contendo semente única que fica aderida por um só ponto à parede do fruto (pericarpo).

O LCC (responsável por cerca de 25% do peso total da castanha), apesar de seu amplo potencial industrial, ainda é considerado um subproduto do agronegócio do caju com baixo valor agregado, porém consiste em uma das fontes naturais mais diversificadas de compostos fenólicos e cada vez mais encontra aplicações na química fina (GARRISON et al., 2017; PIUS; MGANI, 2019)

Atualmente existem dois tipos de cajueiro: o comum e o anão-precoce. O primeiro, conhecido também como gigante, possui altura que varia de 8 a 15 metros, com uma copa com 12 a 16 metros de envergadura, chegando a ultrapassar os 20 metros em alguns casos (FIGURA 3A). As plantas de cajueiro comum propagadas por sementes apresentam a primeira floração entre 2 e 5 anos e podem levar até 13 anos para atingir a estabilidade quanto à produção de frutos. Já as propagadas por via assexuada atingem a maturidade na produção em 2 anos. Em relação à produtividade de castanhas há plantas que produzem de 1 kg até 100 kg de fruto por safra. O peso do pedúnculo vai de 20 g a 500 g e do fruto pode variar de 3 g a 33 g. O cajueiro anão-precoce, também conhecido como cajueiro de 6 meses, apresenta porte reduzido e copa com estrutura homogênea (FIGURA 3B), produzindo frutos já no primeiro ano de plantio (CAVALCANTI; NETO; BARROS, 2013).

Figura 3 - Cajueiro: (a) comum ou gigante; (b) anão precoce.

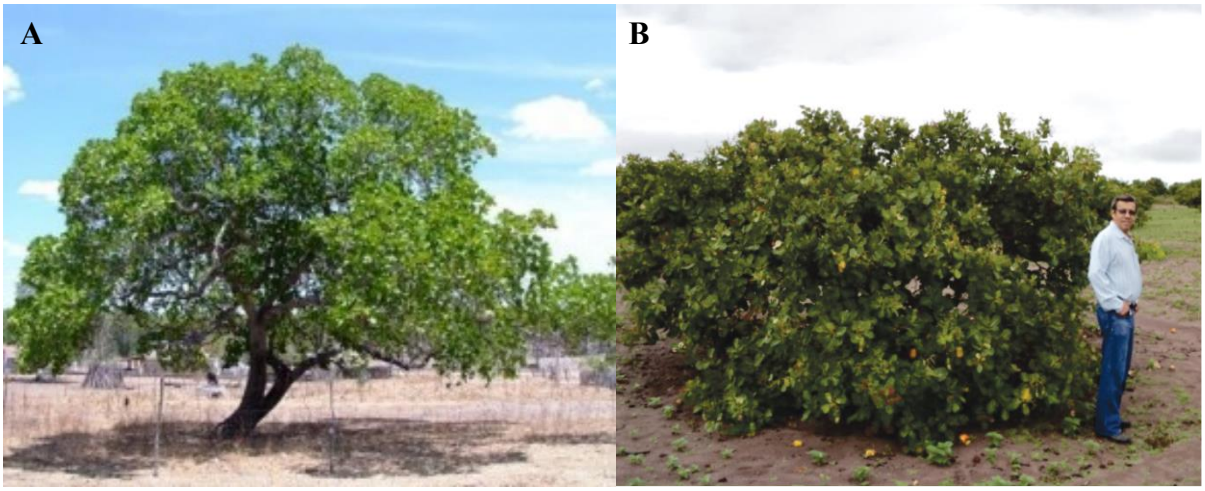

Fonte: Elaborada pela autora (2022).

As condições ideais para o cultivo do cajueiro incluem temperaturas de até 40°C e umidade do ar entre 65 e 85%, com índice pluviométrico superior a 800 mm e inferior a 1600 mm anuais (EMPARN, 2013). As baixas temperaturas são prejudiciais à floração e à frutificação da planta, que é conhecida por sua tolerância à seca (OLIVEIRA et al., 2019). É interessante

que o ciclo de chuvas esteja distribuído entre cinco e sete meses, com posterior estação seca bem definida, permitindo, assim, que o período de floração e frutificação da planta ocorra nessa estação. Além disso, um solo profundo, fértil, com pH em torno de 6,5, de composição arenosa e bem drenado são outras características que favorecem o bom desenvolvimento do cultivo desta planta (SÁ; PAIVA; MARINHO, 2000).

A. occidentale é uma planta de grande capacidade adaptativa, sendo facilmente cultivada, o que garante sua ampla distribuição geográfica (AWODUN et al., 2015). Desta forma, seu cultivo é favorecido tanto em regiões de clima temperado quanto em regiões subtropicais e tropicais. Esse fato tornou favorável a expansão do cultivo da planta, ocorrida sobretudo no período das grandes navegações, quando foi levada para os continentes africano e asiático em virtude da exploração por novos territórios protagonizada por europeus, principalmente portugueses (DENDENA; CORSI, 2014).

A nível mundial, as áreas que concentram a maior produção do caju incluem o Sudeste da Ásia, África Ocidental, África Oriental e Brasil (BERRY; SARGENT, 2011; DENDENA; CORSI, 2014; CISSE, et. al, 2021; RULLIER; RICAU, 2015). A produção mundial de castanha de caju supera os 4 milhões de toneladas por ano (OLIVEIRA et al., 2019), destacando-se Vietnã, Nigéria, Índia e Costa do Marfim como maiores produtores (SERRANO; PESSOA, 2016). O Brasil é o sexto maior produtor mundial de castanhas de caju (BRAINER; VIDAL, 2020).

No Brasil, 90% da renda gerada por meio do cultivo do cajueiro provém dos processos de beneficiamento da castanha, haja visto seu elevado valor econômico imposto no mercado internacional (BARRETTO et al., 2014). O cultivo da frutífera é bastante favorecido na região Nordeste do país, principalmente nos estados do Ceará, Piauí e Rio Grande do Norte que, juntos, respondem por mais de 90% da produção nacional de caju, sendo explorados não apenas o fruto, mas também os chamados subprodutos que agregam importante valor ao agronegócio dessa frutífera tropical (LEITE et al., 2016; OLIVEIRA et al., 2019; SALEHI et al., 2019; CONAB, 2021).

Dados do Instituto Brasileiro de Geografia e Estatística (IBGE) mostram que a produção nacional de castanhas de caju ultrapassou as 110 mil toneladas no ano de 2021, com uma área plantada de 427.874 hectares e mais de 426 mil hectares de área colhida. O estado do Ceará sempre é destaque em termos de produção da fruta, não sendo diferente em 2021, uma vez que o estado contribuiu com 63.076 toneladas do total produzido no país (FIGURA 4) (IBGE, 2021). De acordo com dados da Companhia Nacional de Abastecimento (Conab), os principais destinos de exportação da castanha de caju brasileira são países como Estados Unidos,

Canadá, Vietnã e China (CONAB, 2021).

Figura 4 – Produção da safra de castanha de caju (em toneladas) correspondente ao ano de 2021 no Brasil e nas unidades da federação.

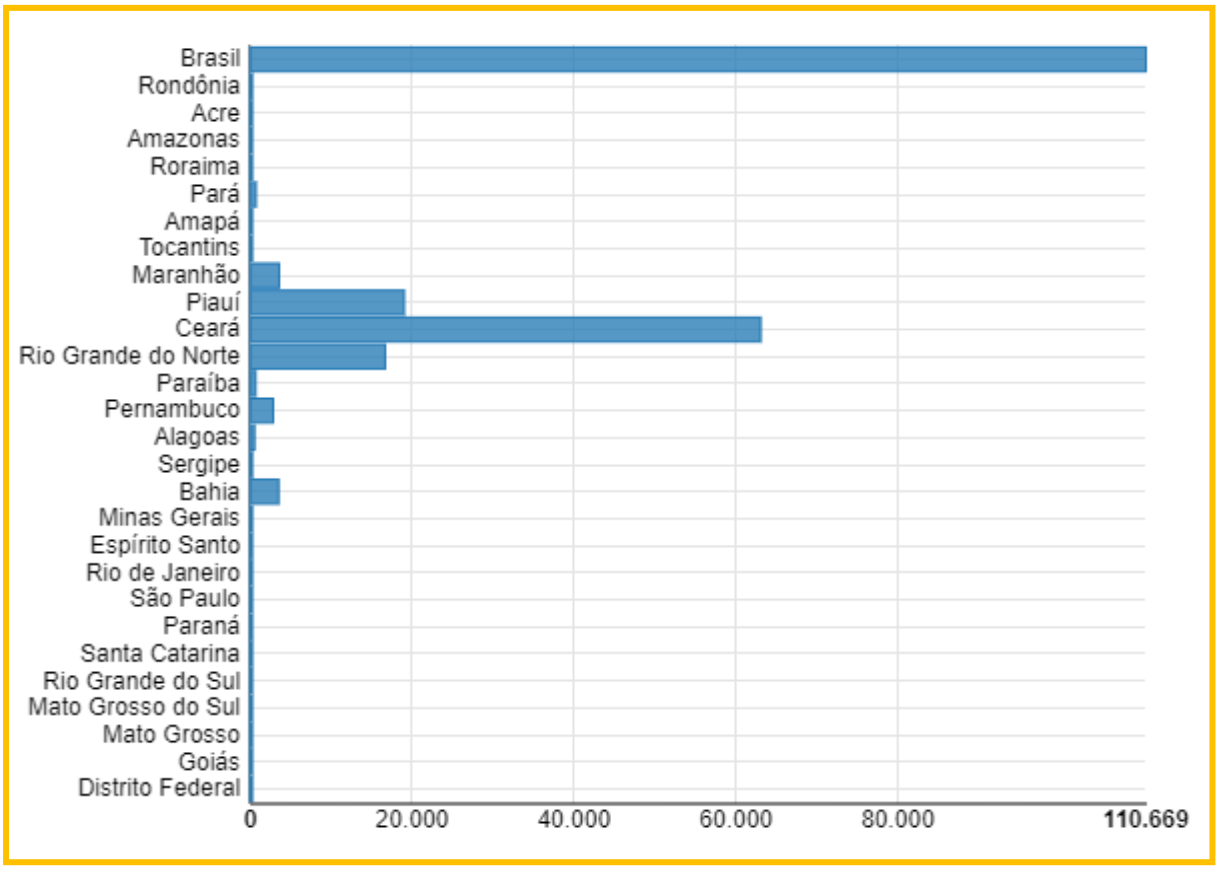

Fonte: IBGE – Levantamento Sistemático da Produção Agrícola (2022).

A área plantada em território nacional para o cajueiro é a segunda maior para espécies frutíferas, ficando atrás apenas do cultivo de laranja, gerando anualmente cerca de 250 mil empregos diretos e indiretos. Os pequenos produtores de caju representam 75% do total, com áreas de cultivo inferiores a 20 hectares. Apesar da importância do cajueiro para a economia nacional, estima-se que não há grandes investimentos para o melhoramento e manutenção dos pomares, haja visto que cerca de 75% dos pedúnculos são perdidos durante o processo de desenvolvimento e colheita do caju, de modo que apenas 350 mil toneladas são aproveitados pelas indústrias que fabricam sucos, doces e refrigerantes (SERRANO; PESSOA, 2016).

Apesar dos grandes números de produção, quedas acentuadas na produção dos pomares de caju vêm ocorrendo, conforme ilustra o gráfico da Figura 5. Este decréscimo pode ser justificado pelos extensos períodos de seca (índices pluviométricos muito abaixo da média),

que culmina no abortamento das flores. Outra causa importante para a queda nos rendimentos é a ocorrência cada vez maior de pragas nas lavouras, como as doenças causadas por fungos, por exemplo (SERRANO; PESSOA, 2016).

Figura 5 – Quantidade produzida de castanha de caju (em toneladas) durante o período 2009 a 2020 no Brasil.

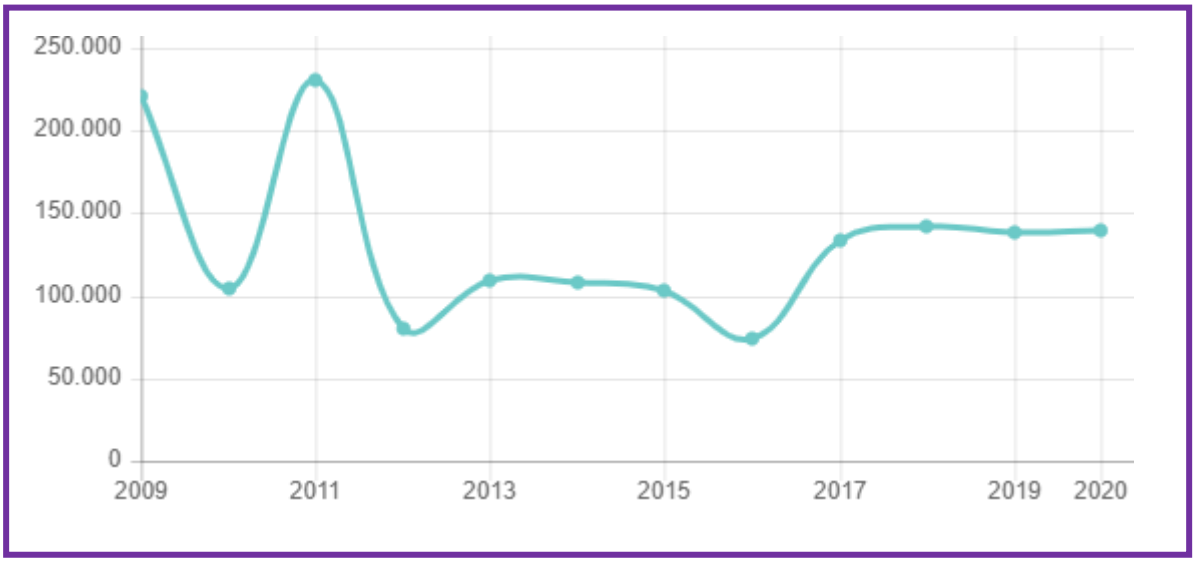

Fonte: IBGE – Levantamento Sistemático da Produção Agrícola (2022).

3.2 Mofo preto, antracnose e oídio: doenças fúngicas que afetam a cultura do cajueiro

Dentro da grande variedade de doenças pelas quais o cajueiro pode ser acometido, a maioria delas é causada por fungos. Os sintomas provocados pelas doenças na parte aérea da planta são mais perceptíveis não apenas pela fácil observação como também em virtude dos danos causados à produção, embora todas as partes da planta possam ser afetadas pelas doenças que atingem os cultivos (FREIRE et al., 2002).

A seguir, são apresentadas algumas das principais doenças fúngicas que atacam a cultura do cajueiro anualmente, sobretudo no Brasil, comprometendo, assim, o rendimento na produção dos pomares.

3.2.1 Mofo preto

Caracterizado por ser um parasita obrigatório, *Pilgeriella anacardii* Arx & Müller, o fungo causador do mofo preto, atua colonizando as folhas do cajueiro (FREIRE et al., 2002).

Os sintomas iniciais da doença incluem a presença de manchas na parte superior das folhas que caracterizam a insuficiência na produção de clorofila, evoluindo para a presença de uma camada escura de aparência aveludada formada pelo micélio na porção inferior das folhas (FIGURA 6). Após penetrar nos estômatos, o patógeno impede o desenvolvimento foliar devido à redução na troca de oxigênio entre a planta e o meio ambiente, levando à murcha e queda prematura das folhas. Epidemias severas vêm acometendo os pomares de cajueiro, sobretudo na zona costeira do Nordeste brasileiro (VIANA et al., 2012).

A ocorrência da doença se dá a partir do início da estação chuvosa atingindo seu ponto de maior severidade ao término desse período, fato que coincide com a emissão de novas folhagens por parte das plantas de *A. occidentale* (CARDOSO et al., 2005). Acibenzolar-S-metil (ASM) além de defensivos a base de oxicloreto de cobre são muitas vezes empregados para o controle da doença, além do plantio de clones de cajueiro que apresentam certo grau de resistência ao patógeno, configurando-se esta como uma opção ecologicamente correta além de economicamente viável de manejo da doença (VIANA et al., 2012).

Figura 6 – Folha de cajueiro mostrando sintomas em estágio mais avançado de mofo preto.

Fonte: Lima et al. (2019).

3.2.2 Antracnose

Causada pelo fungo *Colletotrichum gloeosporioides* (Penz.) Penz. & Sacc. (FIGUEIRÊDO et al., 2012), a antracnose figura, em vários países, como uma das principais fitopatologias que atingem a cultura do cajueiro, comprometendo o rendimento na produção de castanhas e pedúnculos (NAKPALO et al., 2017). O fungo ataca inflorescências, galhos, maturis (castanhas jovens), pseudofrutos, além de frutos e folhas jovens da planta. Em estágios mais avançados, ocorre a morte de folhas e inflorescências, além da necrose e queda de maturis (UACIQUETE; KORSTEN; VAN DER WAALS, 2013). Nas folhas jovens, os primeiros

sintomas são manchas pardas que se tornam avermelhadas conforme a folha envelhece e a doença evolui. Já nos maturis, pedúnculos e castanhas, manchas escuras com rachaduras podem ser observadas, inviabilizando o consumo do fruto e pseudofruto (FIGURA 7) (CARDOSO, 2019).

Períodos de ocorrência de precipitação favorecem o ataque do micro-organismo, sendo, no Brasil, o período de janeiro a julho e durante os meses de agosto e setembro as épocas mais favoráveis para a ocorrência da doença no campo. O mês de setembro é reportado na literatura como sendo o de incidência mais severa da doença, pois há ocorrência da chamada "chuva do caju" que favorece a disseminação do patógeno pelos pomares (FREIRE et al., 2002).

Figura 7 – (a) Folhas, (b) Maturi, (c) Castanhas e (d) Pedúnculo de cajueiro apresentando sintomas de antracnose.

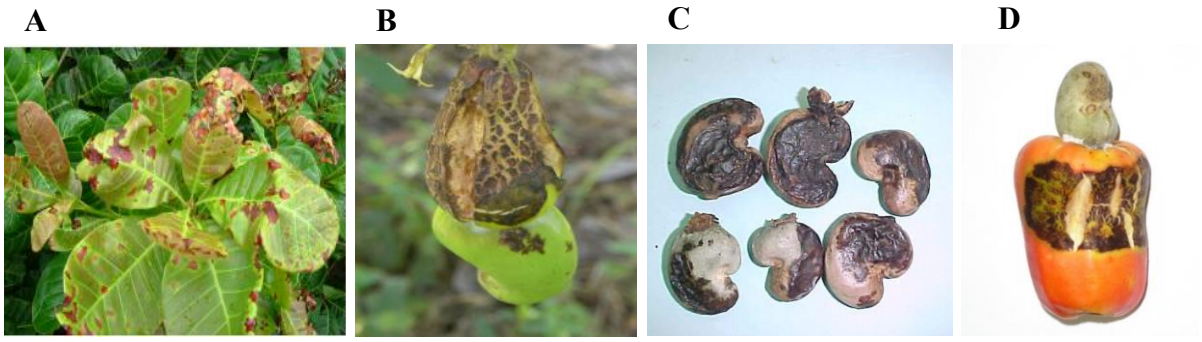

Fonte: Cardoso (2019).

O controle da antracnose no campo vem sendo realizado por intermédio da aplicação de variados fungicidas a base de oxiclorato de cobre, hidróxido de cobre, carbamato de zinco com manganês em períodos em que há floração e frutificação, quando os tecidos jovens estão mais suscetíveis ao ataque do patógeno. No entanto, devido às questões ambientais e aos custos, assim como observado para o controle das demais doenças, estudos para minimizar o emprego de fungicidas e procurar meios de controle alternativos vêm sendo realizados de modo que a inserção de pomares constituídos de clones de cajueiro anão precoce resistentes à essa doença pode consistir em uma alternativa ao uso de defensivos agrícolas (FREIRE et al., 2002).

3.2.3 Oídio

O oídio (também conhecida como cinza do cajueiro) é a doença mais antiga na cultura do caju. Era considerada uma patologia secundária, sem grande importância, porém, nos

últimos anos, é a doença que mais afeta as plantações de caju no Brasil (LIMA, 2017). A primeira descrição da doença foi feita em 1898, quando o micro-organismo causador da patologia foi identificado em plantas coletadas no estado de São Paulo e nomeado como *Oidium anacardii* Noack, descrito como parasita das inflorescências, frutos e folhas do cajueiro (FREIRE et al., 2002; PINTO et al., 2014). Posteriormente, verificou-se que a doença é causada pelo estado anamórfico de *Erysiphe quercicola* (que recebe o nome de *Pseudoidium anacardii* (Noack) U. Braun & R.T.A.Cook), parasita obrigatório do cajueiro, pertencente à ordem *Erysiphales* que consiste em um grupo de mais de 800 espécies de patógenos que estão notadamente envolvidos no parasitismo de mais de 1500 gêneros de plantas, especialmente em plantas que compõem a família Anacardiaceae (PINTO et al., 2018).

O oídio causa prejuízos na cultura do caju por afetar tanto a castanha quanto o pedúnculo, além das folhas e inflorescências, levando, ainda, ao abortamento das flores. Outro sintoma característico é a formação de uma camada branca-acinzentada sobre as folhas (FIGURA 8) (SERRANO et al., 2013). Essa patologia, apesar de afetar plantações de várias regiões do país, vem notadamente sendo mais frequente no Nordeste e compromete não apenas as folhas maduras do cajueiro, mas também tem-se observado ultimamente que os sintomas aparecem cada vez mais em folhas jovens e vêm comprometendo mais da metade das áreas produtoras de caju no Nordeste brasileiro, sendo que, quando não há intervenções com produtos químicos, pode comprometer até 100% dos pomares (LIMA, 2017; MARTINS et al., 2018).

Figura 8 - Sintomas do oídio em cajueiro nas folhas, fruto e pedúnculo.

Fonte: (CARDOSO et al., 2012).

A agressividade e dispersão geográfica do oídio vêm aumentando rapidamente nos últimos anos no Brasil, comprometendo significativamente a produção de caju. Em virtude disso, ainda são poucos os trabalhos que investigam formas de mitigar os problemas causados

por essa patologia (LIMA, 2017). As epidemias estão se tornando cada vez mais graves e comuns, podendo começar durante o período de floração da planta e se estender até o estágio final de produção (PINTO et al., 2018).

Na tentativa de combater o oídio vários métodos têm sido utilizados, dentre eles a pulverização de produtos químicos à base de enxofre tem-se mostrado eficaz no controle do micro-organismo, contudo, há os inconvenientes ambientais além de custos com mão de obra para a aplicação (CARDOSO et al., 2012). Pesquisas recentes conduzidas pela Embrapa Agroindústria Tropical apontam que alguns clones de cajueiro já introduzidos na natureza apresentam resistência ao oídio, fato bastante relevante para o desenvolvimento de tecnologias que possam levar ao controle da doença por intermédio da implantação de pomares constituídos por clones mais resistentes (FREIRE, 2015).

3.3 Clones de cajueiro anão precoce

Os cajueiros do tipo comum (gigantes) constituíam os pomares desta frutífera no Brasil até meados da década de 70, com o plantio sendo realizado empregando as sementes. No entanto, isso culminava em rendimentos insuficientes (menos de 250kg/ha de castanha), além de heterogeneidade dos cultivos sobretudo em relação à qualidade da castanha e do pedúnculo (BARROS, 2022).

A partir da década de 1960, seleções fenotípicas deram origem ao cajueiro tipo anão precoce, de modo que as mudas desse tipo foram inseridas na agricultura a partir da década de 1980 (SERRANO; OLIVEIRA, 2013) e, desde então, seu cultivo vem ganhando espaço nas lavouras devido a vários fatores: a planta apresenta porte baixo (inferior a 5 m), o que facilita o processo manual de colheita; frutificação e florescimento já no primeiro ano de existência da planta; pedúnculo suculento; maior rendimento considerando a relação amêndoa/castanha; facilidade na remoção da película da amêndoa (despeliculagem); pedúnculo com maior tempo de conservação; consistência da polpa (CAVALCANTI; NETO; BARROS, 2013; SERRANO; OLIVEIRA, 2013; SERRANO; PESSOA, 2016). Esses fatores também são favoráveis do ponto de vista do interesse econômico, uma vez que a implantação de pomares constituídos por clones de cajueiro tipo anão precoce favorece a uniformidade nas características consideradas relevantes para o comércio do caju, como teor de açúcares, peso e aspecto do pedúnculo, aparência e qualidade das castanhas. Além disso, proporciona ao produtor efetuar a colheita manual, poda, aplicação de defensivos agrícolas de modo mais eficiente somado à ocorrência

da propagação vegetativa dos clones, fatos que representam um progresso no cultivo do cajueiro (CARDOSO et al., 1999).

Os avanços tecnológicos propiciaram a introdução de clones melhorados de cajueiro tipo anão-precoce nas lavouras e, dentre os clones cultivados no Brasil, destacam-se o 'CCP 06', o 'CCP 09', o 'CCP 76', o 'CCP 1001', o 'Embrapa 50', o 'Embrapa 51', o 'BRS 226', o 'BRS 265' e o 'BRS 189'. Ainda estão presentes em áreas cultivadas os clones 'BRS 253', 'BRS 274', 'BRS 275', 'FAGA1' e 'FAGA 11' (LIMA, 2017).

Dentre os clones mencionados, destacam-se o 'CCP 76' obtido na década de 1980 e com cultivo favorecido tanto em regime sequeiro quanto irrigado, com aproveitamento do pedúnculo para o mercado de mesa devido ao seu sabor agradável, e da castanha bastante explorada no mercado de amêndoas. O clone 'BRS 189' foi lançado no ano 2000 e indicado para cultivo irrigado no estado do Ceará apresentando excelentes características que o tornam atrativo para o mercado de mesa. O clone 'BRS 226' teve seu lançamento para plantio comercial em regime sequeiro no ano de 2002 para exploração da amêndoa, e o clone 'BRS 265' lançado no ano de 2006 apresenta características que o tornam recomendável tanto para o mercado de mesa (consumo *in natura*) quanto para o mercado de castanha (BARROS, 2022).

Apesar das grandes vantagens advindas da inserção de clones de cajueiro anão precoce nos pomares, também houve problemas quanto ao aumento na suscetibilidade a doenças devido à redução na variabilidade genética, tendo em vista que indivíduos oriundos de clonagem apresentam genótipos idênticos em todas as gerações. Desse modo, se um indivíduo é suscetível a determinada doença, as gerações advindas dele também conservarão essa característica. Além disso, tem-se o fator do desequilíbrio em virtude do aumento na área plantada, levando ao surgimento de novas doenças causadas por micro-organismos além do aumento das já existentes (CARDOSO et al., 1999; LIMA, 2017). Por outro lado, alguns clones apresentam resistência a determinadas doenças. Os clones 'BRS 226', 'CCP 76', 'BRS 265' e 'BRS 189' mostram respostas distintas em relação à resistência e suscetibilidade às doenças mofo preto, antracnose e oídio e esse fato torna esses clones atraentes não só pelas características mencionadas quanto pela possibilidade de serem empregados graças a sua maior resistência a doenças (PINTO et al., 2018; LIMA et al., 2019), justificando a sua seleção para este estudo.

3.4 Interação planta-patógeno e os mecanismos de defesa das plantas: A biossíntese de COVs

O ataque constante de variados tipos de micro-organismos patogênicos confere às plantas um fator de proteção por meio da ativação de mecanismos que envolvem a fortificação da parede celular, produção de enzimas que degradam patógenos, suicídio celular, além da biossíntese de metabólitos que apresentam atividade antimicrobiana (TIKU, 2018). Em muitos casos, as plantas conseguem desenvolver resistência a esses agressores (ALLWOOD et al., 2011; MHLONGO et al., 2018; JOGAIAH; ABDELRAHMAN, 2019). A resistência desenvolvida por parte do hospedeiro é entendida como a capacidade que ele apresenta de evitar ou atrasar a penetração do patógeno em suas estruturas, comprometendo o desenvolvimento do processo de infecção (IRITI; FAORO, 2009; PINTO, 2016). Porém, os mecanismos que regem essa resistência ainda não estão completamente elucidados, mas sabe-se que esse processo envolve a liberação de moléculas pelos patógenos que desencadeiam um mecanismo de reconhecimento por parte do hospedeiro, levando à biossíntese de moléculas objetivando minimizar os danos causados pelo patógeno (GUPTA et al., 2015; JOGAIAH; ABDELRAHMAN, 2019).

Dentre os compostos que são biossintetizados pelas plantas por meio de seus mecanismos de defesa, destacam-se os compostos orgânicos voláteis (COVs), que são metabólitos secundários geralmente lipofílicos, de baixos ponto de ebulição e massa molecular, além de elevada pressão de vapor em condições naturais (LUBES; GOODARZI, 2017). Esses compostos podem atuar como mediadores da relação entre plantas e patógenos, desempenhando funções antibacteriana, antifúngica ou antioxidante (LÓPEZ-GRESA et al., 2017).

A variedade de compostos voláteis emitidos pelas plantas está diretamente relacionada às condições ambientais a que são submetidas, de modo que o estresse biótico e o abiótico contribuem para essa variedade (CALO et al., 2015). Estes compostos também podem atuar na expressão ou silenciamento dos genes de defesa, permitindo que as plantas interajam entre si em condições naturais de campo (KISHIMOTO et al., 2005). Estas interações podem potencializar os efeitos antimicrobianos dos compostos quando analisados individualmente, logo, os metabólitos voláteis podem ser, em conjunto, responsáveis pelo efeito antimicrobiano do óleo essencial de uma planta (DOS SANTOS et al., 2019).

Como resposta à infecção por patógenos, importantes COVs já foram descritos na literatura, como os voláteis de folhas verdes (GLV do inglês *green leaf volatiles*), terpenos, terpenoides, aldeídos e salicilato de metila. Compostos químicos dessas classes apresentam potentes efeitos antimicrobianos e auxiliam no sistema de defesa das plantas (ALGARRA

ALARCON et al., 2015).

3.4.1 Voláteis de folhas verdes (GLVs - green leaf volatiles)

Os COVs incluem uma variedade muito grande de compostos que são biossintetizados pelas plantas. Dentro dessa perspectiva, destacam-se os chamados voláteis de folhas verdes (GLV, do inglês *green leaf volatiles*) que são compostos químicos produzidos e liberados quando há ocorrência de algum tipo de estresse ao qual a planta é submetida, como ataque de herbívoros ou fitopatógenos (LÓPEZ-GRESA et al., 2017). Logo, a formação e consequente liberação dos GLVs (que pode ocorrer segundos após a perturbação provocada) consiste em um importante mecanismo de defesa direta das plantas além de permitirem que a comunicação entre esses vegetais seja realizada (defesa indireta). A partir do momento em que são lançados ao ambiente, os GLVs também funcionam como sinalizadores que permitem às plantas vizinhas reconhecerem que algo no ambiente pode consistir em uma ameaça e, assim, ativem seus mecanismos de defesa antes mesmo de entrarem em contato efetivo com o estresse que desencadeou a sua liberação pelas plantas nos arredores (MATSUI; KOEDUKA, 2016; WAKAI et al., 2019; SARANG; RUDZIŃSKI; SZMIGIELSKI, 2021).

Os GLVs são expressos junto com outros tipos de COVs, como terpenoides e derivados de aminoácidos. Os voláteis de folhas verdes são compostos que incluem álcoois, aldeídos e ésteres com uma cadeia principal de 6 átomos de carbono (C6) em sua estrutura. Estes compostos são biossintetizados em plantas superiores a partir de ácidos graxos insaturados por meio de reações que têm início na ativação da via da lipoxigenase (LOX) e dá sequência à reação catalisada de dioxigenação dos ácidos graxos, como o linoleico e o linolênico, dando origem a hidroperóxidos. Em seguida, a enzima hidroperóxido liase (HPL) atua na reação que fornece C6 aldeídos que, por sua vez, podem sofrer isomerização, desidrogenação e esterificação para fornecer álcoois e ésteres além de formas isoméricas dos aldeídos. Todo esse processo se inicia com a degradação de lipídios das membranas tanto por processos fisiológicos de desenvolvimento das planta como por intermédio de estresses provocados (UL HASSAN; ZAINAL; ISMAIL, 2015; VINCENTI et al., 2019). A figura 9 ilustra o processo de formação de alguns GLVs.

Figura 9 - Caminho biossintético seguindo a rota lipoxigenase (LOX) para a produção de GLVs, especificamente aldeídos e álcoois.

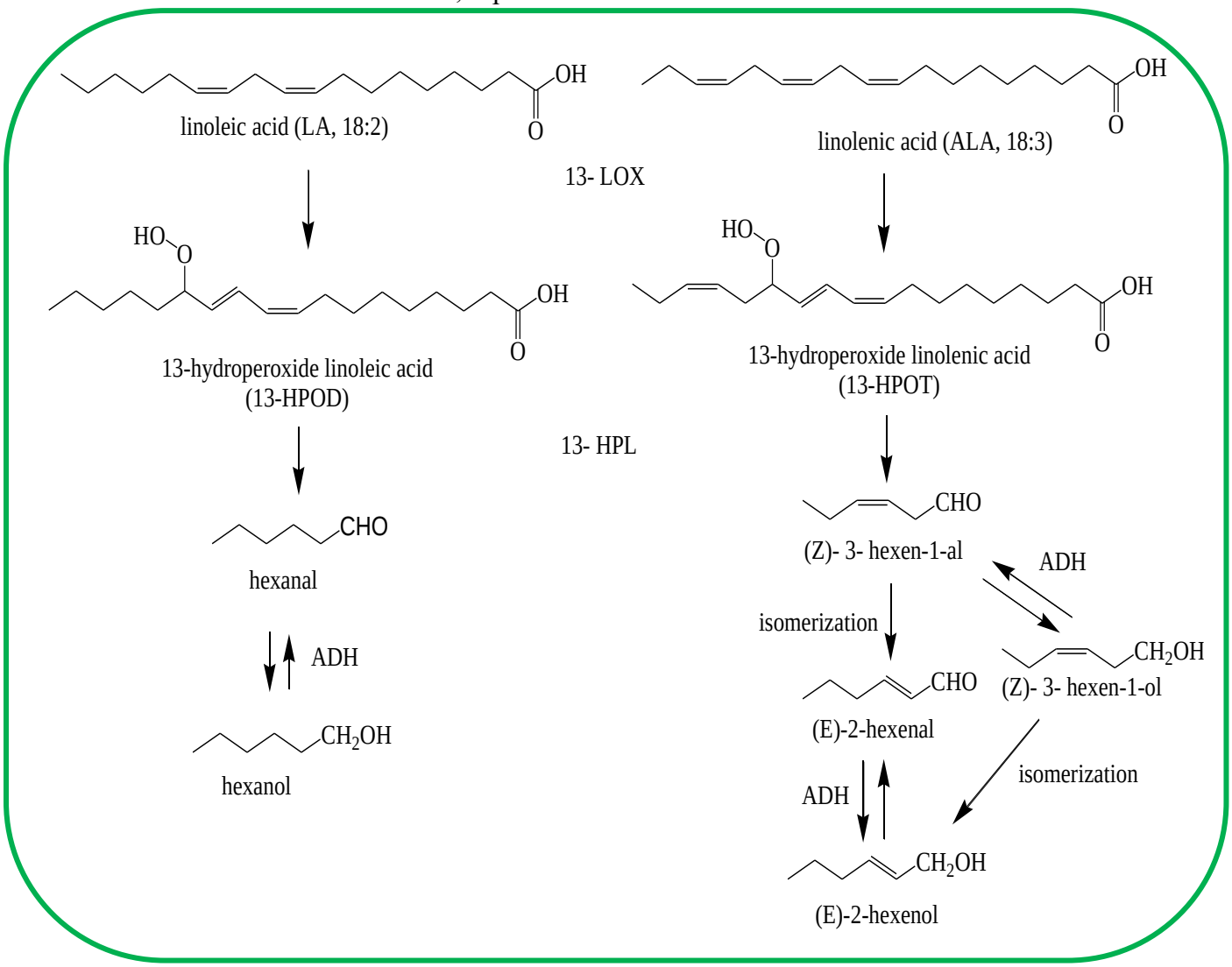

Legenda: 13-LOXs participam da produção de ácido 13-hidroperoxi-(9Z,11E)-octadecadienoico (13-HPOD) e 13-HPOT. 13-HPLs (hidroperóxido liase) atuam em 13-HPOD e 13-HPOT levando à formação de aldeídos C6. A ocorrência de reações de isomerização de aldeídos ocorre naturalmente ou por via enzimática (isomerase) para a produção de isômeros. As reações de desidrogenação, catalisadas pela ação de álcool desidrogenase (ADH) e esterificação de aldeídos, levam à produção de álcoois e ésteres, respectivamente (VINCENTI et al., 2019).

Compostos como (*E*)-2-hexenal, (*Z*)-3-hexenal e (*Z*)-3-hexenol são GLVs bastante conhecidos por proporcionarem a indução do acúmulo de ácido jasmônico, levarem à expressão de genes de defesa, além da biossíntese de outros compostos para agirem no sistema de defesa das plantas (SUGIMOTO et al., 2021). A Figura 10 mostra os GLVs mais encontrados em plantas.

Figura 10 - Estruturas químicas dos GLVs mais encontrados em plantas.

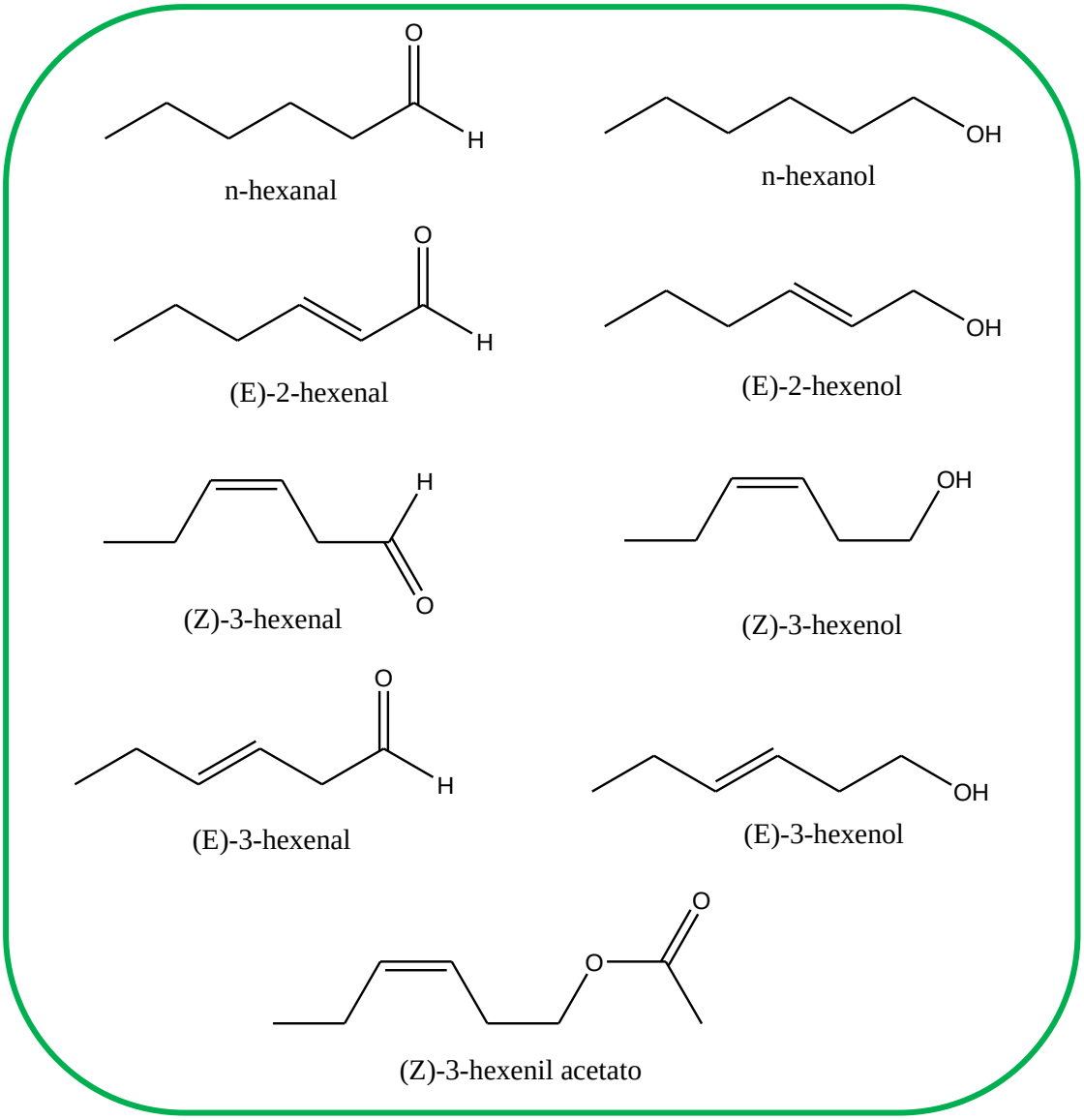

Fonte: (MATSUI; KOEDUKA, 2016).

Pesquisas recentes confirmam que devido às suas propriedades químicas distintas, os GLVs podem desempenhar papéis diferentes como por exemplo, o caso dos aldeídos C6 que se mostram muito eficientes na defesa direta contra fungos. Isso se deve ao fato dos grupos formil nos aldeídos apresentarem um potencial eletrofílico significativo, sobretudo quando há insaturações nas porções alfa e beta à carbonila, como no composto (*E*)-2-hexenal, por exemplo, o que contribui significativamente para o comprometimento no crescimento de patógenos, pois os aldeídos C6 são propensos a sofrer reações com várias moléculas biológicas, inclusive àquelas que eliminam funções vitais das células do micro-organismo (TANAKA et al., 2018).

Dessa forma, os GLVs atuam como mecanismo de defesa das plantas contra patógenos e podem, também, em conjunto com ácido jasmônico, ácido salicílico, etileno e

outros fitormônios, modular a resistência sistêmica adquirida (SAR) na mesma planta e em plantas vizinhas, preparando-as, portanto, para ataques futuros. Os GLVs podem ser biossintetizados por uma determinada parte da planta que foi atacada e se deslocarem para partes ainda não atacadas com o objetivo de desencadear a ativação de genes de defesa. Isso também acontece com plantas que ainda não foram atacadas, mas que estão próximas a plantas danificadas e podem, assim, terem alterados seus níveis de metabólitos relacionados à defesa (SHARIFI-RAD et al., 2017; TANAKA et al., 2018).

Estudos apontam que esses compostos podem substituir os produtos químicos empregados na agricultura em diferentes fases do cultivo objetivando não apenas o tratamento à base de produtos naturais como também a proteção das plantas contra o ataque de micro-organismos que comprometem os pomares (WAKAI et al., 2019). Além disso, a seleção de plantas ricas em GLVs, que indicam maior resistência a patógenos, consiste em uma ferramenta útil de aproveitamento dessa importante característica para que sejam implantados pomares melhorados e com indivíduos mais resistentes visando garantir cultivos mais saudáveis mitigando, assim, os problemas advindos com a infestação por micro-organismos (EFFAH et al., 2022).

3.4.2 Terpenos e derivados

Além dos GLVs, os COVs biossintetizados e emitidos pelas plantas incluem compostos de diferentes classes de produtos naturais que também atuam no sistema de defesa das plantas, como os terpenos, os ácidos, as cetonas, as aminas, além de álcoois, ésteres e aldeídos com diferentes números de átomos de carbono. Estes compostos fazem parte da composição dos chamados óleos voláteis, que consistem em líquidos hidrofóbicos contendo compostos químicos voláteis obtidos a partir de plantas (CALO et al., 2015; MAHIZAN et al., 2019).

Os óleos voláteis têm sido usados em diversos sistemas tradicionais de cura em todo o mundo desde os tempos antigos devido às suas atividades biológicas. Já foram descritos mais de 3000 óleos voláteis, dentre os quais estima-se que um décimo seja relevante para as indústrias farmacêutica, nutricional e cosmética. Vários óleos voláteis são de importante interesse em pesquisas por apresentarem atividade citotóxica e essa atividade se deve às interações complexas que ocorrem entre as diferentes classes de compostos como fenóis,

aldeídos, cetonas, álcoois, ésteres, éteres ou hidrocarbonetos presentes nesses óleos (SHARIFI-RAD et al., 2017).

Os óleos voláteis são oriundos de diversas partes da planta, como folhas, flores, cascas de caule, galhos, semente e até mesmo das raízes, podem ser extraídos empregando-se métodos que podem fazer uso de solventes orgânicos, destilação e métodos combinados para obtenção de maiores rendimentos, a depender do caso (MAHIZAN et al., 2019). Devido à riqueza e diversidade em sua composição, os óleos voláteis apresentam diferentes atividades biológicas, dentre elas, a antimicrobiana. Por isso, eles são tidos como uma das mais potentes fontes de grupos de produtos naturais para a obtenção de antifúngicos mais seguros (CALO et al., 2015; HAQUE et al., 2016; MAHIZAN et al., 2019). Os fatores que determinam a atividade dos óleos voláteis são a composição, os grupos funcionais presentes nos componentes ativos e suas interações sinérgicas (GUIMARÃES et al., 2019).

Um dos mecanismos de ação dos óleos voláteis como agentes antimicrobianos é a capacidade de seus constituintes de penetrar nas células dos micro-organismos através da membrana celular e causar inibição nas propriedades funcionais das células (BAJPAI; BAEK; KANG, 2012). A atividade antimicrobiana dos constituintes de um conjunto complexo de metabólitos voláteis geralmente não é atribuída a um composto específico, uma vez que o efeito sinérgico deve ser levado em consideração, ou seja, certos compostos podem atuar na modulação dos efeitos antimicrobianos de outros (RUSSO et al., 2015; GUIMARÃES et al., 2019).

Muitos estudos já descritos na literatura corroboram a eficácia dos óleos voláteis como antifúngicos contra várias cepas, embora não se tenham elucidado por completo os mecanismos que regem essa importante atividade (ABAD; ANSUATEGUI; BERMEJO, 2007; DA CRUZ CABRAL; FERNÁNDEZ PINTO; PATRIARCA, 2013). Exemplos desses estudos incluem o tratamento com óleos voláteis contra cepas dos fitopatógenos *Phytophthora infestans* (SOYLU; SOYLU; KURT, 2006) e *Botrytis cinerea* (SOYLU; KURT; SOYLU, 2010) que provocou a perda da integridade da parede celular e da permeabilidade da membrana plasmática desses fungos com importantes alterações morfológicas nas hifas. Em *Candida albicans* a ocorrência de apoptose foi evidenciada pela inibição da filamentação e ruptura da membrana citoplasmática (ZUZARTE et al., 2012). Em relação ao fungo *Aspergillus flavus*, óleos voláteis inibiram a produção de aflatoxinas (importantes micotoxinas biossintetizadas por esses micro-organismos) em virtude de danos significativos acarretados às membranas das hifas e conidióforos expostos ao óleo essencial (FERREIRA et al., 2013). Em *A. niger*, verificaram-se danos irreversíveis à parede celular, membrana celular e diversas organelas celulares. Os

resultados relataram evidente ruptura das membranas citoplasmáticas e organelas intracelulares, descolamento da membrana plasmática da parede celular, além de danos aos compartimentos das hifas (TOLOUEE et al., 2010). Os óleos voláteis podem, ainda, causar inibição da biossíntese de ergosterol na membrana plasmática dos fungos e danos mitocondriais (SHARIFI-RAD et al., 2017).

A literatura reporta o amplo espectro de atividade antimicrobiana dos monoterpenos, destacando os efeitos inseticidas e, sobretudo, a eficácia de monoterpenos cíclicos e não cíclicos como potentes antifúngicos (HIMEJIMA et al., 1992; KLEPZIG; SMALLEY; RAFFA, 1996; OBARA; HASEGAWA; KODAMA, 2002; LUO et al., 2004; KISHIMOTO et al., 2005; YAMASAKI et al., 2007; SHIMADA et al., 2014; QUINTANA-RODRIGUEZ et al., 2015). Dentre eles, podem ser citados como exemplos o terpinen-4-ol, γ-terpineno, α-terpineno, terpinoleno, α-pineno, 1,8-cineol, ρ-cimeno, (+)-limoneno, β-mirceno, (+)-β-pineno, (±)-linalol, α-felandreno e α-terpineol (Figura 11) cujos estudos os descrevem como sendo ativos contra os patógenos de plantas *Alternaria alternata*, *Aspergillus* spp. *Saccharomyces cerevisiae*, *Mucor mucedo*, *Colletotrichum lindemuthianum* e *Botrytis cinerea*. Estudos sugerem ainda que nos monoterpenos hidroxilados a ação antimicrobiana é potencializada devido às ligações de hidrogênio com sítios ativos das enzimas promovendo a sua inativação, o que acarreta em disfunção ou até ruptura da membrana celular (ALGARRA ALARCON et al., 2015; GUIMARÃES et al., 2019; MAHIZAN et al., 2019).

Os monoterpenos também apresentam significativa importância nos mecanismos de defesa e comunicação entre plantas, já que as rotas biossintéticas são ativadas para a emissão desses compostos em resposta à presença de patógenos, visando mitigar os efeitos das infestações. Desta forma, o estudo dos monoterpenos como compostos antimicrobianos constitui em uma importante ferramenta com grande potencial para desenvolvimento de defensivos agrícolas à base de produtos naturais objetivando auxiliar no combate aos prejuízos causados nas lavouras pelos micro-organismos (YAMASAKI et al., 2007; SHIMADA et al., 2014; ALGARRA ALARCON et al., 2015).

Figura 11 – Estrutura química de alguns compostos monoterpênicos já relatados na literatura com relação à sua atividade antifúngica.

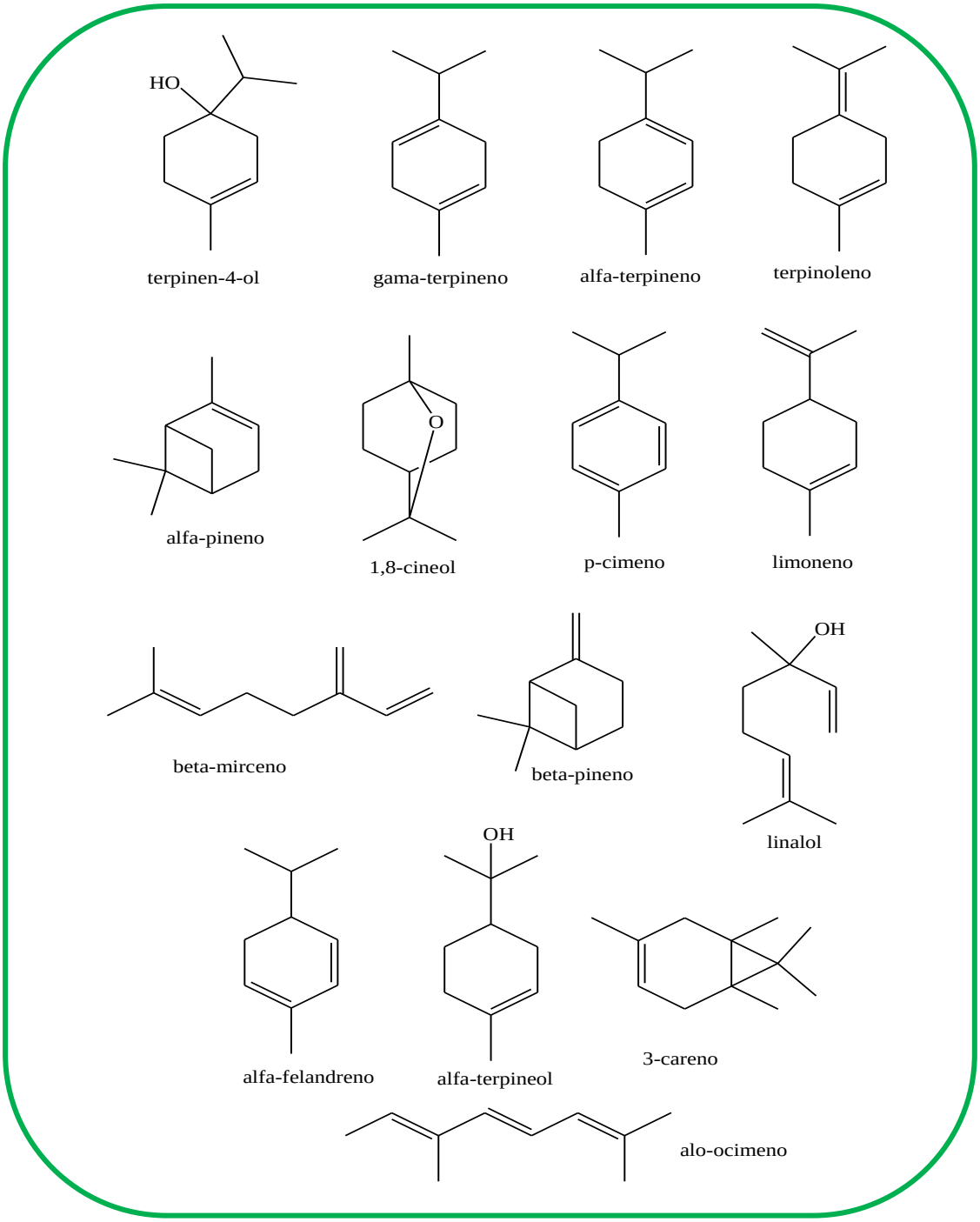

Fonte: Algarra Alarcon et al. (2015); Mahizan et al. (2019).

Além dos monoterpenos, óleos ricos em sesquiterpenos também têm a sua atividade antimicrobiana amplamente relatada na literatura (BARRERO et al., 2005; FORTUNA et al., 2011; BRUNO et al., 2013; MAHIZAN et al., 2019; NAWROT; GORNOWICZ-POROWSKA; NOWAK, 2020; MASI et al., 2021; NAWROT et al., 2021). No caso das lactonas

sesquiterpênicas, a literatura reporta que as mais ativas são as de caráter mais apolar ou de baixa polaridade (BARRERO et al., 2000) e a atividade antimicrobiana está relacionada à estrutura esquelética específica desses compostos que contêm um anel de lactona acoplado a um exo-metileno, fator que culmina na inibição de enzimas celulares por intermédio de uma adição nucleofílica. Ésteres e grupos hidroxila, quando presentes como substituintes, potencializam e aumentam e biodisponibilidade dos compostos, tornando-os lipofílicos ou hidrofílicos. A lipofilicidade permite que esses compostos penetrem de uma forma mais eficaz nas paredes celulares dos micro-organismos (NAWROT et al., 2021).

Dos terpenoides de ocorrência natural, os sesquiterpenos e as lactonas sesquiterpênicas são os mais relatados do ponto de vista de atividade antifúngica contra diversas cepas e muitos estudos têm sido feitos em relação a essa importante característica desses compostos (ABAD; ANSUATEGUI; BERMEJO, 2007). Os mecanismos que regem essa atividade ainda permanecem pouco compreendidos, embora se discuta que eles envolvam a ruptura da membrana celular em virtude da natureza lipofílica dos compostos pertencentes a essa classe de terpenoides (PEREIRA et al., 2017; NAWROT; GORNOWICZ-POROWSKA; NOWAK, 2020; NAWROT et al., 2021).

3.5 Compostos orgânicos voláteis de *Anacardium occidentale*

Por meio de pesquisas na literatura sobre os COVs oriundos do cajueiro, foi realizado um levantamento, sem limitação de período, objetivando-se identificar os compostos já relatados para *A. occidentale* em termos de metabólitos voláteis. Com base nessa pesquisa, verificou-se que tanto o pedúnculo, quanto as folhas e fruto são investigados, sendo mais comumente encontrados dados para os voláteis das duas primeiras estruturas da planta. No entanto, em relação às plantas de cajueiro tipo anão precoce, não foram encontrados estudos acerca de seus COVs.

A Tabela 1 contém informações acerca dos COVs já relatados na literatura para *A. occidentale*. De acordo com os dados apresentados, observa-se uma grande variedade de compostos pertencentes a classes químicas bastante variadas, como hidrocarbonetos, cetonas, ácidos, ésteres, álcoois.

Em relação ao pedúnculo, verifica-se que os ésteres são os constituintes químicos mais abundantes nessa estrutura da planta, seguidos de ácidos carboxílicos, aldeídos, álcoois e cetonas de cadeia curta. Nas castanhas também predominam hidrocarbonetos oxigenados, com destaque para os ácidos carboxílicos de cadeia curta.

No caso das folhas, verifica-se que os terpenos são os compostos majoritários, onde a presença de monoterpenos e sesquiterpenos é abundante. Com relação ao presente estudo realizado com clones de cajueiro tipo anão precoce, foi possível verificar que as plantas investigadas, semelhante ao que ocorre com as plantas de cajueiro gigante relatadas na literatura, também apresentam, em sua maioria, compostos terpênicos sendo emitidos pelas folhas.

Tabela 1 – COVs já relatados na literatura para o cajueiro (*A. occidentale*) (continua).

	Composto	Fórmula molecular	Classe química	Parte da planta	Referência
1	Pentanoato de etila	$C_7H_{14}O_2$	éster	pedúnculo	(BICALHO; REZENDE, 2001)
2	Hexanoato de metila	$C_7H_{14}O_2$	éster	pedúnculo	(BICALHO; REZENDE, 2001)
3	2-Metil-2-butenoato de etila	$C_8H_{14}O_2$	éster	pedúnculo	(BICALHO; REZENDE, 2001)
4	Hexanoato de etila	$C_8H_{16}O_2$	éster	pedúnculo	(BICALHO; REZENDE, 2001)
5	(*Z*)-3-Hexanoato de etila	$C_8H_{14}O_2$	éster	pedúnculo	(BICALHO; REZENDE, 2001)
6	(*E*)-3-Hexanoato de etila	$C_8H_{14}O_2$	éster	pedúnculo	(BICALHO; REZENDE, 2001)
7	2-Hexanoato de etila	$C_8H_{16}O_2$	éster	pedúnculo	(BICALHO; REZENDE, 2001)
8	2-Hidroxi-4-metilpentanoato de etila	$C_8H_{16}O_3$	éster	pedúnculo	(BICALHO; REZENDE, 2001)
9	Benzoato de metila	$C_8H_8O_2$	éster	pedúnculo	(BICALHO; REZENDE, 2001)

Tabela 1 – COVs já relatados na literatura para o cajueiro (*A. occidentale*) (continuação).

	Composto	Fórmula molecular	Classe química	Parte da planta	Referência
10	Isopentanoato de pentila	$C_{10}H_{20}O_2$	éster	pedúnculo	(BICALHO; REZENDE, 2001)
11	2-Metil-2-butanoato de butila	$C_9H_{18}O_2$	éster	pedúnculo	(BICALHO; REZENDE, 2001)
12	Benzoato de etila	$C_9H_{10}O_2$	éster	pedúnculo	(BICALHO; REZENDE, 2001)
13	Octanoato de etila	$C_{10}H_{20}O_2$	éster	pedúnculo	(BICALHO; REZENDE, 2001)
14	Benzenoacetato de etila	$C_{10}H_{12}O_2$	éster	pedúnculo	(BICALHO; REZENDE, 2001)
15	2-Octenoato de etila	$C_{10}H_{18}O_2$	éster	pedúnculo	(BICALHO; REZENDE, 2001)
16	2-Metil-2-butenoato de hexila	$C_{11}H_{22}O_2$	éster	pedúnculo	(BICALHO; REZENDE, 2001)
17	(*Z*)-Cinamato de etila	$C_{11}H_{12}O_2$	éster	pedúnculo	(BICALHO; REZENDE, 2001)
18	(*E*)-Cinamato de metila	$C_{10}H_{10}O_2$	éster	pedúnculo	(BICALHO; REZENDE, 2001)

Tabela 1 – COVs já relatados na literatura para o cajueiro (*A. occidentale*) (continuação).

	Composto	Fórmula molecular	Classe química	Parte da planta	Referência
19	Decanoato de etila	$C_{12}H_{24}O_2$	éster	pedúnculo	(BICALHO; REZENDE, 2001)
20	(*E*)-Cinamato de etila	$C_{11}H_{12}O_2$	éster	pedúnculo	(BICALHO; REZENDE, 2001)
21	Dodecanoato de etila	$C_{14}H_{28}O_2$	éster	pedúnculo	(BICALHO; REZENDE, 2001)
22	Hexadecanoato de etila	$C_{18}H_{36}O_2$	éster	pedúnculo	(BICALHO; REZENDE, 2001)
23	Tiglato de etila	$C_7H_{12}O_2$	éster	flores	(MAIA; ANDRADE; ZOGHBI, 2000; SALEHI et al., 2019)
24	Salicilato de metila	$C_8H_8O_3$	éster	flores	(SALEHI et al., 2019)
25	Acetato de etila	$C_4H_8O_2$	éster	pedúnculo	(SALEHI et al., 2019)
26	Butanoato de etila	$C_6H_{12}O_2$	éster	pedúnculo	(SALEHI et al., 2019)
27	Propanoato de etila	$C_5H_{10}O_2$	éster	pedúnculo	(SALEHI et al., 2019)
28	*trans*-2-butenoato de etila	$C_6H_{10}O_2$	éster	pedúnculo	(SALEHI et al., 2019)
29	*trans*-2-hexenoato de etila	$C_8H_{14}O_2$	éster	pedúnculo	(SALEHI et al., 2019)
30	*trans*-3-hexanoato de etila	$C_8H_{14}O_2$	éster	pedúnculo	(SALEHI et al., 2019)

Tabela 1 – COVs já relatados na literatura para o cajueiro (*A. occidentale*) (continuação).

	Composto	Fórmula molecular	Classe química	Parte da planta	Referência
31	Acetato de isoamila	$C_7H_{14}O_2$	éster	pedúnculo	(SALEHI et al., 2019)
32	2-Butenoato de metila	C_5H_8O	éster	pedúnculo	(SALEHI et al., 2019)
33	2-Hexanoato de metila	$C_7H_{14}O_2$	éster	pedúnculo	(SALEHI et al., 2019)
35	Dietil ftalato	$C_{12}H_{14}O_4$	éster	LCC	(PATEL; BANDYOPADHYAY; GANESH, 2006)
36	2-Metil-2-butenoato de butila	$C_9H_{18}O_2$	éster	pedúnculo	(BICALHO; REZENDE, 2001)
37	2-Butenoato de etila	$C_6H_{10}O$	éster	pedúnculo	(BICALHO; REZENDE, 2001)
38	3-Metilbutanoato de etila	$C_7H_{14}O_2$	éster	pedúnculo	(BICALHO; REZENDE, 2001)
39	Tetradecanoato de etila	$C_{16}H_{32}O_2$	éster	pedúnculo	(BICALHO; REZENDE, 2001)
40	Benzoato de hexila	$C_{13}H_{18}O_2$	éster	pedúnculo	(BICALHO; REZENDE, 2001)
41	2-Metil-2-butenoato de metila	$C_6H_{10}O_2$	éster	pedúnculo	(BICALHO; REZENDE, 2001)

Tabela 1 – COVs já relatados na literatura para o cajueiro (*A. occidentale*) (continuação).

	Composto	Fórmula molecular	Classe química	Parte da planta	Referência
42	3-Metilbutanoato de metila	$C_6H_{12}O_2$	éster	pedúnculo	(BICALHO; REZENDE, 2001)
43	(*E*)-3-Hexenoato de etila	$C_8H_{14}O_2$	éster	pedúnculo	(BICALHO; REZENDE, 2001)
44	2-Metilbutanoato de etila	$C_7H_{14}O_2$	éster	pedúnculo	(BICALHO; REZENDE, 2001; GARRUTI et al., 2003)
45	Benzoato de benzila	$C_{14}H_{12}O_2$	éster	folhas	(KOSSOUOH et al., 2008)
46	Salicilato de benzila	$C_{14}H_{12}O_3$	éster	folhas	(KOSSOUOH et al., 2008)
47	γ-Nonalactona	$C_9H_{16}O_2$	lactona	pedúnculo	(BICALHO; REZENDE, 2001)
48	γ-Dodecalactona	$C_{12}H_{22}O_2$	lactona	pedúnculo	(BICALHO; REZENDE, 2001)
49	γ-Hexalactone	$C_6H_{10}O_2$	lactona	pedúnculo	(BICALHO; REZENDE, 2001)
50	δ-Octalactone	$C_8H_{14}O_2$	lactona	pedúnculo	(BICALHO; REZENDE, 2001)

Tabela 1 – COVs já relatados na literatura para o cajueiro (*A. occidentale*) (continuação).

	Composto	Fórmula molecular	Classe química	Parte da planta	Referência
51	Ácido octanoico	$C_8H_{16}O_2$	ácido carboxílico	pedúnculo	(BICALHO; REZENDE, 2001)
52	Ácido nonanoico	$C_9H_{18}O_2$	ácido carboxílico	pedúnculo	(BICALHO; REZENDE, 2001)
53	Ácido decanoico	$C_{10}H_{20}O_2$	ácido carboxílico	pedúnculo	(BICALHO; REZENDE, 2001)
54	Ácido dodecanoico	$C_{12}H_{24}O_2$	ácido carboxílico	pedúnculo	(BICALHO; REZENDE, 2001)
55	Ácido tetradecanoico	$C_{14}H_{28}O_2$	ácido carboxílico	pedúnculo	(BICALHO; REZENDE, 2001)
56	Ácido hexadecanoico	$C_{16}H_{32}O_2$	ácido carboxílico	pedúnculo	(BICALHO; REZENDE, 2001)
57	Ácido ocatadecanoico	$C_{18}H_{36}O_2$	ácido carboxílico	pedúnculo	(BICALHO; REZENDE, 2001)

Tabela 1 – COVs já relatados na literatura para o cajueiro (*A. occidentale*) (continuação).

	Composto	Fórmula molecular	Classe química	Parte da planta	Referência
58	Ácido palmítico	$C_{16}H_{32}O_2$	ácido carboxílico	castanha	(MAIA; ANDRADE; ZOGHBI, 2000; RICO; BULLÓ; SALAS-SALVADÓ, 2016; SALEHI et al., 2019)
59	Ácido oleico palmítico	$C_{16}H_{32}O_2$	ácido carboxílico	castanha	(MAIA; ANDRADE; ZOGHBI, 2000; SALEHI et al., 2019)
60	Ácido *trans*-linoleico	$C_{18}H_{32}O_2$	ácido carboxílico	LCC, folhas, castanha	(GUO et al., 2016; SALEHI et al., 2019)
61	Ácido 2-metil-butanoico	$C_5H_{10}O_2$	ácido carboxílico	pedúnculo	(SALEHI et al., 2019)
62	Ácido 3-metil-butanoico	$C_5H_{10}O_2$	ácido carboxílico	pedúnculo	(SALEHI et al., 2019)
63	Ácido acético	$C_2H_4O_2$	ácido carboxílico	castanha, pedúnculo, folhas	(SALEHI et al., 2019)
64	Ácido anacárdico dieno	$C_{22}H_{32}O_3$	ácido carboxílico	LCC	(PATEL; BANDYOPADHYAY; GANESH, 2006)

Tabela 1 – COVs já relatados na literatura para o cajueiro (*A. occidentale*) (continuação).

	Composto	Fórmula molecular	Classe química	Parte da planta	Referência
65	Ácido anacárdico monoeno	$C_{22}H_{34}O_3$	ácido carboxílico	LCC	(PATEL; BANDYOPADHYAY; GANESH, 2006)
66	Ácido anacárdico trieno	$C_{22}H_{30}O_3$	ácido carboxílico	LCC	(PATEL; BANDYOPADHYAY; GANESH, 2006)
67	C8:0 Ácido octanoico	$C_8H_{16}O_2$	ácido carboxílico	pedúnculo	(BICALHO; REZENDE, 2001)
68	C9:0 Ácido nonanoico	$C_9H_{18}O_2$	ácido carboxílico	pedúnculo	(BICALHO; REZENDE, 2001a)
69	C10:0 Ácido decanoico	$C_{10}H_{20}O_2$	ácido carboxílico	pedúnculo	(BICALHO; REZENDE, 2001
70	C14:0 Ácido tetradecanoico	$C_{14}H_{28}O_2$	ácido carboxílico	pedúnculo	(BICALHO; REZENDE, 2001)
71	C18:0 Ácido octadecanoico	$C_{18}H_{36}O_2$	ácido carboxílico	pedúnculo	(BICALHO; REZENDE, 2001)

Tabela 1 – COVs já relatados na literatura para o cajueiro (*A. occidentale*) (continuação).

	Composto	Fórmula molecular	Classe química	Parte da planta	Referência
72	C12: 0 Ácido dodecanoico	$C_{12}H_{24}O_2$	ácido carboxílico	pedúnculo, folhas, casca do caule, castanha	(BICALHO; REZENDE, 2001; RICO; BULLÓ; SALAS-SALVADÓ, 2016)
73	C16:0 Ácido hexadecanoico	$C_{16}H_{32}O_2$	ácido carboxílico	castanha, folhas	(BICALHO; REZENDE, 2001; KOSSOUOH et al., 2008; MONTANARI et al., 2012; GA OLATUNJI, 2015; RICO; BULLÓ; SALAS-SALVADÓ, 2016)
74	Ácido 1,2-benzeno dicarboxílico	$C_8H_6O_4$	ácido carboxílico	folhas	(KOSSOUOH et al., 2008)
75	Ácido 17-octadecenoico	$C_{18}H_{34}O_2$	ácido carboxílico	castanhas, pedúnculo	(DE LOURDES CARDEAL; GUIMARÃES; PARREIRA, 2005)
76	Benzaldeído	C_7H_6O	aldeído	pedúnculo	(BICALHO; REZENDE, 2001)
77	2-Metil-2-pentenal	$C_6H_{10}O$	aldeído	pedúnculo	(SALEHI et al., 2019)
78	3-Metil-1-butanol	$C_5H_{12}O$	aldeído	pedúnculo	(SALEHI et al., 2019)

Tabela 1 – COVs já relatados na literatura para o cajueiro (*A. occidentale*) (continuação).

	Composto	Fórmula molecular	Classe química	Parte da planta	Referência
79	4-Etilbenzaldeído	$C_9H_{10}O$	aldeído	pedúnculo	(SALEHI et al., 2019)
80	Octanal	$C_8H_{16}O$	aldeído	pedúnculo	(SALEHI et al., 2019)
81	*trans*-2-hexenal	$C_6H_{10}O$	aldeído	pedúnculo	(SALEHI et al., 2019)
82	Hexanal	$C_6H_{12}O$	aldeído	pedúnculo, castanha	(DE LOURDES CARDEAL; GUIMARÃES; PARREIRA, 2005)
83	Fenilacetaldeído	C_8H_8O	aldeído	pedúnculo	(BICALHO; REZENDE, 2001)
84	Nonanal	$C_9H_{18}O$	aldeído	pedúnculo, castanha, folhas	(BICALHO; REZENDE, 2001; SALEHI et al., 2019)
85	Decanal	$C_{10}H_{20}O$	aldeído	pedúnculo	(BICALHO; REZENDE, 2001)
86	(*E*)-2-Decenal	$C_{10}H_{18}O$	aldeído	pedúnculo	(BICALHO; REZENDE, 2001)
87	Furfural	$C_5H_4O_2$	aldeído	castanha, pedúnculo	(MAIA; ANDRADE; ZOGHBI, 2000; BICALHO; REZENDE, 2001)

Tabela 1 – COVs já relatados na literatura para o cajueiro (*A. occidentale*) (continuação).

	Composto	Fórmula molecular	Classe química	Parte da planta	Referência
88	p-Anisaldeído	$C_8H_8O_2$	aldeído	folhas	(KOSSOUOH et al., 2008)
89	6-Metil-5-hepten-2-ona	$C_8H_{14}O$	cetona	pedúnculo	(BICALHO; REZENDE, 2001)
90	Acetofenona	C_8H_8O	cetona	pedúnculo	(BICALHO; REZENDE, 2001)
91	3-Hidróxi-2-butanona	$C_4H_8O_2$	cetona	pedúnculo	(BICALHO; REZENDE, 2001)
92	6-Metil-5-hepten-2-ona acetofenona	$C_8H_{14}O$	cetona	castanha, pedúnculo	(MAIA; ANDRADE; ZOGHBI, 2000; BICALHO; REZENDE, 2001)
93	2-Nonadecanona	$C_{19}H_{38}O$	cetona	folhas	(KOSSOUOH et al., 2008)
94	6,10,14-Trimetil-2-pentadecanone	$C_{18}H_{36}O$	cetona	folhas	(KOSSOUOH et al., 2008)
95	7,9-Diterbutil-1-oxaspiro-[4,5]-deca-6,9-Dieno-2,8-diona	$C_{17}H_{24}O_3$	cetona	folhas	(KOSSOUOH et al., 2008)
96	Mentona	$C_{10}H_{18}O$	cetona	folhas	(KOSSOUOH et al., 2008)
97	1-Octanol	$C_8H_{18}O$	álcool	pedúnculo	(BICALHO; REZENDE, 2001; GARRUTI et al., 2003)

Tabela 1 – COVs já relatados na literatura para o cajueiro (*A. occidentale*) (continuação).

	Composto	Fórmula molecular	Classe química	Parte da planta	Referência
98	Hexadecanol	$C_{16}H_{34}O$	álcool	pedúnculo, flores	(MAIA; ANDRADE; ZOGHBI, 2000; BICALHO; REZENDE, 2001)
99	Octadecanol	$C_{18}H_{38}O$	álcool	pedúnculo	(BICALHO; REZENDE, 2001)
100	(*E*)-Hex-2-enol	$C_6H_{12}O$	álcool	castanha	(SALEHI et al., 2019)
101	(*Z*)-Hex-3-enol	$C_6H_{12}O$	álcool	castanha	(SALEHI et al., 2019)
102	1-Butanol	C_4H_9OH	álcool	pedúnculo	(SALEHI et al., 2019)
103	1-Hexanol	$C_6H_{14}O$	álcool	pedúnculo	(GARRUTI et al., 2003)
104	1-Pentanol	$C_5H_{12}O$	álcool	pedúnculo	(GARRUTI et al., 2003)
105	2-Butoxietanol	$C_6H_{14}O_2$	álcool	pedúnculo	(GARRUTI et al., 2003)
106	2-Hexanol	$C_6H_{14}O$	álcool	pedúnculo	(GARRUTI et al., 2003)
107	3-Hexanol	$C_6H_{14}O$	álcool	pedúnculo	(GARRUTI et al., 2003)
108	1-Epi-cubenol	$C_{15}H_{26}O$	álcool	folhas	(KOSSOUOH et al., 2008)
109	1-Octen-3-ol	$C_8H_{16}O$	álcool	folhas	(KOSSOUOH et al., 2008)
110	1,4-Dimetilbenzeno	C_8H_{10}	álcool	folhas	(KOSSOUOH et al., 2008)
111	1,10-Diepi-cubenol	$C_{15}H_{26}O$	álcool	folhas	(KOSSOUOH et al., 2008)
112	7-Octadieno-3,6-diol	$C_8H_{14}O_2$	álcool	folhas	(KOSSOUOH et al., 2008)

Tabela 1 – COVs já relatados na literatura para o cajueiro (*A. occidentale*) (continuação).

	Composto	Fórmula molecular	Classe química	Parte da planta	Referência
113	Mentha-1,4-dien-7-ol	$C_{10}H_{16}O$	álcool	folhas	(KOSSOUOH et al., 2008)
114	Cardanol dieno	$C_{21}H_{32}O$	fenol	LCC	(MORAIS et al., 2017)
115	Cardanol trieno	$C_{21}H_{30}O$	fenol	LCC	(MORAIS et al., 2017)
116	Cardol diene	$C_{21}H_{32}O_2$	fenol	LCC	(MORAIS et al., 2017)
117	Cardol monoeno	$C_{21}H_{34}O_2$	fenol	LCC	(MORAIS et al., 2017)
118	Cardol trieno	$C_{21}H_{30}O_2$	fenol	LCC	(MORAIS et al., 2017)
119	Agatisflavona		fenol	folhas	(VELAGAPUDI et al., 2018)
120	o-Cimeno	$C_{10}H_{16}$	terpeno	pedúnculo	(BICALHO; REZENDE, 2001)
121	Limoneno	$C_{10}H_{16}$	terpeno	pedúnculo, folhas, castanhas	(BICALHO; REZENDE, 2001; DE LOURDES CARDEAL; GUIMARÃES; PARREIRA, 2005; KOSSOUOH et al., 2008)
122	α-Cubebeno	$C_{15}H_{24}$	terpeno	pedúnculo, folhas	(BICALHO; REZENDE, 2001; KOSSOUOH et al., 2008)

Tabela 1 – COVs já relatados na literatura para o cajueiro (*A. occidentale*) (continuação).

	Composto	Fórmula molecular	Classe química	Parte da planta	Referência
123	α-Copaeno	$C_{15}H_{24}$	terpeno	pedúnculo, folhas	(MAIA; ANDRADE; ZOGHBI, 2000; BICALHO; REZENDE, 2001a; KOSSOUOH et al., 2008; MONTANARI et al., 2012; SALEHI et al., 2019)
124	α-cis-Bergamoteno	$C_{15}H_{24}$	terpeno	pedúnculo, folhas	(BICALHO; REZENDE, 2001; KOSSOUOH et al., 2008)
125	β-Cariofileno	$C_{15}H_{24}$	terpeno	pedúnculo	(BICALHO; REZENDE, 2001)
126	α-*trans*-bergamoteno	$C_{15}H_{24}$	terpeno	pedúnculo, folhas	(BICALHO; REZENDE, 2001; KOSSOUOH et al., 2008)
127	γ-Muuroleno	$C_{15}H_{24}$	terpeno	pedúnculo	(BICALHO; REZENDE, 2001)
128	β-Bisaboleno	$C_{15}H_{24}$	terpeno	pedúnculo	(BICALHO; REZENDE, 2001)

Tabela 1 – COVs já relatados na literatura para o cajueiro (*A. occidentale*) (continuação).

	Composto	Fórmula molecular	Classe química	Parte da planta	Referência
129	γ-Cadineno	$C_{15}H_{24}$	terpeno	pedúnculo, folhas	(BICALHO; REZENDE, 2001; KOSSOUOH et al., 2008; MONTANARI et al., 2012)
130	δ-Cadineno	$C_{15}H_{24}$	terpeno	pedúnculo; folhas	(MAIA; ANDRADE; ZOGHBI, 2000; BICALHO; REZENDE, 2001; KOSSOUOH et al., 2008; MONTANARI et al., 2012; SALEHI et al., 2019)
131	α-Calacoreno	$C_{15}H_{20}$	terpeno	pedúnculo	(BICALHO; REZENDE, 2001)
132	α-Muurulol	$C_{15}H_{26}O$	terpeno	pedúnculo	(BICALHO; REZENDE, 2001)
133	α-Cadinol	$C_{15}H_{26}O$	terpeno	pedúnculo	(BICALHO; REZENDE, 2001)
134	Curcufenol	$C_{15}H_{22}O$	terpeno	pedúnculo	(BICALHO; REZENDE, 2001)

Tabela 1 – COVs já relatados na literatura para o cajueiro (*A. occidentale*) (continuação).

	Composto	Fórmula molecular	Classe química	Parte da planta	Referência
135	Geranilcetona	$C_{13}H_{22}O$	terpeno	pedúnculo	(BICALHO; REZENDE, 2001)
136	1,8-Cineol	$C_{10}H_{18}O$	terpeno	folhas	(SALEHI et al., 2019)
137	(*E*)-β-Ocimeno	$C_{10}H_{16}$	terpeno	folhas	(MAIA; ANDRADE; ZOGHBI, 2000; EGONYU et al., 2013)
138	Cariofileno	$C_{15}H_{24}$	terpeno	folhas	(MONTANARI et al., 2012)
139	α-Humuleno	$C_{15}H_{24}$	terpeno	folhas	(MONTANARI et al., 2012)
140	α-Muuroleno	$C_{15}H_{24}$	terpeno	folhas	(KOSSOUOH et al., 2008; MONTANARI et al., 2012)
141	β -Selineno	$C_{15}H_{24}$	terpeno	folhas	(KOSSOUOH et al., 2008; MONTANARI et al., 2012)
142	δ-Selineno	$C_{15}H_{24}$	terpeno	folhas	(KOSSOUOH et al., 2008; MONTANARI et al., 2012)
143	Aromadendreno	$C_{15}H_{24}$	terpeno	folhas	(KOSSOUOH et al., 2008; MONTANARI et al., 2012)
144	Biciclogermacreno	$C_{15}H_{24}$	terpeno	folhas	(KOSSOUOH et al., 2008; MONTANARI et al., 2012)

Tabela 1 – COVs já relatados na literatura para o cajueiro (*A. occidentale*) (continuação).

	Composto	Fórmula molecular	Classe química	Parte da planta	Referência
145	Germacreno B	$C_{15}H_{24}$	terpeno	folhas	(KOSSOUOH et al., 2008; MONTANARI et al., 2012)
146	Germacreno D	$C_{15}H_{24}$	terpeno	folhas	(KOSSOUOH et al., 2008; MONTANARI et al., 2012)
147	α-Amorfeno	$C_{15}H_{24}$	terpeno	folhas	(KOSSOUOH et al., 2008; MONTANARI et al., 2012)
148	β-Chamigreno	$C_{15}H_{24}$	terpeno	folhas	(MONTANARI et al., 2012)
149	δ-Cadinol	$C_{15}H_{26}O$	terpeno	folhas	(MONTANARI et al., 2012)
150	(*Z*)-Ocimeno	$C_{10}H_{16}$	terpeno	folhas	(EGONYU et al., 2013)
151	Alloocimeno	$C_{10}H_{16}$	terpeno	folhas	(EGONYU et al., 2013)
152	Cardanol (C13)	$C_{19}H_{32}O$	terpeno	LCC	(PATEL; BANDYOPADHYAY; GANESH, 2006)
153	Cardanol (C15)	$C_{21}H_{34}O$	terpeno	LCC	(PATEL; BANDYOPADHYAY; GANESH, 2006)

Tabela 1 – COVs já relatados na literatura para o cajueiro (*A. occidentale*) (continuação).

	Composto	Fórmula molecular	Classe química	Parte da planta	Referência
154	Cardanol (C17)	$C_{23}H_{38}O$	terpeno	LCC	(PATEL; BANDYOPADHYAY; GANESH, 2006)
155	Cardol	$C_{21}H_{36}O_2$	terpeno	LCC	(PATEL; BANDYOPADHYAY; GANESH, 2006)
156	6-Cadineno	$C_{15}H_{26}$	terpeno	pedúnculo	(BICALHO; REZENDE, 2001)
157	p-Cimeneno	$C_{10}H_{14}$	terpeno	folhas	(KOSSOUOH et al., 2008)
158	3-Careno	$C_{10}H_{16}$	terpeno	folhas	(KOSSOUOH et al., 2008)
159	4a-H,10a-H-Guaia-1(5)-6-dieno	$C_{15}H_{24}$	terpeno	folhas	(KOSSOUOH et al., 2008)
160	4b-H,10a-H-Guaia-1(5)-6-diene	$C_{15}H_{24}$	terpeno	folhas	(KOSSOUOH et al., 2008)
161	9-Epi-β-cariofileno	$C_{15}H_{24}$	terpeno	folhas	(KOSSOUOH et al., 2008)
162	10-Epi-cubenol	$C_{15}H_{26}O$	terpeno	folhas	(KOSSOUOH et al., 2008)
163	10-Epi-γ-eudesmol	$C_{15}H_{26}O$	terpeno	folhas	(KOSSOUOH et al., 2008)
164	16-Caurene	$C_{20}H_{32}$	terpeno	folhas	(KOSSOUOH et al., 2008)
165	Allo-aromadendreno	$C_{15}H_{24}$	terpeno	folhas	(KOSSOUOH et al., 2008)
166	Aristolone	$C_{15}H_{22}O$	terpeno	folhas	(KOSSOUOH et al., 2008)

Tabela 1 – COVs já relatados na literatura para o cajueiro (*A. occidentale*) (continuação).

	Composto	Fórmula molecular	Classe química	Parte da planta	Referência
167	Carvenona	$C_{10}H_{16}O$	terpeno	folhas	(KOSSOUOH et al., 2008)
168	Álcool cariofileno	$C_{15}H_{26}O$	terpeno	folhas	(KOSSOUOH et al., 2008)
169	Óxido de cariofileno	$C_{15}H_{24}O$	terpeno	folhas	(KOSSOUOH et al., 2008)
170	Citronelal	$C_{10}H_{18}O$	terpeno	folhas	(KOSSOUOH et al., 2008)
171	Citronelol	$C_{10}H_{20}O$	terpeno	folhas	(KOSSOUOH et al., 2008)
172	*cis*-calameneno	$C_{15}H_{22}$	terpeno	folhas	(KOSSOUOH et al., 2008)
173	Óxido de cis-linalol	$C_{10}H_{18}O$	terpeno	folhas	(KOSSOUOH et al., 2008)
174	*cis*-p-ment-2-en-1-ol	$C_{10}H_{18}O$	terpeno	folhas	(KOSSOUOH et al., 2008)
175	Chavicol	$C_9H_{10}O$	terpeno	folhas	(KOSSOUOH et al., 2008)
176	Criptona	$C_9H_{14}O$	terpeno	folhas	(KOSSOUOH et al., 2008)
177	Cubenol	$C_{15}H_{26}O$	terpeno	folhas	(KOSSOUOH et al., 2008)
178	Elemol	$C_{15}H_{26}O$	terpeno	folhas	(KOSSOUOH et al., 2008)
179	Epi-globulol	$C_{15}H_{26}O$	terpeno	folhas	(KOSSOUOH et al., 2008)
180	Epi-α-cadinol	$C_{15}H_{26}O$	terpeno	folhas	(KOSSOUOH et al., 2008)
181	Epi-α-muurolol	$C_{15}H_{26}O$	terpeno	folhas	(KOSSOUOH et al., 2008)
182	Eremofileno	$C_{15}H_{24}$	terpeno	folhas	(KOSSOUOH et al., 2008)
183	Etilbenzeno	C_8H_{10}	terpeno	folhas	(KOSSOUOH et al., 2008)
184	Farnesol	$C_{15}H_{26}O$	terpeno	folhas	(KOSSOUOH et al., 2008)

Tabela 1 – COVs já relatados na literatura para o cajueiro (*A. occidentale*) (continuação).

	Composto	Fórmula molecular	Classe química	Parte da planta	Referência
185	Geraniol	$C_{10}H_{18}O$	terpeno	folhas	(KOSSOUOH et al., 2008)
186	Geranil formato	$C_{11}H_{18}O_2$	terpeno	folhas	(KOSSOUOH et al., 2008)
187	Germacreno A	$C_{15}H_{24}$	terpeno	folhas	(KOSSOUOH et al., 2008)
188	Globulol	$C_{15}H_{26}O$	terpeno	folhas	(KOSSOUOH et al., 2008)
189	Guaia-6,9-dieno	$C_{15}H_{24}$	terpeno	folhas	(KOSSOUOH et al., 2008)
200	Tiglato de hexila	$C_7H_{12}O_2$	terpeno	folhas	(KOSSOUOH et al., 2008)
201	Epóxido de humuleno II	$C_{15}H_{24}O$	terpeno	folhas	(KOSSOUOH et al., 2008)
202	Intermedeol	$C_{15}H_{26}O$	terpeno	folhas	(KOSSOUOH et al., 2008)
203	Cânfora de zimbro	$C_{15}H_{26}O$	terpeno	folhas	(KOSSOUOH et al., 2008)
204	Linalool	$C_{10}H_{18}O$	terpeno	folhas	(KOSSOUOH et al., 2008)
205	Mentha-1(7),8-dieno	$C_{10}H_{16}$	terpeno	folhas	(KOSSOUOH et al., 2008)
206	Óxido de manoil	$C_{20}H_{34}O$	terpeno	folhas	(KOSSOUOH et al., 2008)
207	Metil chavicol	$C_{10}H_{12}O$	terpeno	folhas	(KOSSOUOH et al., 2008)
208	Metil eugenol	$C_{11}H_{14}O_2$	terpeno	folhas	(KOSSOUOH et al., 2008)
209	Linolenato de metila	$C_{19}H_{32}O_2$	terpeno	folhas	(KOSSOUOH et al., 2008)
210	Mesitileno	C_9H_{12}	terpeno	folhas	(KOSSOUOH et al., 2008)
211	Sulfeto de menta	$C_{15}H_{24}S$	terpeno	folhas	(KOSSOUOH et al., 2008)
212	Mirceno	$C_{10}H_{16}$	terpeno	folhas	(KOSSOUOH et al., 2008)

Tabela 1 – COVs já relatados na literatura para o cajueiro (*A. occidentale*) (continuação).

	Composto	Fórmula molecular	Classe química	Parte da planta	Referência
213	Cânfora	$C_{10}H_{16}O$	terpeno	folhas	(KOSSOUOH et al., 2008)
214	Felandral	$C_{10}H_{16}O$	terpeno	folhas	(KOSSOUOH et al., 2008)
215	Fitol	$C_{20}H_{40}O$	terpeno	folhas	(KOSSOUOH et al., 2008)
216	*p*-cimen-7-ol	$C_{10}H_{14}O$	terpeno	folhas	(KOSSOUOH et al., 2008)
217	*p*-cimeno	$C_{10}H_{14}$	terpeno	folhas	(KOSSOUOH et al., 2008)
218	*p*-menta-1,5-dien-7-ol	$C_{10}H_{16}O$	terpeno	folhas	(KOSSOUOH et al., 2008)
219	*p*-menta-1,5-dien-8-ol	$C_{10}H_{16}O$	terpeno	folhas	(KOSSOUOH et al., 2008)
220	*p*-mentha-1(7),2-dien-8-ol	$C_{10}H_{16}O$	terpeno	folhas	(KOSSOUOH et al., 2008)
221	*p*-menta-1(7),4(8)-dieno	$C_{10}H_{16}$	terpeno	folhas	(KOSSOUOH et al., 2008)
222	Piperitone	$C_{10}H_{16}O$	terpeno	folhas	(KOSSOUOH et al., 2008)
223	Borneol	$C_{10}H_{18}O$	terpeno	folhas	(KOSSOUOH et al., 2008)
224	Cadina-1,4-dieno	$C_{15}H_{24}$	terpeno	folhas	(KOSSOUOH et al., 2008)
225	Cadina-3,5-dieno	$C_{15}H_{24}$	terpeno	folhas	(KOSSOUOH et al., 2008)
226	Canfeno	$C_{10}H_{16}$	terpeno	folhas	(KOSSOUOH et al., 2008)
227	Sabineno	$C_{10}H_{16}$	terpeno	folhas	(KOSSOUOH et al., 2008)
228	Álcool santolina	$C_{10}H_{18}O$	terpeno	folhas	(KOSSOUOH et al., 2008)
229	Salvial-4(14)-en-1-ona	$C_{15}H_{24}O$	terpeno	folhas	(KOSSOUOH et al., 2008)
230	Selina-3,5-dieno	$C_{15}H_{24}$	terpeno	folhas	(KOSSOUOH et al., 2008)

Tabela 1 – COVs já relatados na literatura para o cajueiro (*A. occidentale*) (continuação).

	Composto	Fórmula molecular	Classe química	Parte da planta	Referência
231	Selina-3,7(11)-dieno	$C_{15}H_{24}$	terpeno	folhas	(KOSSOUOH et al., 2008)
232	Selina-4(15),7(11)-dieno	$C_{15}H_{24}$	terpeno	folhas	(KOSSOUOH et al., 2008)
233	Terpinen-4-ol	$C_{10}H_{18}O$	terpeno	folhas	(KOSSOUOH et al., 2008)
234	Terpinoleno	$C_{10}H_{16}$	terpeno	folhas	(KOSSOUOH et al., 2008)
235	Timol	$C_{10}H_{14}O$	terpeno	folhas	(KOSSOUOH et al., 2008)
236	*trans*-Calameneno	$C_{15}H_{22}$	terpeno	folhas	(KOSSOUOH et al., 2008)
237	*trans*-Carveol	$C_{10}H_{16}O$	terpeno	folhas	(KOSSOUOH et al., 2008)
238	*trans*-2-Ciclohexen-1-ol	$C_{10}H_{18}O$	terpeno	folhas	(KOSSOUOH et al., 2008)
239	Óxido trans-linalol	$C_{10}H_{18}O_2$	terpeno	folhas	(KOSSOUOH et al., 2008)
240	*trans*-p-Ment-2-en-1-ol	$C_{10}H_{18}O$	terpeno	folhas	(KOSSOUOH et al., 2008)
241	*trans*-Piperitol	$C_{10}H_{18}O$	terpeno	folhas	(KOSSOUOH et al., 2008)
242	*trans*-Fitol	$C_{20}H_{40}O$	terpeno	folhas	(KOSSOUOH et al., 2008)
243	*trans*-Sabinol	$C_{10}H_{16}O$	terpeno	folhas	(KOSSOUOH et al., 2008)
244	Valenceno	$C_{15}H_{24}$	terpeno	folhas	(KOSSOUOH et al., 2008)
245	Viridiflorol	$C_{15}H_{26}O$	terpeno	folhas	(KOSSOUOH et al., 2008)
246	Ilanga-2,4(15)-dieno	$C_{15}H_{22}$	terpeno	folhas	(KOSSOUOH et al., 2008)
247	Zonareno	$C_{15}H_{24}$	terpeno	folhas	(KOSSOUOH et al., 2008)
248	α-Cadineno	$C_{15}H_{24}$	terpeno	folhas	(KOSSOUOH et al., 2008)

Tabela 1 – COVs já relatados na literatura para o cajueiro (*A. occidentale*) (continuação).

	Composto	Fórmula molecular	Classe química	Parte da planta	Referência
249	α-Fenchol	$C_{10}H_{18}O$	terpeno	folhas	(KOSSOUOH et al., 2008)
250	Acetato de α-fenchil	$C_{12}H_{20}O_2$	terpeno	folhas	(KOSSOUOH et al., 2008)
251	α-Felandreno	$C_{10}H_{16}$	terpeno	folhas	(KOSSOUOH et al., 2008)
252	α-Terpineno	$C_{10}H_{16}$	terpeno	folhas	(KOSSOUOH et al., 2008)
253	α-Terpineol	$C_{10}H_{18}O$	terpeno	folhas	(KOSSOUOH et al., 2008)
254	α-Tujeno	$C_{10}H_{16}$	terpeno	folhas	(KOSSOUOH et al., 2008)
255	α-Selineno	$C_{15}H_{24}$	terpeno	folhas	(KOSSOUOH et al., 2008)
256	β-Acoradieno	$C_{15}H_{24}$	terpeno	folhas	(KOSSOUOH et al., 2008)
257	β-Bourboneno	$C_{15}H_{24}$	terpeno	folhas	(KOSSOUOH et al., 2008)
258	β-Bulneseno	$C_{15}H_{24}$	terpeno	folhas	(KOSSOUOH et al., 2008)
259	β-Cedreno	$C_{15}H_{24}$	terpeno	folhas	(KOSSOUOH et al., 2008)
260	β-Cubebeno	$C_{15}H_{24}$	terpeno	folhas	(KOSSOUOH et al., 2008)
261	β -Elemeno	$C_{15}H_{24}$	terpeno	folhas	(KOSSOUOH et al., 2008)
262	β-Felandreno	$C_{10}H_{16}$	terpeno	folhas	(KOSSOUOH et al., 2008)
263	β-Terpineol	$C_{10}H_{18}O$	terpeno	folhas	(KOSSOUOH et al., 2008)
264	δ-Amorfeno	$C_{15}H_{24}$	terpeno	folhas	(KOSSOUOH et al., 2008)
265	δ-Elemeno	$C_{15}H_{24}$	terpeno	folhas	(KOSSOUOH et al., 2008)
266	γ-2-Cadineno	$C_{15}H_{24}$	terpeno	folhas	(KOSSOUOH et al., 2008)

Tabela 1 – COVs já relatados na literatura para o cajueiro (*A. occidentale*) (continuação).

	Composto	Fórmula molecular	Classe química	Parte da planta	Referência
267	γ-Amorfeno	$C_{15}H_{24}$	terpeno	folhas	(KOSSOUOH et al., 2008)
268	γ-Elemeno	$C_{15}H_{24}$	terpeno	folhas	(KOSSOUOH et al., 2008)
269	γ-Gurjuneno	$C_{15}H_{24}$	terpeno	folhas	(KOSSOUOH et al., 2008)
270	γ-Pinocarveol	$C_{10}H_{16}O$	terpeno	folhas	(KOSSOUOH et al., 2008)
271	γ-Terpineno	$C_{10}H_{16}$	terpeno	folhas	(KOSSOUOH et al., 2008)
272	Butirato de (*E*)-3-Hexenila	$C_{10}H_{18}O_2$	terpeno	folhas	(KOSSOUOH et al., 2008)
273	Isovalerato de (E)-3-hexenila	$C_{11}H_{20}O_2$	terpeno	folhas	(KOSSOUOH et al., 2008)
274	(*E*)-β-Farneseno	$C_{15}H_{24}$	terpeno	folhas	(KOSSOUOH et al., 2008)
275	(*E*)-β-Ionona	$C_{13}H_{20}O$	terpeno	folhas	(KOSSOUOH et al., 2008)
276	(*E*,*E*)-α-Farneseno	$C_{15}H_{24}$	terpeno	folhas	(KOSSOUOH et al., 2008)
277	2-metil butirato de (*Z*)-3-hexenila	$C_{11}H_{20}O_2$	terpeno	folhas	(KOSSOUOH et al., 2008)
278	Benzoato de (*Z*)-3-hexenila	$C_{13}H_{16}O_2$	terpeno	folhas	(KOSSOUOH et al., 2008)
279	Isovalerato de (*Z*)-3-hexenila	$C_{11}H_{20}O_2$	terpeno	folhas	(KOSSOUOH et al., 2008)
280	(Z)-3-Hexenoato de (*Z*)-3-hexenila	$C_{12}H_{20}O_2$	terpeno	folhas	(KOSSOUOH et al., 2008)
281	Butirato de (*Z*)-3-hexenila	$C_{10}H_{18}O_2$	terpeno	folhas	(KOSSOUOH et al., 2008; EGONYU et al., 2013)
282	α-Ylangeno	$C_{15}H_{24}$	terpeno	folhas	

Tabela 1 – COVs já relatados na literatura para o cajueiro (*A. occidentale*) (continuação).

	Composto	Fórmula molecular	Classe química	Parte da planta	Referência
283	Ácido 2-furano-metanol butanóico	$C_8H_{10}O_3$	terpeno	castanhas, pedúnculo	(DE LOURDES CARDEAL; GUIMARÃES; PARREIRA, 2005)
284	1,3-Dihidroxi-2propanona	C_3H_6O	terpeno	castanhas, pedúnculo	(DE LOURDES CARDEAL; GUIMARÃES; PARREIRA, 2005)
285	2-Octilciclopropanooctanal	$C_{19}H_{36}O$	terpeno	castanhas, pedúnculo	(DE LOURDES CARDEAL; GUIMARÃES; PARREIRA, 2005)
286	Éster de 1-butanol de ácido acético	$C_6H_{12}O$	terpeno	castanhas, pedúnculo	(DE LOURDES CARDEAL; GUIMARÃES; PARREIRA, 2005)
287	Éster de 2-propen-1-ol de ácido acético	$C_{16}H_{22}O_3$	terpeno	castanhas, pedúnculo	(DE LOURDES CARDEAL; GUIMARÃES; PARREIRA, 2005)
288	Éster 3-hexen-1-ol de ácido acético	$C_8H_{14}O$	terpeno	castanhas, pedúnculo	(DE LOURDES CARDEAL; GUIMARÃES; PARREIRA, 2005)

Tabela 1 – COVs já relatados na literatura para o cajueiro (*A. occidentale*) (continuação).

	Composto	Fórmula molecular	Classe química	Parte da planta	Referência
289	Hexanoato de 2-propenila	$C_9H_{16}O_2$	terpeno	castanhas, pedúnculo	(DE LOURDES CARDEAL; GUIMARÃES; PARREIRA, 2005)
290	Oxalato de amônio	$C_2H_8N_2O_4$	sal orgânico	castanhas, pedúnculo	(DE LOURDES CARDEAL; GUIMARÃES; PARREIRA, 2005)
291	Pentanoato de 3-metilbutila	$C_{10}H_{20}O_2$	éster	castanhas, pedúnculo	(DE LOURDES CARDEAL; GUIMARÃES; PARREIRA, 2005)
292	α-Pineno	$C_{10}H_{16}$	hidrocarboneto	pedúnculo, folhas	(DE LOURDES CARDEAL; GUIMARÃES; PARREIRA, 2005; MORONKOLA; KASALI; EKUNDAYO, 2007; KOSSOUOH et al., 2008)

Tabela 1 – COVs já relatados na literatura para o cajueiro (*A. occidentale*) (continuação).

	Composto	Fórmula molecular	Classe química	Parte da planta	Referência
293	β-Pineno	$C_{10}H_{16}$	hidrocarboneto	pedúnculo, folhas, castanha	(DE LOURDES CARDEAL; GUIMARÃES; PARREIRA, 2005; KOSSOUOH et al., 2008)
294	*trans*-Cariofileno	$C_{15}H_{24}$	hidrocarboneto	pedúnculo, folhas, castanha	(DE LOURDES CARDEAL; GUIMARÃES; PARREIRA, 2005; KOSSOUOH et al., 2008)
295	Naftaleno	$C_{10}H_{8}$	hidrocarboneto	pedúnculo	(BICALHO; REZENDE, 2001)
296	Tridecano	$C_{13}H_{28}$	hidrocarboneto	pedúnculo	(BICALHO; REZENDE, 2001)
297	Tetradecano	$C_{14}H_{30}$	hidrocarboneto	pedúnculo, folhas	(BICALHO; REZENDE, 2001, 2001; MONTANARI et al., 2012)
298	Pentadecano	$C_{15}H_{32}$	hidrocarboneto	pedúnculo	(BICALHO; REZENDE, 2001)

Tabela 1 – COVs já relatados na literatura para o cajueiro (*A. occidentale*) (continuação).

	Composto	Fórmula molecular	Classe química	Parte da planta	Referência
299	Hexadecano	$C_{16}H_{34}$	hidrocarboneto	pedúnculo	(BICALHO; REZENDE, 2001)
300	Heptadecano	$C_{17}H_{36}$	hidrocarboneto	pedúnculo	(BICALHO; REZENDE, 2001)
301	Octadecano	$C_{18}H_{38}$	hidrocarboneto	pedúnculo	(BICALHO; REZENDE, 2001)
302	Nonadecano	$C_{19}H_{40}$	hidrocarboneto	pedúnculo	(BICALHO; REZENDE, 2001)
303	Eicosano	$C_{20}H_{42}$	hidrocarboneto	pedúnculo	(BICALHO; REZENDE, 2001)
304	1-O-trans-Cinamoil-D-Glucopiranose	$C_{15}H_{18}O_7$	hidrocarboneto	pedúnculo	(MICHODJEHOUN-MESTRES; AMRAOUI; BRILLOUET, 2009)

Fonte: Elaborada pela autora (2022).

3.6 Metabolômica e interação planta-patógeno

Apesar do interesse cada vez mais crescente nos mecanismos e compostos envolvidos nas interações entre plantas e micro-organismos, sobretudo os patogênicos, estudos metabolômicos são menos frequentes na literatura, em contraste com os estudos genômicos e transcriptômicos que são realizados com maior frequência a fim de identificar os mecanismos genéticos relacionados a essas interações (CASTRO-MORETTI et al., 2020; GUPTA; SCHILLACI; ROESSNER, 2022).

As interações que ocorrem entre as plantas e os micro-organismos, sejam eles patogênicos ou não, exercem grande influência sobre a fisiologia dos hospedeiros, sendo essas interações um campo de estudos em desenvolvimento e de grande importância, sobretudo, para a produção agrícola. Graças à importância desse tipo de interação, a metabolômica vem, nos últimos anos, desenvolvendo métodos e técnicas para ampliar o conhecimento do ponto de vista quantitativo e qualitativo das interações entre plantas e fungos patogênicos. (ALLWOOD et al., 2011; CHEN; MA; CHEN, 2019; GUPTA; SCHILLACI; ROESSNER, 2022).

As doenças que afetam diretamente as plantas e que são causadas por fungos consistem em uma das principais ameaças à segurança alimentar no mundo todo, logo, entender as interações que acontecem entre fungos e plantas é de suma importância para o controle das fitopatologias. A metabolômica não apenas fornece uma abordagem qualitativa e quantitativa para determinar a patogênese de fungos fitopatogênicos, mas também ajuda a elucidar os mecanismos de defesa das plantas hospedeiras (CHEN; MA; CHEN, 2019).

Uma vez detectada a presença de fitopatógenos, as reações metabólicas das plantas sofrem significativas alterações. No caso do metabolismo secundário, as mudanças incluem a produção de hormônios de defesa, como ácido salicílico e jasmonatos, além de outros compostos, tanto fixos como voláteis, que são biossintetizados como forma de prevenir ou minimizar os efeitos do ataque do agressor (WILLIAM ALLWOOD et al., 2010). Nesse contexto, a metabolômica tem desempenhado um papel de extrema importância na distinção entre doença e simbiose (GUPTA; SCHILLACI; ROESSNER, 2022).

Os estudos relatados na literatura acerca das interações entre plantas e patógenos, apesar de menos corriqueiros que os estudos baseados em outras ciências ômicas, mostram a importância da metabolômica como ferramenta crucial para a compreensão das mudanças nos perfis químicos das plantas causadas por situações diversas. A metabolômica auxilia, ainda, na identificação de plantas com maior resistência tanto ao ataque de pragas na agricultura como a outras situações que lhes causam estresse biótico ou abiótico. Exemplos desses relatos incluem

os trabalhos de LÓPEZ-GRESA et al. (2017) que identificaram, por meio de metabolômica global com a técnica de GC-EM, COVs como (*Z*)-3-hexenol além dos ácidos acético, propiônico, isobutírico, butírico e vários monoterpenos. Esses compostos foram apontados como responsáveis pela resposta imune diferencial das folhas infectadas de tomateiro Rio Grande frente a cepas virulentas ou avirulentas de *Pseudomonas syringae*. As informações obtidas ampliam o conhecimento do sistema de defesa dessas plantas e sugerem a possibilidade de desenvolvimento de plantas projetadas para maior resistência ao patógeno.

Estudos metabolômicos conduzidos por (CHOO, 2010) mostraram que os níveis de flavonóides, fenilpropanóides e terpenóides aumentaram nas linhagens de cevada resistentes após a ocorrência de infecção por cepas de *Fusarium* ilustrando a importância desses metabólitos no mecanismo de defesa desse vegetal. Além disso, linhagens de trigo também apresentaram mudanças acentuadas em seus perfis de metabólitos voláteis após a infecção por *F. graminearum* (PARANIDHARAN et al., 2008).

Jones e colaboradores empregaram a metabolômica para investigar as modificações nos perfis químicos de arroz infectados por *M. oryzae*, que causa a doença fúngica mais grave nas plantações dessa commodity, comprometendo os rendimentos dos cultivos. Descobriram que os níveis de alanina nas amostras submetidas ao contágio foi maior do que nas amostras sadias e sugeriram que o aumento nesse metabólito é causador da morte celular (JONES et al., 2011).

O acometimento de cultivares de milho pelo fungo *Ustilago maydis*, causador de tumores, promoveu o aumento na biossíntese de vários compostos, como ácido fenilpropiônico, tirosina, ácido chiquímico; e os níveis de derivados do ácido hidroxicinâmico (HCA) e antocianinas também se mostraram elevados, destacando a diferença em relação às cultivares sadias que não apresentaram tais alterações (DOEHLEMANN et al., 2008).

Estudos relacionados à infecção de arroz, soja, alface e batata por cepas de *R. solani* destacaram que, para o caso da soja, a infecção pelo fungo resultou na maior biossíntese de carboidratos, perturbações nas vias de aminoácidos e ativação das vias biossintéticas de isoflavonoides, α-linolenato e fenilpropanoides. Essas vias são conhecidas por exibirem propriedades antioxidantes e bioatividade, fatos que auxiliam a soja a contra-atacar o patógeno *R. solani* (ALIFERIS; FAUBERT; JABAJI, 2014).

B. cinerea é um patógeno que causa grandes perdas na agricultura por acometer diferentes tipos de culturas. Análises metabolômicas globais foram realizadas com morango, uva, tomate e *Arabidopsis* infectados com *B. cinerea* (LLOYD et al., 2011; GRECO et al., 2012; AGUDELO-ROMERO et al., 2015; CAMAÑES et al., 2015; NEGRI et al., 2017; HU et al.,

2019). No caso do morango, a diferenciação do perfil metabólico foi identificada logo no estágio inicial da doença quando, inclusive, os sintomas não eram perceptíveis, fato de extrema importância, pois permite o diagnóstico precoce da doença, o que pode levar à diminuição de perdas nos pomares (HU et al., 2019). Para as cultivares de uva, metabolômica global empregando a técnica de RMN possibilitou detectar mudanças significativas nos metabólitos. Este estudo revelou que a infecção por *B. cinerea* causa alterações metabólicas significativas na uva, sendo que a biossíntese de fenilpropanoides, flavonoides e sacarose juntamente com glicerol, ácido glucônico e succinato foi aumentada nas plantas doentes, estando esses compostos diretamente associados ao crescimento do fitopatógeno nas uvas (GRECO et al., 2012).

Portanto, os estudos metabolômicos para a identificação de modificações nos perfis de metabólitos, sejam eles voláteis ou fixos, empregando-se técnicas analíticas adequadas, consistem em uma ferramenta valiosa para a compreensão dos mecanismos que regem as interações entre plantas e fitopatógenos e podem possibilitar melhorias na agricultura a partir da identificação de quais metabólitos conferem maior resistência às plantas permitindo, assim, o desenvolvimento de defensivos agrícolas à base de produtos naturais inócuos ao meio ambiente, bem como a implantação de pomares com indivíduos com características que envolvam a resistência aos patógenos (CHEN; MA; CHEN, 2019).

4. METODOLOGIA

4.1 Material vegetal: Origem e coleta

A seleção dos clones de cajueiro tipo anão precoce ‘CCP76’, ‘BRS226’, ‘BRS189’ e ‘BRS265’ foi feita de acordo com informações acerca das características que os tornam atrativos no mercado (como descrito no item 3.3) além de informações concernentes à resistência e suscetibilidade dos mesmos em relação às doenças mofo preto, antracnose e oídio (TABELA 2).

Tabela 2 – Comportamento dos clones em relação a diferentes fitopatologias.

Clone	Mofo preto	Antracnose	Oídio
‘CCP76’	Suscetível	Resistente	Parcialmente resistente
‘BRS226’	Resistente	Resistente	Resistente
‘BRS189’	Suscetível	Resistente	Suscetível
‘BRS265’	Resistente	Suscetível	Parcialmente resistente

Fonte: (LIMA et al., 2019; PINTO et al., 2018).

O perfil metabolômico de compostos orgânicos voláteis dos clones de cajueiro foi investigado no período de março a dezembro do ano de 2019, a partir da coleta de folhas e castanhas de plantas pertencentes ao Campo Experimental da Embrapa, localizado no município de Pacajus, a 54 km de Fortaleza, no estado do Ceará - Brasil (coordenadas geográficas do local: 4 ° 10 'S e 38 ° 27 'W e altitude de 60 m acima do nível do mar). O pomar foi implantado em maio de 2011 sob o regime de sequeiro e contém 16 linhas com 30 cajueiros em cada uma. As linhas do pomar são divididas em quatro blocos (delineamento de blocos ao acaso), cada linha consistindo em um tipo de clone de cajueiro anão da Embrapa codificado como ‘CCP76’, ‘BRS226’, ‘BRS189’ e ‘BRS265’. Defensivos agrícolas não são aplicados nesta área.

De cada um dos quatro tipos de clones avaliados, cinco plantas foram selecionadas para a coleta de amostras durante todo o período de estudo.

4.1.1 Coleta de material vegetal (folhas) para a investigação do perfil de voláteis em relação às doenças mofo preto e antracnose

Para o estudo do perfil dos COVs das plantas em resposta à doença mofo preto, causada por *Pilgeriella anacardii* Arx & Müller, foram realizadas coletas mensais das folhas de 20 plantas, cinco plantas de cada clone, no período de março a julho do ano de 2019. De cada planta foram coletadas 3 folhas de mesmo tamanho (aproximadamente 9 cm), totalizando 60 amostras por coleta.

Para a investigação do perfil dos COVs das mesmas plantas em relação à resposta à doença antracnose, causada por *Colletotrichum gloeosporioides*, os mesmos procedimentos foram adotados, porém com coletas mensais de julho a dezembro de 2019.

As folhas frescas foram coletadas no período da manhã, no intervalo de 9 às 11h, e colocadas no interior de *vials* de vidro de 20 mL com tampa de rosca contendo septo de silicone/PTFE (Supelco, Bellefonte, PA, EUA), específicos para análise por CG-EM. Após a coleta, os frascos contendo o material a ser analisado foram colocados dentro de uma caixa de isopor contendo um banho de gelo e transportados para o Laboratório Multiusuário de Química de Produtos Naturais (LMQPN) da Embrapa Agoindústria Tropical-CE, onde as análises usando CG-EM foram realizadas, em triplicata (FIGURA 12).

Figura 12 – Representação da disposição dos clones de cajueiro anão precoce utilizados no estudo e das coletas das amostras de folhas no campo.

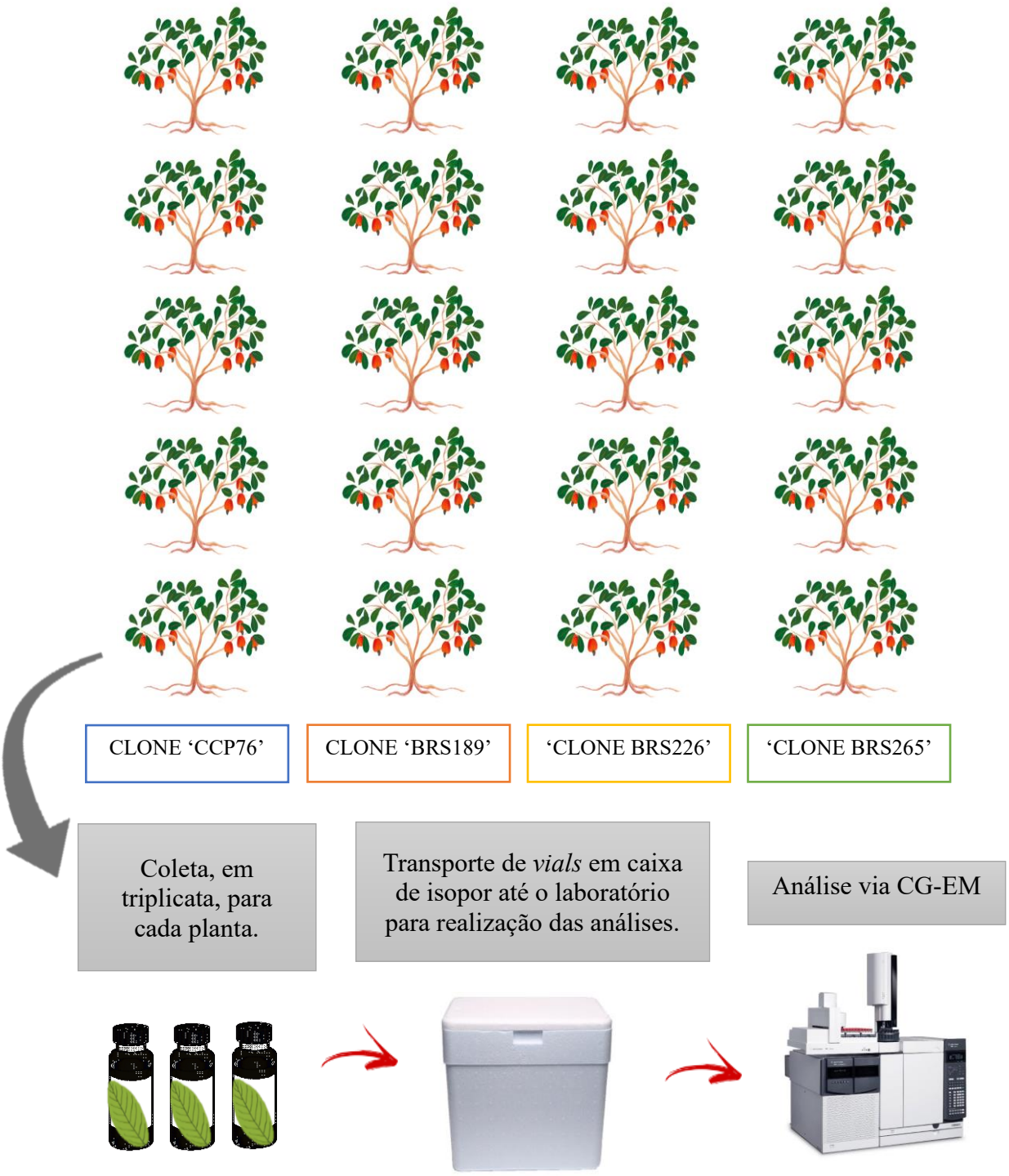

Fonte: Elaborada pela autora (2020).

4.1.2 Coleta de material vegetal (castanhas) para a investigação do perfil de voláteis em relação à doença oídio

A investigação do perfil de metabólitos voláteis emitidos pelos clones em relação à resposta ao ataque de *Pseudoidium anacardii* (F. Noack) U. Braun & R.T. A. Cook, patógeno causador do oídio, foi realizada por intermédio da coleta de amostras de castanhas no mês de outubro de 2019. Apesar de infestações por oídio também acometerem as folhas, no ano em que as análises foram realizadas não houve ataque nessa estrutura da planta, sendo, portanto, investigada a resposta química por parte das castanhas.

As análises das castanhas foram realizadas por meio de uma coleta no mês de outubro. Foram coletadas castanhas dos quatro clones estudados (‘CCP76’, ‘BRS226’, ‘BRS189’ e ‘BRS265’) com tamanho aproximado de 5 centímetros e sem sintomas da doença, além da coleta de castanhas com sintomas da doença para o clone suscetível ‘BRS189’. Assim como na coleta das folhas, para cada um dos quatro tipos de clone foram selecionadas 5 plantas para o estudo, sendo que, de cada planta, foi coletada uma castanha aparentemente sem sintomas do oídio, sendo colocada no interior de um frasco de vidro de 150 mL, totalizando cinco castanhas para cada tipo de clone. O mesmo procedimento foi adotado para coleta das castanhas com sintomas da doença. As coletas foram realizadas em triplicata, perfazendo-se um total de 15 amostras (FIGURA 13).

Todas as análises das folhas e castanhas foram realizadas a partir de amostras coletadas das mesmas cinco plantas inicialmente selecionadas de cada clone.

Figura 13 – Esquema da organização das amostras de castanhas coletadas no mês de outubro.

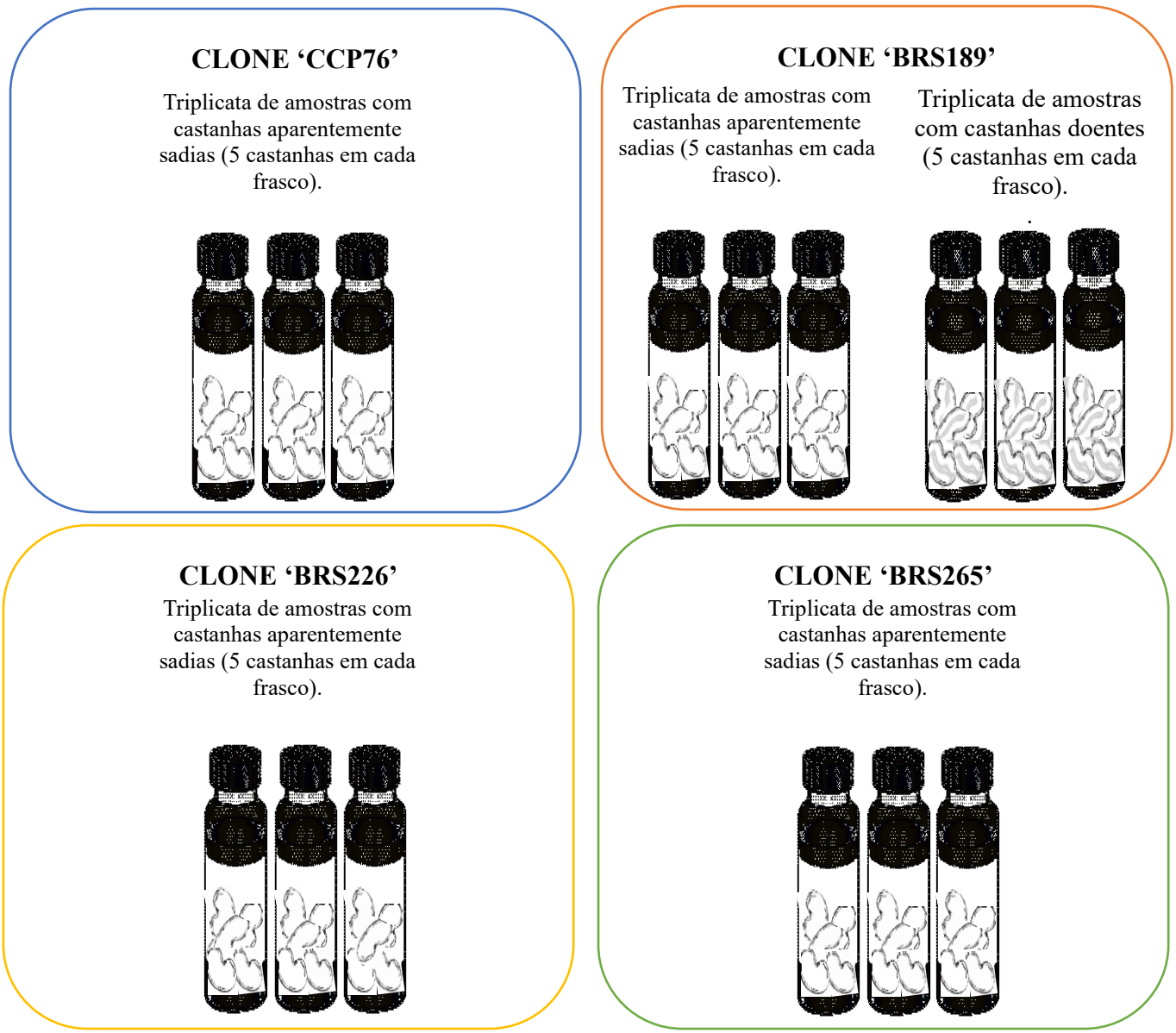

Fonte: Elaborada pela autora (2020).

4.2 Extração por SPME e análise dos compostos orgânicos voláteis por CG-EM

Para a extração de compostos voláteis das folhas e das castanhas foi utilizada a técnica de microextração em fase sólida (SPME) via *headspace*, utilizando condições experimentais baseadas em estudos anteriores (ROUSEFF et al., 2008). Para as análises de folhas, os *vials* contendo as amostras foram pré-incubados a 30 °C por 30 min sem agitação. Na sequência, a fibra cinza do tipo divinilbenzeno/carboxeno/polidimetilsiloxano (DVB/CAR/PDMS) de 1 cm (Supelco, Bellefonte, PA, EUA) foi exposta no interior dos *vials*,

no espaço livre, para a adsorção dos compostos voláteis durante 15 minutos. Após o período de captura dos compostos, a fibra foi removida dos *vials* e enviada ao injetor do cromatógrafo gasoso, onde permaneceu por 3 min para dessorção térmica (a 260 °C) dos analitos capturados. As análises foram feitas no modo automático.

Para as análises dos compostos voláteis das castanhas, o procedimento adotado foi a injeção manual, tendo em vista o tamanho dos frascos utilizados para acomodar as amostras não serem compatíveis com o equipamento. Desse modo, os frascos contendo as amostras foram pré-incubados em banho-maria (Cientec, CT-226) a 35 °C por 30 min sem agitação. Em seguida, a fibra cinza do tipo divinilbenzeno/carboxeno/polidimetilsiloxano (DVB/CAR/PDMS) de 1 cm (Supelco, Bellefonte, PA, EUA) foi exposta no interior dos frascos, no espaço livre, para a adsorção dos compostos voláteis durante 15 min (FIGURA 14). Após o período de captura dos compostos, a fibra foi retirada dos frascos e enviada ao injetor do cromatógrafo gasoso, onde permaneceu por 3 min para dessorção térmica (a 260 °C) dos analitos capturados.

O cromatógrafo a gás utilizado nas análises foi um sistema GC 7890B da Agilent Technologies Espanha, SL, Madri, acoplado a um espectrômetro de massa com analisador quadrupolo (5977A MSD Agilent Technologies Espanha, SL, Madri). A coluna usada no cromatógrafo a gás para a separação dos compostos foi do tipo HP5-MS ((5% fenil)-dimetilpolisiloxano) com 30m x 0,25mm de diâmetro interno e espessura do filme de 0,25µm. As análises foram feitas no modo *splitless*, usando gás hélio como transportador dos analitos, com vazão de 1 mL/min. Além disso, a eluição dos compostos pela coluna ocorreu com variação de temperatura, sendo que, inicialmente, a coluna foi mantida em 40 ºC e programada para 260 ºC a uma taxa de 7 ºC min^{-1}.

Figura 14 - Representação da metodologia empregada na extração dos compostos voláteis de castanhas de cajueiro.

Fonte: Elaborada pela autora (2019).

Para obtenção dos espectros de massa, foi utilizada a ionização por impacto de elétrons (70 eV), analisando uma faixa de massa de 50 a 600 Da. A temperatura usada na linha de transferência foi de 280°C sendo a da fonte de ionização 230 °C e quadrupolo a 150 °C. A identificação dos compostos obtidos foi realizada comparando os espectros de massa adquiridos com os presentes na Biblioteca NIST 2.0, 2012 (National Institute of Standards and Technology, Gaithersburg, Md, EUA) que acompanha o software MassHunter Workstation - Qualitative Analysis versão B.06.00 Agilent Technologies, além da comparação, tanto com o índice de retenção da série homóloga de n-alcanos C8-C30 (Supelco, 49451-U, Bellefonte, PA, EUA) quanto com dados da literatura (ADAMS, 2017).

4.3 Tratamento de dados e análise quimiométrica

Os dados de aquisição das análises obtidos com o software MassHunter Workstation foram submetidos ao tratamento no *software* MS-Dial (disponível para *download* gratuito por meio do link http://prime.psc.riken.jp/compms/msdial/main.html) para deconvolução e alinhamento de todos os cromatogramas, bem como para a construção de matrizes. Dessa forma, os dados do perfil metabólico dos clones já alinhados e deconvoluídos, foram organizados em uma planilha do Excel, onde os compostos identificados foram dispostos nas colunas e os nomes das amostras nas linhas, formando assim uma matriz de dados.

As informações das áreas dos picos dos compostos voláteis obtidos nos cromatogramas foram submetidas à normalização, utilizando a base da web Metaboanalyst 4.0 (www.metaboanalyst.ca) que também auxiliou na realização das análises quimiométricas multivariadas, como Análise Discriminante por Mínimos Quadrados Parciais (PLS-DA), Análise de Componentes Principais (PCA) e OLPS-DA, além da construção de *heatmaps* e de gráficos de análise de agrupamento hierárquico (HCA) de acordo com o protocolo fornecido (CHONG et al., 2019).

5 Metabolômica de voláteis de folhas de cajueiro: Avaliação de biomarcadores de resistência associados ao mofo preto (*Pilgeriella anacardii* Arx & Müller)

Volatile metabolomics from cashew leaves: Assessment of resistance biomarkers associated with black mold (*Pilgeriella anacardii* Arx & Müller)

Debora B. de Sousa, Gisele S. da Silva, Jhonyson A. C. Guedes, Luiz A. L. Serrano, Marlon V. V. Martins, Tigressa H. S. Rodrigues, Edy S. de Brito, Davila Zampieri, Mary A. S. Lima, and Guilherme J. Zocolo

Artigo publicado em *Journal of the Brazilian Chemical Society*

https://dx.doi.org/10.21577/0103-5053.20220078

ABSTRACT

Black mold, a disease caused by the fungus *Pilgeriella anacardia* Arx & Müller, affects cashews (*Anacardium occidentale*). Some cashew clones are more resistant to the pathogen; however, little is known about the chemical profile responsible for this trait. The investigation of volatile organic compounds (VOCs) from leaves of dwarf cashew clones resistant (BRS 226 and BRS 265) and susceptible (CCP 76 and BRS 189) to the pathogen was carried out. Leaves were collected during the months of disease incidence and decline (March to July 2019, Brazil), and VOCs were analyzed by gas chromatography-mass spectrometry (GC-MS) combined with chemometric tools. The GC-MS analysis tentatively identified 96 compounds. Partial least squares discriminant analysis (PLS-DA), orthogonal partial least squares discriminant analysis (OPLS-DA), hierarchical cluster analysis (HCA), and ROC curves analysis were useful in dividing VOCs into distinct resistance and associated chemical susceptibility groups for different clones. The VOCs in the leaves of the resistant clones were identified as alcohols and aldehydes containing six carbons: (*E*)-hex-2-enal, hex-3-en-1-ol, (*Z*)-hex-2-en-1-ol, (*E*)-hex-2-en-1-ol, and hexan-1-ol. Moreover, α-pinene, pseudolimonene, α-phellandrene, β-myrcene, sylvestrene, β-cis-ocimene, methyl salicylate, myrtenol, α-copaene, γ-muurolene, germacrene D, valencene, and germacrene B were also detected in these samples and may be candidate chemical biomarkers for cashew resistance to *P. anacardii*.

Keywords: *Anacardium occidentale*, resistance, susceptibility, *Pilgeriella anacardii*, chemometric analysis, biomarkers

Introduction

The cashew tree (*Anacardium occidentale* L.) is a plant originally from Brazil that is cultivated with great importance in the semi-arid region of the country, occupying approximately 500 thousand hectares. Its main product is cashew nut, an important commodity that generates approximately US$ 100 million per year for the country. The world's largest consumers of cashew nuts are India, the United States, and the European Union (IBGE, 2017).

Common cashew trees are large plants with a height that can exceed 10 m, which makes manual harvesting impossible with consequent loss of cashew pulp. To maximize the use of cashew products, from the 1980s onwards Brazil consolidated a strong genetic improvement program, resulting in the provision of 12 clonal genotypes, 10 of which are called dwarf-cashew (height less than 4 m). Dwarf-cashew clones allow manual harvesting of fruits, increasing the use and quality of cashew nuts and pulps, and favor the achievement of more productive orchards (CAVALCANTI; RESENDE, 2010).

However, some cultivars of dwarf-cashew clones have suffered severe attacks of a black mold, which is caused by the phytopathogen *Pilgeriella anacardii* Arx & Müller (Mycobank Database, 2020). This fungus is characterized by being an obligatory parasite that colonizes the lower part of the mature leaves of the cashew tree, where it is possible to observe the formation of a layer of black mycelium (FREIRE et al., 2002). The first symptom of the disease is the occurrence of spots indicative of insufficiency in the production of chlorophyll, which results in the yellowing of the leaves at the beginning of the rainy season. This disease is highly disseminated in orchards that produce cashews in May, just after two months of intense rain in the semi-arid region (FREIRE et al., 2002).

Owing to the lack of fungicides registered to control black mold disease in cashew cultivars, the use of genetic resistance presented by some clones has been reported as an efficient and economically viable alternative for the implantation of orchards (VIANA et al., 2012). Besides, the understanding of the chemical compound profile related to this resistance may favor the cashew clone breeding program in the search for new genotypes with resistance to diseases, as well as for the development of biopesticidal organic compounds.

The literature reports that when plants are under attack by pathogenic microorganisms, they biosynthesize volatile organic compounds (VOCs) that have antibacterial, antifungal, and antioxidant functions as signs of defense responses. Thus, metabolomic studies are frequently performed to identify the mechanisms related to plant-pathogen interactions (LÓPEZ-GRESA et al., 2017; MHLONGO et al., 2018).

The dwarf-cashew clones BRS 265 and BRS 226 were resistant to the attack of the *P. anacardii*, whereas BRS 189 and CCP 76 were susceptible to black mold disease (LIMA et al., 2019). According to these results, this work reports the investigation of the chemical profile of VOCs emitted from leaves of resistant and susceptible dwarf-cashew clones in response to the incidence and decline of black mold disease. The VOCs were analyzed by gas chromatographymass spectrometry (GC-MS), and the spectral data were interpreted using chemometric tools to identify possible chemical biomarkers.

2. Experimental

2.1 Plant material

The leaves of the cashew clones CCP 76, BRS 226, BRS 189, and BRS 265 were collected at the Embrapa Agroindústria Tropical (Experimental Field), located in the municipality of Pacajus, Ceará State, Brazil (geographical coordinates of the place: 4°10’S and 38°27’W and altitude of 60 m above sea level). The orchard of these clone types of dwarf cashews was planted in May 2011 under a rainfed regime. Since implantation, the orchard has received all the cultural treatments recommended by Serrano and de Oliveira (SERRANO; OLIVEIRA, 2013). Agrochemicals with probable action on black mold were not applied to the area.

Sample collection was conducted from March to July 2019, with one collection per month. From each of the four types of clones evaluated, five plants were selected, from which three leaves of the same size (approximately 9 cm) were collected, totaling 60 samples per collection. Leaf samples collected in March did not show disease symptoms for any clone type.

The leaf samples collected in April and May showed features associated with symptoms of the disease for clones CCP 76 and BRS 189. In June and July, no leaf samples showed symptoms of the disease. Fresh leaf samples were collected in the morning period. The samples were placed inside 20 mL vials with screw caps containing silicone septum/polytetrafluoroethylene (PTFE) (Supelco, Bellefonte, PA, USA), specific for analysis

using GC-MS. After collection, the vials containing the samples were placed inside a Styrofoam box containing an ice bath until GC-MS analysis was carried out in triplicate.

2.2 Extraction and analysis of the volatile organic compounds

Solid-phase microextraction (SPME) using the headspace technique was used to extract volatile compounds from the leaves of each investigated cashew clone. The experimental conditions for SPME analyses were according to Rouseff et al (ROUSEFF et al., 2008). The vials containing the samples were pre-incubated at 30 ºC for 30 min without shaking, and a divinylbenzene/carboxen/polydimethylsiloxane (DVB/CAR/PDMS) gray fiber of 1 cm (Supelco, Bellefonte, PA, USA) was exposed inside the vials for the adsorption of volatile compounds for 15 min in the headspace. After the extraction time, the fiber was removed from the vials and sent to the gas chromatograph injector, where it remained for 3 min for thermal desorption (at 260 °C) of the captured analytes. The elution of the compounds through the column occurred with temperature variation, and the initial column temperature was maintained at 40 °C and programmed to 260 ºC at a rate of 7 ºC min^{-1}.

The gas chromatograph used in the analysis was a 7890B GC System from Agilent Technologies Spain (Madrid, Spain) coupled to a mass spectrometer with a quadrupole analyzer (5977A MSD Agilent Technologies Spain). The column used was HP5-MS ((5%-phenyl)-dimethylpolysiloxane) with an internal diameter of 30 m × 0.25 mm internal diameter and a film thickness of 0.25 µm. The analyses were performed in splitless mode, using helium gas as the carrier of the analytes, at a flow rate of 1 mL min^{-1}.

To obtain the mass spectra, electron impact ionization at 70 eV was used, with a mass range of 50-600 Da. The temperature used in the transfer line was 280 °C and the ionization source was 150 °C. The identification of the obtained compounds was performed by comparing the acquired mass spectra with those present in the NIST 2.0 Library, 2012 (National Institute of Standards and Technology, Gaithersburg, MD, USA) database that accompanies the MassHunter Workstation-Qualitative Analysis software version B.06.00 Agilent Technologies (California, USA) in addition to comparing the retention index of the homologous series of n-alkanes C8-C30 (Supelco, 49451-U, Bellefonte, PA, USA) and with data from the literature (ADAMS, 2017).

2.3 Chemometric analysis

The acquisition data for the analysis obtained using the MassHunter Workstation software were processed on the MS-DIAL platform for deconvolution and alignment of the chromatograms. Furthermore, the metabolic profile data were organized in a spreadsheet (Excel, Microsoft) (MICROSOFT, 2021), where the identified compounds were arranged in columns and the sample names in rows, thus forming a data matrix.

The peak areas of the VOCs obtained via chromatograms were normalized by the sum treated on the cube root transformation scale that transform the response variable from y to y1/3 and it was the type of transformation that provided a better normal distribution of the data obtained. Data were scaled according to the Pareto scale using the MetaboAnalyst 4.0 web base (METABOANALYST, 2019). In addition, multivariate chemometric analyses were performed, such as partial least squares-discriminant analysis (PLS-DA) and orthogonal projections to latent structures-discriminant analysis (OPLS-DA), beyond the construction of heat maps, hierarchical cluster analysis (HCA) graphs. Furthermore, multivariate ROC curves were generated through cross-validation to complement biomarker identification analyses, where two thirds (2/3) of the samples are used to assess the importance of the feature and the main features are then used to build classification models which are validated on 1/3 of the samples that were left out. The procedure was repeated several times to calculate the performance and confidence interval of each model. This entire procedure was also performed using the MetaboAnalyst 5.0 web base according to the protocol provided by Chong (CHONG; WISHART; XIA, 2019).

Results

The pathogen

P. anacardii colonized the lower part of the mature cashew leaves (Figure S1, Supplementary Information (SI) section). From there, the fungus prevents the development of the leaves after penetrating the stomata and causing a reduction in the oxygen exchange between the plant and the environment (VIANA et al., 2012). According to the field observations during the collecting months (March, April, May, June, and July), the presence of the pathogen could be observed with different intensities. Between March and April, it was already possible to observe the presence of the fungus. However, there was no significant intensity when compared to May, when there was a severe infection, followed by a disease decline in June and July. These

observations are in accordance with the literature, which reports that the first symptoms of the disease can be observed at the beginning of the rainy season, reaching its most serious point in May, coinciding with the end of the rainy season in Northeast Brazil (FREIRE et al., 2002).

Profile of volatile organic compounds (VOCs)

Ninety-six compounds were tentatively identified from the four types of clones during the five months of analysis (Table S1, SI section). Most compounds belong to the terpene class. However, alcohols, esters, ketones, and aldehydes with short chains have also been identified. The results are in agreement with compounds already reported in the literature for the genus Anacardium, based on bibliographic research that takes into account family, genus, and species (BICALHO; REZENDE, 2001; GARRUTI et al., 2003; CEVA-ANTUNES et al., 2006; DZAMIC et al., 2009; CARDOSO et al., 2010; AGILA; BARRINGER, 2011; GEBARA et al., 2011; LING et al., 2016; SALEHI et al., 2019b; LIU et al., 2020). Thus, the confirmation by the literature that these compounds have already been identified in plants of the cashew tree genus, family, and species corroborates the fact that the compounds tentatively identified are products of plant biosynthesis and not of the fungus.

Data analysis

Owing to the amount and complexity of the data obtained, the results are presented as follows: metabolomic profile of each clone to verify the response of each clone along with the disease progress (March, April, and May) and decline (June and July). Comparisons were made between the profile of volatile organic compounds of clones resistant and susceptible to *P. anacardii*, aiming to verify which metabolites differ from the most resistant clones in relation to those susceptible clones; therefore, they could be biomarkers in response to pathogen attack.

Thus, the metabolic profiles of the clone BRS 226 (resistant to *P. anacardii*) were compared against the clones BRS 189 and CCP 76 (susceptible) as well as the comparison between BRS 265 (resistant) and the clones BRS 189 and CCP 76 was made on different models (PLS-DA and OPLS-DA). To check the accuracy and reliability of the model, the R^2Y and Q^2 parameters were used, called the explained variance, which provides a measure of fit of the model in relation to the original data, and the variable Q^2, called the predicted variance, which provides the internal consistency of the measure between the original and predictive data of the cross-validation (Table S2, SI section). Models with R^2Y and Q^2 values close to one were

considered excellent. However, values above 0.5 are accepted when the sample components are highly complex. The closer these two parameters are to 1, the more stable and reliable the model (CHAGAS-PAULA et al., 2015a).

In addition to the PLS-DA and OPLS-DA analyses, multivariate ROC curves were also constructed to identify possible biomarkers of resistance to black mold disease. As an important statistical tool, ROC curve graphs allow tests in which the rate of true positives (sensitivity) on the y-axis is plotted against the rate of false positives (specificity) on the x-axis. From this graph, it is possible to obtain the area under the curve (AUC). AUC is a measure of the accuracy of a diagnostic test, that is, a measure of the discriminatory ability of a test to verify whether a specific condition is present or absent (BÜNGER; MALLET, 2016; HOO; CANDLISH; TEARE, 2017; YU et al., 2019). Assessing the usefulness of a biomarker identified by ROC curve tests based on its AUC can be done so that values between 0.9-1.0 are considered excellent. Already between 0.8-0.9 are classified as good; 0.7-0.8 are regular; 0.6-0.7 consider themselves poor; 0.5-0.6 indicates the test has no diagnostic value (XIA et al., 2013). For this study, all curves constructed with a model 3 (with ten features) display a good performance and proved to be excellent in predicting compounds that may be candidates for biomarkers of resistance to black mold disease.

Analysis of the profile of volatile organic compounds of clone BRS 226 (resistant to P. anacardii) during the months of infestation and non-infestation

Discriminant analysis by partial least squares score graph (PLS-DA) (FIGURE 15a) explained 60.6% of the total variance through the first two components and showed intersections between the metabolite profiles in March and April, suggesting a similar volatile pattern for the initial months of infection. Volatile similarity was also observed between May (peak severity) and June-July (declining severity). The PLS-DA loading graph (FIGURE 15b) showed that (*E*)-hex-2-enal (2), (*Z*)-hex-3-en-1-ol (3), (*Z*)-hex-2-en-1-ol (4), (*E*)-hex-2-en-1-ol (5), hexan-1-ol (6), β-pinene (15), and oct-1-en-3-ol (16) may be associated with the differentiation between samples in May, June, and July, with the first two months of analysis (March and April). In contrast, camphene (12), α-fenchene (13), octan-3-one (18), limonene (24), β-cis-ocimene (27), and p-mentha-3,8-diene (30) may be associated with the differentiation in the profile of volatile compounds in March and April concerning the others.

The variable importance in the projection (VIP) graphs show the most relevant metabolites in the response model with values above 1.0. The VIP graph (FIGURE 15c)

constructed with data referring to samples from the BRS 226 clone over the months of March to July highlights that the most important compounds in the projection for the month of May include (*E*)-hex-2-enal (2), (*Z*)-hex-2-en-1-ol (4), hexan-1-ol (6), and α-phellandrene (20), which were reported in the literature for Anacardiaceae (MAIA; ANDRADE; ZOGHBI, 2000; DE AQUINO; ARAÚJO; SILVEIRA, 2017), a fact that corroborates that such compounds are plant biosynthesis products. These compounds can be considered as potential candidates for defense biomarkers of this clone against *P. anacardii*, considering that, in May, the severity of the pathogen in the field was observed with greater intensity in relation to the other months.

Figure 15. (A) Partial Least Squares Discriminant Analysis (PLS-DA) score and (B) loading, (C) graph of Variables of Importance in Projection (VIP) built with the volatile compounds identified in the 'BRS 226' clone over May to July.

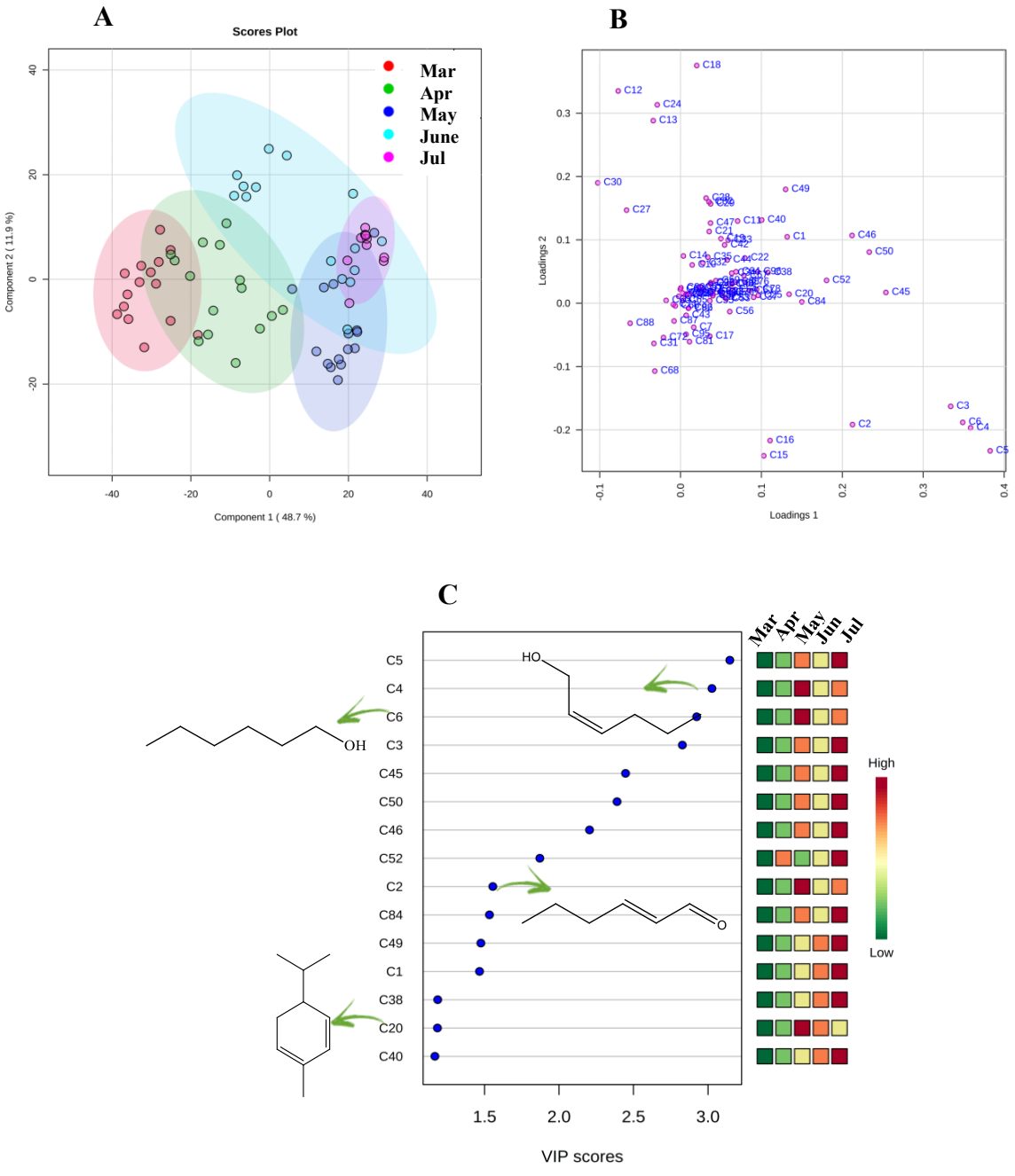

Source: Author (2019).

The heatmap graph (Figure S2, SI section) shows that compounds (*E*)-hex-2-enal (2), (*Z*)-hex-3-en-1-ol (3), (*Z*)-hex-2-en-1-ol (4), (*E*)-hex-2-en-1-ol (5), hexan-1-ol (6), β-

pinene (15), and oct-1-en-3-ol (16) (SALEHI et al., 2019a) showed a more pronounced increase in concentration in May, corroborating the data already pointed out by the VIP.

Comparative analysis of the volatile compound profiles of clones BRS 226 (resistant to P. anacardii) vs. BRS 189 (susceptible to P. anacardii)

The analysis for the behavior of the BRS 226 (resistant) and BRS 189 (susceptible), from March to July show, through the HCA graph (Figure S3a, SI section), that the volatile profiles are distinct for both clones (two groups). Within the large group of clone BRS 226, samples from March and April were grouped based on similarities in the metabolite profile, and samples from May, June, and July formed another group. The same pattern was observed for clone BRS 189. Thus, it is inferred that the samples have a similar chemical profile when the first signs of the pathogen are verified in the field. During the month of greatest severity, the metabolite profile changes in response to the stress to which the plants are subjected.

The PLS-DA (Figure S3b, SI section) score graph shows that most samples of the BRS 226 clone are found in the positive part of component 2, while the BRS 189 samples occupy the negative part of this component. It is still possible to verify that the differentiation in the profile of volatile compounds of the resistant clone (BRS 226) begins as early as March. All samples, except for July were found in the negative part of component 1. For the BRS 189 clone, there was significant differentiation in the volatile profile from April, since the samples from that month onwards are in the positive part of component 1. PLS-DA loading (Figure S3c, SI section) revealed that camphene (12), α-fenchene (13), β-myrcene (17), octan-3-one (18), pseudolimonene (19), limonene (24), sylvestrene (26), and β-cis-ocimene (27) (DZAMIC et al., 2009; ZOGHBI et al., 2014; SALEHI et al., 2019) are VOCs related to discrimination between samples.

Using a supervised analysis tool, an orthogonal partial least squares discriminant analysis (OPLS-DA) graph was constructed with samples from clones BRS 226 and BRS 189 for May. This analysis was carried out to verify which VOCs were responsible for the differentiation between resistant and susceptible clones in the month of greatest disease severity.

The construction of the OPLS-DA score graph (FIGURE 16a) allowed us to verify the formation of two completely separate groups, which showed the different chemical responses of plants to the disease. The values of the quality parameters for the model were

satisfactory: R2Y = 0.886 and Q2 = 0.869, suggesting that there was a statistically significant difference between the metabolic profiles of the analyzed samples.

An S-plot dispersion graph (FIGURE 16b) was constructed to analyze the variables responsible for the separation between the groups observed in the OPLS-DA score graph. Discriminating compounds, that is, those at the ends of the graph axis and away from the center, common to both groups of samples, are highlighted by red circles. On the negative axis of the S-Plot are the compounds responsible for the discrimination of the susceptible clone (BRS 189), while on the positive axis there are the metabolites related to the resistant clone (BRS 226).

The VIP score graph (FIGURE 16c) corroborates the results obtained in the OPLS-DA S-Plot, which presents important antimicrobial VOCs already reported in the literature (IIJIMA, 2014). Thus, the biosynthesis of (*Z*)-hex-3-en-1-ol (3), (*Z*)-hex-2-en-1-ol (4), (*E*)-hex-2-en-1-ol (5), hexan-1-ol (6), oct-1-en-3-ol (16) and β-myrcene (17) (DZAMIC et al., 2009; SALEHI et al., 2019; LIU et al., 2020), present in the samples of the resistant clone in the month of greatest infestation (May), may participate as biomarkers in the defense mechanism of plants of BRS 226 clone.

The ROC curve (FIGURE 16d) constructed with the samples referring to both clones in the month of greatest infestation of *P. anacardii* in the field shows, through the AUC value, that the data provide a good diagnosis of which compounds contribute to the defense of the plants. The selection panel (FIGURE 16e) corroborates the compounds highlighted by the VIP graph as being identified in the samples of resistant clones (BRS 226) and also highlights the α-fenchene compound (13), a fact that reiterates that these compounds may be participating of the plant's defense mechanism and contributing to its greater resistance to the pathogen's attack.

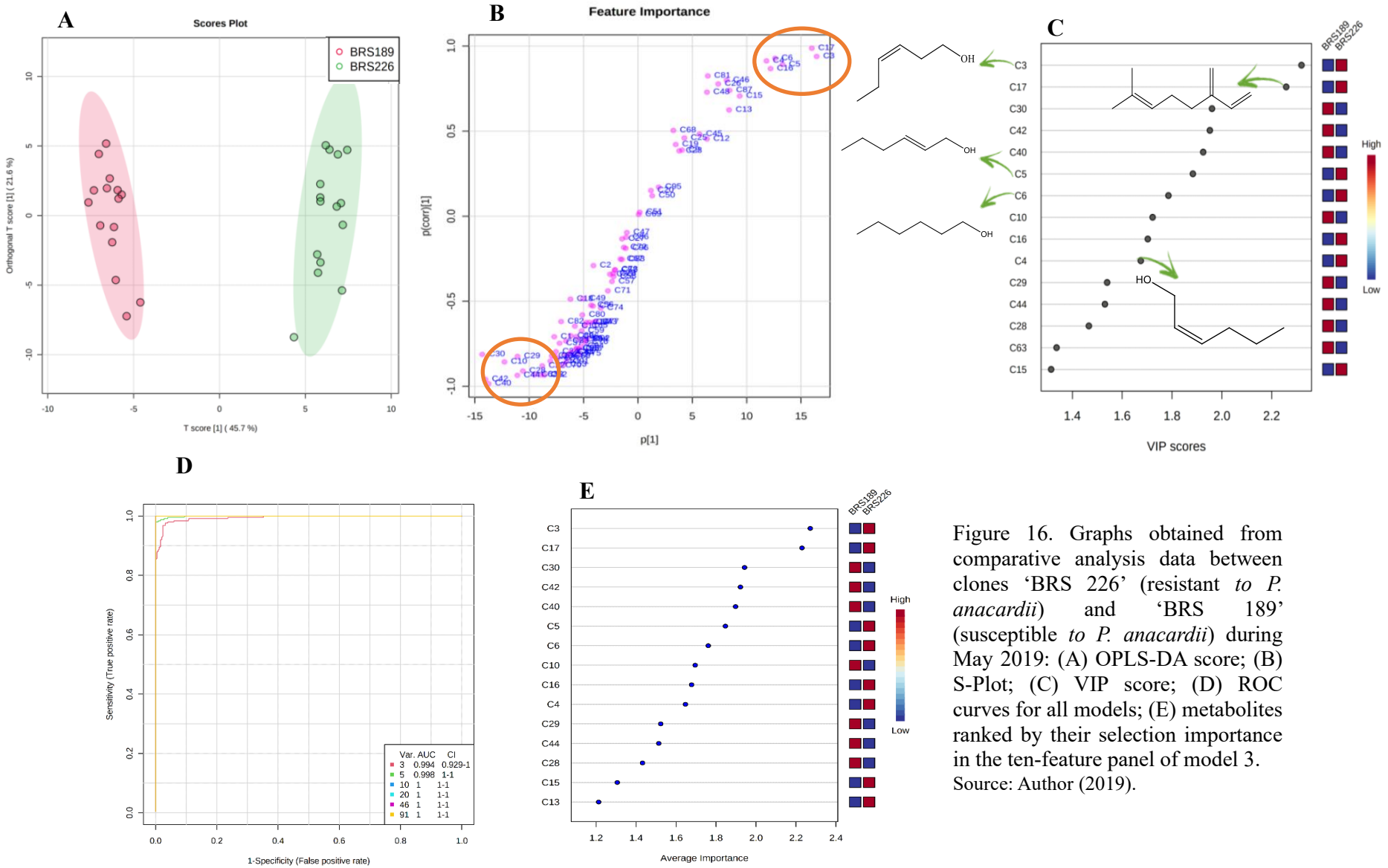

Figure 16. Graphs obtained from comparative analysis data between clones 'BRS 226' (resistant *to P. anacardii*) and 'BRS 189' (susceptible *to P. anacardii*) during May 2019: (A) OPLS-DA score; (B) S-Plot; (C) VIP score; (D) ROC curves for all models; (E) metabolites ranked by their selection importance in the ten-feature panel of model 3.
Source: Author (2019).

Comparative analysis of the volatile compound profiles of BRS 226 clones (resistant to P. anacardii) vs. CCP 76 (susceptible to P. anacardii)

The comparative analysis between the clones BRS 226 and CCP 76, resistant and susceptible, respectively, allows verification through HCA (Figure S4a, SI section) that the samples present a distinct volatile profile because the samples of the clones were separated into two large groups.

PLS-DA (Figure S4b, SI section) corroborates the separation of the HCA so that the samples referring to the BRS 226 clone are arranged on the positive part of component 2, whereas the samples from the CCP 76 clone are on the negative part of the same component. It is also worth mentioning that the samples referring to the BRS 226 clone are found, almost in their entirety (except for July), in the negative part of component 1. This shows that the defense compounds against pathogen attack were carried out in March when the presence of the fungus was first perceived. The CCP 76 clone, on the other hand, seems to initiate a change in metabolite biosynthesis only from April. Therefore, later when compared to BRS 226, a fact that may be associated with the susceptibility of this clone to the disease. The separation into two groups relative to each clone was confirmed by PLS-DA loading (Figure S4c, SI section), suggesting that camphene (12), α-fenchene (13), β-myrcene (17), and β-cis-ocimene (27) (DZAMIC et al., 2009; SALEHI et al., 2019) are discriminators between the two clones.

A OPLS-DA using data from May was performed to verify which metabolites were responsible for differentiating the samples from the resistant clone BRS 226 about the susceptible clone CCP 76 in the month of greatest disease severity. The OPLS-DA score graph (FIGURE 17a) suggests that plants have different chemical responses to infection by *P. anacardii*. The values of R2Y = 0.830 and Q2 = 0.806 were satisfactory, suggesting a statistically significant difference between the metabolic profiles of the samples analyzed.

Through the S-plot dispersion graph (FIGURE 17b), it was possible to identify the variables responsible for the separation between the groups observed in the OPLS-DA score graph. On the negative axis of the S-Plot are the compounds responsible for the discrimination of the resistant clone (BRS 226), while on the positive axis there are metabolites related to the susceptible clone (CCP 76).

β-Myrcene (17), sylvestrene (26), and myrtenol (48) were identified by VIP as the most abundant VOCs in the resistant clone in the month of May (FIGURE 17c) and were highlighted as candidates for resistance biomarkers of clone BRS 226, when compared with the

susceptible clone CCP 76.

The construction of the ROC curve (FIGURE 17d) for the samples of the clones BRS 226 and ‘CCP 76’ shows good performance and, through Figure 17e, it can be seen that the compounds (E,E)-hexa-2,4-dienal (9), (Z)-butanoic acid, 3-hexenyl ester (45) in addition to myrtenol (48) are the ones that appear in greater abundance in the resistant clone in the period of greatest pathogen infestation in the field. Therefore, they can act in the defense mechanism of this plant, contributing to its greater resistance against *P. anacardii*.

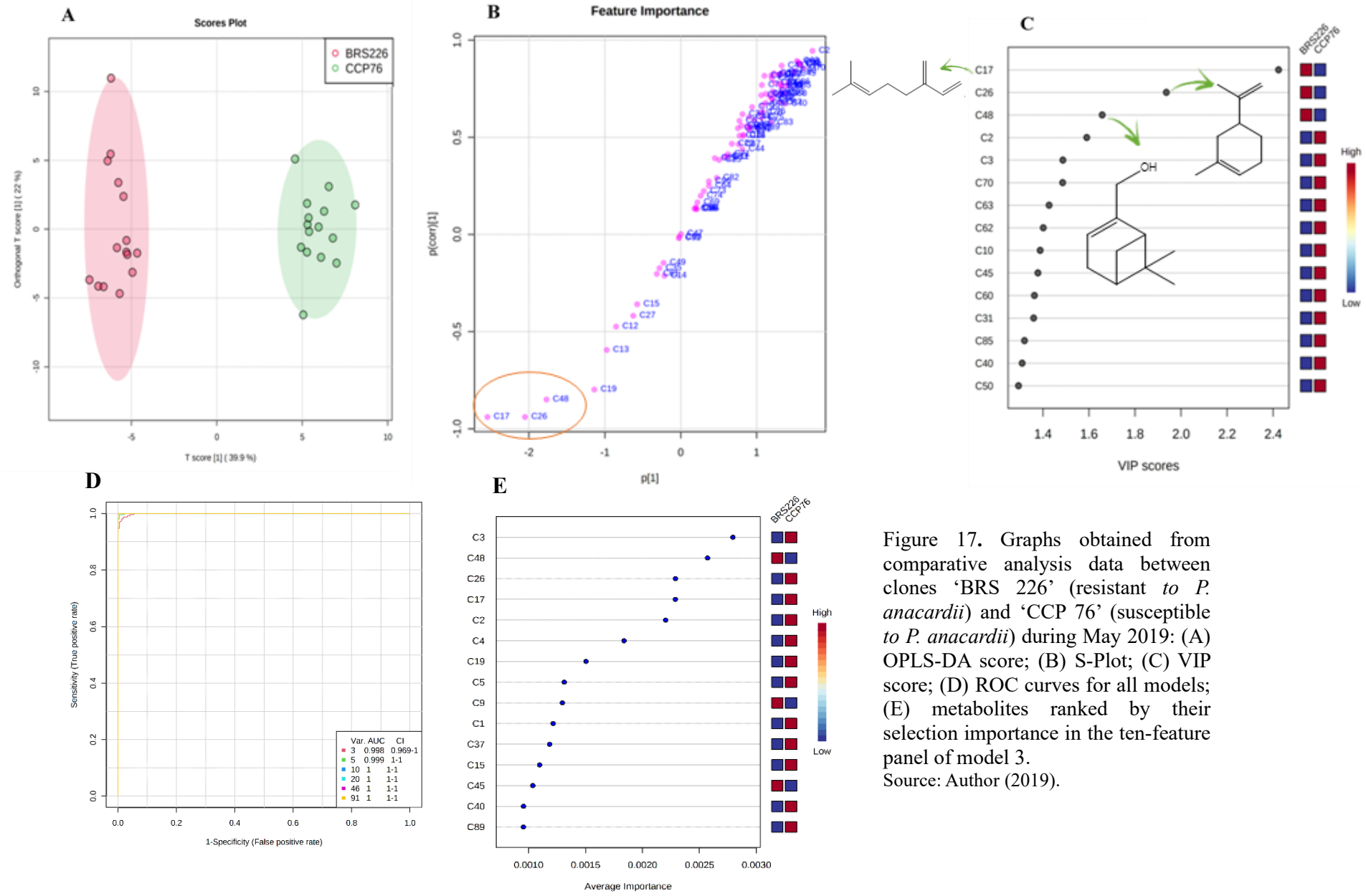

Figure 17. Graphs obtained from comparative analysis data between clones 'BRS 226' (resistant *to P. anacardii*) and 'CCP 76' (susceptible *to P. anacardii*) during May 2019: (A) OPLS-DA score; (B) S-Plot; (C) VIP score; (D) ROC curves for all models; (E) metabolites ranked by their selection importance in the ten-feature panel of model 3.
Source: Author (2019).

Analysis of the profile of volatile organic compounds of clone BRS 265 (resistant to P. anacardii) during the months of infestation and non-infestation

The PLS-DA graph for BRS 265 clone revealed a separation between the samples over the five months of analysis (FIGURE 18a) and showed the difference in the profile of VOCs of the clone according to the presence or absence of disease. The PLS-DA loading graph (FIGURE 18b) showed that the compounds (*E*)-hex-2-enal, (2), (*Z*)-hex-3-en-1-ol (3), (*Z*)-hex-2-en-1-ol (4), (*E*)-hex-2-en-1-ol (5), hexan-1-ol (6), α-pinene (11), β-cis-ocimene (27), and β-*trans*-ocimene (28) were responsible for the separation of the samples according to the different months of analysis.

Compounds present in the VIP (FIGURE 18c) include those already reported in the literature for cashews, such as (*E*)-hex-2-enal, (2), α-pinene (11), β-*cis*-ocimene (27), α-copaene (54), γ-muurolene (78), and valencene (84) (LIU et al., 2020b), with high concentrations in May and a decrease in June and July; therefore, they are potential response biomarkers to attack by the phytopathogen that causes black mold. These compounds have been reported in the literature for their antimicrobial activity (IIJIMA, 2014; MNEIMNE et al., 2016; SMERIGLIO et al., 2019).

The generated heatmap (Figure S5, SI section) for the BRS 265 clone shows that many compounds had their concentration increased in May and maintained high concentrations in June and July, an interesting fact since this clone has already been reported in the literature as being more resistant to black mold when compared to CCP 76, BRS 189 and BRS 226 (LIMA et al., 2019a). Hexanal (1), (*E*)-hex-2-enal, (2), hex-4-en-1-ol (7), α-pinene (11), octan-3-one (18), δ-3-carene (21), β-*cis*-ocimene (27), terpinolene (31), (*Z*)-hex-3-en-1-ol, propanoate (32), (*E*)-hex-2-en-1-ol, propanoate (33), *p*-mentha-1,3,8-triene (34), α-ylangene (53), β-cubebene (55), β-bourbonene (56), valencene (84), and γ-cadinene (89) may be associated with resistance of the BRS 265 clone against the pathogen. These compounds have already been reported in the literature for cashew trees leaf and fruit (DZAMIC et al., 2009; CARDOSO et al., 2010; DE AQUINO; ARAÚJO; SILVEIRA, 2017; SALEHI et al., 2019 SMERIGLIO et al., 2019; LIU et al., 2020).

Figure 18. (A) Partial Least Squares Discriminant Analysis (PLS-DA) score and (B) loading, and (C) graph of Variables of Importance in Projection (VIP) constructed with the volatile compounds identified in the ‘BRS 265’ clone from May to July.

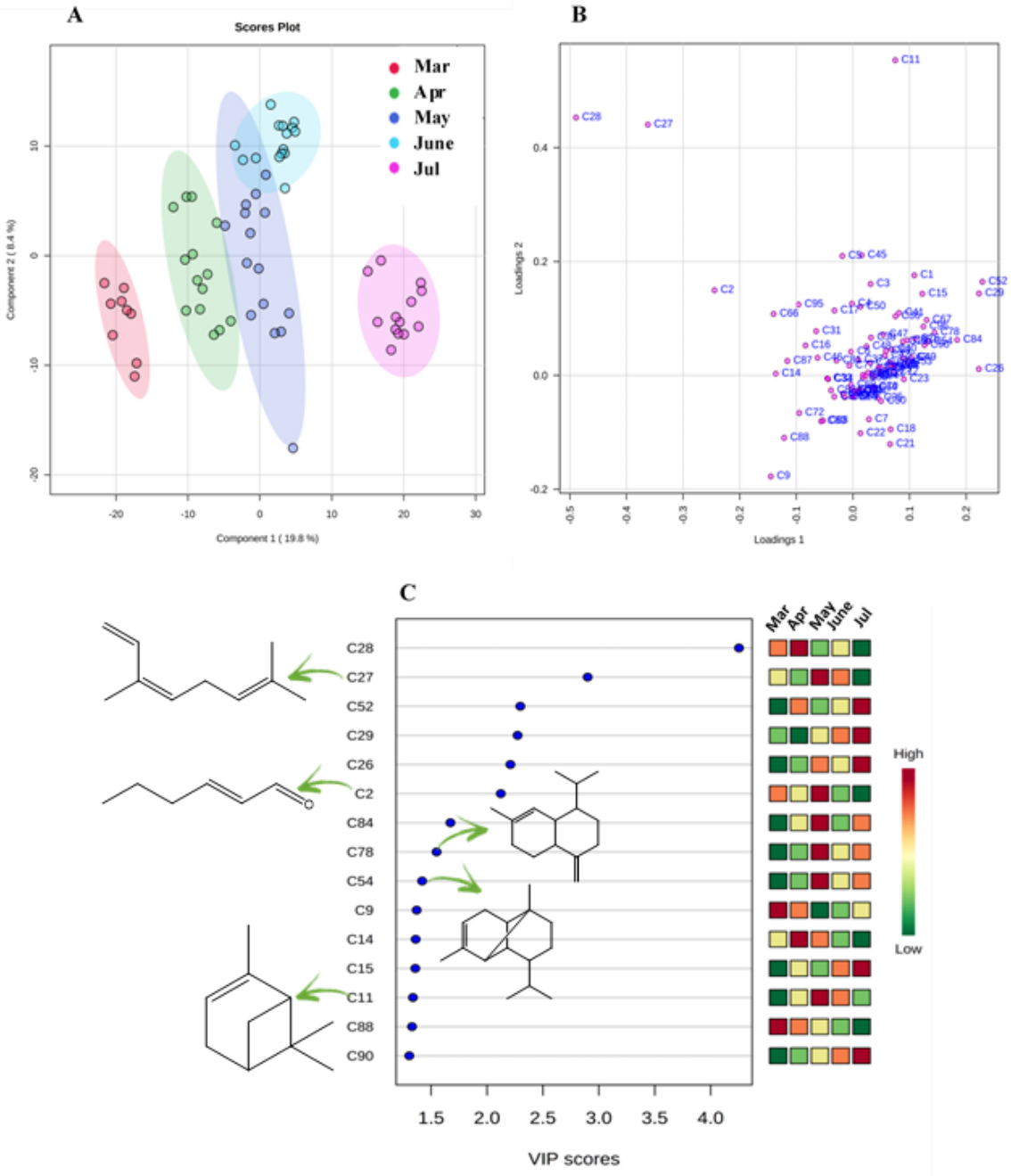

Source: Author (2019).

Comparative analysis of the volatile compound profiles of clones BRS 265 (resistant to P. anacardii) vs. BRS 189 (susceptible to P. anacardii)

Hierarchical clustering analysis (HCA) (Figure S6a, SI section) was constructed based on the chemical profile data of VOCs biosynthesized by BRS 265 and BRS 189 clones from March to July, showed a clear separation between them. This corroborates the hypothesis that the resistance of certain clones involves the biosynthesis of volatile organic compounds that assist in pathogen resistance (PONZIO et al., 2013).

Partial least squares discriminant analysis (PLS-DA), where the 2D score graph (Figure S6b, SI section) explains 35.4% of the total variance. It corroborates the results obtained in the HCA regarding the segregation of the samples, and it is possible to verify that samples from BRS 189 are located in the negative quadrant of component 2. The samples from clone BRS 265 are in the positive quadrant of the same component. The PLS-DA loading graph (Figure S6c, SI section) shows the influence of variables on the samples and highlights some metabolites that were responsible for separating the groups over the months, being (Z)-hex-3-en-1-ol (3), (*Z*)-hex-2-en-1-ol (4), (*E*)-hex-2-en-1-ol (5), and (*Z*)-butanoic acid, 3-hexenyl ester (45) (SALEHI et al., 2019; LIU et al., 2020b) the main discriminants of the resistant clone samples (BRS 265) in relation to the susceptible one (BRS 189).

The volatile metabolite profiles for May of both clones were compared to identify candidate biomarkers for resistance to *P. anacardii*. The OPLS-DA score graph (FIGURE 19a) explains 51.2% of the total variance and suggests that the clones behave differently in terms of biosynthesis and emission of volatile organic compounds in response to infection *by P. anacardii*. The values of the quality parameters for the models R2Y = 0.930 and Q2 = 0.911 suggest that there is a statistically significant difference between the metabolic profiles of the samples.

The S-plot dispersion graph (FIGURE 19b) shows, on the negative axis, the compounds responsible for the discrimination of the susceptible clone (BRS 189), while on the positive axis there are the metabolites related to the resistant clone (BRS 265), all highlighted by a red circle.

The VIP score (FIGURE 19c) contains molecules already reported in the literature with antimicrobial activity (DA SILVA et al., 2012; MNEIMNE et al., 2016), such as α-pinene (11), oct-1-en-3-ol (16), β-*cis*-ocimene (27), chrysantenone (36), methyl salicylate (47), and α-copaene (54), which were more abundant in the samples of the resistant clone in May, corroborating the data presented by the S-Plot analysis. Thus, these compounds are highlighted

as candidates for resistance biomarkers of the BRS 265 clone when compared with the susceptible BRS 189 clone.

The construction of the ROC curve (FIGURE 19d) allowed corroborating the presence of the compounds α-pinene (11), β-*cis*-ocimene (27), chrysantenone (36), and α-copaene (54) (FIGURE 19e) already highlighted by the VIP in the pathogen-resistant clone. In addition to confirming these compounds, p-mentha-3,8-diene (30), (4*E*,6*Z*)-alloocimene (38), *neo*-*allo*-ocimene (40), and (*Z*)-2-hexenyl butyrate (42) are also highlighted.

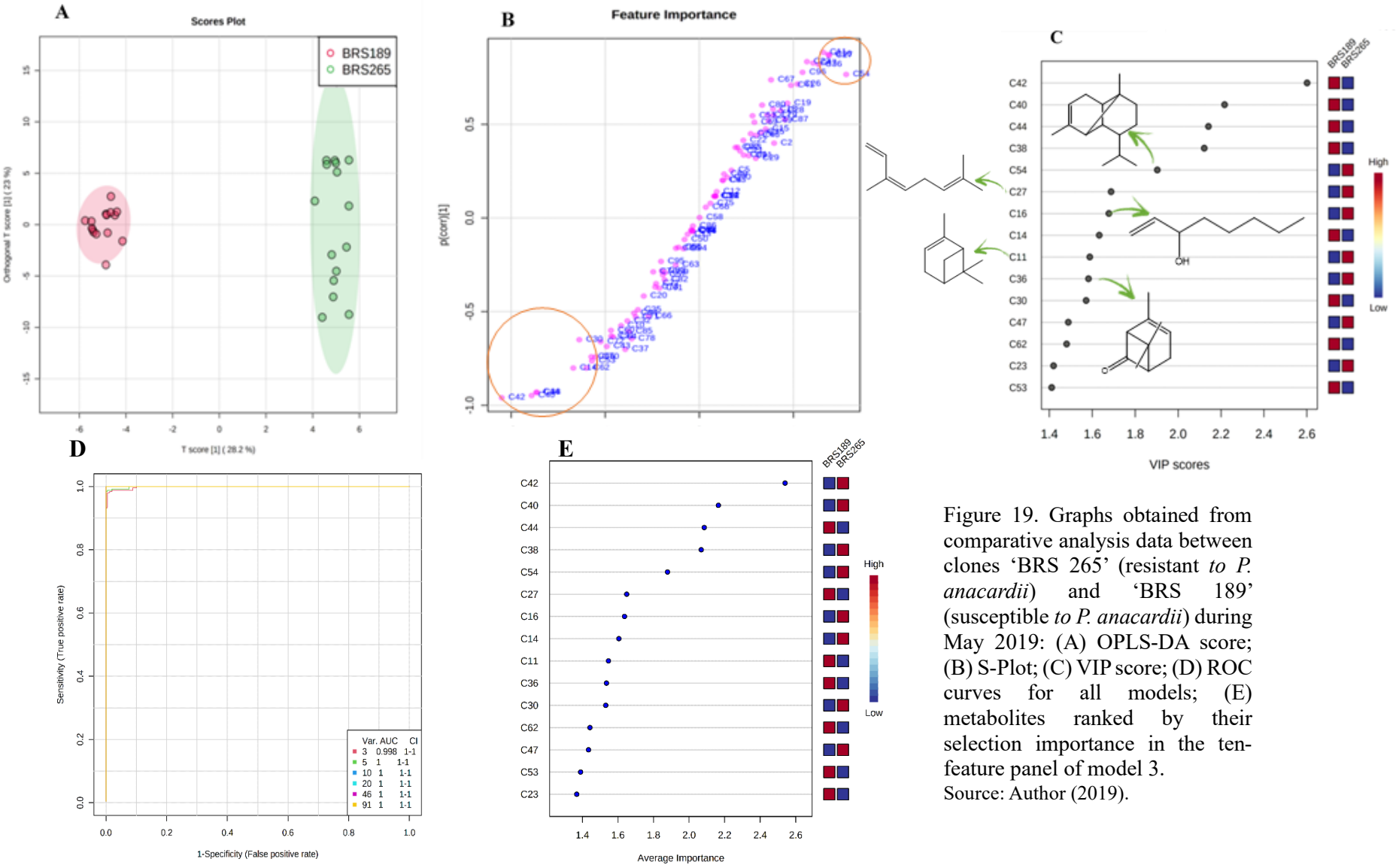

Figure 19. Graphs obtained from comparative analysis data between clones 'BRS 265' (resistant *to P. anacardii*) and 'BRS 189' (susceptible *to P. anacardii*) during May 2019: (A) OPLS-DA score; (B) S-Plot; (C) VIP score; (D) ROC curves for all models; (E) metabolites ranked by their selection importance in the ten-feature panel of model 3.
Source: Author (2019).

Comparative analysis of the volatile compound profiles of BRS 265 clones (resistant to P. anacardii) vs. CCP 76 (susceptible to P. anacardii)

The HCA results (Figure S7a, SI section) showed differences between the profiles of VOCs emitted by the two clones over the five months of analysis because it was possible to observe the clear separation of samples from both clones into two large groups from March to July.

The PLS-DA score (Figure S7b, SI section) confirmed the separation observed in the HCA. In negative values of component 2, there are samples related to clone BRS 265, and in positive values of the same component, there are samples from CCP 76. The samples for March and April of both clones were found in the negative part of component 1. However, the samples for May, June, and July are located in the positive part of component 1. This fact shows that an increase in the disease severity leads to a similar volatile pattern, indicating the biosynthesis of metabolites that can defend them from the attack of the pathogen. The PLS-DA loading graph (Figure S7c, SI section) highlights that the discrimination biomarkers include *neo*-*allo*-ocimene (40), (*E*)-butanoic acid, 2-hexenyl ester (42) (SALEHI et al., 2019; LIU et al., 2020) for the CCP 76 clone and, in relation to BRS 265, the compounds β-myrcene (17), and chrysantenone (36).

OPLS-DA models were built to identify VOCs responsible for the differentiation of both clones in May. The OPLS-DA score graph (FIGURE 20a) explains 46.7% of the total variance and shows that the clones behave differently in the biosynthesis and emission of metabolites in response to black mold. The values of the quality parameters for the model were satisfactory: $R^2Y = 0.976$ and $Q^2 = 0.961$, suggesting that there was a statistically significant difference between the metabolic profiles of the samples analyzed.

The S-plot dispersion graph (FIGURE 20b) shows which variables were responsible for the separation between the groups observed in the score graph. The compounds responsible for the discrimination of the resistant clone (BRS 265) are located on the negative axis, while on the positive axis there are metabolites related to the susceptible clone (CCP 76).

The VIP score (FIGURE 20c) corroborate the results obtained in the OPLS-DA S-Plot, which presents VOCs already reported in the literature with antimicrobial activity (KIRCHNER et al., 2010; GIWELI et al., 2012; ISMAIL et al., 2013; FALAHATI et al., 2015; HRISTOVA et al., 2015). Terpenes and esters derivatives, such as α-pinene (11), pseudolimonene (19), sylvestrene (26), β-*cis*-ocimene (27), methyl salicylate (47), *cis*-3-

hexenyl isovalerate (49), α-copaene (54), acoradien (73), germacrene D (80) and germacrene B (96) were the most abundant in the samples of the resistant clone BRS 265 in May and were highlighted as biomarkers candidates for its resistance of the BRS 265 clone when compared with the susceptible clone (CCP 76).

Through the analysis of the ROC curve (FIGURE 20d) it is possible to corroborate the compounds highlighted by the analysis of VIP scores, and the compounds (*E*)-hex-2-en1-ol (5), β-*trans*-ocimene (28), (*Z*)-butanoic acid, 3-hexenyl ester (45) and acoradien (73) as present in samples from the resistant clone compared to the susceptible clone (FIGURE 20e).

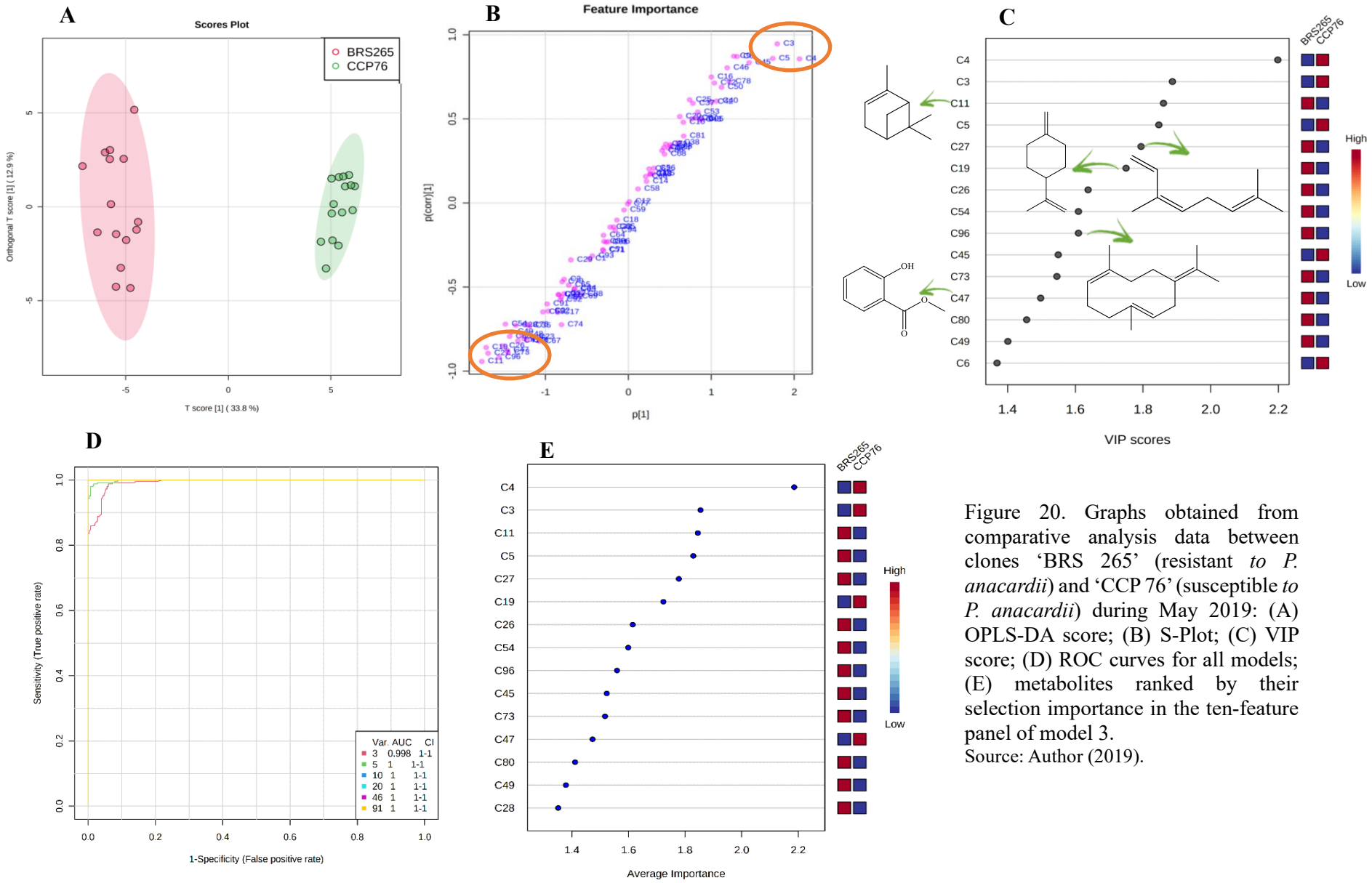

Figure 20. Graphs obtained from comparative analysis data between clones 'BRS 265' (resistant *to P. anacardii*) and 'CCP 76' (susceptible *to P. anacardii*) during May 2019: (A) OPLS-DA score; (B) S-Plot; (C) VIP score; (D) ROC curves for all models; (E) metabolites ranked by their selection importance in the ten-feature panel of model 3.
Source: Author (2019).

Analysis of the profile of volatile compounds from the BRS 189 clone (susceptible to P. anacardii) during the months of infestation and non-infestation

The PLS-DA graph (FIGURE 21a) shows differences in the profile of VOCs emitted by the leaves of the BRS 189 clone in each month of analysis. Samples related to May formed a group that hardly intercepted the sample groups from other months. This fact is interesting when correlated with the observations made in the field, since in May, the plants were under conditions of greater infestation of the pathogen; therefore, their metabolic response tends to be different, aiming at their defense against biotic stress.

On the other hand, the sample groups in March and April showed a cross between each other, suggesting some similarity in the metabolic profile in these months. In addition, according to observations made in the field in March and April, the presence of the pathogen was already observed but without much severity, with the beginning of the infection attributed to that period. In June, there was a sharp drop in disease severity, so the profile of the metabolites was similar, in part, to that observed in July, when there were milder symptoms.

The PLS-DA loading graph (FIGURE 21b) suggests that VOCs are responsible for separating samples into groups, including (*Z*)-hex-3-en-1-ol (3), (*Z*)-hex-2-en-1-ol (4), (*E*)-hex-2-en-1-ol (5), hexan-1-ol (6), oct-1-en-3-ol (16), and guaia-1(10),11-diene (87), all of which have already been reported in the literature for the species *occidentale* (SALEHI et al., 2019a).

According to the VIP (FIGURE 21c), 3-octanone (18), (4*E*,6*Z*)-*allo*-ocimene (38), *cis*-pinocamphone (44), and α-ylangene (53) (LIU et al., 2020) contributed the most to the description of variables in May.

The heatmap (Figure S8, SI section) constructed based on the Euclidean distance measurement with the profile of volatile metabolites biosynthesized from March to July by the BRS 189 clone showed that there are differences in the plant metabolome according to the presence and absence of the pathogen. The metabolites α-thujene (10), octan-3-one (18), and terpinolene (31) (PAPAGEORGIOU; ASSIMOPOULOU; YANNOVITS-ARGIRIADIS, 1999; MONTANARI et al., 2012; BORTOLUCCI et al., 2018; SALEHI et al., 2019) showed a significant increase in concentration in May, which coincides with the period of increase in the severity of the disease in the field.

Figure 21. (A) Partial Least Squares Discriminant Analysis (PLS-DA) score and (B) loading, and (C) graph of Variables of Importance in Projection (VIP) constructed with the volatile compounds identified in the ‘BRS 189’ clone from March to July.

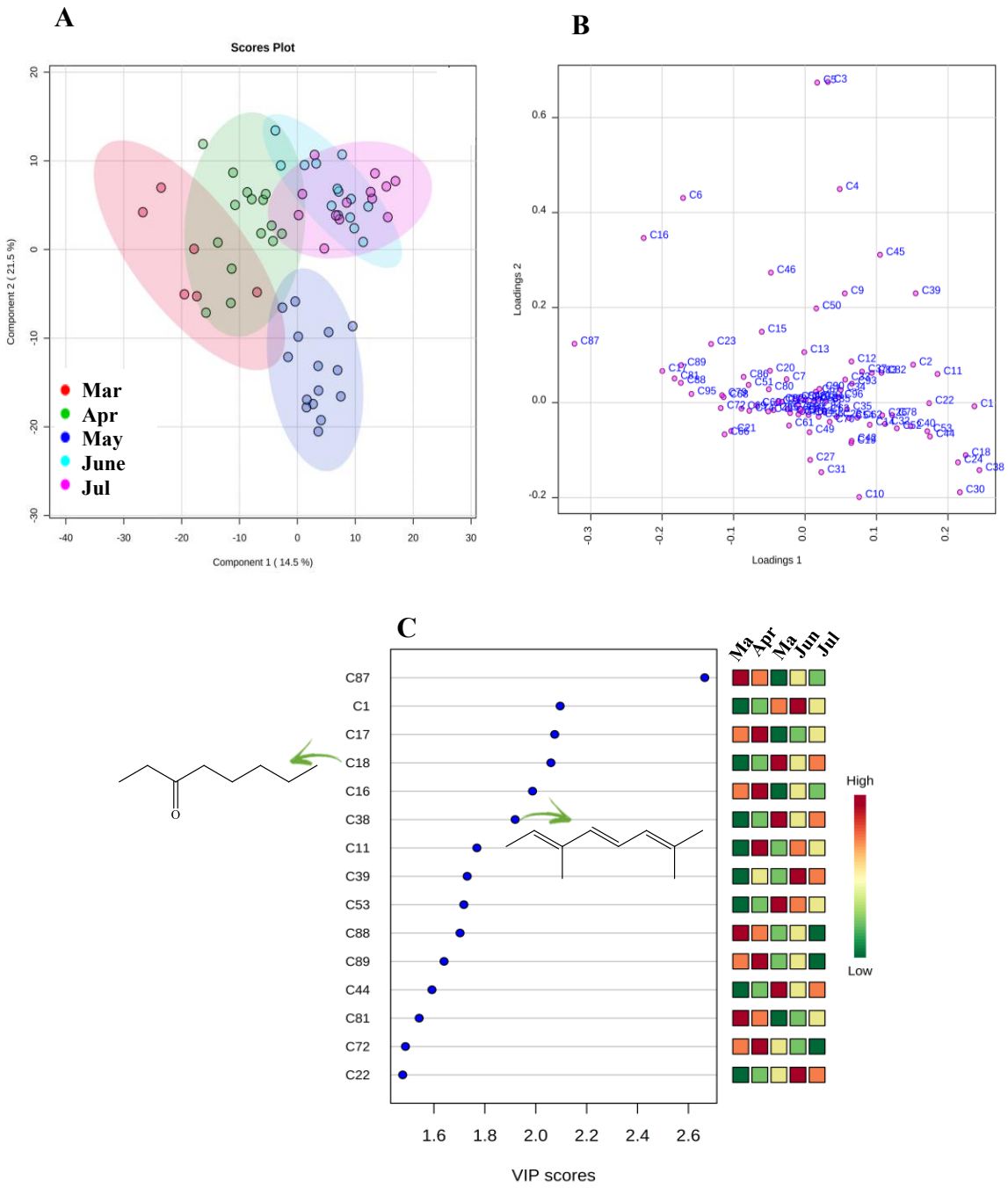

Source: Author (2019).

Analysis of the volatile compound profile of the CCP 76 clone (susceptible to P. anacardii) during months of infestation and non-infestation

The discrimination between the samples of the CCP 76 clone over the months of analysis was verified through the construction of a PLS-DA score graph (FIGURE 22a). PLS-DA loading (FIGURE 22b) showed that separation of the monthly profiles occurred because of the presence of (*E*)-hex-2-enal (2), (*Z*)-hex-3-en-1-ol (3), (*Z*)-hex-2-en-1-ol (4), (*E*)-hex-2-en-1-ol (5), hexan-1-ol (6), (*E,E*)-2,4-hexadienal (9), α-thujene (10), α-pinene (11), oct-1-en-3-ol (16), octan-3-one (18), α- phellandrene (20), o-cymene (25), (*Z*)-butanoic acid, 3-hexenyl ester (45), α-terpineol (46), and *cis*-3-hexenyl valerate (50).

The VIP (FIGURE 22c) highlights that (*Z*)-hex-3-en-1-ol (3), octan-3-one (18), α-phellandrene (20), and valencene (84) (KOSSOUOH et al., 2008; SALEHI et al., 2019) had higher concentrations in May, suggesting a relationship with a plant defense mechanism in the face of most diseases.

The heatmap (Figure S9, SI section) shows that compounds (*E*)-hex-2-enal (2), (*Z*)-hex-3-en-1-ol (3), (*Z*)-hex-2-en-1-ol (4), (*E*)-hex-2-en-1-ol (5), hexan-1-ol (6), hex-4-en-1-ol (7), (*E,E*)-2,4-hexadienal (9), 1-octen 3-ol (16), octan-3-one (18), o-cymene (25), (*Z*)-butanoicacid, 3-hexenyl ester (45), α-terpineol (46), cis-valerate -3-hexenyl (50), and γ-muurolene (78) showed an increase in concentration in May. Many of these metabolites have been reported in the literature for the Anacardiaceae family (MAIA; ANDRADE; ZOGHBI, 2000b; DEVECI et al., 2010; SOSA-MOGUEL et al., 2018; SALEHI et al., 2019).

The metabolites highlighted by the VIP and heatmap graphics can be associated with a plant defense system when the occurrence of the disease becomes more severe (CALO et al., 2015a). The compounds highlighted for the CCP 76 clone have already been reported in the literature for *A. occidentale* (CEVA-ANTUNES et al., 2006; GEBARA et al., 2011; CHAGAS-PAULA et al., 2015b; LIU et al., 2020); therefore, they provide support for the fact that these compounds are products of the plant metabolism and not of the microorganism, and can therefore act together as a system of an attempt to defend plants against phytopathogen attack, especially in times of increased disease severity.

Figure 22. (A) Graphs of PLS-DA score, (B) loading, and (C) VIP score from the analyses during the months of March to July 2019 for the ‘CCP 76’ clone.

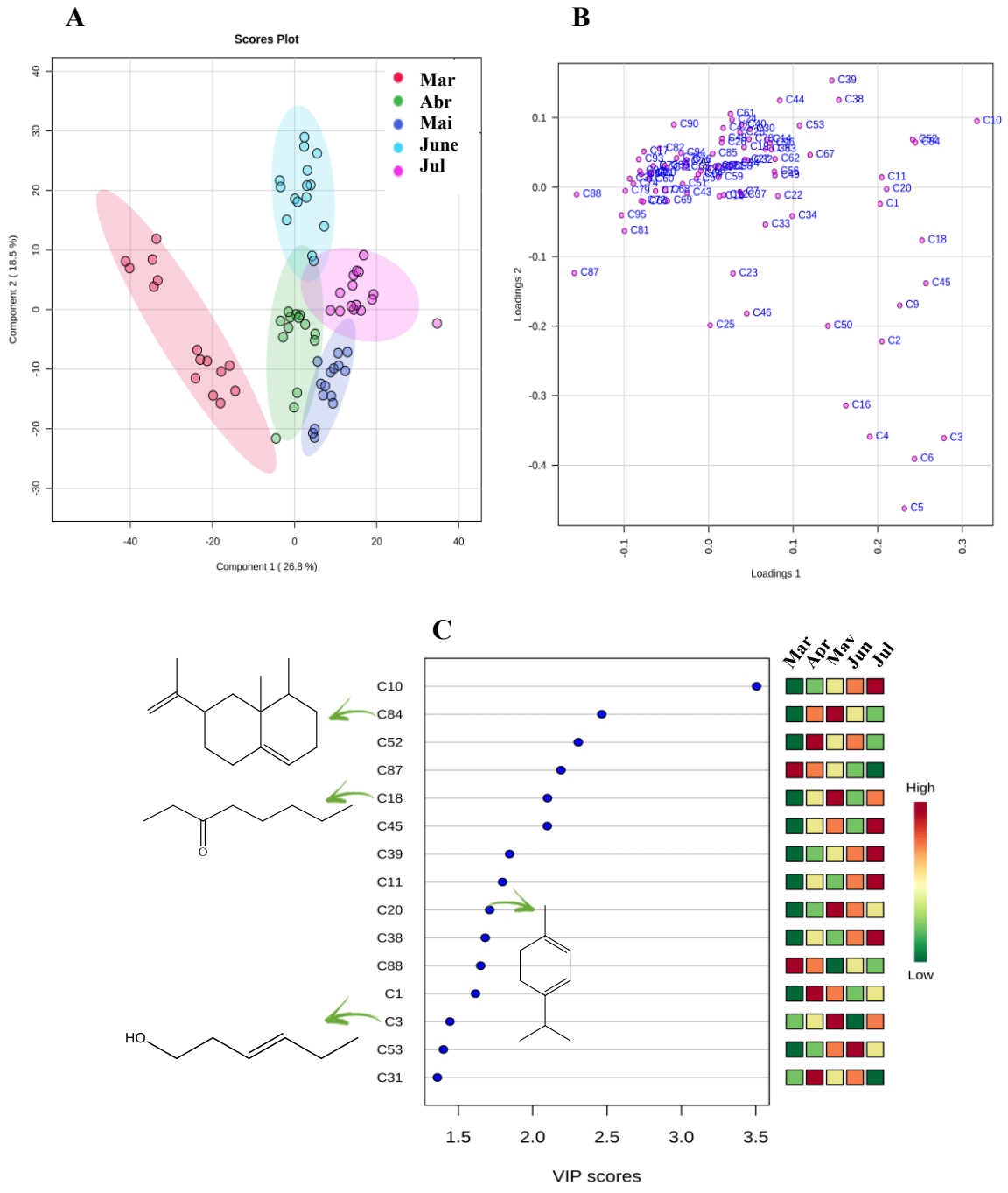

Source: Author (2019).

Discussion

The variety of VOCs emitted by plants is directly relatedto the environment to which they are subjected to biotic and abiotic stresses (CALO et al., 2015). They also act as the

expression or silencing of defense genes. This allows plants to interact with each other under natural conditions in the field (DOS SANTOS et al., 2019). Interactions between VOCs can potentiate the antimicrobial effects of the compounds when analyzed individually through a process of synergism (DOS SANTOS et al., 2019).

VOCs commonly exhibit antimicrobial activity due to the presence of various classes of compounds, such as terpenes, alcohols, acids, esters, aldehydes, ketones, amines, among others (CALO et al., 2015). The antimicrobial activity of the constituents of a complex set of volatile metabolites is generally not attributed to a specific compound, since the synergistic effect must be taken into account. Indeed, certain compounds can modulate the antimicrobial effects of others (BAJPAI; BAEK; KANG, 2012). One of the mechanisms of action of volatiles oils as antimicrobial agents is the ability of their constituents to penetrate the cells of microorganisms through the cell membrane and inhibit the cell's functional properties (BAJPAI; BAEK; KANG, 2012).

Volatile compounds such as aldehydes, alcohols, and esters of the six carbon atoms biosynthesized by leaves from higher plants are known as green leaf volatiles (GLVs). They are reported in the literature as important compounds in the defense and signaling mechanisms of plants against attack by herbivores, bacteria, and phytopathogenic fungi, in addition to being involved in communication processes between plants (TANAKA et al., 2018). Under normal conditions, plants biosynthesize these compounds; however, under stress conditions, including those caused by the presence of phytopathogens, this biosynthesis occurs more quickly (KISHIMOTO et al., 2008; PONZIO et al., 2013; AMEYE et al., 2018). GLVs are biosynthesized through the enzymatic pathway of lipoxygenase (LOX), which relies on the performance of various enzymes that convert lipid substrates into defense molecules (VINCENTI et al., 2019). Figure S10 (SI section) illustrates this biosynthetic pathway for the production of C6 aldehydes and alcohols (UL HASSAN; ZAINAL; ISMAIL, 2015).

It was possible to observe, for the samples referring to the plants of the clones resistant to *P. anacardii*, the biosynthesis of short-chain aldehydes and alcohols, especially in the month of the greatest occurrence of the pathogen in the field (May). Therefore, the metabolites highlighted by the VIP, heatmap graphics and confirmed by ROC curve analysis can be associated with the defense system of the host against the pathogen (CASTRO-MORETTI et al., 2020).

Short-chain aldehydes are present in low concentrations in healthy plant leaves. However, their concentration may increase when the plant is exposed to attack by herbivores, insects, and microorganisms such as fungi (KISHIMOTO et al., 2008). This fact justifies the

increase in the concentration of these compounds in the samples of resistant clones (BRS 226 and BRS 265) during the period of infection. These compounds, which have remarkable antifungal activity, modulate plant defense responses, leading to the biosynthesis of phytoalexins. n-Hexanal and (*Z*)-3-hexenal are biosynthesized through the cleavage of 13-hydroperoxides from linoleic and linolenic acids catalyzed by hydroperoxide lyase (HPL), whereas (*Z*)-3-hexenal can easily be converted into its (*E*)-2-hexenal isomer, which also has antimicrobial activity (KISHIMOTO et al., 2008). The biosynthesis of these compounds by plants attacked by fungi is reported to be responsible for inducing greater resistance in the host in the face of attack by phytopathogens (UL HASSAN; ZAINAL; ISMAIL, 2015).

The biosynthesis of C6 alcohols is related to the response of the plant in an attempt to prevent the entry of the pathogen into plant cells (SCALA et al., 2013; LÓPEZ-GRESA et al., 2017). The BRS 226 clone is reported in the literature to be less affected by *P. anacardi*, thus the biosynthesis of compounds (*Z*)-hex-3-en-1-ol (3), (*Z*)-hex-2-en-1-ol (4), (*E*)-hex-2-en-1-ol (5), and hexan-1-ol (6), observed, especially in May, corroborates the fact that the plants of this clone emit a chemical response in order to defend themselves against the attack of the fungus, which may contribute to confer resistance to the pathogen.

Regarding the antimicrobial activity of volatile compounds, it is necessary to highlight the importance of the effects that may arise from the interaction between them. These effects can be additive, antagonistic or synergistic and depend on the concentration and number of compounds emitted by the plant (DOS SANTOS et al., 2019). Thus, some compounds highlighted for the susceptible clones according to the VIP have reports of antimicrobial activity, however, the fact that the BRS 189 and CCP 76 clones are more affected by *P. anacardii* than BRS 226 and BRS 265 clones may be due to the insufficient concentration of these compounds to guarantee the protection of the plants. Another possibility is the antagonistic effect provoked by the interaction of these emitted compounds; that is, the isolated compounds present activity; however, their mixture does not present significant activity.

Concerning the resistant clone, BRS 265, similar to what was observed for BRS 226, there was an increase in the biosynthesis of compounds such as hexanal (1), (*E*)-hex-2-enal, (2), hex-4-en-1-ol (7), can be associated with the defense mechanism of plants that do so in an attempt to prevent the microorganism from penetrating its cellular structure (SCALA et al., 2013).

In addition to C6 aldehydes and alcohols, compounds that include terpenes, such as α-pinene, δ-3-carene, β-myrcene, methyl salicylate, β-cis-ocimene, terpinolene, and α-copaene, also stood out in the investigated samples of cashew clones resistant to *P. anacardii* and may

therefore be biomarker candidates for resistance by these plants in black mold. Studies have reported that oils rich in these compounds show significant antifungal activity (POWERS et al., 2018).

Terpenes are compounds that are biosynthesized by plants and have various functions, such as attracting pollinators and herbivore predators, in addition to being responsible for the defense response of plants against phytopathogens, highlighting, in this aspect, monoterpenes (RAMAK et al., 2014). In which many isoprenoids can be biosynthesized from damaged tissues through the activation of defense genes, aiming to protect the plant from the penetration of the pathogen in its cells (KISHIMOTO et al., 2005; MIHAI; POPA, 2015; HAQUE et al., 2016). The variety and concentration of terpenes are decisive factors for the success of the antimicrobial activity of a set of volatile compounds emitted by plants (MIHAI; POPA, 2015). Thus, the effects that the interaction between the compounds can cause, which can be additive, antagonistic, or synergistic, must be considered (IIJIMA, 2014).

The diversity in the structure of monoterpenes is related to the types of cations that are produced during the process of biosynthesis of these compounds from geranyl pyrophosphate (GPP) and linalyl pyrophosphate (LPP) and neryl pyrophosphate (NPP) isomers. (MAHIZAN et al., 2019a). Monoterpenes can be cyclic or acyclic, whereas monoterpenoids originate through biochemical reactions that give them the functions of esters, alcohols, ethers, aldehydes, and ketones. The monoterpene precursors are isopentenyl diphosphate (IPP) and its allylic isomer dimethylallyl diphosphate (DMAPP). The two possible biosynthetic pathways for the synthesis of IPP and DMAPP are the methyl-erythritol-4-phosphate (MEP) and acetate-mevalonate (MVA) pathways (DORTA et al., 2014; HAQUE et al., 2016; MAHIZAN et al., 2019).

The biosynthesis of cyclic monoterpenes such as α-pinene occurs through the formation of a linear acyclic intermediate from the isomerization of the initial geranyl diphosphate cation. Cycling produces an α-terpinyl cation, which undergoes secondary cycling. The biosynthesis of acyclic monoterpenes, such as myrcene and β-cis-ocimene, also involves isomerization of the geranyl diphosphate cation, but without cyclization processes (Figure S11, SI section) (MIHAI; POPA, 2015; HAQUE et al., 2016).

Thus, the monoterpenes highlighted at higher concentrations in the samples of resistant clones contribute to the defense of these plants against the fungus that causes black mold.

Conclusions

In this study, it was possible to observe different behaviors of VOC biosynthesis in dwarf cashew clones according to the stress caused by *P. anacardii* infestations. BRS 265 and BRS 226 showed resistance to *P. anacardii* in the analyzed periods. Chemometric analyzes for spectral data of BRS 265 allowed to identify (*E*)-hex-2-enal (2), α-pinene (11), pseudolimonene (19), sylvestrene (26), β-*cis*-ocimene (27), methyl salicylate (47), α-copaene (54), γ-muurolene (78), germacrene D (80), valencene (84), and germacrene B (96) as VOCs associated with its defense mechanism. On the other hand, (*E*)-hex-2-enal (2), (*Z*)-hex-3-en-1-ol (3), (*Z*)-hex-2-en-1-ol, (4), (*Z*)-hex-2-en-1-ol (5), hexan-1-ol (6), β-myrcene (17), α-phellandrene (20), sylvestrene (26), and myrtenol (48) are for clone BRS 226. The chemometric data also made it possible to verify that the metabolite profile of susceptible clones were similar and the compounds octan-3-one (18), (4E,6Z)-alloocimene (38), cis-pinocamphone (44) and α-ylangene (53) for clone BRS 189 and (*Z*)-hex-3-en-1-ol (3), octan-3-one (18), α-phellandrene (20), butanoic acid, 3-hexenyl ester, (*Z*)- (51) and valencene (84) for CCP 76 can be biomarkers of the presence of the pathogen. These findings suggested some VOCs involved in the host's attempt to combat the pathogen *P. anacardii* and provided an important step to carry out studies of the development of natural pesticides to protect orchards cashew trees.

Supplementary Information

Supplementary data (table about chemical composition of volatile oil of dwarf cashew trees, table about multivariate analysis, figures about heatmaps analysis, HCAs analysis, PLS-DA analysis, figures about biosynthetic path following the LOX route for the production of green leaf volatiles and biosynthesis of acyclic and cyclic monoterpenes from geranyl diphosphate, chromatograms, and mass spectra) are available free of charge at http://jbcs.sbq.org.br as PDF file.

Acknowledgments

The authors gratefully acknowledge the financial support from the National Council for Scientific and Technological Development (CNPq, Conselho Nacional de Desenvolvimento Científico e Tecnológico), National Institute of Science and Technology - INCT BioNat, grant No. 465637/2014-0, Brazil, and the Coordination for the Improvement of Higher Education

Personnel (Coordenação de Aperfeiçoamento de Pessoal de Nível Superior - CAPES, Finance Code 001).

Author Contributions

Debora B. de Sousa was responsible for methodology, formal analysis, investigation, resources, data curation, writing original draft; Gisele S. da Silva for investigation, writing review and editing; Jhonyson A. C. Guedes for investigation, writing review and editing; Luiz A. L. Serrano for conceptualization, investigation, writing review and editing; Marlon V. V. Martins for conceptualization, investigation, resources, writing review and editing; Tigressa H. S. Rodrigues for conceptualization, investigation, resources, writing review and editing; Edy S. de Brito for conceptualization, writing review and editing, supervision; Davila Zampieri for conceptualization, writing review and editing, supervision; Mary A. S. Lima for conceptualization, writing review and editing, supervision; Guilherme J. Zocolo for conceptualization, methodology, resources, writing review and editing, supervision, project administration, funding acquisition.

Supplementary Information

Figure S1. Cashew leaf showing symptoms in a more advanced stage of black mould. (Author, 2019).

Source: Author (2019).

Table S1 - Chemical composition of volatile oil of dwarf cashew trees (*to be continued*).

	Compound	RI Literature	RI Found[a]	Match[b]	R. Match[c]	Chemical Class	Molecular Formula	*m/z*	RT (min)[d]
1	hexanal	801	802	837	841	aldehyde	$C_6H_{12}O$	100.1	3.777
2	(*E*)-hex-2-enal	846	848	931	950	alcohol	$C_6H_{10}O$	98.1	4.709
3	(*Z*)-hex-3-en-1-ol	853	855	958	961	alcohol	$C_6H_{12}O$	100.1	4.728
4	(*Z*)-hex-2-en-1-ol	859	864	879	881	alcohol	$C_6H_{12}O$	100.1	4.891
5	(*E*)-hex-2-en-1-ol	854	858	804	813	alcohol	$C_6H_{12}O$	100.1	4.922
6	hexan-1-ol	863	870	836	852	alcohol	$C_6H_{14}O$	101.1	4.934
7	hex-4-en-1-ol	871	870	735	741	alcohol	$C_6H_{12}O$	100.1	4.996
8	cyclohexanol	869	873	801	820	aldehyde	$C_6H_{12}O$	100.1	5.041
9	(*E,E*)-hexa-2,4-dienal	907	918	682	842	terpene	C_6H_8O	100.1	5.854
10	α-thujene	924	930	901	923	terpene	$C_{10}H_{16}$	136.1	6.119
11	α -pinene	932	938	954	957	terpene	$C_{10}H_{16}$	136.1	6.411
12	camphene	946	951	948	963	terpene	$C_{10}H_{16}$	136.1	6.455
13	α -fenchene	945	948	835	843	terpene	$C_{10}H_{16}$	136.1	6.495
14	7-ethenylbicyclo[4.2.0]oct-1-ene	955	958	828	867	terpene	$C_{10}H_{14}$	134.1	6.698
15	β-pinene	974	981	929	930	terpene	$C_{10}H_{16}$	136.1	7.124
16	oct-1-en-3-ol	974	980	859	879	alcohol	$C_8H_{16}O$	128.1	7.136
17	β-myrcene	988	992	918	918	terpene	$C_{10}H_{16}$	136.1	7.224
18	octan-3-one	979	987	906	911	ketone	$C_8H_{16}O$	128.1	7.286
19	pseudolimonene	1003	995	798	825	terpene	$C_{10}H_{16}$	136.1	7.441

Table S1 - Chemical composition of volatile oil of dwarf cashew trees (*continuation*).

	Compound	RI Literature	RI Found[a]	Match[b]	R. Match[c]	Chemical Class	Molecular Formula	*m/z*	RT (min)[d]
20	α -phellandrene	1002	1003	915	922	terpene	$C_{10}H_{16}$	136.1	7.455
21	δ-3-carene	1008	1009	866	916	terpene	$C_{10}H_{16}$	136.1	7.643
22	δ-2-carene	1001	1007	744	744	terpene	$C_{10}H_{16}$	136.1	7.693
23	α -terpinene	1014	1017	931	937	terpene	$C_{10}H_{16}$	136.1	7.912
24	limonene	1024	1026	952	953	terpene	$C_{10}H_{16}$	136.1	7.987
25	o-cymene	1022	1026	937	943	hydrocarbon	$C_{10}H_{14}$	134.1	8.131
26	sylvestrene	1025	1031	909	921	terpene	$C_{10}H_{16}$	136.1	8.200
27	β-*cis*-ocimene	1032	1036	943	944	terpene	$C_{10}H_{16}$	136.1	8.368
28	β-*trans*-ocimene	1044	1049	912	912	terpene	$C_{10}H_{16}$	136.1	8.725
29	γ-terpinene	1054	1060	953	963	terpene	$C_{10}H_{16}$	136.1	8.800
30	*p*-mentha-3,8-diene	1068	1070	891	897	terpene	$C_{10}H_{16}$	136.1	9.032
31	terpinolene	1086	1090	931	942	terpene	$C_{10}H_{16}$	136.1	9.263
32	(*Z*)-3-hexen-1-ol, propanoate	1095	1099	804	875	ester	$C_9H_{16}O_2$	156.1	9.670
33	(*E*)-2-hexen-1-ol, propanoate	1103	1100	733	736	ester	$C_9H_{16}O_2$	156.1	9.714
34	p-mentha-1,3,8-triene	1108	1110	851	932	terpene	$C_{10}H_{14}$	134.1	9.901
36	chrysanthenone	1127	1115	634	634	terpene	$C_{10}H_{14}O$	150.1	10.007
35	*cis*-2-p-menthen-1-ol	1118	1124	897	917	alcohol	$C_{10}H_{18}O$	154.1	10.176
37	(*E,E*)-2,6-dimethyl-octa-1,3,5,7-tetraene,	1132	1129	956	967	hydrocarbon	$C_{10}H_{14}$	134.1	10.189

Table S1 - Chemical composition of volatile oil of dwarf cashew trees (*continuation*).

	Compound	RI Literature	RI Found[a]	Match[b]	R. Match[c]	Chemical Class	Molecular Formula	*m/z*	RT (min)[d]
38	(4E,6Z)-*allo*-ocimene	1128	1128	942	942	terpene	$C_{10}H_{16}$	136.1	10.346
39	limonene oxide, trans-	1137	1140	749	805	terpene	$C_{10}H_{16}O$	152.1	10.514
40	*neo*-*allo*-ocimene	1140	1141	942	942	terpene	$C_{10}H_{16}$	136.1	10.533
41	*cis*-3-hexenyl iso-butyrate	1142	1142	649	755	ester	$C_{10}H_{18}O_2$	170.1	10.577
42	2-hexenyl butyrate	1193	1191	787	789	ester	$C_{10}H_{18}O_2$	170.2	11.580
43	hexyl butanoate	1191	1194	806	838	ester	$C_{10}H_{20}O_2$	172.0	11.589
44	*cis*-pinocamphone	1172	1177	951	960	ketone	$C_{10}H_{16}O$	152.1	11.598
45	(*Z*)-butanoic acid, 3-hexenyl ester	1184	1186	939	944	ester	$C_{10}H_{18}O_2$	168.9	11.610
46	α -terpineol	1186	1191	924	925	terpene	$C_{10}H_{18}O$	152.1	11.643
47	methyl salicylate	1190	1197	875	908	ester	$C_8H_8O_3$	152.0	11.703
48	myrtenol	1194	1198	896	913	alcohol	$C_{10}H_{16}O$	152.1	11.722
49	*cis*-3-hexenyl isovalerate	1232	1231	931	938	ester	$C_{11}H_{20}O_2$	184.0	12.366
50	*cis*-3-hexenyl valerate	1279	1282	895	915	ester	$C_{11}H_{20}O_2$	184.0	13.461
51	δ-elemene	1335	1340	913	929	terpene	$C_{15}H_{24}$	204.2	14.581
52	α -cubebene	1348	1353	941	955	terpene	$C_{15}H_{24}$	204.2	14.812
53	α -ylangene	1373	1376	947	948	terpene	$C_{15}H_{24}$	204.2	15.256
54	α -copaene	1374	1376	949	952	terpene	$C_{15}H_{24}$	204.2	15.262
55	β-cubebene	1387	1384	862	877	terpene	$C_{15}H_{24}$	204.2	15.450

Table S1 - Chemical composition of volatile oil of dwarf cashew trees (*continuation*).

	Compound	RI Literature	RI Found[a]	Match[b]	R. Match[c]	Chemical Class	Molecular Formula	*m/z*	RT (min)[d]
56	β-bourbonene	1387	1391	822	833	terpene	$C_{15}H_{24}$	204.2	15.519
57	isolongifolene	1389	1396	891	905	terpene	$C_{15}H_{24}$	204.2	15.525
58	β-elemene	1389	1395	898	899	terpene	$C_{15}H_{24}$	204.2	15.537
59	sativene	1390	1396	858	863	terpene	$C_{15}H_{24}$	204.2	15.594
60	longifolene	1407	1401	873	877	hydrocarbon	$C_{15}H_{24}$	204.2	15.662
61	isocaryophyllene	1408	1411	850	862	terpene	$C_{15}H_{24}$	204.2	15.850
62	α -gurjunene	1409	1415	912	920	hydrocarbon	$C_{15}H_{24}$	204.2	15.944
63	α -cedrene	1422	1425	885	897	hydrocarbon	$C_{15}H_{24}$	204.2	15.982
64	β-cedrene	1419	1420	885	897	hydrocarbon	$C_{15}H_{24}$	204.2	16.013
65	β-gurjunene	1431	1434	897	905	hydrocarbon	$C_{15}H_{24}$	204.2	16.175
66	β-humulene	1436	1430	854	855	hydrocarbon	$C_{15}H_{24}$	204.2	16.182
67	γ-elemene	1434	1437	927	930	terpene	$C_{15}H_{24}$	204.2	16.300
68	β-copaene	1430	1436	891	891	terpene	$C_{15}H_{24}$	204.2	16.332
69	α -guaiene	1437	1442	894	897	terpene	$C_{15}H_{24}$	204.2	16.388
70	α -himachalene	1449	1447	899	903	terpene	$C_{15}H_{24}$	204.2	16.469
71	patchoulene	1454	1455	839	841	terpene	$C_{15}H_{24}$	204.2	16.638
72	neoclovene	1452	1454	864	866	terpene	$C_{15}H_{24}$	204.2	16.701
73	acoradien	1464	1463	791	810	terpene	$C_{15}H_{24}$	204.2	16.780

Table S1 - Chemical composition of volatile oil of dwarf cashew trees (*continuation*).

	Compound	RI Literature	RI Found[a]	Match[b]	R. Match[c]	Chemical Class	Molecular Formula	*m/z*	RT (min)[d]
74	(*Z*)-beta-caryophyllene	1464	1467	961	961	terpene	$C_{15}H_{24}$	204.2	16.789
75	aromadendrene	1439	1441	906	910	terpene	$C_{15}H_{24}$	204.2	16.796
76	alloaromadendrene	1458	1462	917	919	terpene	$C_{15}H_{24}$	204.2	16.838
77	γ-gurjunene	1475	1472	874	879	terpene	$C_{15}H_{24}$	204.2	16.920
78	γ-muurolene	1478	1479	950	953	terpene	$C_{15}H_{24}$	204.2	17.120
79	α -amorphene	1483	1483	933	935	terpene	$C_{15}H_{24}$	204.2	17.170
80	germacrene D	1480	1487	903	952	terpene	$C_{15}H_{24}$	204.2	17.176
81	α-muurolene	1500	1498	946	956	terpene	$C_{15}H_{24}$	204.2	17.289
82	β-selinene	1489	1492	904	916	terpene	$C_{15}H_{24}$	204.2	17.326
83	viridiflorene	1496	1494	865	889	terpene	$C_{15}H_{24}$	204.2	17.345
84	valencene	1496	1491	900	913	terpene	$C_{15}H_{24}$	204.2	17.376
85	δ-selinene	1492	1496	894	926	terpene	$C_{15}H_{24}$	204.2	17.433
86	γ-patchoulene	1502	1503	879	897	terpene	$C_{15}H_{24}$	204.2	17.545
87	guaia-1(10),11-diene	1509	1505	837	846	terpene	$C_{15}H_{24}$	204.2	17.551
88	β-bisabolene	1505	1509	867	883	terpene	$C_{15}H_{24}$	204.2	17.595
89	γ-cadinene	1513	1512	933	937	terpene	$C_{15}H_{24}$	204.2	17.683
90	β-cadinene	1518	1519	881	886	terpene	$C_{15}H_{24}$	204.2	17.708
91	δ-cadinene	1522	1522	944	948	terpene	$C_{15}H_{24}$	204.2	17.815

Table S1 - Chemical composition of volatile oil of dwarf cashew trees (*conclusion*).

	Compound	RI Literature	RI Found[a]	Match[b]	R. Match[c]	Chemical Class	Molecular Formula	*m/z*	RT (min)[d]
92	α -cadinene	1537	1536	801	802	terpene	$C_{15}H_{24}$	204.2	17.953
93	cadina-1,4-diene	1533	1533	893	894	terpene	$C_{15}H_{24}$	204.2	18.064
94	selina-3,7(11)-diene	1545	1543	897	901	terpene	$C_{15}H_{24}$	204.2	18.146
95	guaia-3,9-diene	1556	1556	801	823	terpene	$C_{15}H_{24}$	204.2	18.334
96	germacrene B	1569	1565	873	914	terpene	$C_{15}H_{24}$	204.2	18.609

[a]RI: retention index; [b]Match: it is a correspondence factor between the spectrum of the analyzed compound and the spectrum of the library NIST (direct match); [c]R. Match: it is a match factor for the unknown and the library spectrum ignoring any peaks in the unknown that are not in the library spectrum (reverse search); [d]RT: retention time (minutes).

Table S2 - Multivariate analysis of partial least squares discriminant analysis (PLS-DA) and orthogonal partial least squares discriminant analysis (OPLS-DA) models from different groups for the metabolic profile of cashew clones against black mold.

Model	Type	R^2Y	Q^2
'BRS 226'	PLS-DA	0.964	0.909
'BRS 226' *vs* 'BRS 189'	PLS-DA	0.952	0.901
	OPLS-DA	0.886	0.869
'BRS 226' *vs* 'CCP 76'	PLS-DA	0.957	0.922
	OPLS-DA	0.830	0.806
'BRS 265'	PLS-DA	0.986	0.965
'BRS 265' *vs* 'BRS 189'	PLS-DA	0.958	0.907
	OPLS-DA	0.930	0.911
'BRS 265' vs 'CCP 76'	PLS-DA	0.965	0.932
	OPLS-DA	0.976	0.961
'CCP 76'	PLS-DA	0.971	0.919
'BRS 189'	PLS-DA	0.953	0.810

Figure S2. Heatmap graph constructed based on the volatile compounds identified in the leaf samples of the 'BRS 226' clone over the months of March to July 2019. In the scale, the red color represents the compounds with a higher relative abundance and the blue color represents the compounds with lower relative abundance and the class refers to the months of study. Analyzes performed in triplicate samples.

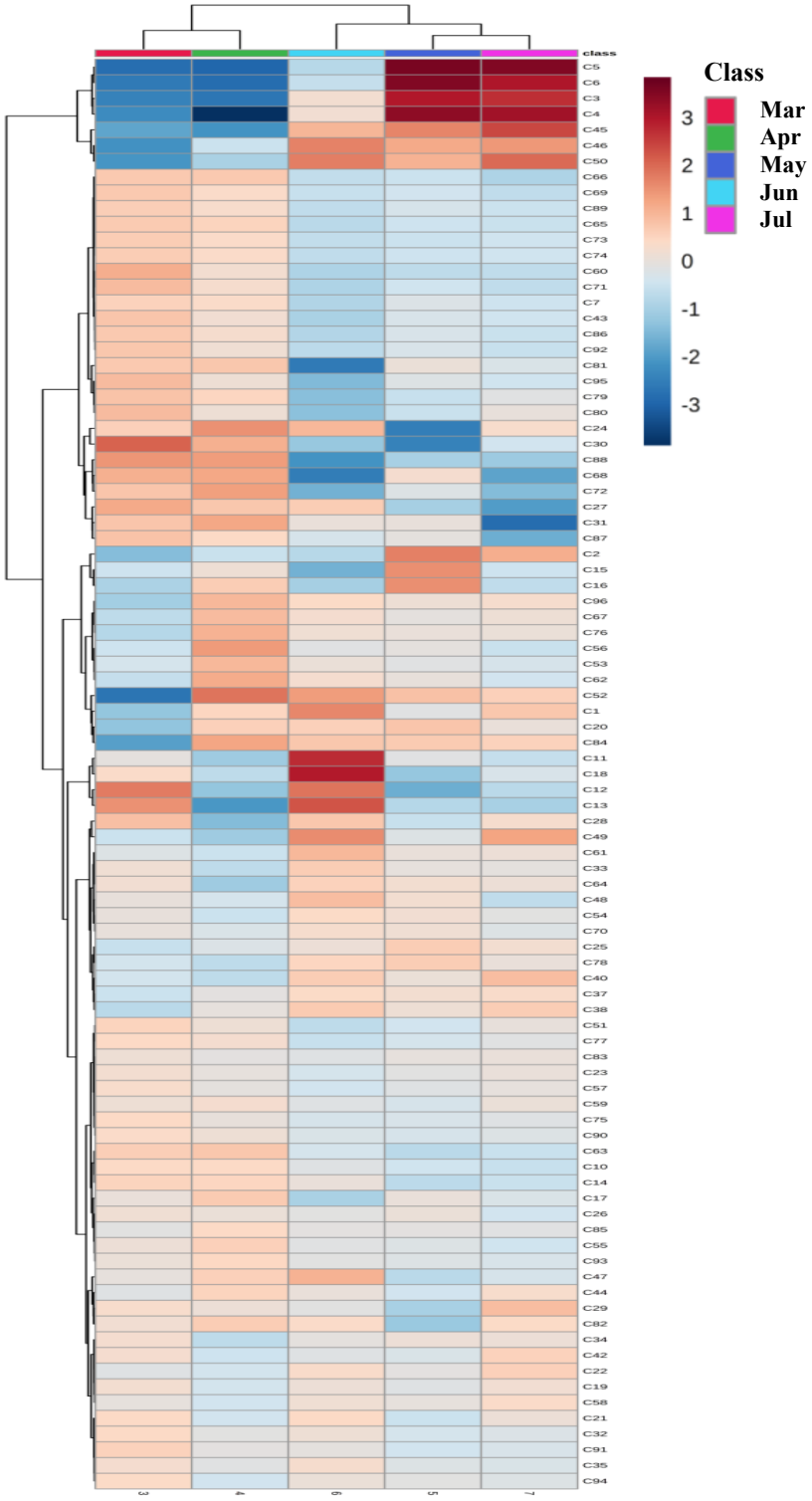

Source: Author (2019).

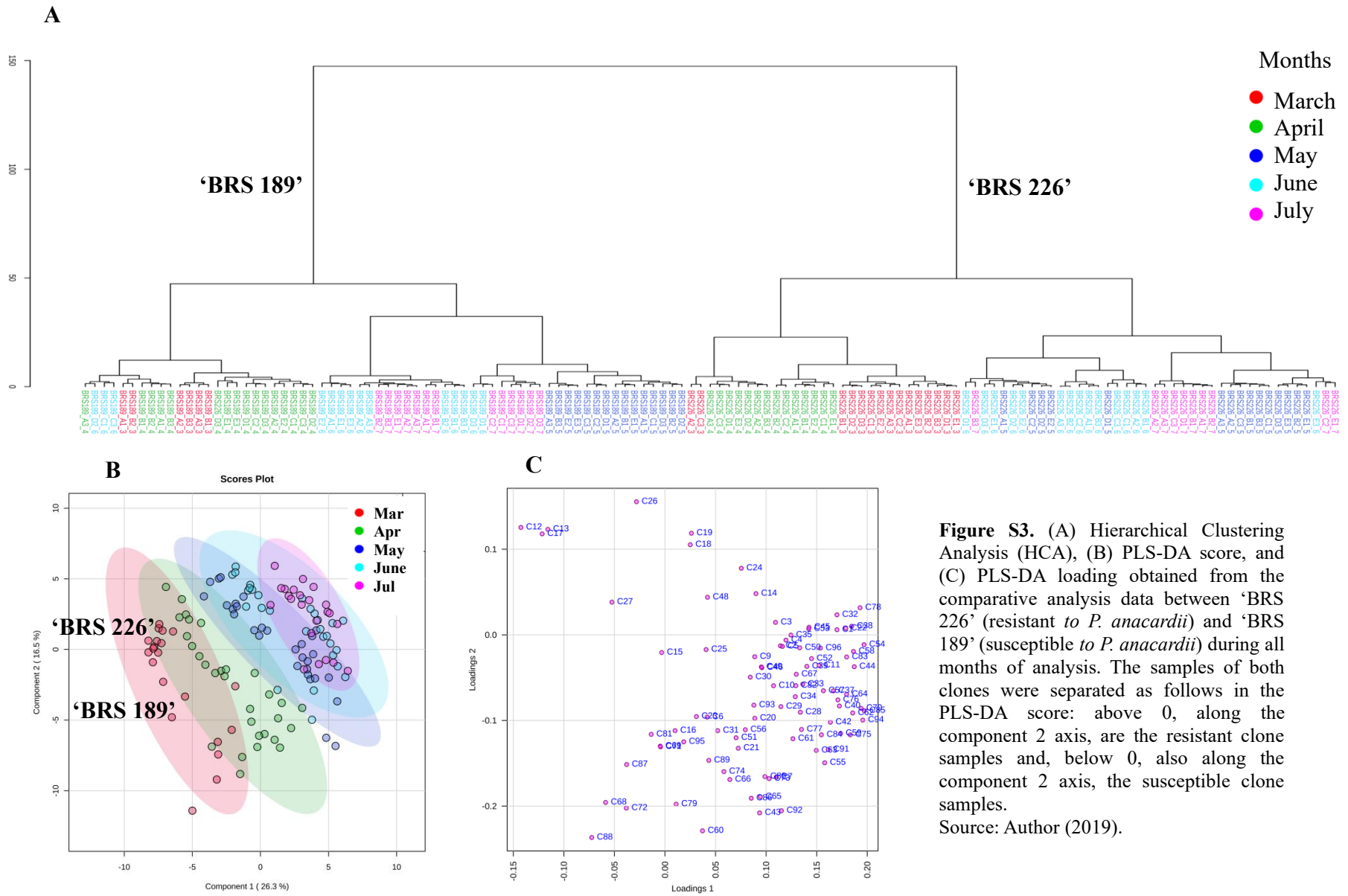

Figure S3. (A) Hierarchical Clustering Analysis (HCA), (B) PLS-DA score, and (C) PLS-DA loading obtained from the comparative analysis data between ‘BRS 226’ (resistant *to P. anacardii*) and ‘BRS 189’ (susceptible *to P. anacardii*) during all months of analysis. The samples of both clones were separated as follows in the PLS-DA score: above 0, along the component 2 axis, are the resistant clone samples and, below 0, also along the component 2 axis, the susceptible clone samples.
Source: Author (2019).

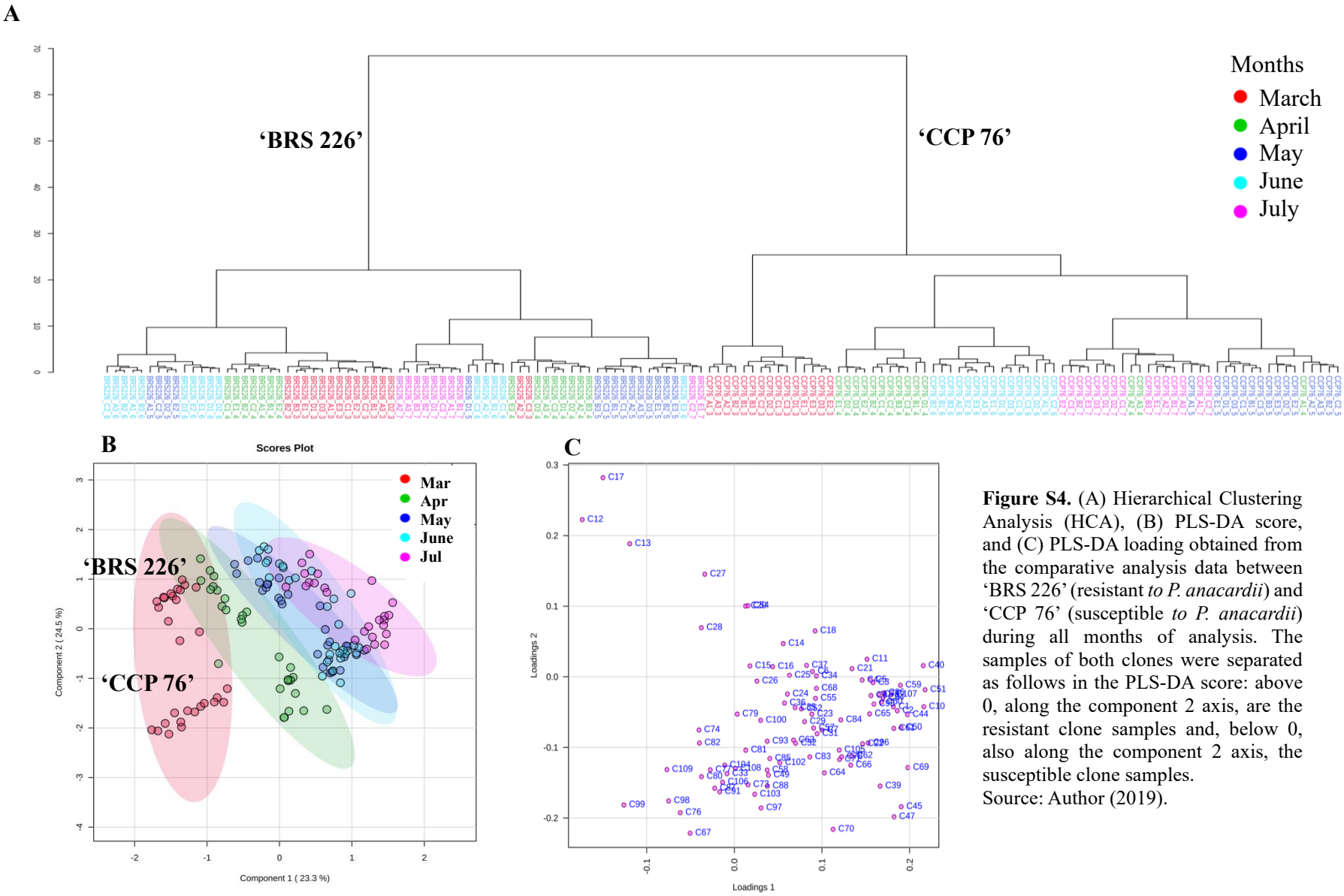

Figure S4. (A) Hierarchical Clustering Analysis (HCA), (B) PLS-DA score, and (C) PLS-DA loading obtained from the comparative analysis data between 'BRS 226' (resistant *to P. anacardii*) and 'CCP 76' (susceptible *to P. anacardii*) during all months of analysis. The samples of both clones were separated as follows in the PLS-DA score: above 0, along the component 2 axis, are the resistant clone samples and, below 0, also along the component 2 axis, the susceptible clone samples.
Source: Author (2019).

Figure S5. Heatmap graph constructed based on the volatile compounds identified in the leaf samples of the 'BRS265' clone over the months of March to July 2019. In the scale, the red color represents the compounds with a higher relative abundance and the blue color represents the compounds with lower relative abundance and the class refers to the months of study. Analyzes performed in triplicate samples.

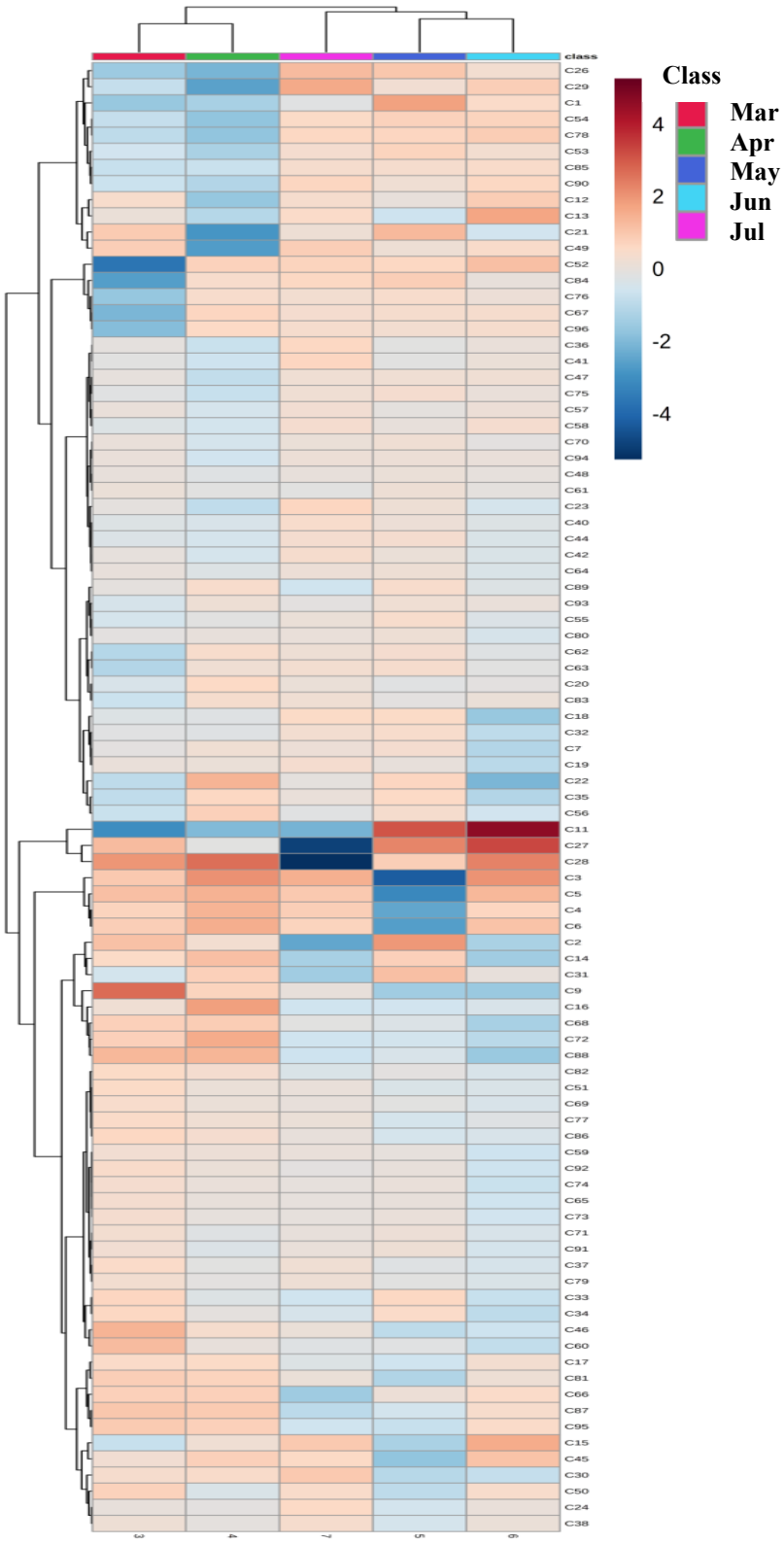

Source: Author (2019).

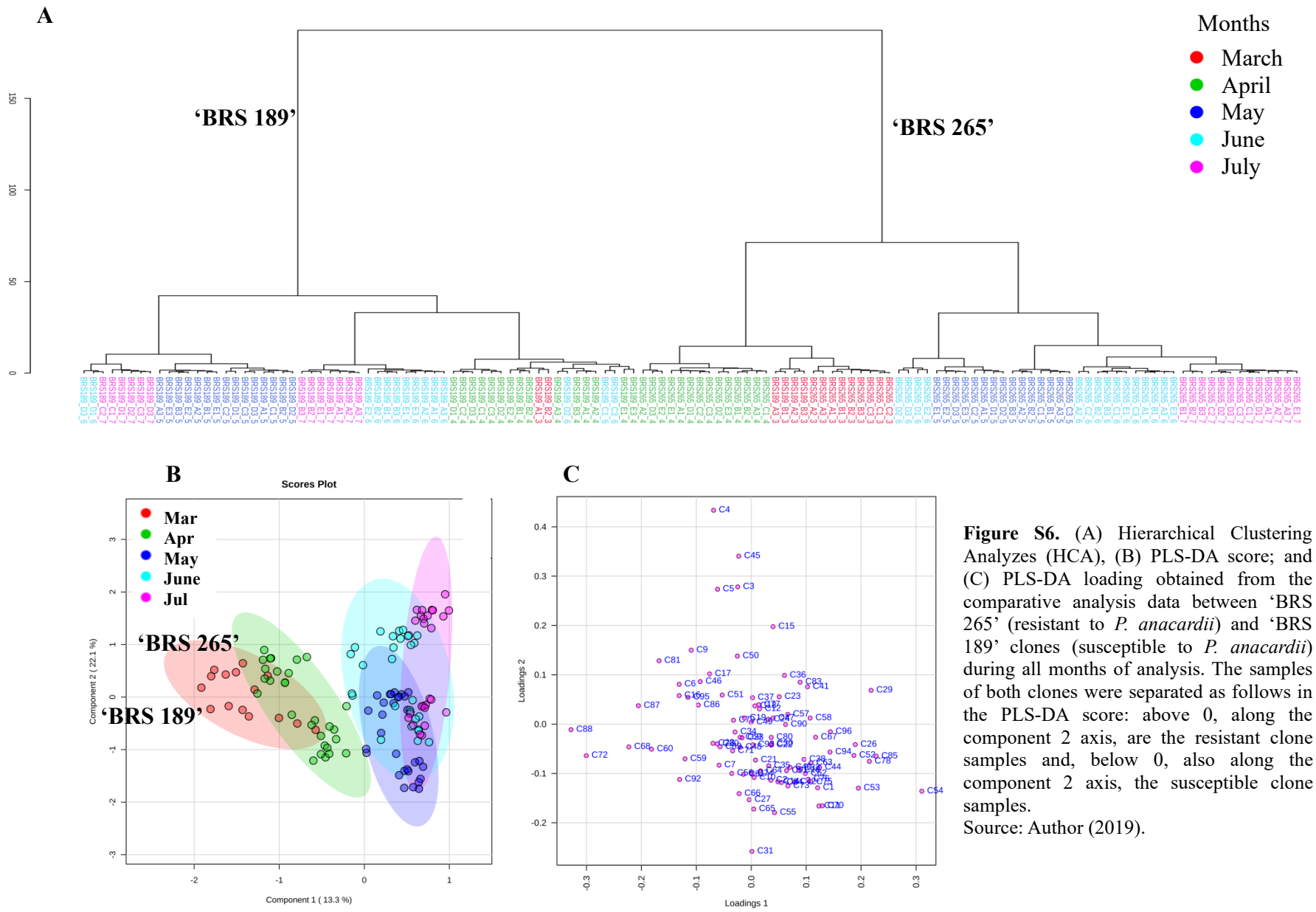

Figure S6. (A) Hierarchical Clustering Analyzes (HCA), (B) PLS-DA score; and (C) PLS-DA loading obtained from the comparative analysis data between ‘BRS 265’ (resistant to *P. anacardii*) and ‘BRS 189’ clones (susceptible to *P. anacardii*) during all months of analysis. The samples of both clones were separated as follows in the PLS-DA score: above 0, along the component 2 axis, are the resistant clone samples and, below 0, also along the component 2 axis, the susceptible clone samples.
Source: Author (2019).

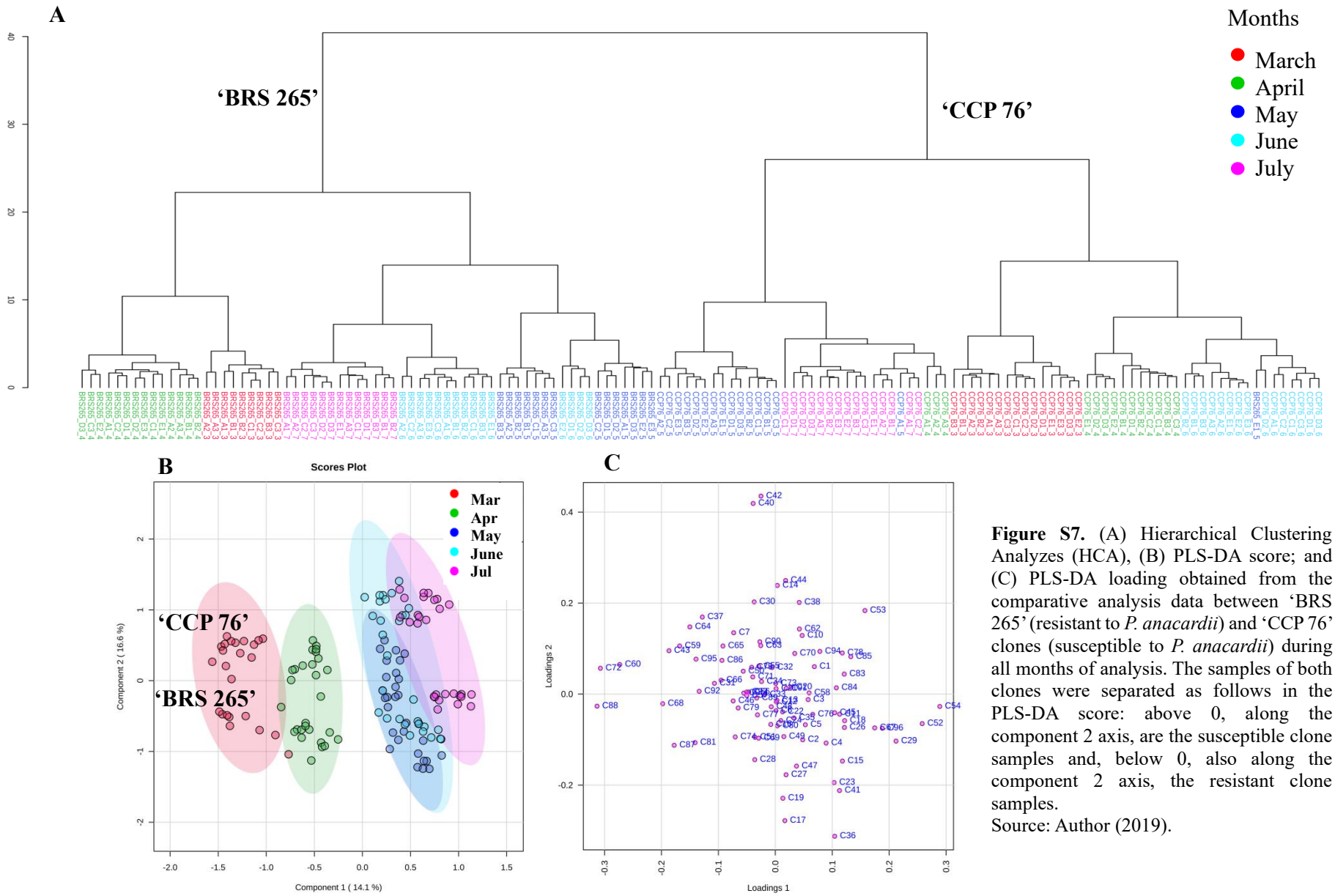

Figure S7. (A) Hierarchical Clustering Analyzes (HCA), (B) PLS-DA score; and (C) PLS-DA loading obtained from the comparative analysis data between 'BRS 265' (resistant to *P. anacardii*) and 'CCP 76' clones (susceptible to *P. anacardii*) during all months of analysis. The samples of both clones were separated as follows in the PLS-DA score: above 0, along the component 2 axis, are the susceptible clone samples and, below 0, also along the component 2 axis, the resistant clone samples.
Source: Author (2019).

Figure S8. Heatmap graph constructed based on the volatile compounds identified in the leaf samples of the 'BRS189' clone over the months of March to July 2019. In the scale, the red color represents the compounds with a higher relative abundance and the blue color represents the compounds with lower relative abundance and the class refers to the months of study. Analyzes performed in triplicate samples.

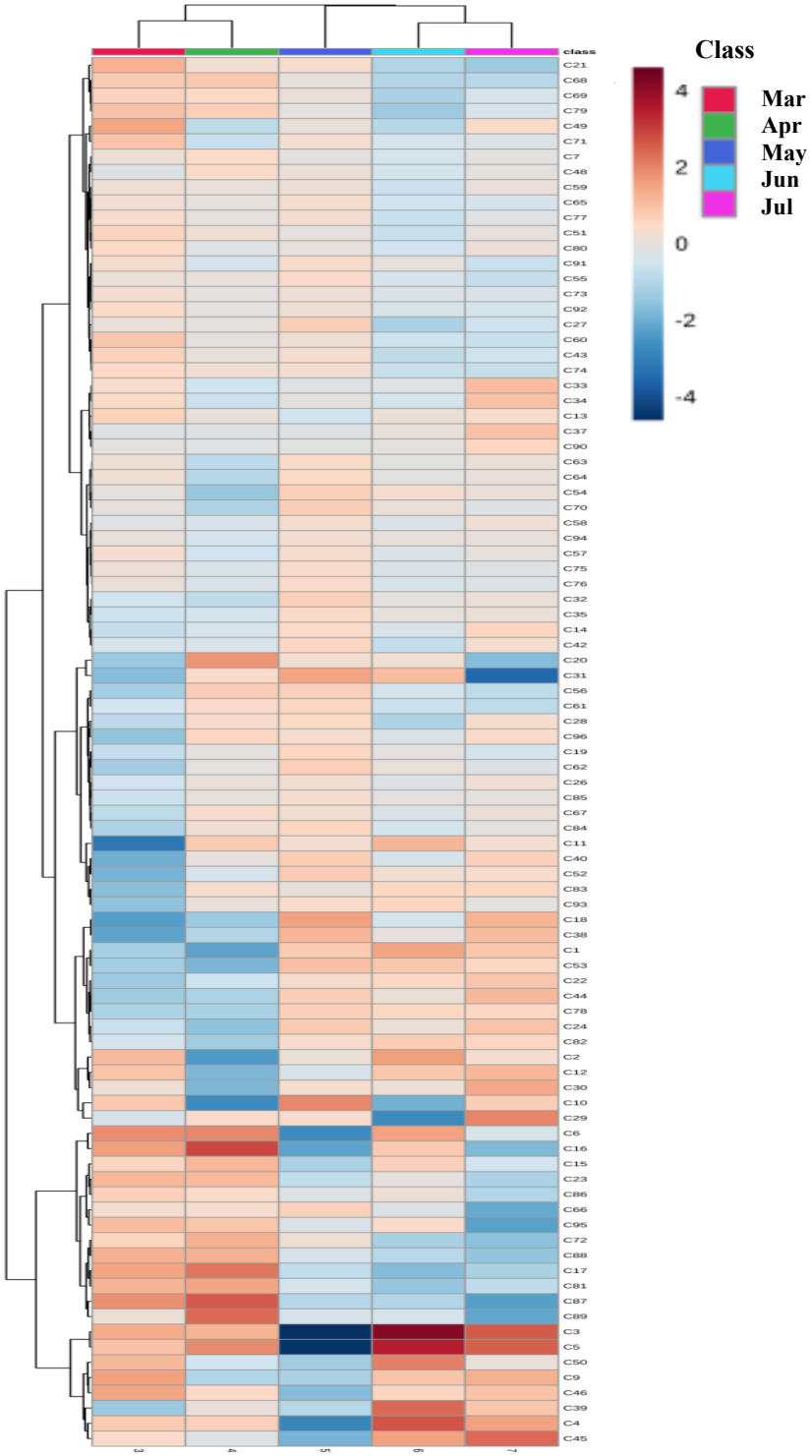

Source: Author (2019).

Figure S9. Heatmap graph constructed based on the volatile compounds identified in the leaf samples of the 'CCP76' clone over the months of March to July 2019. In the scale, the red color represents the compounds with a higher relative abundance and the blue color represents the compounds with lower relative abundance and the class refers to the months of study. Analyzes performed in triplicate samples.

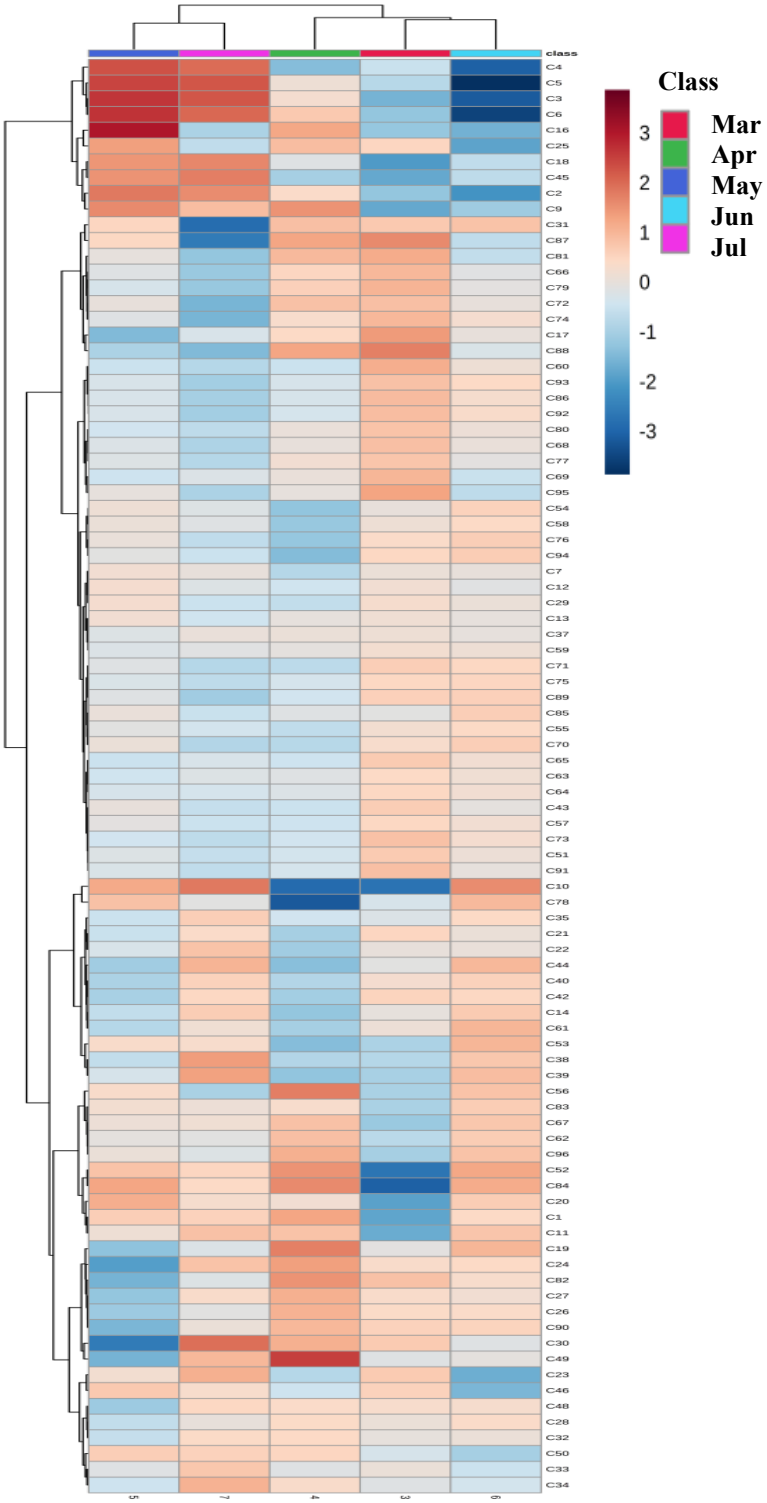

Source: Author (2019).

Figure S10. Biosynthetic path following the LOX route for the production of green leaf volatiles, specifically aldehydes and alcohols. 13-LOXs participate in the production of 13-hydroperoxy-(9Z,11E)-octadecadienoic acid (13-HPOD) and 13-HPOT. 13-HPLs (hydroperoxide lyase) act on 13-HPOD and 13-HPOT leading to the formation of C6 aldehydes. The occurrence of isomerization reactions of aldehydes occurs naturally or by enzymatic route (isomerase) for the production of isomers. Dehydrogenation reactions, catalyzed by alcohol dehydrogenase (ADH) and esterification of aldehydes leads to the production of alcohols and esters, respectively.

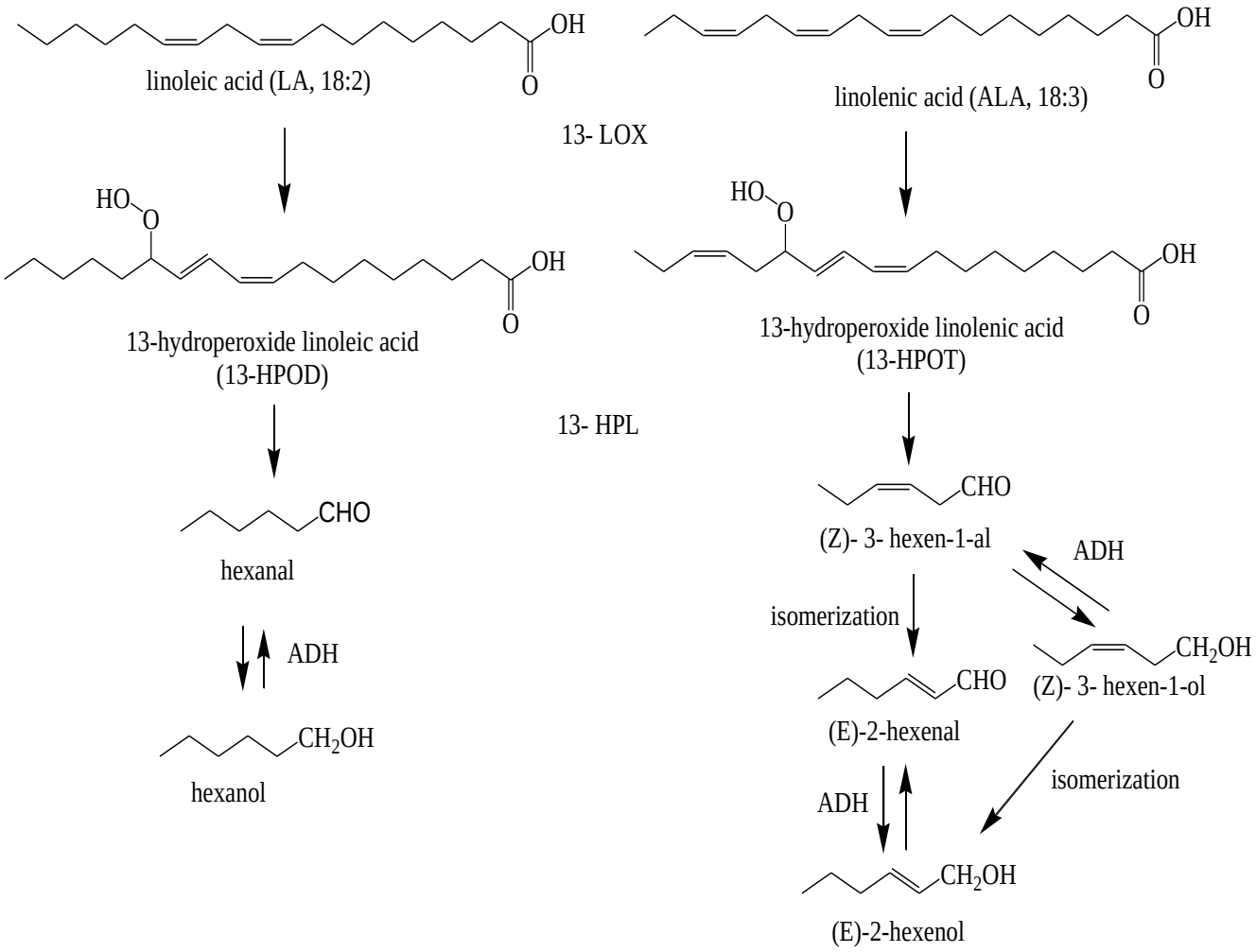

Figure S11. Biosynthesis of acyclic and cyclic monoterpenes from geranyl diphosphate.

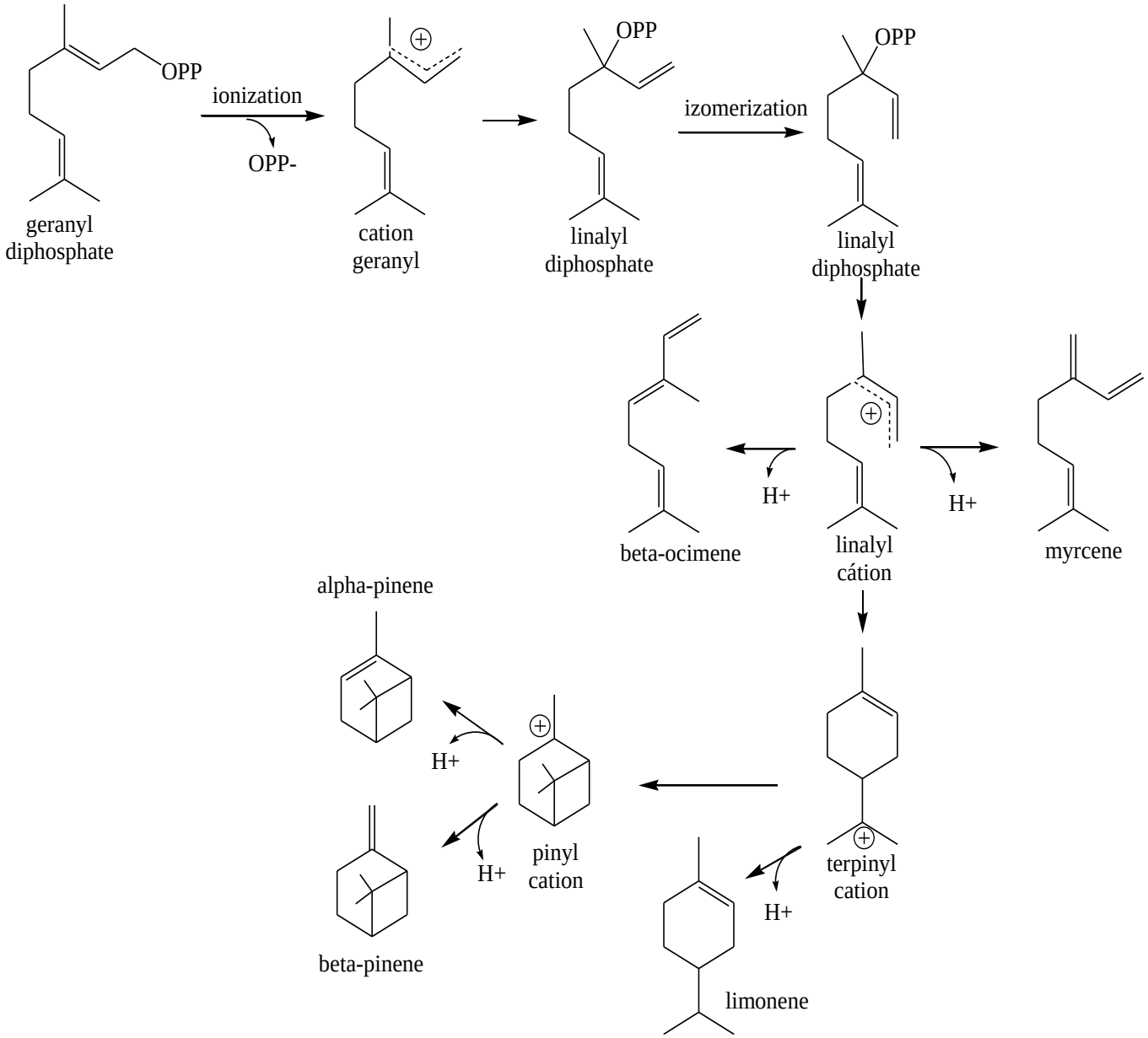

Figure S12. (a) Chromatogram referring to the resistant clone 'BRS 265' in the month of May. (b) Mass spectra (electron impact ionization at 70 eV) of some compounds identified as candidate biomarkers of resistance to *P. anacardii*.

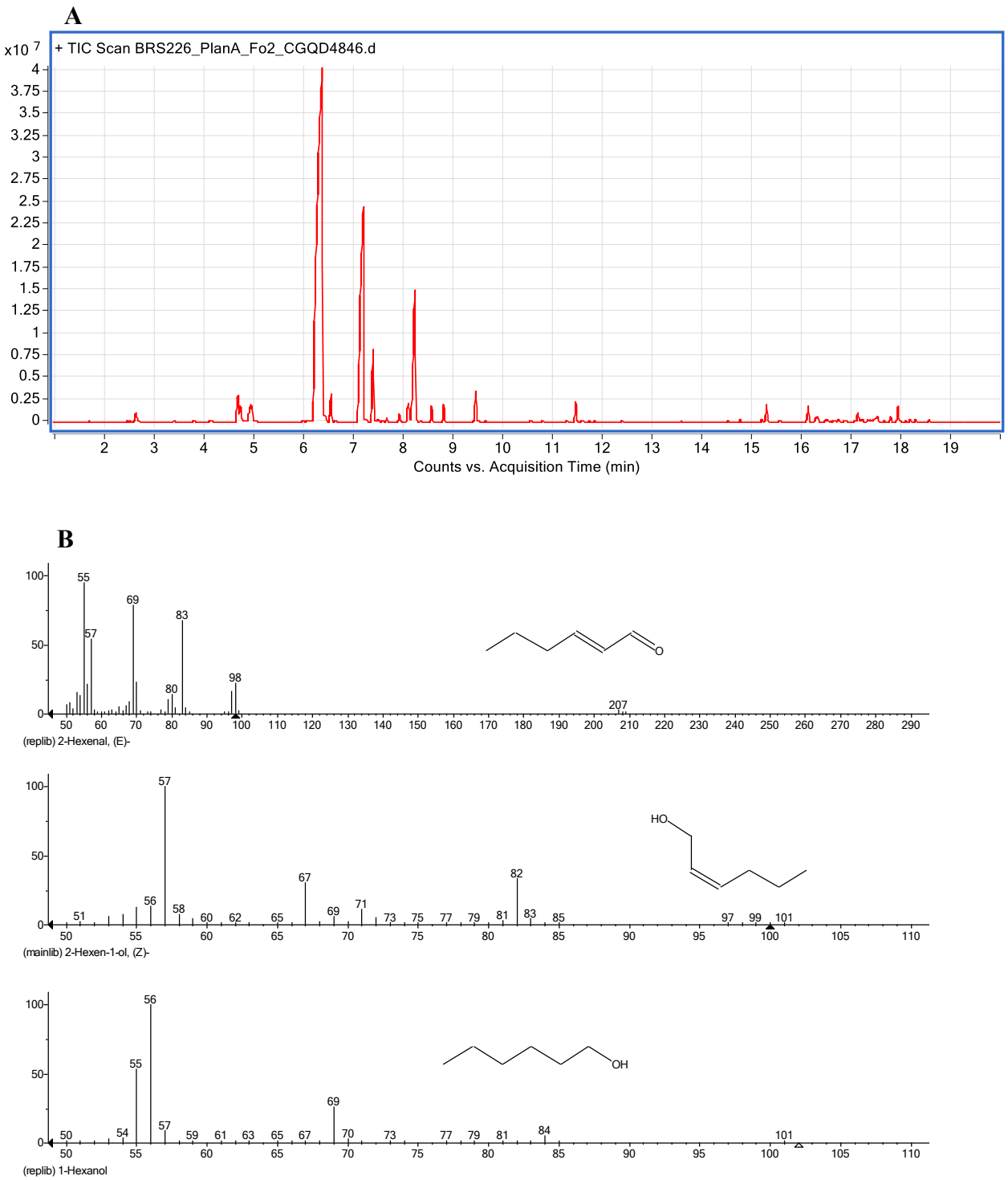

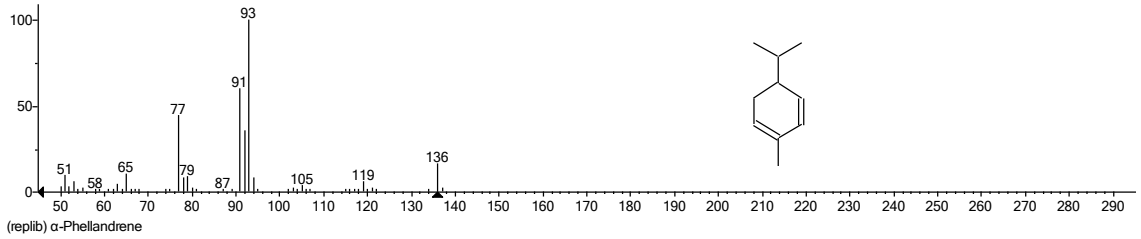

Figure S13. (a) Chromatogram referring to the resistant clone 'BRS 265' in the month of May. (b) Mass spectra (electron impact ionization at 70 eV) of some compounds identified as candidate biomarkers of resistance to *P. anacardii*.

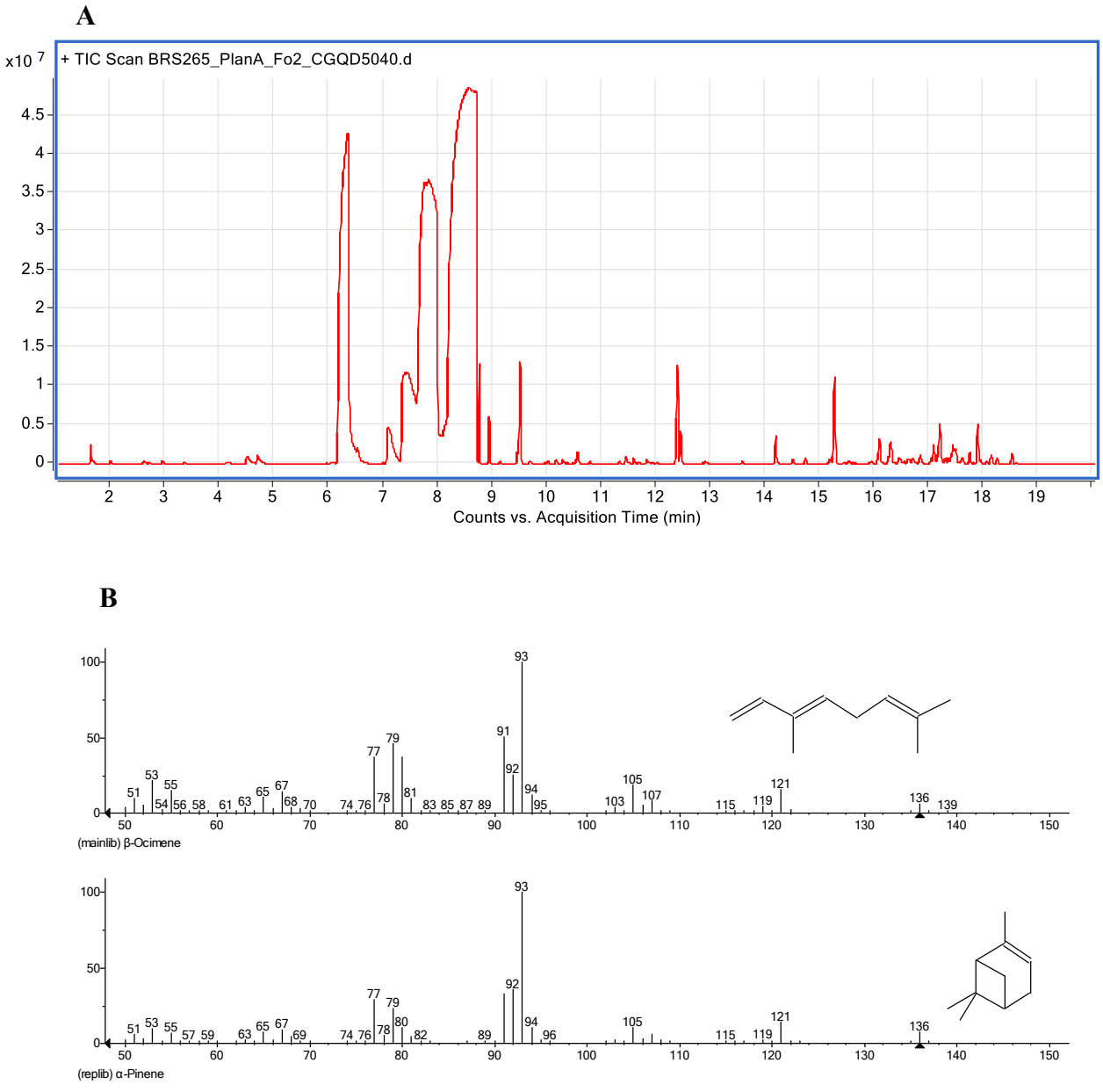

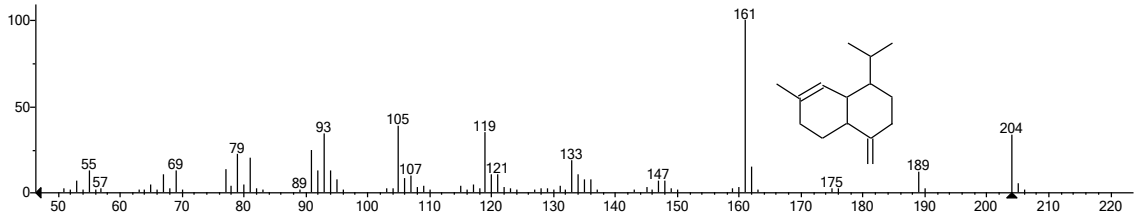

(mainlib) γ-Muurolene

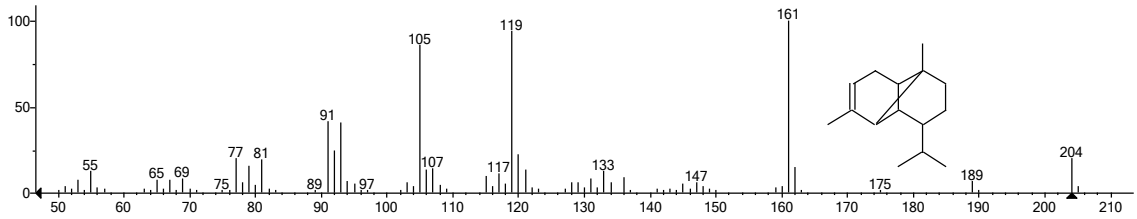

(mainlib) .alfa.-Copaene

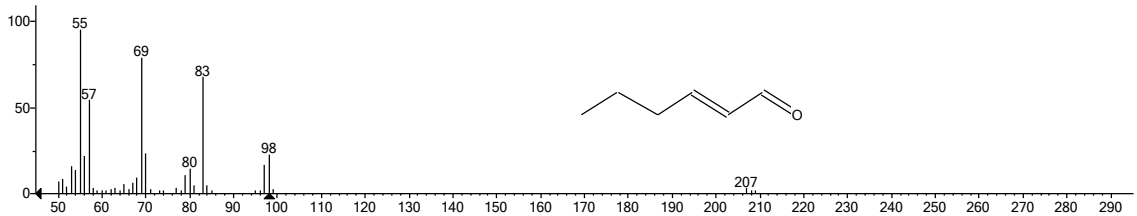

(replib) 2-Hexenal, (E)-

6 Perfil metabolômico de compostos orgânicos voláteis de folhas de clones de cajueiro por HS-SPME/GC-MS para identificação de candidatos a marcadores de resistência à antracnose

---

Metabolomic profile of volatile organic compounds from leaves of cashew clones by HS-SPME/GC-MS for the identification of candidates for anthracnose resistance markers

Debora B. de Sousa, Gisele S. da Silva, Luiz A. L. Serrano, Marlon V. V. Martins, Tigressa H. S. Rodrigues, Mary A. S. Lima, and Guilherme J. Zocolo

Artigo submetido ao periódico *Journal of Chromatography B*

ABSTRACT

Anthracnose caused by *Colletotrichum gloeosporioides* affects the leaves, inflorescences, nuts, and peduncles of cashew trees (*Anacardium occidentale*). The use of genetically improved plants and the insertion of dwarf cashew clones that are more resistant to phytopathogens are strategies to minimize the impact of anthracnose on cashew production. However, resistance mechanisms related to the biosynthesis of secondary metabolites remain unknown. Thus, this study promoted the investigation of the profile of volatile organic compounds of resistant cashew clone leaves ('CCP 76', 'BRS 226' and 'BRS 189') and susceptible ('BRS 265') to *C. gloeosporioides*, in the periods of non-infection and infection of the pathogen in the field (July-December 2019 - Brazil). Seventy-eight compounds were provisionally identified. Chemometric analyses, such as Principal Component Analysis (PCA), Discriminating Partial Least Squares Analysis (PLS-DA), Discriminating Analysis of Orthogonal Partial Least Squares (OPLS-DA), and Hierarchical Cluster Analysis (HCA), separated the samples into different groups, highlighting hexanal, (*E*)-hex-2-enal, (*Z*)-hex-2-en-1-ol, (*E*)-hex-3-en-1-ol, in addition to α-pinene, α-terpinene, γ-terpinene, β-pinene, and δ-3-carene, in the samples of the resistant clones in comparison to the susceptible clone. According to the literature, these metabolites have antimicrobial activity and are therefore chemical marker candidates for resistance to *C. gloeosporioides* in cashew trees.

Keywords: *Anacardium occidentale*, Resistance, Phytopathogen, Anthracnose, Chemometric analyzes, Markers.

1. INTRODUCTION

Originating in the northeast region of Brazil, *Anacardium occidentale* L. is considered the most important species among the 20 species of the *genus Anacardium*, adapting well in temperate, subtropical, and tropical regions (LEITE et al., 2016; SALEHI et al., 2019). It has a prominent position in the Brazilian economy, especially in the North and Northeast regions (EMMANUELLE et al., 2016; MUNTALA et al., 2020) because of the cashew nut trade, as well as the pseudo fruit widely used in the food and beverage industries (LÓPEZ; LUCAS, 2010). However, the quality and yield of cashew trees are greatly affected by fungal attack (WONNI, 2017).

Anthracnose is one of the most important fungal diseases in cashew orchards (FREIRE et al., 2002) and is caused by *Colletotrichum gloeosporioides*, which affects both young and adult plants (SHARMA; KULSHRESTHA, 2015; VELOSO et al., 2021). The pathogen causes the fall of leaves and young cashew nuts in addition to inflorescence death (FREIRE et al., 2002; UACIQUETE; KORSTEN; VAN DER WAALS, 2013; VELOSO et al., 2021). In Brazil, during August and September, when the so-called “rain of the cashew” occurs in the northeast region, the disease can reach a high level of spread and severity, leading to losses that can exceed 50% in production (FREIRE et al., 2002a).

As an alternative to using pesticides, planting of early dwarf cashew clones has been carried out because of its high genetic variability, which is an important factor with great potential for the selection of cashew clones that are more resistant to anthracnose (CARDOSO et al., 1999; FREIRE et al., 2002). However, little is known about the mechanisms of biosynthesis of secondary metabolites that lead to the greater resistance of these plants to *C. gloeosporioides*.

Volatile organic compounds (VOCs) emitted by plants can act as mediators in the relationship between plants and pathogens, performing antibacterial, antifungal or antioxidant functions (LÓPEZ-GRESA et al., 2017; LUBES; GOODARZI, 2017), in addition to being able to act in the expression or silencing of defense genes, a fact that allows plants to interact with each other in natural field conditions (KISHIMOTO et al., 2005). Within this context, the richness of secondary metabolites of plants of the genus *Anacardium* has been widely reported

in the literature, as larvicidal, antimicrobial, anti-inflammatory, and antioxidant activities are attributed to metabolites biosynthesized by various parts of the plant, such as leaves, stems, fruits, and pseudo fruits (LEITE et al., 2016).

Therefore, this study aimed to investigate the profile of volatile metabolites emitted by the leaves of the four cashew clones 'CCP 76', 'BRS 226', 'BRS 189' (resistant to *C. gloeosporioides*), and 'BRS 265' (susceptible to *C. gloeosporioides*). The analysis was carried out over the months of infestation and non-infestation, covering the period from July to December 2019, in Brazil, through the analysis of volatile organic compounds using gas chromatography coupled with mass spectrometry (CG-EM) (LUBES; GOODARZI, 2017). Through the use of chemometric tools, it was possible to obtain a better organization of the data to identify candidates for resistance markers for cashew anthracnose (CHEN; MA; CHEN, 2019).

2. MATERIALS AND METHODS

2.1. Plant material

The clones 'CCP 76', 'BRS 226' and 'BRS 189' are the clones selected for the study, the most resistant to anthracnose, while the clone 'BRS 265' is reported as the least resistant to this phytopathology. In addition, these clones are among the most commonly employed in agriculture because of the various characteristics that make them attractive from a commercial point of view (LIMA et al., 2019).

Leaves were collected from plants grown in the Embrapa Agroindústria Tropical (Experimental Field), located in the municipality of Pacajus, in the state of Ceará, Brazil (geographical coordinates: 4 ° 10 S and 38 ° 27 'W and altitude of 60 m above sea level). The field was planted under rainfed conditions in 2011. Since the implantation, the orchard has received all the cultural treatments recommended by (SERRANO; OLIVEIRA, 2013), and no pesticides have been applied with action on anthracnose in this area.

To analyze the profile of volatile compounds emitted by the leaves of the plants, given the presence and absence of *C. gloeosporioides* infestation in the field, one collection per month was carried out from July to December 2019. From each of the four types of clones evaluated, five plants were selected for the entire study, so that three leaves of the same size (approximately 9 cm) were collected, totaling 60 samples collected monthly.

Fresh leaves were collected in the morning and placed inside 20 mL glass vials, specifically for analysis by CG-EM, with a screw cap containing a silicone septum/PTFE (Supelco, Bellefonte, PA, USA). To be transported to the laboratory where the analysis was carried out, vials containing the samples were placed inside a polystyrene box containing an ice bath (Fig. S1, supplementary material).

2.2 Extraction and analysis of the volatile organic compounds

The volatile organic compounds were analyzed using a GC 7890 B system from Agilent Technologies Spain, SL, Madrid, coupled to a mass spectrometer with a quadrupole analyzer (5977A MSD Agilent Technologies Spain, SL, Madrid). The column used in the gas chromatograph for the separation of the analytes was of the HP5-MS ((5% phenyl) - dimethylpolysiloxane) type with 30m x 0.25mm internal diameter and 0.25µm film thickness, using the splitless mode in the analyses and helium gas, with a flow rate of 1 mL/min, as the carrier gas.

For the extraction of volatile compounds from the leaves of the cashew clones investigated, the solid-phase microextraction (SPME) technique was used via headspace, using experimental conditions based on studies by (ROUSEFF et al., 2008).

The vials containing the samples were pre-incubated, without shaking, at 30°C for 30 min, after which 1 cm gray fiber (Supelco, Bellefonte, PA, USA) coated with divinylbenzene, carboxene, or polydimethylsiloxane (DVB / CAR / PDMS) was exposed to the headspace space inside the vials for the adsorption of volatile compounds for 15 min. Then, the fiber was removed from the vials and sent to the chromatographic injector, where it remained for 3 min for the thermal desorption of the analytes at 260°C. The temperature ramp used was an initial temperature of 40°C, ranging from 40°C to 260°C at a rate of 7°C/min, and maintained at 260°C for 5 min. All analyses were performed in automatic mode and in triplicate.

The mass spectra were obtained in the positive mode according to the ionization mode by electron impact (70 eV) and analyzed in the mass range of 50–600 Da. The temperatures used in the ionization source and transfer line were 150 and 280°C, respectively. The comparison of the acquired mass spectra with those present in the NIST 2.0 Library, 2012 (National Institute of Standards and Technology, Gaithersburg, MD, USA) that accompanies the MassHunter Workstation–Qualitative Analysis software version B.06.00 Agilent Technologies, in addition to the comparison, both with the retention index of the homologous series of n-alkanes C8-C30 (Supelco, 49451-U, Bellefonte, PA, USA) and with data from the

literature (ADAMS, 2017), was used to identify the compounds extracted from the samples.

2.3. Chemometric analysis

The chromatograms from the analyses performed on the gas chromatograph and processed in the MassHunter Workstation software were subjected to alignment and deconvolution using the MS-Dial software to construct matrices. The data were organized in spreadsheets (Excel, Microsoft), where the lines contained the names of the analyzed samples and the columns contained the names of the tentatively identified compounds.

For the performance of chemometric analyses, such as Principal Component Analysis (PCA), Partial Least Squares-Discriminant Analysis (PLS-DA), Orthogonal Partial Least Squares Discriminant Analysis (OPLS-DA), and Hierarchical Clustering Analyses (HCA), the data were subjected to normalization by sum treatment on the cube root transformation scale and staggered according to the Pareto scale using the Metaboanalyst 4.0 web platform (www.metaboanalyst.ca) following the provided protocol (CHONG; WISHART; XIA, 2019).

3. RESULTS AND DISCUSSION

3.1 The pathogen

The leaf samples of the clones were collected from July to December to verify the behavior of the emission of volatile organic compounds during the non-occurrence and occurrence of infestation of the pathogen in the field. Thus, in July (when the first symptoms of the disease were observed in the field, but without severity), leaves without symptoms of the disease were collected, except for the clone 'BRS 265', which had some associated symptoms. In August and September, the clone plants 'BRS 265' had severe symptoms of anthracnose, while the plants of the other clones showed little signs of the disease. In October, there were still signs of the presence of the pathogen in the field, so the susceptible clone still had symptoms of the disease. In November and December, samples from all clones did not show symptoms of anthracnose.

3.2 Profile of volatile organic compounds (VOCs)

During the six months of analysis, seventy-eight volatile organic compounds, such

as terpenes, alcohols, esters, and aldehydes, were tentatively identified from the samples of the four types of cashew clones analyzed (Table S1, supplementary material). The chemical profile of volatile compounds in the samples is shown according to literature data for the genus *Anacardium*. The bibliographic research was carried out taking into account family, genus, and species (BICALHO; REZENDE, 2001; GARRUTI et al., 2003; CEVA-ANTUNES et al., 2006; DZAMIC et al., 2009; CARDOSO et al., 2010; AGILA; BARRINGER, 2011; LING et al., 2016; SALEHI et al., 2019; LIU et al., 2020).

The analysis of the chromatograms in periods of greater infestation of the pathogen in the field allowed verifying that there are differences in the profiles of volatile organic compounds of the clones. The most resistant clones (FIGURE 23a, 23b e 23c) maintain the biosynthesis of compounds with antimicrobial activity and it is possible to verify a large amount of biosynthesized compounds. As for the susceptible clone, there is a decrease in the amount as well as in the intensity of the peaks in this period (FIGURE 23d). This makes it possible to emphasize that the clone is less resistant to the pathogen that causes anthracnose has a reduced efficiency in the biosynthesis of compounds with antimicrobial action in this period of greater infestation of *C. gloeosporioides* in the field.

Figure 23. (a) Chromatogram related to the resistant clone samples 'CCP 76'; (b) chromatogram related to the resistant clone samples ‘BRS 226’; (c) chromatogram related to the resistant clone samples ‘BRS 189’; (d) chromatogram related to the susceptible clone samples ‘BRS 265’ during the period of *C. gloeosporioides* infestation in the field (August).

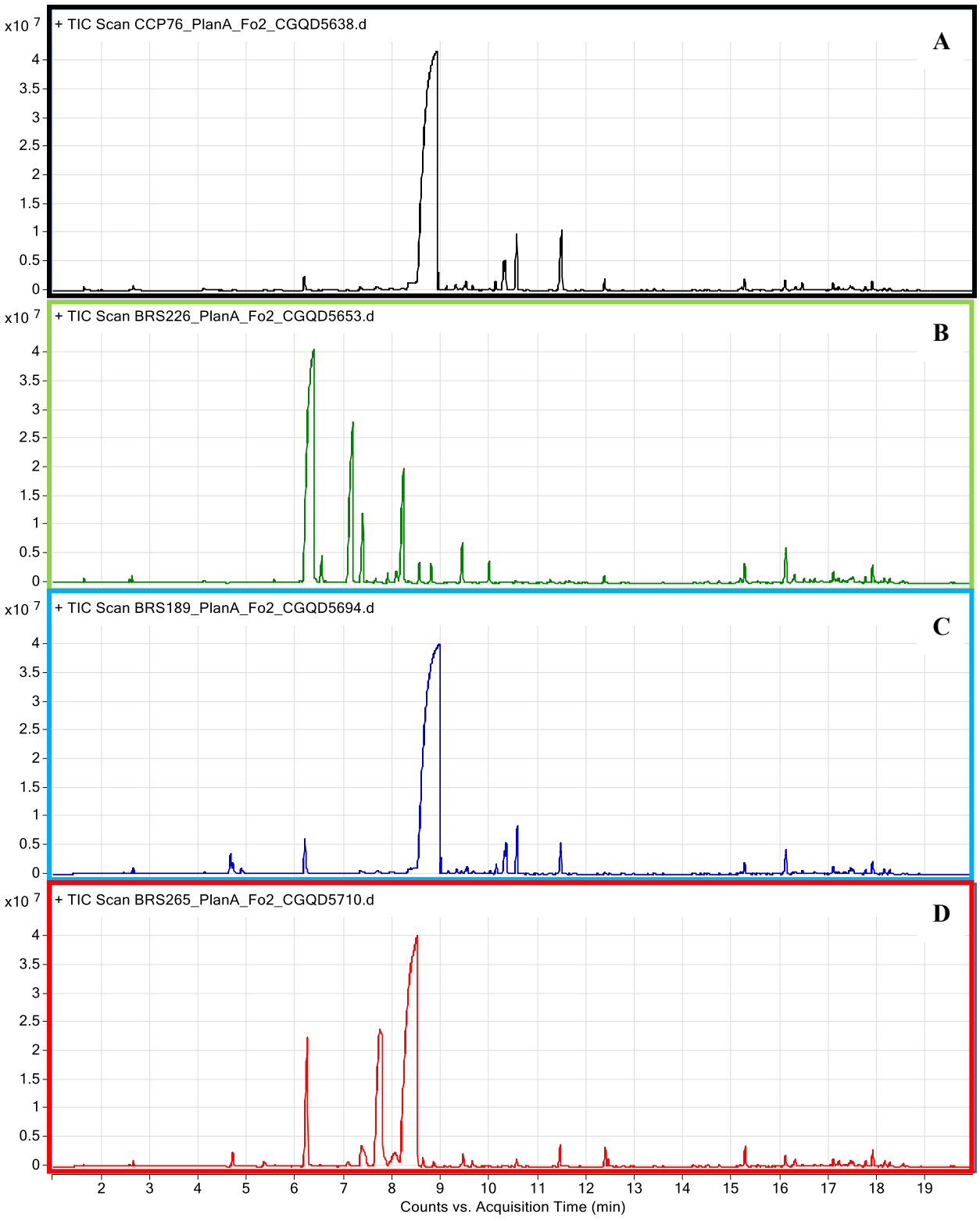

Source: Author (2019).

3.3 Data analysis

Owing to the large amount of data obtained, the results of the individual profiles of each clone will be presented according to the progress (July, August, and September) and decline (October, November, and December) of the disease in the field. To verify which compounds may be contributing to the greater *C. gloeosporioides* resistance of the plants of clones 'CCP 76', 'BRS 226' and 'BRS 189', the results of the profile of volatile compounds from these plants were compared with those obtained for the susceptible clone, 'BRS 265', according to the models presented in Table 3 that had their validity and predictive capacity evaluated according to the parameters R^2Y and Q^2. Values above 0.5 are accepted when the sample components are highly complex; however, the closer these parameters are to 1, the more stable and reliable the model will be (CHAGAS-PAULA et al., 2015b).

Table 3 - Multivariate analysis of PLS-DA and OPLS-DA models from different groups for the metabolic profile of cashew clones against *C. gloeosporioides*.

Model	Type	R^2Y	Q^2
'CCP 76'	PLS-DA	0,956	0,843
'CCP 76' *vs* 'BRS 265'	PLS-DA	0,996	0,982
	OPLS-DA	0,903	0,886
'BRS 226'	PLS-DA	0,980	0,951
'BRS 226' *vs* 'BRS 265'	PLS-DA	0,992	0,971
	OPLS-DA	0,914	0,834
'BRS 189'	PLS-DA	0,933	0,873
'BRS 189' *vs* 'BRS 265'	PLS-DA	0,995	0,987
	OPLS-DA	0,723	0,709
'BRS 265'	PLS-DA	0,931	0,864

3.3.1 Analysis of the profile of volatile organic compounds of clone 'CCP 76' (resistant to C. gloeosporioides) during the months of infestation and non-infestation

The PLS-DA score graph, which explains 47.2% of the total variance (Fig. S2A, supplementary material), shows that the samples for July (beginning of the infestation), November, and December (months without infestation) were found on the positive part of component 2, separated from the samples for August and September (highest infestation), and October (lowest infestation), which were mostly found on the negative part of the same component. The PLS-DA loading graph (Fig. S2B, supplementary material) suggests which metabolites are responsible for separating the samples into groups over the months, among which hexanal (**1**), hexan-1-ol (**6**), *cis*-pinocamphone (**30**), terpinen-4-ol (**31**), and α-bergamotene (**56**) have been reported in the literature for the Anacardiaceae family (ALMA et al., 2004; DE OLIVEIRA NOBRE et al., 2015; SALEHI et al., 2019).

According to the VIP (Fig. S2C, supplementary material) for the months of greatest disease severity (August and September), hexanal (**1**), thuja-2,4(10)-diene (**11**), p-mentha-1(7), 8-diene (**15**), δ-3-carene (**16**), limonene (**18**), o-cymene (**19**), and γ-terpinene (**22**) (Courtois et al., 2012; Salehi et al., 2019) had high concentrations, but decreased in later months. In the low months (October) and non-infestation (November and December), β-*cis*-ocimene (**20**), γ-terpinene (**22**), caryophyllene (**48**), α-bergamotene (**56**), cis-muurola- 3,5-diene (**57**), γ-muurolene (**61**), β-selinene (**65**), viridiflorene (**67**), and α-cadinene (**75**) (ALMA et al., 2004; SALEHI et al., 2019; LIU et al., 2020) contributed the most to the details of the variables, especially in December, when they showed the highest concentration.

A heatmap (Fig. S3, supplementary material) showed that p-mentha-1(7), 8-diene (**15**), α-terpinene (**17**), limonene (**18**), cis-pinocanphone (**30**), and terpinen-4-ol (**31**) (PAPAGEORGIOU; ASSIMOPOULOU; YANNOVITS-ARGIRIADIS, 1999; MONTANARI et al., 2012; BORTOLUCCI et al., 2018; SALEHI et al., 2019) were significantly increased in August. Terpinolene (**24**), *cis*-3-hexenyl valerate (**38**), δ-elemene (**39**), α-gurjunene (**47**), aromadendrene (**53**), and α-himachalene (**55**) (DZAMIC et al., 2009; GEBARA et al., 2011; SALEHI et al., 2019) were present in higher concentrations in September.

3.3.2 Comparative analysis of the volatile organic compounds profile of clones 'CCP 76' (resistant to C. gloeosporioides) vs 'BRS 265' (susceptible to C. gloeosporioides) during the months of infestation and non-infestation

The HCA graph (FIGURE 24a) shows, by the clear separation between the samples of the two clones into two large clusters, that the metabolic profile of the resistant clone is different from that of the clone susceptible to the pathogen.

The PCA score graph (principal component analysis) (FIGURE 24b) explains 49.1% of the total variance and corroborates the separation observed in the HCA. On the negative part of component 1, there are the clone 'BRS 265' samples and, on the positive part of the same component, there are the samples related to the clone 'CCP 76'. The PCA loading graph (FIGURE 24c) highlights α-pinene (**9**), α-phellandrene (**14**), δ-3-carene (**16**) (DZAMIC et al., 2009; SALEHI et al., 2019), who were responsible for separating the samples from the 'BRS 265' clone about the 'CCP 76'. The compounds α-terpinene (**17**), γ-terpinene (**22**), (4*E*, 6*Z*)-*allo*-ocimene (**28**) (PAPAGEORGIOU; ASSIMOPOULOU; YANNOVITS-ARGIRIADIS, 1999; DZAMIC et al., 2009; COURTOIS et al., 2012; SALEHI et al., 2019) can be highlighted as discriminating the samples of the 'CCP 76' clone in relation to the 'BRS 265'.

The OPLS-DA graph (FIGURE 25a) was constructed with samples from the months of greatest infestation (August and September) from both clones to verify which metabolites were responsible for differentiating them during this period. The values of the quality parameters for the model were satisfactory: $R^2Y = 0.903$ and $Q^2 = 0.886$, suggesting that there was a statistically significant difference between the metabolic profiles of the samples analyzed.

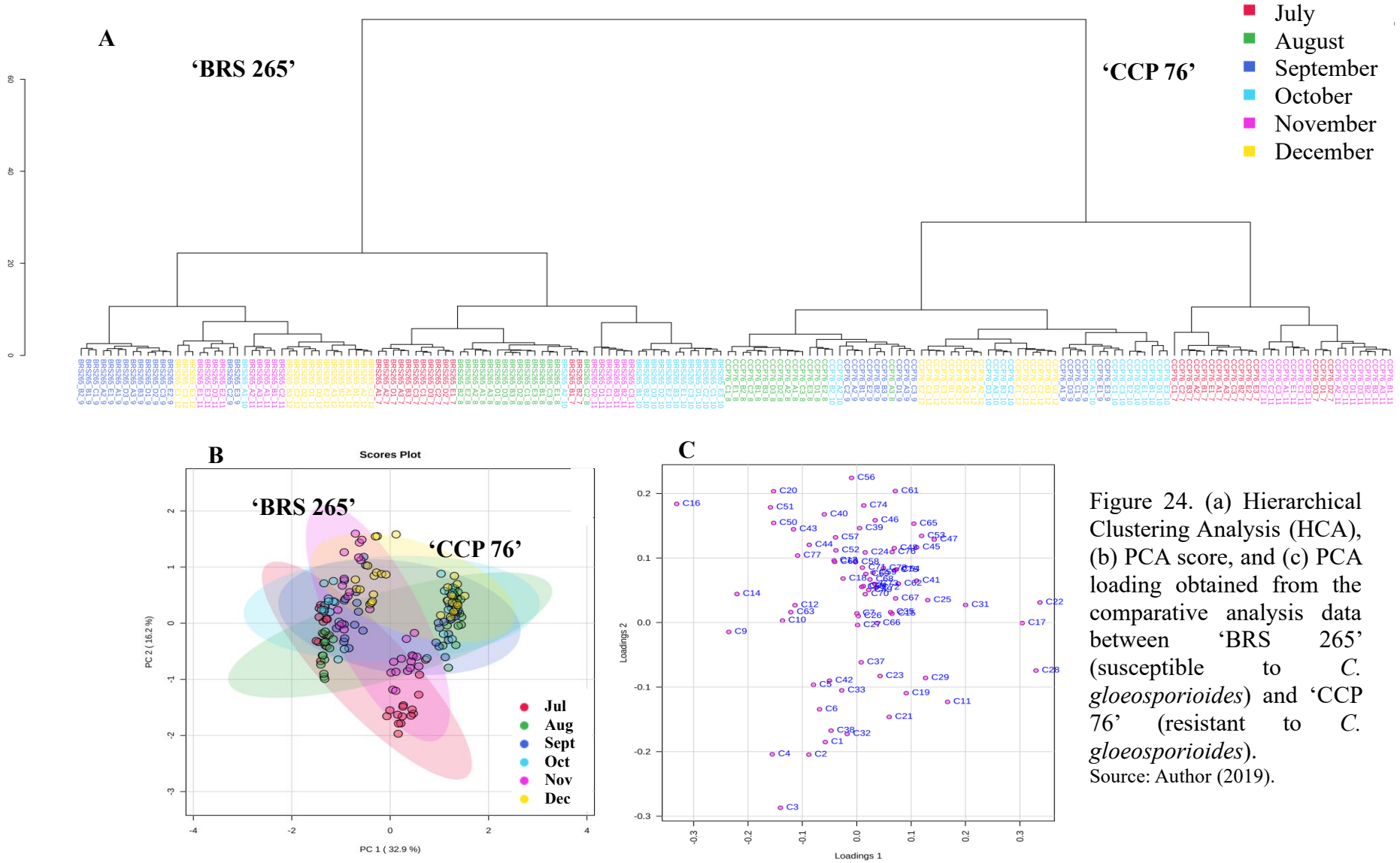

Figure 24. (a) Hierarchical Clustering Analysis (HCA), (b) PCA score, and (c) PCA loading obtained from the comparative analysis data between 'BRS 265' (susceptible to *C. gloeosporioides*) and 'CCP 76' (resistant to *C. gloeosporioides*).
Source: Author (2019).

The S-plot graph (FIGURE 25b) shows, on the negative axis, the compounds responsible for the discrimination of the susceptible clone (‘BRS 265’), while on the positive axis there are the metabolites related to the resistant clone (‘CCP 76’). These data confirmed the metabolic profile differences observed in the OPLS-DA score graph (FIGURE 25a).

The VIP score (FIGURE 25c) contains molecules already reported in the literature with important antimicrobial activity, as observed in OPLS-DA (KIRCHNER et al., 2010; GIWELI et al., 2012; ISMAIL et al., 2013; FALAHATI et al., 2015; HRISTOVA et al., 2015). Thus, the emission of volatile organic compounds such as thuja-2,4(10)-diene (**11**), α-terpinene (**17**), γ-terpinene (**22**), 3-hexen-1-ol, propanoate, (*Z*)- (**25**), (4*E*, 6*Z*) -*allo*-ocimene (**28**), cis-pinocamphone (**30**), terpinen-4-ol (**31**), α-ylangene (**41**) and α-gurjunene (**47**), which had their presence evidenced in the samples of the resistant clone in the months of greatest infestation (August and September), they may be participating in the defense mechanism of the plants and, therefore, be candidates for resistance biomarkers of the 'CCP 76' clone in relation to anthracnose.

Figure 25. Graphs (a) OPLS-DA score and (b) S-plot, and (c) VIP score obtained from comparative analysis data between clones ‘CCP 76’ (resistant to *C. gloeosporioides*) and ‘BRS 265’ (susceptible to *C. gloeosporioides*) during August and September 2019.

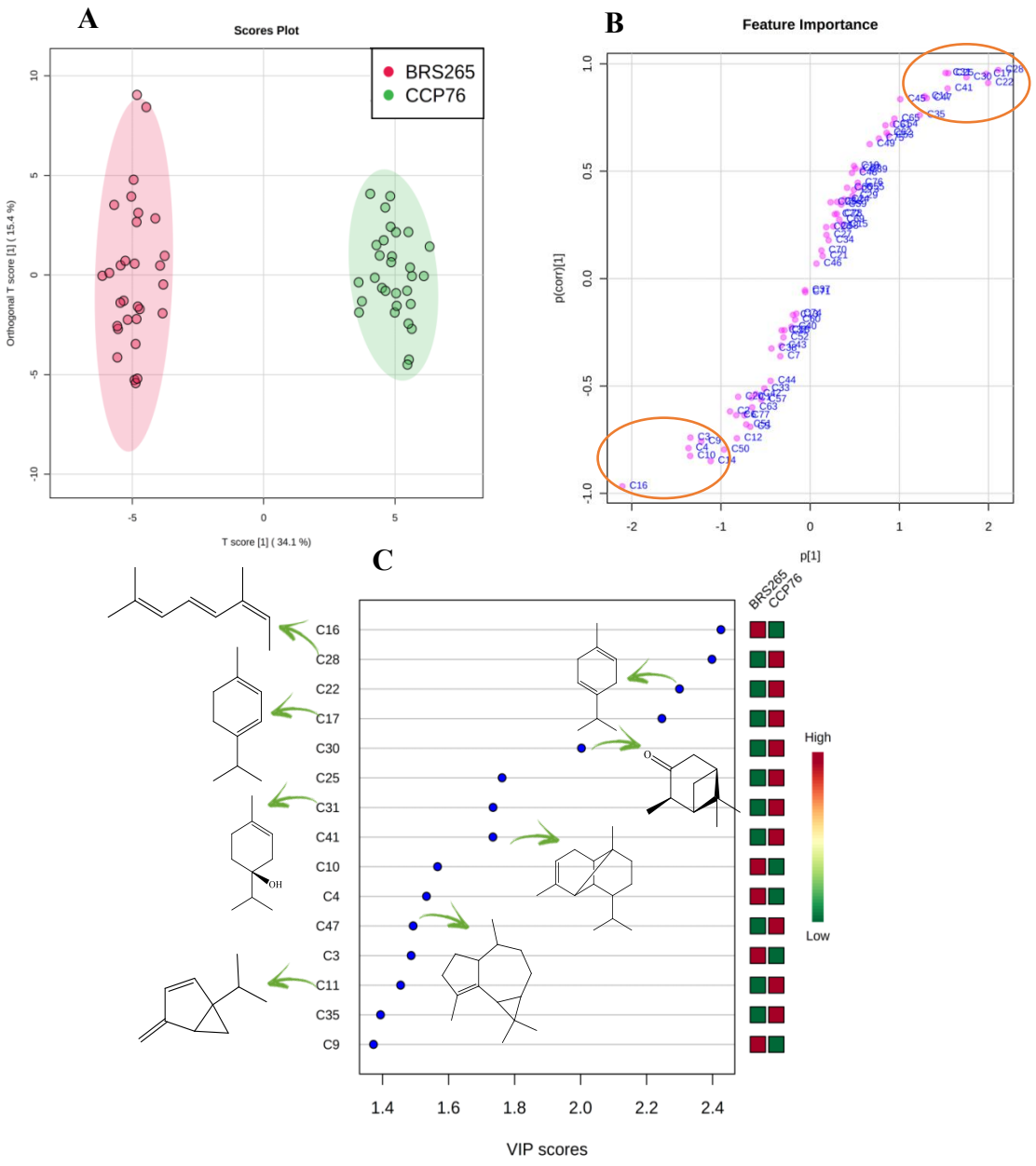

Source: Author (2019).

3.3.3 Analysis of the profile of volatile organic compounds of clone ‘BRS 226’ (resistant to C. gloeosporioides) during the months of infestation and non-infestation

The PLS-DA graph explains 63.2% of the total variance (Fig. S4A, supplementary material) and allows us to verify that the samples referring to July (beginning infestation),

August, and September (severe infestation) present an intersection between themselves, a fact that suggests a similarity in the volatile profile in this period. As for November and December (months without infestation), the samples were almost entirely in the positive part of both components, which suggests differentiation of the metabolite profile in the months of non-infestation (LAOTHAWORNKITKUL et al., 2009).

The PLS-DA loading (Fig. S4B, supplementary material) shows the compounds dispersed throughout the graph; however, those that are located on the negative part of both components are associated with samples from the months of the presence of the pathogen in the field (July, August, and September), such as hexanal (**1**), (*E*)- hex-2-en-1-ol (**7**), thuja-2,4(10) -diene (**11**), α-phellandrene (**14**), p-mentha-1 (7),8-diene (**15**), δ-3-carene (**16**), p-mentha-3,8-diene (**23**), cis-3-hexenyl iso-butyrate (**29**), α-terpineol (**33**), myrtenol (**36**), cis-3-hexenyl-α-methylbutyrate (**37**) and dendrolasin (**78**) (PAPAGEORGIOU; ASSIMOPOULOU; YANNOVITS-ARGIRIADIS, 1999; DZAMIC et al., 2009; COURTOIS et al., 2012; ZOGHBI et al., 2014; SALEHI et al., 2019).

The VIP score (Fig. S4C, supplementary material) highlights the high concentration of compounds with antimicrobial activity in August (high infestation) (CHENG; LIN; CHANG, 2005; DERWICH; BENZIANE; BOUKIR, 2010; HO et al., 2011; ISMAIL et al., 2013; MNEIMNE et al., 2016; PERIGO et al., 2016; SITAREK et al., 2017; JANAH et al., 2018) as hexanal (**1**), α-phellandrene (**14**), p-mentha-1(7), and 8-diene (**15**) (DZAMIC et al., 2009; SALEHI et al., 2019a).

The heatmap (Fig. S5 - supplementary material) shows that the metabolites hexanal (**1**), 2-hexen-1-ol, (*Z*)- (**5**), camphene (**10**), thuja-2,4(10)-diene (**11**), α-phellandrene (**14**), p-mentha-1(7), 8-diene (**15**), δ-3-carene (**16**), 3-hexen-1-ol, propanoate, (*Z*)- (**25**), perylene (**26**), 1,3,8-p-menthatriene (**27**), cis-3-hexenyl iso-butyrate (**29**) and dendrolasin (**78**) (DZAMIC et al., 2009; COURTOIS et al., 2012; ZOGHBI et al., 2014; SALEHI et al., 2019; LIU et al., 2020) had a significant increase in concentration in August and September, a fact that leads to a response from the plants of this clone resistant to the period of greatest infestation of *C. gloeosporioides* as a form of protection, since most of these compounds have reported in the literature about their antimicrobial activity (MONTANARI et al., 2012; IIJIMA, 2014; SINGH et al., 2016).

3.3.4 Comparative analysis of the volatile organic compounds profile of clones 'BRS 226' (resistant to C. gloeosporioides) vs 'BRS 265' (susceptible to C. gloeosporioides) during the

months of infestation and non-infestation

The HCA (FIGURE 26a) and PCA score (FIGURE 26b) graphs show the separation of the samples into two large groups. In the PCA score (explains 48.4% of the total variance) it can be seen that, in the positive part of main component 2, samples are referring to clone 'BRS 265', while in the negative part of the same component, there are samples associated with the clone 'BRS 226'. By analyzing the PCA loading graph (FIGURE 26c), it is observed that the compounds α-pinene (**9**) and β-pinene (**12**) (DZAMIC et al., 2009) are associated with the distinct behavior of the 'BRS 226' clone, while that for 'BRS 265' the compounds are associated with p-mentha-1(7), 8-diene (**15**), δ-3-carene (**16**), limonene (**18**) β-cis-ocimene (**20**).

OPLS-DA graphs were constructed with samples from both clones in August and September (higher infestation in the field). The OPLS-DA score (FIGURE 27a) allowed verification of the separation of clone samples into two large groups, showing that both had different profiles. The values of the parameters $R^2Y = 0.914$ and $Q^2 = 0.834$ for the model were satisfactory, suggesting a statistically significant difference between the metabolic profiles of the samples analyzed (CHAGAS-PAULA et al., 2015b).

The S-plot graph (FIGURE 27b) highlights, on the negative axis, the compounds responsible for the discrimination of the resistant clone ('BRS 226'), such as camphene (**10**), thuja-2,4(10)-diene (**11**), β-pinene (**12**), γ-terpinene (**22**), and neo-dihydro carveol (**34**). While on the positive axis, there are the metabolites related to the susceptible clone ('BRS 265') and p-mentha-1(7), 8-diene (**15**), δ-3-carene (**16**), limonene (**18**), and β-cis-ocimene (**20**). Most of these compounds have already been reported in the literature regarding their antimicrobial activity (GIWELI et al., 2012; MAREI; ABDEL RASOUL; ABDELGALEIL, 2012; MONTANARI et al., 2012; ISMAIL et al., 2013; HERNANDES et al., 2014; MNEIMNE et al., 2016), which justifies the increase in their concentrations during the months of greatest infestation.

The VIP scores (FIGURE 27c) corroborates the results obtained in the OPLS-DA S-plot, highlighting the same compounds in addition to α-pinene (**9**) and α-terpineol (**33**) as candidates for *C. gloeosporioides* resistance markers for clone 'BRS 226'.

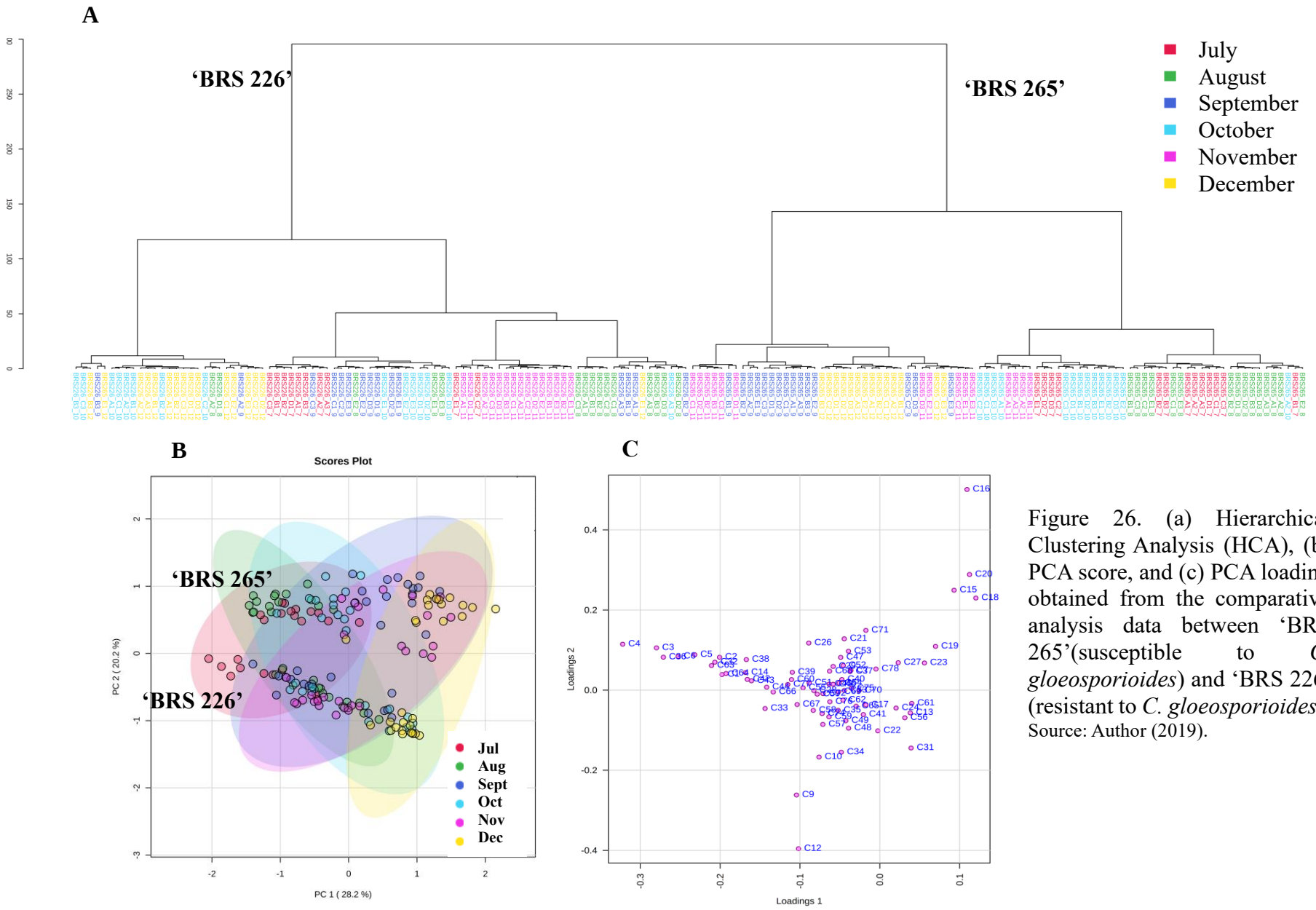

Figure 26. (a) Hierarchical Clustering Analysis (HCA), (b) PCA score, and (c) PCA loading obtained from the comparative analysis data between 'BRS 265'(susceptible to *C. gloeosporioides*) and 'BRS 226' (resistant to *C. gloeosporioides*).
Source: Author (2019).

Figure 27. Graphs (a) OPLS-DA score and (b) S-plot, and (c) VIP score obtained from comparative analysis data between clones ‘BRS 226’ (resistant to *C. gloeosporioides*) and ‘BRS 265’ (susceptible to *C. gloeosporioides*) during August and September 2019.

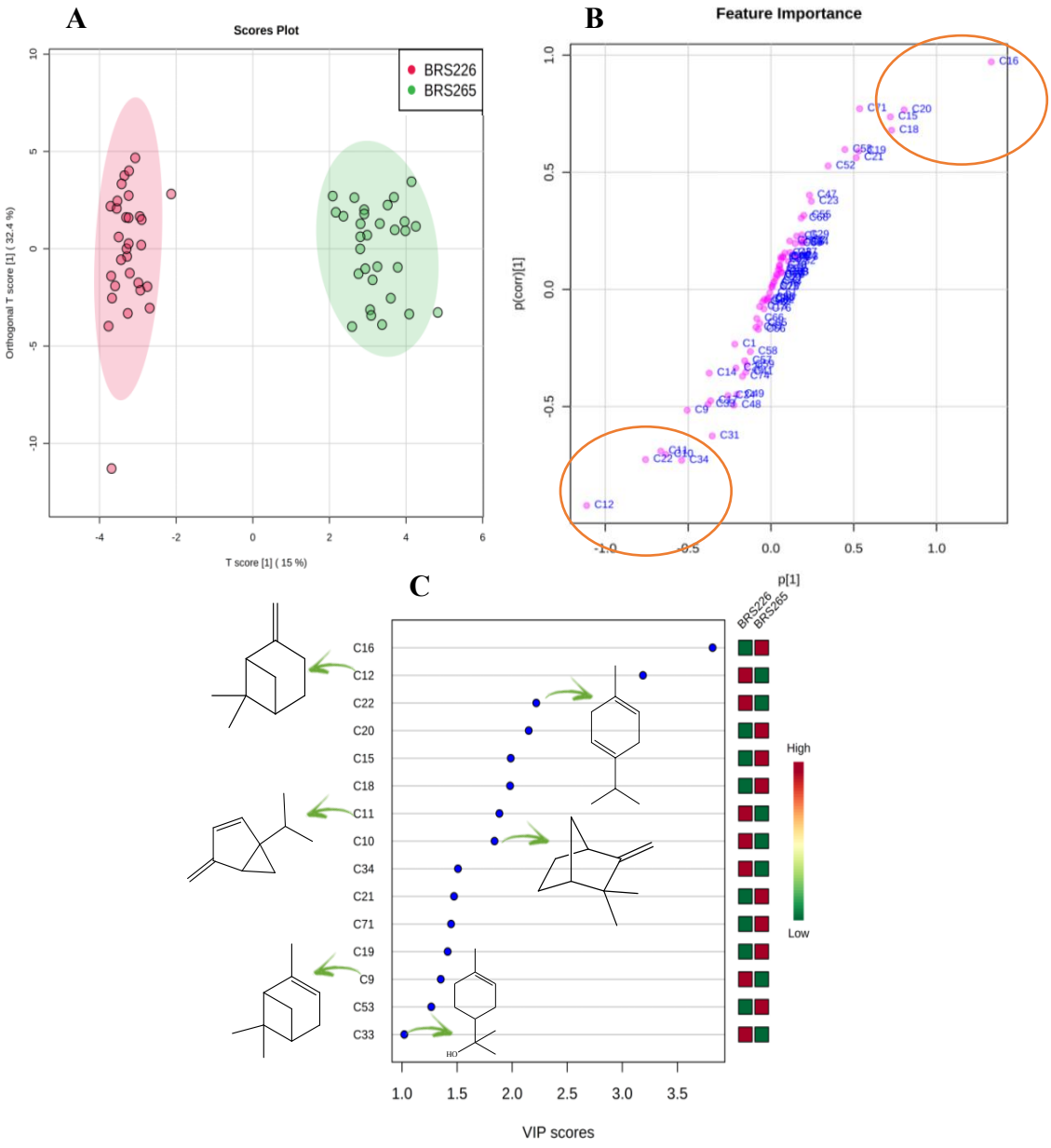

Source: Author (2019).

3.3.5 Analysis of the profile of volatile organic compounds of clone ‘BRS 189’ (resistant to C. gloeosporioides) during the months of infestation and non-infestation

The PLS-DA score graph explained 47% of the total variance (Fig. S6A, supplementary material), which allowed us to verify that the metabolic profile for July

(beginning of the infestation), August, and September (severe infestation) showed some similarity between each other because, in addition to the intersection between the groups of samples, they were found in the negative part of PC1. For November and December (months without infestation), the samples were almost entirely positive for PC1, suggesting differentiation of the metabolite profile in the months of non-infestation.

The PLS-DA loading (Fig. S6B, supplementary material) illustrates the compounds related to the July, August, and September samples as being hexanal (**1**), (*E*)-hex-2-enal (**2**), (*E*)-hex-3-en-1-ol (**3**), (*Z*)-hex-3-en-1-ol (**4**), hexan-1-ol (**6**), and (*Z*)-hex-3-enyl butanoate (**32**) (MORONKOLA; KASALI; EKUNDAYO, 2007; SALEHI et al., 2019; LIU et al., 2020), which can be associated with the defense mechanism of 'BRS 189' plants against the pathogen attack, a fact that makes them more resistant since this clone is reported in the literature as being resistant to anthracnose (LIMA et al., 2019).

According to the VIP (Fig. S6C, supplementary material), in August, the compounds hexanal (**1**), (*E*)-hex-2-enal (**2**), (*E*)-hex-3-en-1-ol (**3**), and (*Z*)-hex-3-en-1-ol (**4**) (MORONKOLA; KASALI; EKUNDAYO, 2007; SALEHI et al., 2019; LIU et al., 2020) showed higher concentrations, but gradually decreased in the following months.

In October, November, and December, it was observed that the compounds α-terpinene (**17**), β-trans-ocimene (**21**), γ-terpinene (**22**), caryophyllene (**48**), γ-muurolene (**61**), α-amorphene (**62**), viridiflorene (**67**), α-muurolene (**69**), γ-patchoulene (**70**) and δ-cadinene (**73**) (DZAMIC et al., 2009; SALEHI et al., 2019a) gradually increased in concentration until a peak in December. Most of these compounds are sesquiterpenes and have considerable antimicrobial activity (IIJIMA, 2014; MÉRILLON, 2018).

The heatmap (Fig. S7, supplementary material) shows that in August, the compounds hexanal (**1**), (*E*)-hex-2-enal (**2**), (*E*)-hex-3-en-1-ol (**3**), (*Z*)-hex-3-en-1-ol (**4**), and (*Z*)-hex-2-en-1-ol (**5**) (MORONKOLA; KASALI; EKUNDAYO, 2007; SALEHI et al., 2019; LIU et al., 2020) showed a significant increase in concentration, but decreased in the following months. In September, thuja-2,4(10)-diene (**11**) and (*Z*)-hex-3-enyl butanoate (**32**) (COURTOIS et al., 2012; SALEHI et al., 2019) were prominent at high concentrations. The final month of infestation (October) shows that compounds (*Z*)-hex-3-en-1-ol (**4**), hexan-1-ol (**6**), and (*E*)-hex-2-en-1-ol (**7**) (COURTOIS et al., 2012; SALEHI et al., 2019; LIU et al., 2020), which show antimicrobial activity (CHENG; LIN; CHANG, 2005; IIJIMA, 2014) are in higher concentrations compared to other months.

3.3.6 Comparative analysis of the volatile organic compounds profile of clones 'BRS 189' (resistant to C. gloeosporioides) vs 'BRS 265' (susceptible to C. gloeosporioides) during the months of infestation and non-infestation

The HCA graph (FIGURE 28a) and PCA score (explaining 57.8% of the total variance) (FIGURE 28b) illustrate the separation between samples from both clones. Through the PCA loading (FIGURE 28c) it can be seen that the differentiation of the samples from the 'BRS 189' clone is related to the compounds (*E*)-hex-2-enal (**2**), (*E*)-hex-3-en-1-ol (**3**), hexan-1-ol (**6**), α-terpinene (**17**), γ-terpinene (**22**), (4*E*,6*Z*)-*allo*-ocimene (**28**) and (*Z*)-hex-3-enyl butanoate (**32**) (MORONKOLA; KASALI; EKUNDAYO, 2007; SALEHI et al., 2019; LIU et al., 2020), while samples from the susceptible clone were discriminated by the presence of the compounds α-pinene (**9**), δ-3-careno (**16**) and β-*cis*-ocimene (**20**) (DZAMIC et al., 2009; SALEHI et al., 2019).

The OPLS-DA score graph (FIGURE 29a) was constructed based on the profiles of August and September, demonstrating the existence of differentiation in the biosynthesis of volatile secondary metabolites from the plants of the resistant clone compared to the clone susceptible to anthracnose. The values of the parameters $R^2Y = 0.723$ and $Q^2 = 0.709$ for the model were satisfactory, suggesting a statistically significant difference between the metabolic profiles of the analyzed samples.

The S-plot scatter plot (FIGURE 29b) shows that on the negative axis are the compounds (*E*)-hex-2-enal (**2**), (*E*)-hex-3-en-1-ol (**3**), hexan-1-ol (**6**), α-terpinene (**17**), γ-terpinene (**22**), and (4*E*,6*Z*)-*allo*-ocimene (**28**), responsible for the discrimination of the resistant clone ('BRS 189'), a fact confirmed by the VIP score graph (FIGURE 29c). On the positive axis, there are metabolites related to the susceptible clone ('BRS 265'), with α-pinene (**9**) and δ-3-carene (**16**) being highlighted.

The compounds indicated in the OPLS-DA S-plot, as well as in the VIP score, have already been proven in the literature (DA SILVA et al., 2012; GIWELI et al., 2012; MONTANARI et al., 2012; ISMAIL et al., 2013; IIJIMA, 2014; FALAHATI et al., 2015).

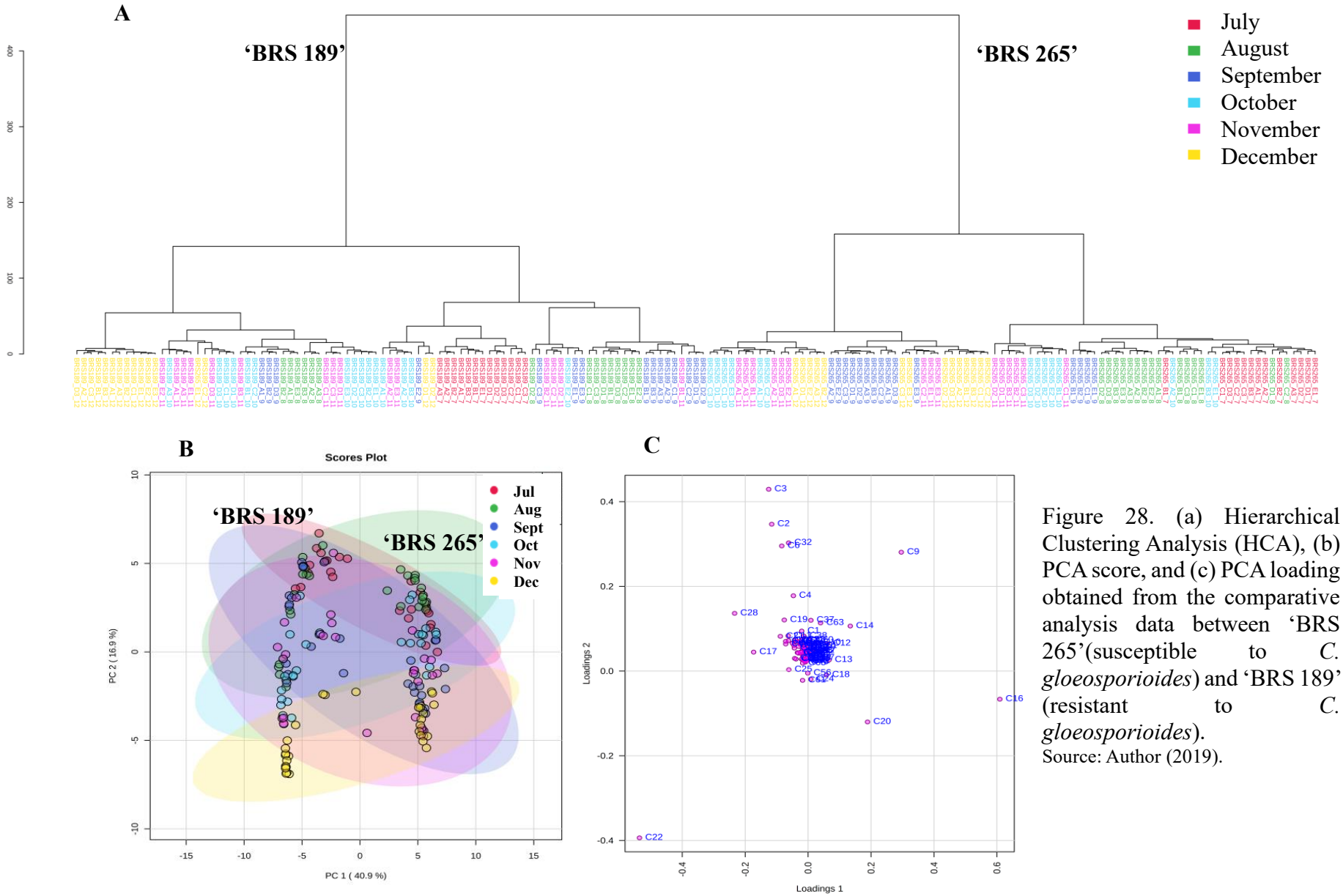

Figure 28. (a) Hierarchical Clustering Analysis (HCA), (b) PCA score, and (c) PCA loading obtained from the comparative analysis data between 'BRS 265'(susceptible to *C. gloeosporioides*) and 'BRS 189' (resistant to *C. gloeosporioides*).
Source: Author (2019).

Figure 29. Graphs (a) OPLS-DA score and (b) S-plot, and (c) VIP score obtained from comparative analysis data between clones ‘BRS 189’ (resistant to *C. gloeosporioides*) and ‘BRS 265’ (susceptible to *C. gloeosporioides*) during August and September 2019.

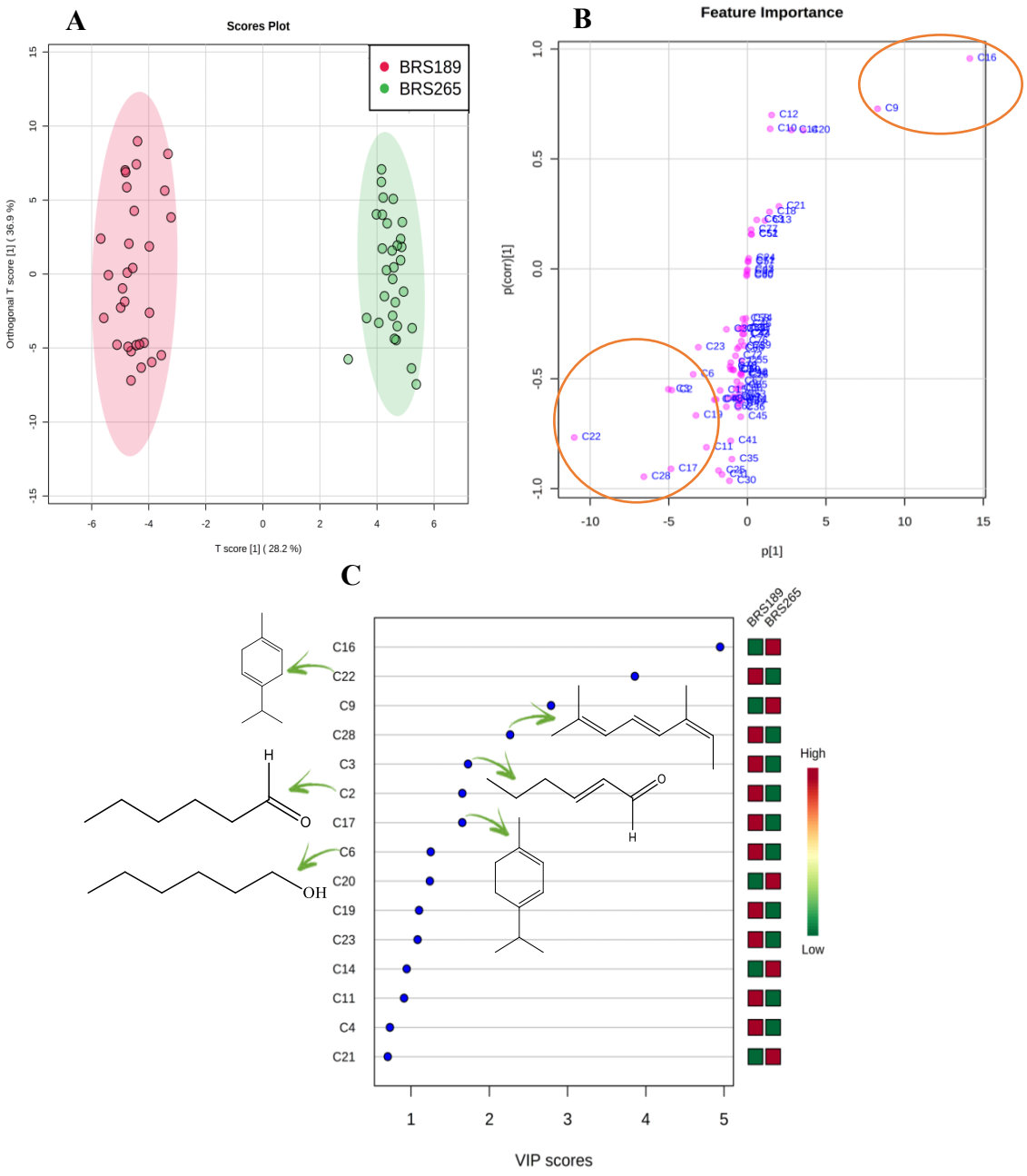

Source: Author (2019).

3.3.7 Analysis of the profile of volatile organic compounds of clone ‘BRS 265’ (susceptible to C. gloeosporioides) during the months of infestation and non-infestation

The PLS-DA score graph explains 45.6% of the total variance (Fig. S8A,

supplementary material) and allows us to verify that the metabolic profiles for July (beginning of the infestation) and August (high infestation) were similar, as they were found in the negative part of PC1, and the samples intersect each other. The samples from September, October, November, and December also showed similarities.

The PLS-DA loading (Fig. S8B, supplementary material) illustrates that compounds (*E*)-hex-2-enal (**2**), (*E*)-hex-3-en-1-ol (**3**), (*Z*)-hex-3-en-1- ol (**4**), hexan-1-ol (**6**), and (*Z*)-hex-3-enyl butanoate (**32**) (MORONKOLA; KASALI; EKUNDAYO, 2007; SALEHI et al., 2019; LIU et al., 2020) are associated with the months of July and August and are the main contributors to the differentiation of these samples in the other months. The compounds β-myrcene (**13**), p-mentha-1(7), 8-diene (**15**), δ-3-carene (**16**), limonene (**18**), o-cymene (**19**), and β-cis-ocimene (**20**) (BICALHO; REZENDE, 2001; DZAMIC et al., 2009; SALEHI et al., 2019) are associated with November and December, when the pathogen in the field is no longer apparent.

The VIP score graph (Fig. S8C, supplementary material) shows the data confirmed by the heatmap (Fig. S9, supplementary material). In July (the beginning of the infestation), α-pinene (**9**) (DZAMIC et al., 2009) showed a higher concentration; however, it gradually decreased in the following months until reaching the lowest concentration in December. In August, (severe infestation), compounds (*E*)-hex-2-enal (**2**), (*E*)-hex-3-en-1-ol (**3**), and (*Z*)-hex-3-enyl butanoate (**32**) (MORONKOLA; KASALI; EKUNDAYO, 2007; SALEHI et al., 2019; LIU et al., 2020) had an increased concentration, but decreased in the following months, which suggests that the plants of this clone are trying to contain the attack promoted by the pathogen because these compounds are associated with the plant defense system (SCALA et al., 2013). In October, when the level of infection was already low, the compounds with the highest concentrations were (*Z*)-hex-3-en-1-ol (**4**) and hexan-1-ol (**6**) (SALEHI et al., 2019; LIU et al., 2020). In November and December, it was observed that the compounds α-terpinene (**17**), β-trans-ocimene (**21**), γ-terpinene (**22**), caryophyllene (**48**), γ-muurolene (**61**), α-amorphene (**62**), viridiflorene (**67**), α-muurolene (**69**), γ-patchoulene (**70**) and δ-cadinene (**73**) (DZAMIC et al., 2009; SALEHI et al., 2019) gradually increased in concentration until reaching a maximum in December.

Because they are beings without mobility, plants need to develop defense mechanisms to interact and protect themselves from variations that may be present in the environment in which they are inserted (DUDAREVA et al., 2006). The interactions that occur between plants and microorganisms are pathogenic or not, because of the significant influence they have on the physiology of the hosts. Therefore, these interactions are a field of study in

development and great importance, especially for agricultural production (ALLWOOD et al., 2011).

Plants can develop resistance to pathogens (ALLWOOD et al., 2011), characterized by their ability to prevent or delay the penetration of the pathogen in their structures, compromising the development of the infection process (PINTO et al., 2016b). The mechanisms that govern this resistance have not yet been fully elucidated, but it is known that this process involves the release of molecules by pathogens that trigger a recognition mechanism by the host, leading to the biosynthesis of compounds with the objective of minimizing damage caused by the aggressor (GUPTA et al., 2015).

Volatile organic compounds are lipophilic compounds that are biosynthesized by plants and released into the atmosphere by structures such as leaves, flowers, and fruits (KOEDUKA, 2018). In many cases, they can have direct toxic effects against bacteria and fungi; thus, through the emission of these compounds, plants can protect themselves against the attack of pathogens (MATSUI et al., 2012; AMEYE et al., 2018; KOEDUKA, 2018), as well as maintain communication with neighboring plants so that they can activate their defense mechanisms early (DUDAREVA et al., 2006; LAOTHAWORNKITKUL et al., 2009).

Owing to the importance of plant-pathogen interactions, metabolomics has stood out in developing methods and techniques to expand knowledge about the compounds involved in this type of interaction (ALLWOOD et al., 2011; CHEN; MA; CHEN, 2019).

Investigation of the chemical profile of VOCs carried out with cashew clones allowed us to verify that plants resistant to the pathogen that causes anthracnose emit a series of compounds with antimicrobial activity that may contribute to their defense against the attack of *C. gloeosporioides* (LIMA et al., 2019).

The compounds hexanal (**1**), thuja-2,4(10)-diene (**11**), p-mentha-1(7),8-diene (**15**), δ-3-carene (**16**), limonene (**18**), o-cymene (**19**), and γ-terpinene (**22**) were highlighted in the VIP graph for the resistant clone ‘CCP 76’. Oils containing high concentrations of these molecules are known to exhibit antimicrobial activity (GIWELI et al., 2012; MONTANARI et al., 2012; MNEIMNE et al., 2016; PERIGO et al., 2016; SÁ et al., 2018). Thus, these compounds may contribute to the greater resistance of this clone to attack by *C. gloeosporioides* (SHARMA; KULSHRESTHA, 2015).

Volatile oils of Anacardiaceae species rich in α-terpinene, limonene, and terpinen-4-ol have significant antimicrobial activity against strains of various phytopathogens (ISMAIL et al., 2013). Additionally, terpinolene, cis-pinocamphone, α-himachalene, and aromadendrene have activity against strains of *Candida* and *Staphylococcus* species and other genera of

phytopathogenic fungi (FRATERNALE et al., 2004; DERWICH; BENZIANE; BOUKIR, 2010; MULYANINGSIH et al., 2011; HRISTOVA et al., 2015; YU et al., 2015) stood out in the heatmap graph of the resistant clone 'CCP 76' during the months of greatest infestation, indicating that defense mechanisms against *C. gloeosporioides* have been activated. The 'CCP 76' clone is reported in the literature to be more resistant to anthracnose when compared to the 'BRS226' and 'BRS 189' clones (LIMA et al., 2019a).

Concerning the other resistant clone 'BRS 226', compounds highlighted during August and September (greatest infestation) include hexanal (**1**), (*Z*)- hex-2-en-1-ol (**5**), camphene (**10**), thuja-2,4(10)-diene (**11**), α- phellandrene (**14**) and p-mentha-1(7), 8-diene (**15**) δ-3-carene (**16**), 3-hexen-1-ol, propanoate, (*Z*)- (**25**), perylene (**26**), 1,3,8-*p*-menthatriene (**27**), *cis*-3-hexenyl iso-butyrate (**29**) and dendrolasin (**78**) whose presence in volatiles oils they give them good antimicrobial activity (GIWELI et al., 2012; MONTANARI et al., 2012; MNEIMNE et al., 2016; PERIGO et al., 2016; SÁ et al., 2018).

The analysis of the samples from the 'BRS 189' clone, similar to the other resistant clones, showed that the compounds hexanal (**1**), (*E*)-hex-2-enal (**2**), (*E*)-hex-3-en-1-ol (**3**), (*Z*)-hex-3-en-1-ol (**4**), (*Z*)-hex-2-en-1-ol, (**5**), thuja-2,4(10)-diene (**11**) and (*Z*)-hex-3-enyl butanoate (**32**) stand out in the months of greatest infestation.

Regarding the 'BRS 265' (susceptible), the presence of the compounds α-pinene (**9**), (*E*)-hex-2-enal (**2**), (*E*)-hex-3-en-1-ol (**3**) has been verified. These compounds have been reported as antimicrobial agents, and the fact that (*Z*)-hex-3-en-1-ol (**4**) and hexan-1-ol (**6**) were found in October in samples of this clone suggests that the plants are still trying to emit a chemical response to the presence of the pathogen (PIESIK et al., 2011; SCALA et al., 2013). Despite this, the 'BRS 265' clone has no resistance to *C. gloeosporioides*, corroborating the importance of the synergistic effect that can occur between the volatiles oil's constituent molecules (ULUKANLI et al., 2014; DO PRADO et al., 2019). Despite not producing α-pinene at high concentrations, other clones biosynthesized other molecules that increased the antimicrobial potential of the set of volatile metabolites emitted and guaranteed their protection against the pathogen (DOS SANTOS et al., 2019).

Many of the compounds highlighted by VIP for resistant clones are monoterpenes, and their antimicrobial action has been described in the literature. The inhibitory action of these compounds occurs through the inhibition of protein synthesis, in addition to granulation, rupture, and inactivation of the cytoplasmic membranes of pathogens. Owing to the pesticide properties of many monoterpenes, they have become natural alternatives for developing pest control agents in crops and are safe, effective, and biodegradable (MAREI; ABDEL RASOUL;

ABDELGALEIL, 2012).

Additionally, compounds known as green leaf volatiles (GLVs) were highlighted in samples from resistant clones. They have six carbon atoms, and can be alcohols, aldehydes, and esters (DUDAREVA et al., 2006). They are biosynthesized by plants to prevent or delay the penetration of pathogens into their structures (MAREI; ABDEL RASOUL; ABDELGALEIL, 2012; SCALA et al., 2013). Thus, these compounds have great potential for controlling crop pathogens (SHIOJIRI et al., 2006; AMEYE et al., 2018).

Due to the antimicrobial activity, especially of hexanal, unsaturated aldehydes (such as hexenal), hexanol, and hexenols, the increase in the concentration of these compounds highlighted by the VIP in August and September corroborates the fact that the plants of the resistant clones emit a chemical response distinct for their defense (IIJIMA, 2014; LAWSON et al., 2020). Studies have reported that GLVs, especially (*Z*)-hex-3-en-1-ol, are considered signaling molecules involved in the process of inducing the defense of plants against attacks by pathogenic microorganisms (LÓPEZ-GRESA et al., 2017). Faced with the presence of pathogens, plants can increase the rate of biosynthesis of these compounds to communicate with other plants and stimulate the biosynthesis of compounds that can defend them from imminent threat (MATSUI et al., 2012; KOEDUKA, 2018).

The main route for the biosynthesis of volatile compounds in green leaves includes the degradation of polyunsaturated fatty acids through the enzymatic action of lipoxygenases (LOX), which promote the oxidation of linoleic or linolenic acids through the addition of oxygen at positions 13 or 9 of these fatty acids to produce their derivatives. The resulting hydroperoxide cleaves are catalyzed by hydroperoxide lyase (HPL), releasing volatile carbonyl fragments such as aldehydes, alcohols, and esters (SALAS; GARCÍA-GONZÁLEZ; APARICIO, 2006). Generally, aldehydes are first biosynthesized and subsequently reduced to their respective C6 alcohols, which are finally converted to their respective esters (MATSUI et al., 2012).

Previous studies have reported that overexpression of HPL in *Arabidopsis* resulted in significant improvement in its defense against the necrotrophic fungal pathogen *Botrytis cinérea*, whereas suppression of this enzyme resulted in greater susceptibility to the pathogen. This indicates that compounds such as C6 aldehydes, alcohols, and esters are important in the defense processes of plants because the suppression of the enzyme that catalyzes the biosynthesis of these compounds results in greater susceptibility of the plant to attack by phytopathogens (KISHIMOTO et al., 2005; MATSUI et al., 2012).

Resistance to certain pathogens can be acquired after the plant is infected with these

microorganisms, increasing the concentration of compounds such as C6 aldehydes and alcohols, even after coming into contact with the fungus; however, they do not develop severe symptoms as they manage to develop structures that guarantee their protection throughout the occurrence of the disease in the field (WALTERS; DANIELL, 2007).

In this context, the increase in the concentration of hexanal, (*E*)-hex-2-enal, (*E*)-hex-3-en-1-ol, and (*Z*)-hex-3-en-1-ol, in addition to terpenic compounds such as limonene, δ-3-carene, γ-terpinene, thuja-2,4(10)-diene, α-phellandrene, α-pinene, β-pinene, and α-terpineol, with antimicrobial activity already reported in the literature against many species of strains such as *Aspergillus niger*, *Cryptococcus neoformans*, and *Candida albicans* (LAWSON et al., 2020) in the plants of the clones most resistant to anthracnose, raises the fact that these individuals are able to activate their defense mechanisms against the attack of *C. gloeosporioides*. Understanding how plants resistant to anthracnose behave in periods of absence or presence of the pathogen in the field in terms of biosynthesis of organic compounds is an essential tool that can lead to the future development of pesticides based on natural products.

4. CONCLUSION

Through this work, it was possible to verify the behavior, from the point of view of VOCs biosynthesis, of cashew clones in the infestation and non-infestation periods of *C. gloeosporioides* in the field. Chemometric analyzes showed, for the resistant clones ‘CCP 76’, ‘BRS 226’ and ‘BRS 189’, a significant increase in the biosynthesis of compounds with high antimicrobial activity reported in the literature compared to the less resistant clone ‘BRS 265’. Hexanal (**1**), thuja-2,4 (10)-diene (**11**), *p*-mentha-1 (7), 8-diene (**15**), δ-3-carene (**16**), α-terpinene (**17**), limonene (**18**), o-cymene (**19**), γ-terpinene (**22**), terpinolene (**24**), cis-pinocamphone (**30**), terpinen-4-ol (**31**), aromadendrene (**53**), and α-himachalene (**55**) stood out in August and September in the clone samples 'CCP 76'. In relation to the clone 'BRS 226', hexanal (**1**), (*Z*) - hex-2-en-1-ol (**5**), camphene (**10**), thuja-2,4 (10) -diene (**11**), α-phellandrene (**14**) and *p*-mentha-1(7),8-diene (**15**), δ-3-carene (**16**), hex-3-en-1-ol, propanoate, (*Z*) - (**25**), perylene (**26**), 1,3,8-*p*-menthatriene (**27**), cis-3-hexenyl iso-butyrate (**29**) and dendrolasin (**78**) were the VOCs associated with the defense mechanism of this resistant clone. For the 'BRS 189' clone, also resistant to the pathogen that causes anthracnose, compounds similar to those of the other resistant clones such as hexanal (**1**), (*E*)-hex-2-enal (**2**), (*E*)-hex-3- en-1-ol (**3**), (*Z*)-hex-3-en-1-ol (**4**), (*Z*)-hex-2-en-1-ol (**5**), thuja-2,4 (10)-diene (**11**) and butanoic (*Z*)-hex-3-enyl

butanoate (**32**) were indicated by chemometric analyzes as participating in the defense mechanism of this clone. In contrast, for the susceptible clone 'BRS 265', α-pinene (**9),** (*E*)-hex-2-enal (**2**), (*E*)-hex-3-en-1-ol (**3**), (*Z*)-hex-3-en-1-ol (**4**), and hexan-1-ol (**6**) were found at higher concentrations during the period of greatest *C. gloeosporioides* infestation. This information regarding the VOC profiles of clones resistant to pathogens that cause anthracnose in cashew trees is important for further research seeking to develop pesticides based on natural products and to understand the behavior of cashew clones against anthracnose.

ACKNOWLEDGMENTS

The authors gratefully acknowledge the financial support from the National Council for Scientific and Technological Development (CNPq, Conselho Nacional de Desenvolvimento Científico e Tecnológico), National Institute of Science and Technology - INCT BioNat, grant # 465637/2014-0, Brazil, and the Coordination for the Improvement of Higher Education Personnel (Coordenação de Aperfeiçoamento de Pessoal de Nível Superior – CAPES, Finance Code 001).

SUPPLEMENTARY MATERIAL: The following are available:

Fig. S1 Schematic representation of how the plants used in this experiment are arranged in the field, highlighting how the monthly collections were made**; Table S1.** Chemical composition of volatile oil of dwarf cashew trees; **Fig. S2.** Heatmap graph constructed based on the volatile compounds identified in the leaf samples of the ‘CCP 76’ clone during the months of July to December 2019; **Fig. S3.** Heatmap graph constructed based on the volatile compounds identified in the leaf samples of the clone ‘BRS 226’ during the months of July to December 2019; **Fig. S4.** Heatmap graph constructed based on the volatile compounds identified in the leaf samples of the 'BRS 189' clone during the months of July to December 2019; **Fig. S5.** Heatmap graph constructed based on the volatile compounds identified in the leaf samples of the 'BRS 265' clone during the months of July to December 2019.

AUTHOR CONTRIBUTIONS

Debora Bezerra de Sousa: Methodology, Formal Analysis, Investigation, Resources, Data curation, Writing – Original Draft. **Gisele Silvestre da Silva**: Investigation, Writing – Review & Editing. **Luiz Augusto Lopes Serrano**: Conceptualization, Investigation, Writing – Review & Editing. **Marlon Vagner Valentim Martins**: Conceptualization, Investigation, Resources, Writing – Review & Editing. **Tigressa Helena Soares Rodrigues**: Conceptualization, Investigation, Resources, Writing – Review & Editing. **Mary Anne Sousa Lima**: Conceptualization, Writing – Review & Editing, Supervision. **Guilherme Julião Zocolo**: Conceptualization, Methodology, Resources, Writing – Review & Editing, Supervision, Project Administration, Funding Acquisition.

Supplementary material

Figure S1. Schematic representation of how the plants used in this experiment are arranged in the field, highlighting how the monthly collections were made.

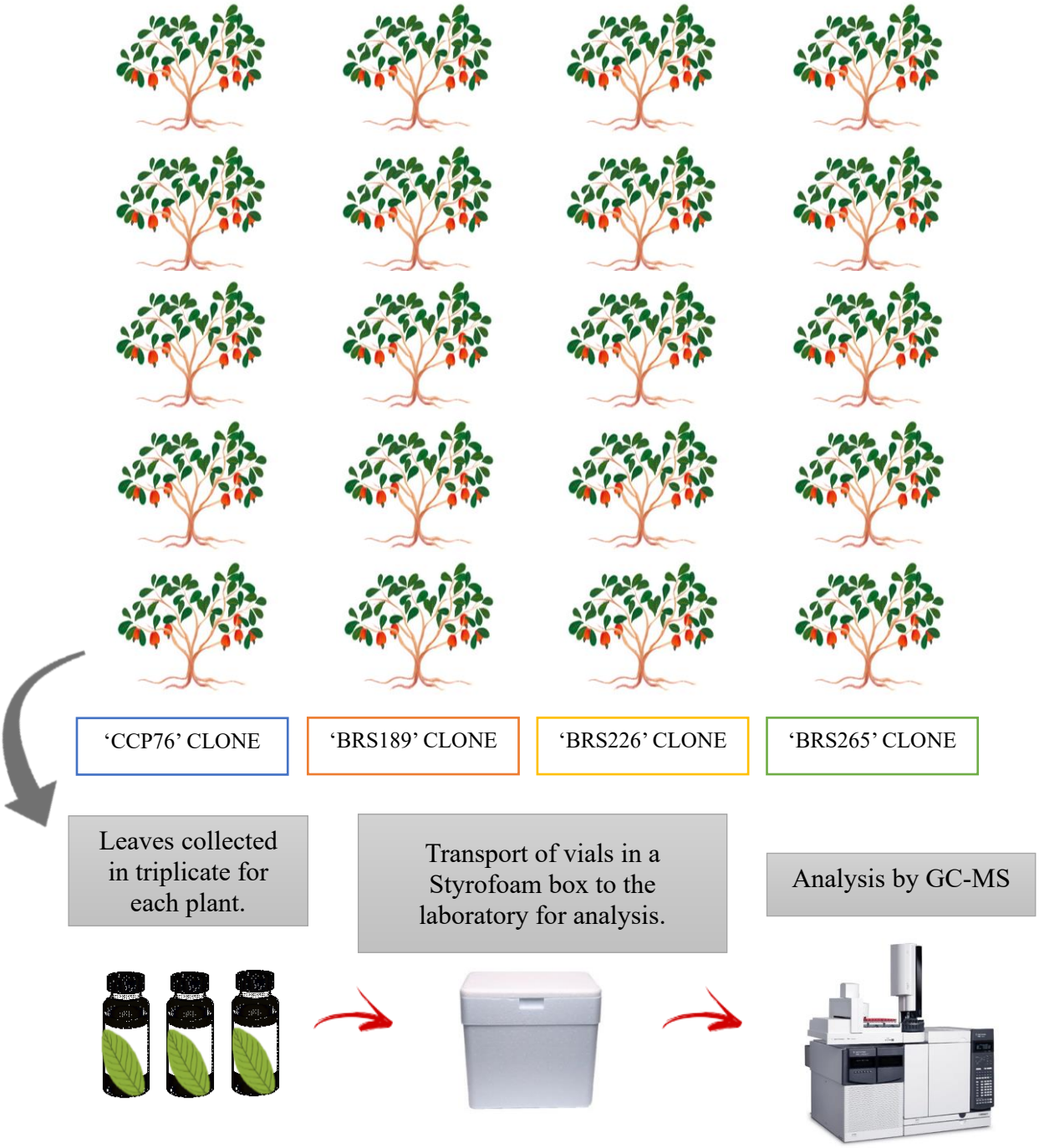

Source: Author (2019).

Table S1 - Chemical composition of volatile oil of dwarf cashew trees (*to be continued*).

	Compound	RI Literature	RI Found[a]	Match[b]	R. Match[c]	Chemical Class	Molecular Formula
1	hexanal	801	801	837	841	aldehyde	$C_6H_{12}O$
2	hex-2-enal	846	843	921	944	aldehyde	$C_6H_{10}O$
3	(*E*)- hex-3-en-1-ol	844	854	916	933	alcohol	$C_6H_{12}O$
4	(*Z*)-hex-3-en-1-ol	850	852	963	965	alcohol	$C_6H_{12}O$
5	(*Z*)- hex-2-en-1-ol	859	863	979	981	alcohol	$C_6H_{12}O$
6	hexan-1-ol	863	864	794	893	alcohol	$C_6H_{14}O$
7	(*E*)- hex-2-en-1-ol	863	855	803	848	alcohol	$C_6H_{12}O$
8	styrene	898	889	859	936	hydrocarbon	C_8H_8
9	α-pinene	932	932	940	943	terpene	$C_{10}H_{16}$
10	camphene	946	949	930	951	terpene	$C_{10}H_{16}$
11	thuja-2,4(10)-diene	953	959	691	813	terpene	$C_{10}H_{14}$
12	β-pinene	974	976	767	844	terpene	$C_{10}H_{16}$
13	β- myrcene	988	989	837	862	terpene	$C_{10}H_{16}$
14	α- phellandrene	1002	1004	760	762	terpene	$C_{10}H_{16}$
15	p-mentha-1(7),8-diene	1003	1002	655	858	terpene	$C_{10}H_{16}$
16	δ-3-carene	1008	1008	768	800	terpene	$C_{10}H_{16}$
17	α-terpinene	1014	1018	927	935	terpene	$C_{10}H_{16}$
18	limonene	1024	1027	880	882	terpene	$C_{10}H_{16}$
19	o-cymene	1022	1026	925	946	hydrocarbon	$C_{10}H_{14}$
20	β-cis-ocimene	1032	1034	943	945	terpene	$C_{10}H_{16}$
21	β-trans-ocimene	1044	1048	925	925	terpene	$C_{10}H_{16}$
22	γ-terpinene	1054	1059	953	963	terpene	$C_{10}H_{16}$
23	p-mentha-3,8-diene	1068	1071	891	897	terpene	$C_{10}H_{16}$
24	terpinolene	1086	1085	853	866	terpene	$C_{10}H_{16}$
25	(*Z*)-hex-3-en-1-ol, propanoate,	1095	1098	682	843	ester	$C_9H_{16}O_2$

Table S1 - Chemical composition of volatile oil of dwarf cashew trees (*continuation*).

	Compound	RI Literature	RI Found[a]	Match[b]	R. Match[c]	Chemical Class	Molecular Formula
26	perylene	1102	1100	822	853	terpene	$C_{20}H_{12}$
27	1,3,8-p-menthatriene	1108	1108	677	834	terpene	$C_{10}H_{14}$
28	(4*E*,6*Z*)-allo-ocimene	1128	1126	901	925	terpene	$C_{10}H_{16}$
29	*cis*-3-hexenyl iso-butyrate	1142	1141	770	835	ester	$C_{10}H_{18}O_2$
30	cis-pinocamphone	1172	1174	944	963	terpene	$C_{10}H_{16}O$
31	terpinen-4-ol	1174	1178	915	921	terpene	$C_{10}H_{18}O$
32	(*Z*)-hex-3-enyl butanoate	1184	1185	931	938	ester	$C_{10}H_{18}O_2$
33	α-terpineol	1186	1191	867	892	terpene	$C_{10}H_{18}O$
34	neo-dihydro carveol	1193	1194	924	939	terpene	$C_{10}H_{18}O$
35	myrtenol	1194	1198	758	775	terpene	$C_{10}H_{16}O$
36	*cis*-3-hexenyl isovalerate	1232	1229	915	937	ester	$C_{11}H_{20}O_2$
37	*cis*-3-hexenyl-α-methylbutyrate	1229	1230	865	876	ester	$C_{11}H_{20}O_2$
38	*cis*-3-hexenyl valerate	1279	1281	895	915	ester	$C_{11}H_{20}O_2$
39	δ-elemene	1335	1337	913	929	terpene	$C_{15}H_{24}$
40	α-cubebene	1348	1350	934	950	terpene	$C_{15}H_{24}$
41	α- ylangene	1373	1373	915	917	terpene	$C_{15}H_{24}$
42	α-copaene	1374	1378	945	949	terpene	$C_{15}H_{24}$
43	β-cubebene	1387	1389	802	826	terpene	$C_{15}H_{24}$
44	β-elemene	1389	1394	865	874	terpene	$C_{15}H_{24}$
45	isolongifolene	1389	1393	818	821	terpene	$C_{15}H_{24}$
46	longifolene	1407	1400	865	873	terpene	$C_{15}H_{24}$
47	α-gurjunene	1409	1414	901	917	terpene	$C_{15}H_{24}$
48	caryophyllene	1417	1423	961	961	terpene	$C_{15}H_{24}$
49	cedrene	1419	1425	849	864	terpene	$C_{15}H_{24}$
50	β-copaene	1430	1432	886	886	terpene	$C_{15}H_{24}$

Table S1 - Chemical composition of volatile oil of dwarf cashew trees (*continuation*).

	Compound	RI Literature	RI Found[a]	Match[b]	R. Match[c]	Chemical Class	Molecular Formula
51	β-gurjunene	1431	1432	890	898	terpene	$C_{15}H_{24}$
52	γ-elemene	1434	1434	907	909	terpene	$C_{15}H_{24}$
53	aromadendrene	1439	1442	842	850	terpene	$C_{15}H_{24}$
54	α-guaiene	1437	1445	894	897	terpene	$C_{15}H_{24}$
55	α- himachalene	1449	1446	850	855	terpene	$C_{15}H_{24}$
56	α-bergamotene	1432	1435	858	891	terpene	$C_{15}H_{24}$
57	*cis*-muurola-3,5-diene	1448	1450	824	893	terpene	$C_{15}H_{24}$
58	neoclovene	1452	1454	845	847	terpene	$C_{15}H_{24}$
59	α-humulene	1452	1457	882	897	terpene	$C_{15}H_{24}$
60	alloaromadendrene	1458	1458	884	886	terpene	$C_{15}H_{24}$
61	γ-muurolene	1478	1479	936	940	terpene	$C_{15}H_{24}$
62	α- amorphene	1483	1481	920	927	terpene	$C_{15}H_{24}$
63	germacrene D	1480	1484	916	937	terpene	$C_{15}H_{24}$
64	β-guaiene	1492	1492	825	832	terpene	$C_{15}H_{24}$
65	β-selinene	1489	1489	895	903	terpene	$C_{15}H_{24}$
66	eremofilene	1496	1492	904	907	terpene	$C_{15}H_{24}$
67	viridiflorene	1496	1497	865	889	terpene	$C_{15}H_{24}$
68	α-selinene	1498	1498	904	916	terpene	$C_{15}H_{24}$
69	α-muurolene	1500	1502	943	954	terpene	$C_{15}H_{24}$
70	γ-patchoulene	1502	1501	879	889	terpene	$C_{15}H_{24}$
71	α-farnesene	1505	1505	948	959	terpene	$C_{15}H_{24}$
72	γ-cadinene	1513	1517	826	839	terpene	$C_{15}H_{24}$
73	δ-cadinene	1522	1525	839	853	terpene	$C_{15}H_{24}$
74	cadina-1,4-diene	1533	1536	811	831	terpene	$C_{15}H_{24}$

Table S1 - Chemical composition of volatile oil of dwarf cashew trees (*conclusion*).

	Compound	RI Literature	RI Found[a]	Match[b]	R. Match[c]	Chemical Class	Molecular Formula
75	α-cadinene	1537	1541	880	880	terpene	$C_{15}H_{24}$
76	selina-3,7(11)-diene	1545	1548	853	879	terpene	$C_{15}H_{24}$
77	germacrene B	1569	1564	871	914	terpene	$C_{15}H_{24}$
78	dendrolasin	1570	1576	828	842	eter	$C_{15}H_{22}O$

[a]RI: retention index;

[b]Match: it is a correspondence factor between the spectrum of the analyzed compound and the spectrum of the library NIST (direct match);

[c]R. Match: it is a match factor for the unknown and the library spectrum ignoring any peaks in the unknown that are not in the library spectrum (reverse search).

Figure S2. Graphs (a) PLS-DA score, (b) loading, and (c) VIP score obtained from the data analysis during July to December 2019 for the clone 'CCP 76'.

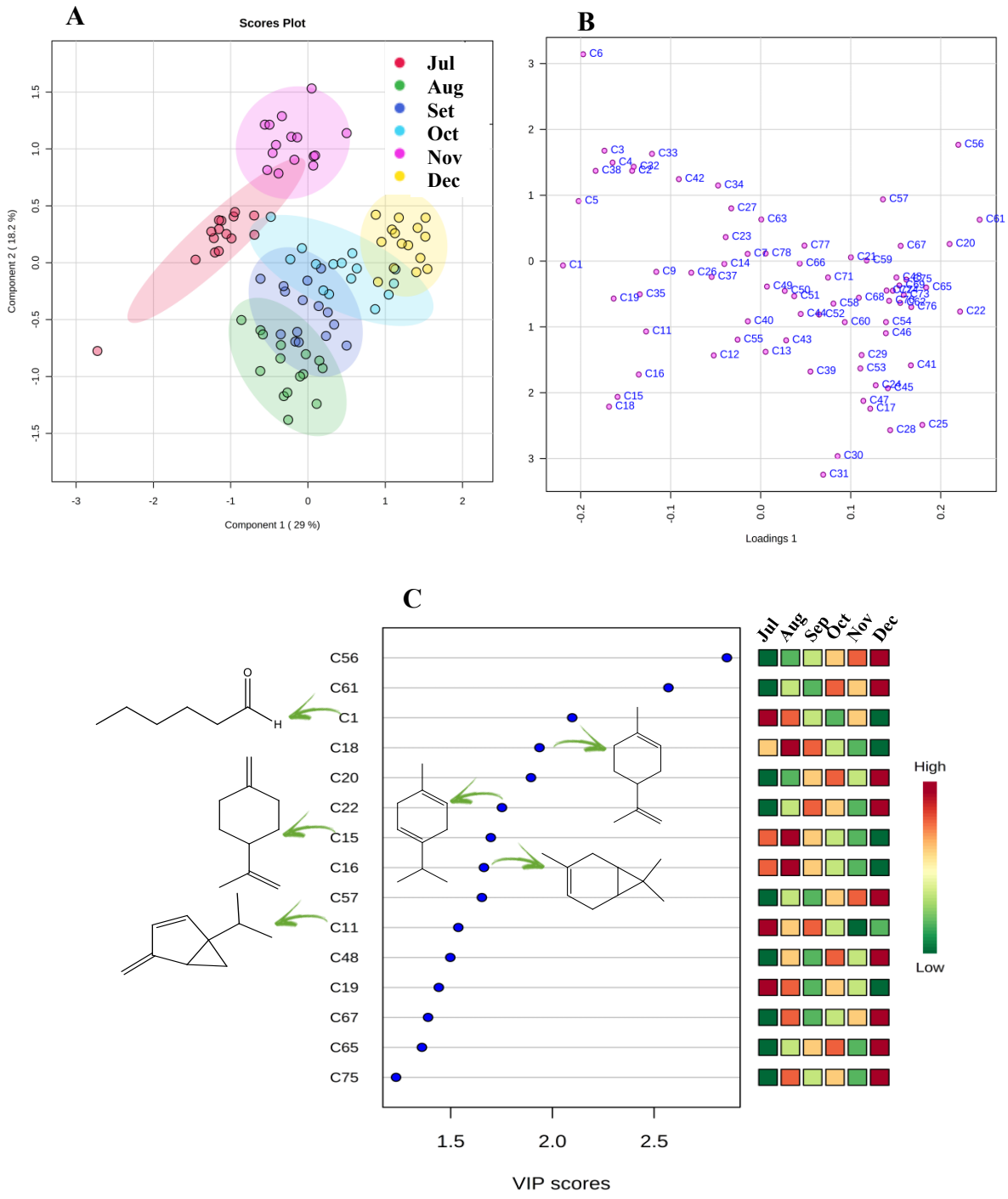

Source: Author (2019).

Figure S3. Heatmap graph constructed based on the volatile compounds identified in the leaf samples of the ‘CCP 76’ clone during the months of July to December 2019.

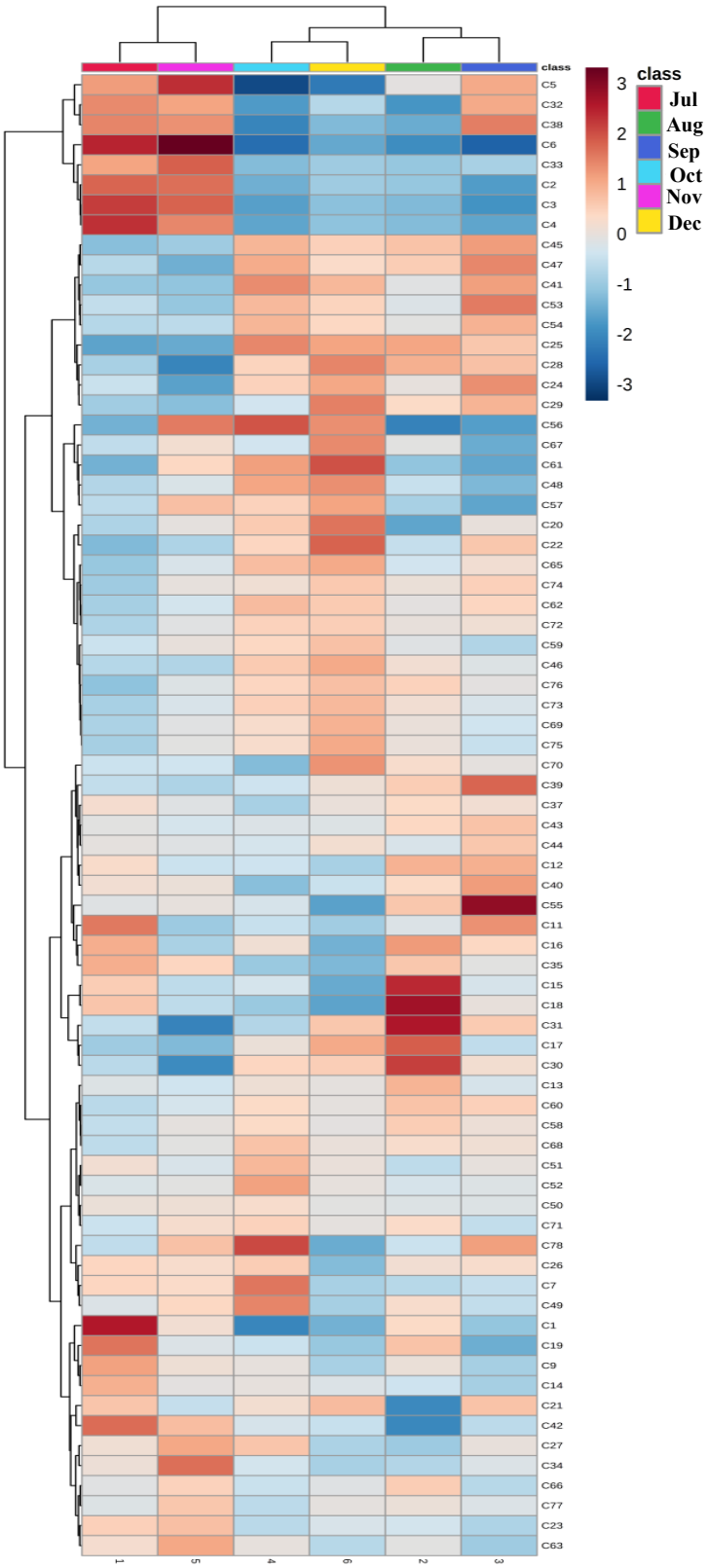

Source: Author (2019).

Figure S4. Graphs (a) de PLS-DA score, (b) loading, and (c) VIP score obtained from the data analysis during July to December 2019 for the clone 'BR226'.

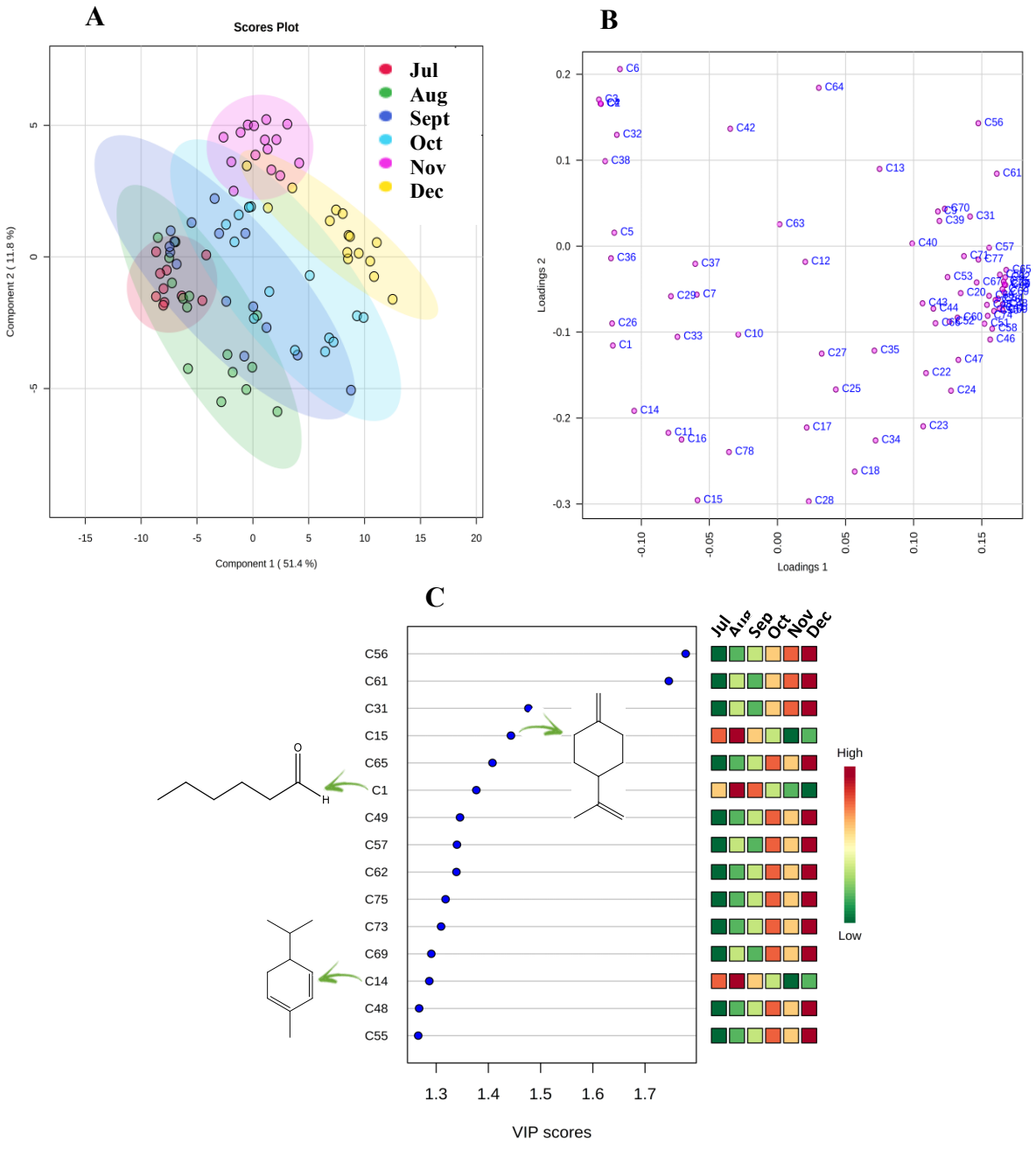

Source: Author (2019).

Figure S5. Heatmap graph constructed based on the volatile compounds identified in the leaf samples of the clone ‘BRS 226’ during the months of July to December 2019.

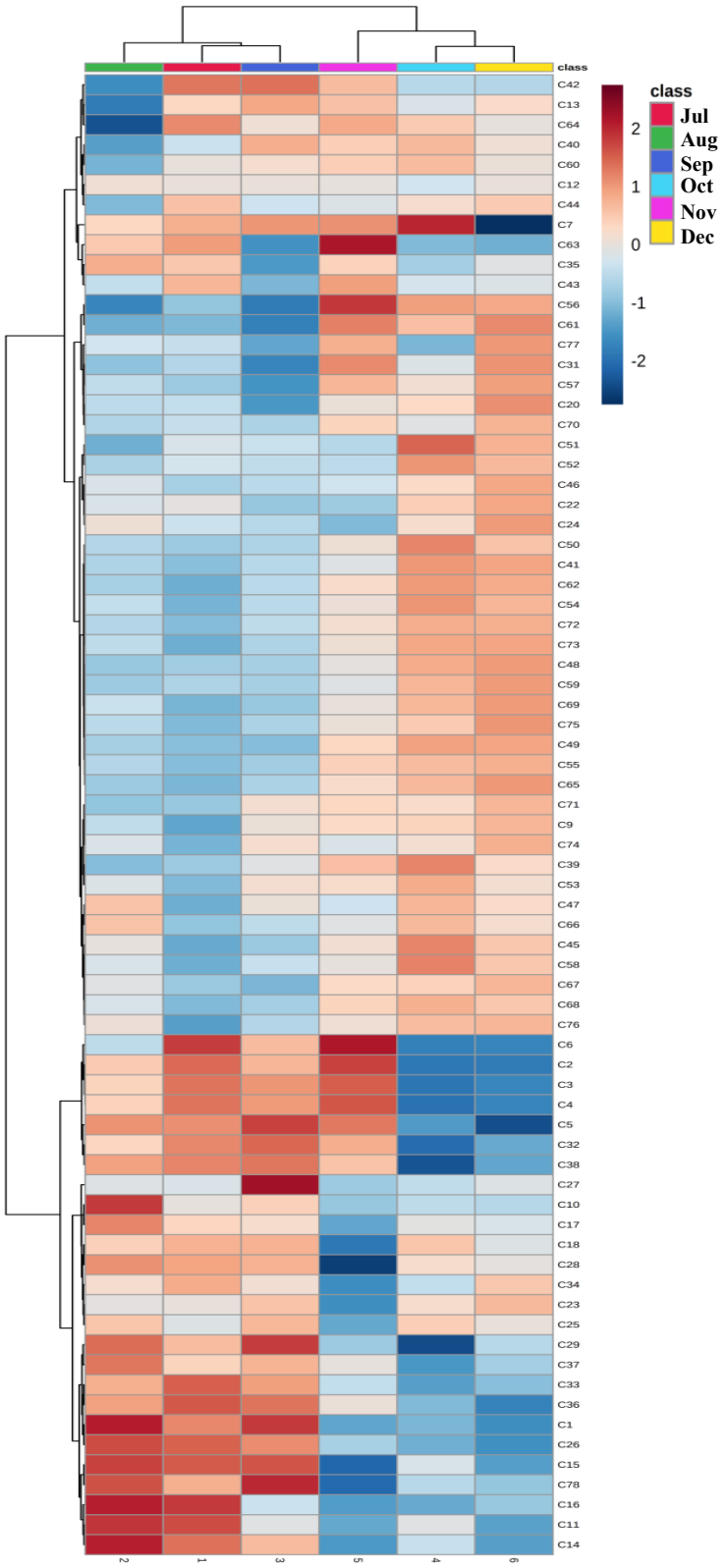

Source: Author (2019).

Figure S6. Graphs (a) PLS-DA score, (b) loading, and (c) VIP score obtained from the data analysis during July to December 2019 for the clone 'BR189'.

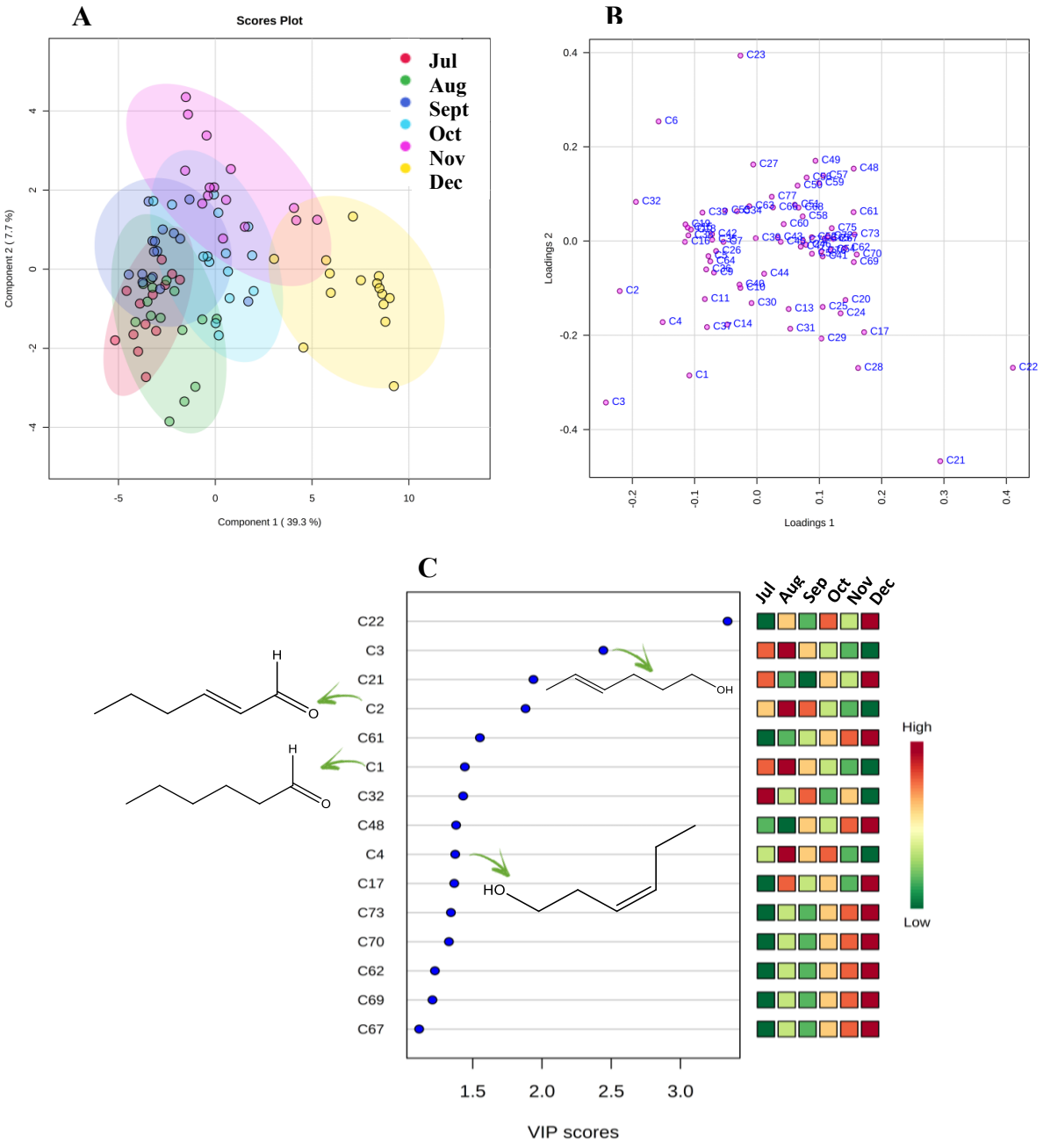

Source: Author (2019).

Figure S7. Heatmap graph constructed based on the volatile compounds identified in the leaf samples of the 'BRS 189' clone during the months of July to December 2019.

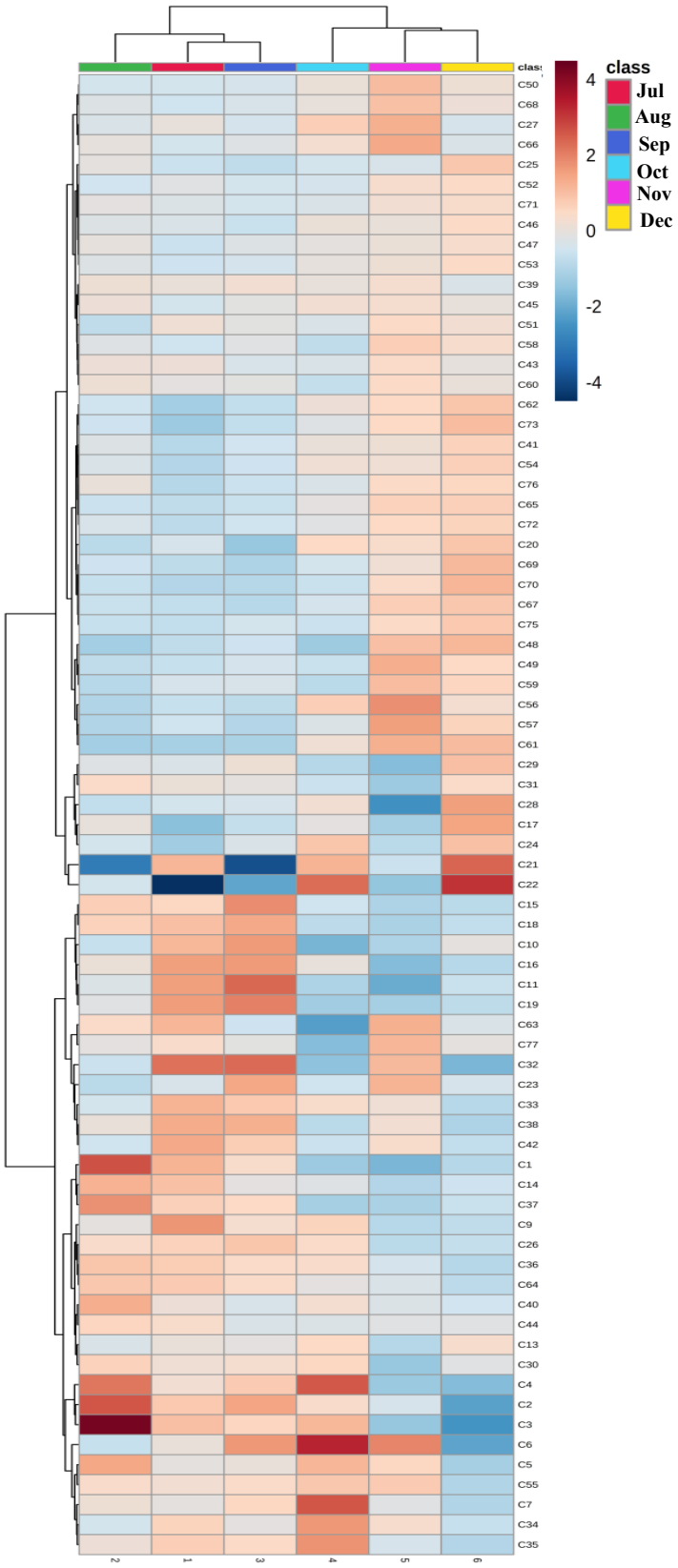

Source: Author (2019).

Figure S8. Graphs (a) PLS-DA score, (b) loading, and (c) VIP score obtained from the data analysis during the months of July to December 2019 for the clone 'BRS 265'.

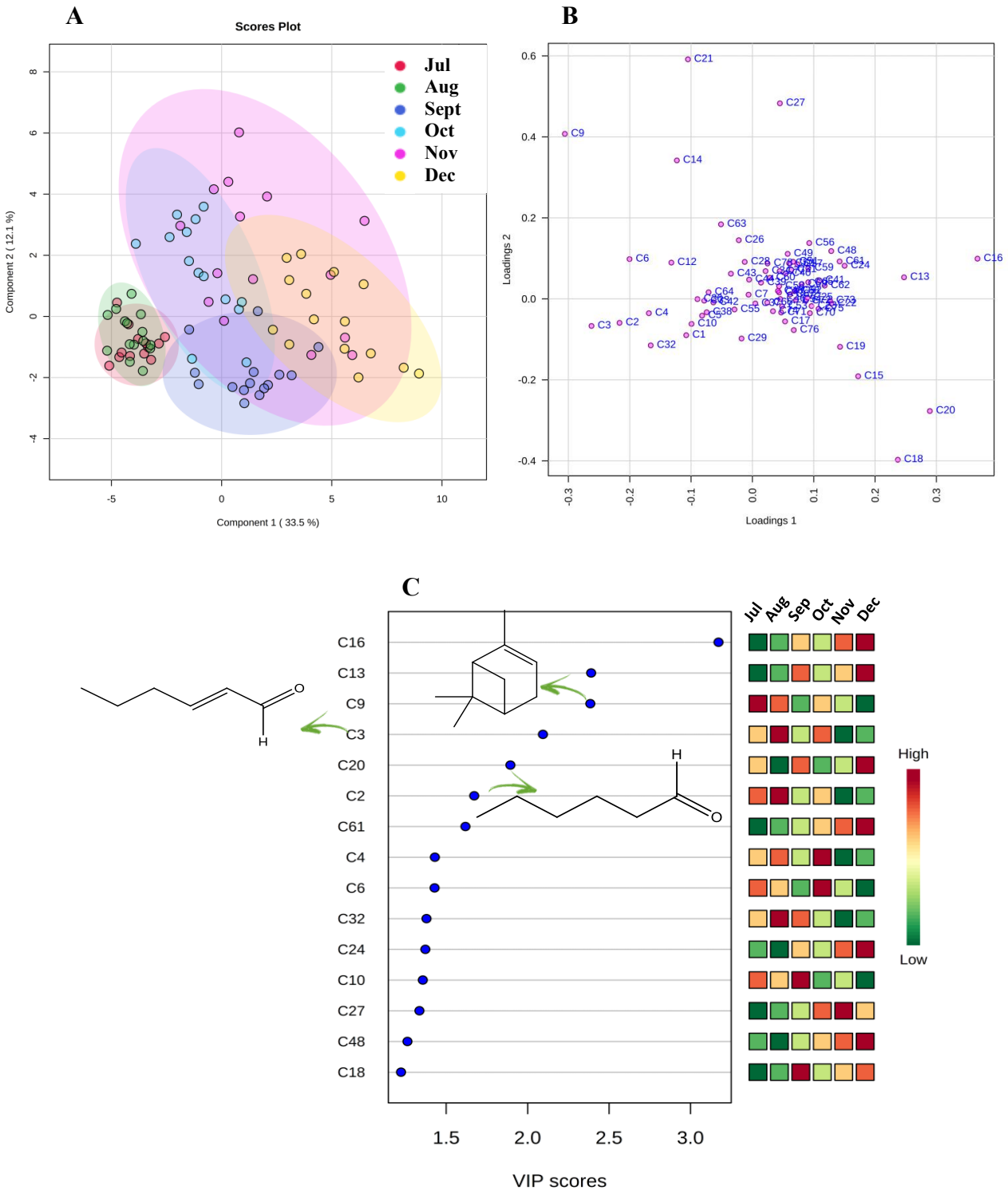

Source: Author (2019).

Figure S9. Heatmap graph constructed based on the volatile compounds identified in the leaf samples of the 'BRS 265' clone during the months of July to December 2019.

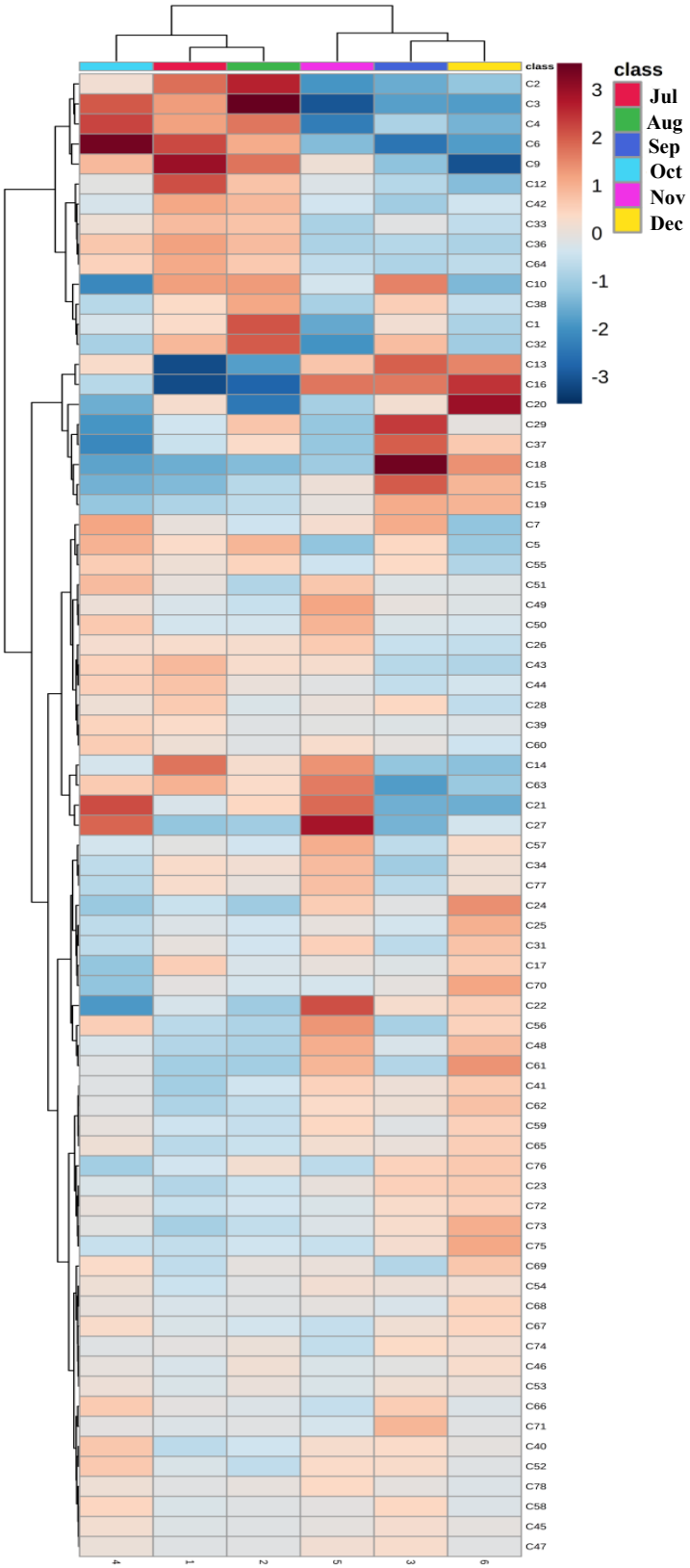

Source: Author (2019).

7 Estudo comparativo de compostos orgânicos voláteis de castanha de caju em resposta ao ataque de *Pseudoidium anacardii* em condições de campo: uma abordagem metabolômica

---

Comparative study of volatile organic compounds from cashew nuts in response to *Pseudoidium anacardii* attack under field conditions: a metabolomics approach

Debora B. de Sousa, Gisele S. da Silva, Luiz A. L. Serrano, Marlon V. V. Martins, Tigressa H. S. Rodrigues, Mary A. S. Lima, and Guilherme J. Zocolo

Artigo submetido ao periódico *Chemistry & Biodiversity*

ABSTRACT

Powdery mildew, a disease caused by the fungus *Pseudoidium anacardii* (F. Noack) U. Braun & R. T. A. Cook, affects the production of cashew nuts. Pathogen-resistant dwarf cashew clones have been implanted in orchards, however, the plant's chemical defense mechanisms are still unknown. The profile of volatile organic compounds (VOCs) emitted by cashew nut samples from clones resistant ('BRS 265', 'CCP 76' and 'BRS 226') and susceptible ('BRS 189') to the disease was investigated. Samples were collected during an infestation period (October 2019, Brazil) and 40 VOCs were provisionally identified by GC-MS. The data obtained underwent partial least squares discriminant analysis (PLS-DA), orthogonal partial least squares discriminant analysis (OPLS-DA), and hierarchical cluster analysis (HCA). Of note are the compounds 3-methyl-1-pentanol, ethyl isovalerate, α-pinene, ethyl tiglate, camphene, β-pinene, β-myrcene, ethyl hexanoate, α-terpinene, β-trans-ocimene, terpinolene, heptanoic acid, ethyl ester, perylene, nonanal, and camphor in the resistant clones, suggesting them as candidates for biomarkers of resistance to *P. anacardii* in cashew nuts.

Keywords: *Anacardium occidentale*, Resistance, *Pseudoidium anacardia*, Cashew nuts, Biomarkers.

Introduction

Belonging to the Anacardiaceae family, *Anacardium occidentale* (popularly known as cashew tree) is a perennial plant originally from Brazil, whose cultivation has become popular in several countries around the world, especially in Vietnam, India, Nigeria, Indonesia, the Philippines, Benin, Guinea-Bissau, and the Ivory Coast, due to its ease of adaptation to different environments. Among the 22 species that constitute the genus, *occidentale* is the most widespread from a commercial point of view (DE BRITO; DE OLIVEIRA SILVA; RODRIGUES, 2018; GYEDU-AKOTO; AMOAH; ODURO, 2019; OLIVEIRA; MOTHÉ; MOTHÉ, 2020). Trees can have different sizes, with the so-called giant cashew tree reaching over 15 m and the plants known as dwarf cashew trees reaching up to 4 m in height (ADIGA et al., 2019). Commercialized products from the cultivation of this fruit tree include the peduncle (false fruit), which is used in the food and beverage industries, and the cashew nut, which develops next to the peduncle and consists of the true fruit of this plant (PATADE et al., 2020).

Rich in fats, proteins, and carbohydrates, cashew nuts are an important product that significantly contributes to the economy of many countries, including Brazil (SALEHI et al., 2019b). This fruit is configured as an achene in the form of a kidney composed of a shell (pericarp) and almond. Cashew nut shells have important and diverse applications, including their use in the paint and lubricant industries. In addition, next to the almond, inside the pericarp, there is a liquid known as cashew nut liquid (CNSL), which has corrosive properties and is used by chemical industries (DE BRITO; DE OLIVEIRA SILVA; RODRIGUES, 2018), CNSL is also a rich source of long-chain unsaturated hydrocarbons that can be used as antioxidants (CHAUHAN; NATH, 2021). The world production of cashew nuts is 5 million tons per year, with Vietnam, Nigeria, India, and the Ivory Coast at the top of the list of largest producers (ADIGA et al., 2019).

In Brazil, where cashew trees have great socioeconomic relevance, it is estimated that the planted area is over 560 thousand hectares. Production exceeds 100,000 tons of cashew nuts, which are exported to countries on the European continent in addition to the United States, Canada, and the Netherlands, guaranteeing employment and income, especially for small and medium Brazilian producers (OLIVEIRA; MOTHÉ; MOTHÉ, 2020).

Despite being a highly resistant plant with a high yield in fruit production, the cashew tree can be compromised by fungal attack (WONNI, 2017). One of the main phytopathologies that affects the cashew tree and has become very important due to the drop in yield in the production of orchards is powdery mildew (FREIRE et al., 2002; LIMA;

MARTINS; CARDOSO, 2019); and its occurrence is recorded not only in Brazil but also in countries such as Mozambique, Tanzania, and Uganda, which are important cashew producers.

Belonging to the order *Erysiphales*, which consists of a group of more than 800 species of pathogens that are notably involved in the parasitism of more than 1500 plant genera, *Pseudoidium anacardii* (F. Noack) U. Braun & RTA Cook, a biotrophic ascomycete, has been identified as the pathogen responsible for this disease, especially in plants of the Anacardiaceae family (PINTO et al., 2016a; FONSECA et al., 2019). Fungal attacks occur on flowers, leaves, peduncles, "maturis" (green-cashews), and cashew nuts, appearing as a grayish powder on these structures, culminating in the loss of nutrients by the plant.(PINTO et al., 2016a) Severe epidemics are becoming increasingly common and can start during the flowering period of the plant and extend to the final stage of production (MARTINS et al., 2018).

The treatment of the disease is carried out in the orchards through the application of sulfur-based compounds sprayed directly on the plants; however, problems of an environmental nature and from the point of view of legislation, in addition to the need for equipment and labor for the application of these products, make the practice difficult. As an alternative to pesticides, cashew plants that are resistant to the pathogen that causes powdery mildew are already being cultivated (PINTO et al., 2018).

In addition to their remarkable resistance to several diseases, many dwarf cashew clones have become attractive for cultivation in orchards because they have high production and begin to bear fruit in the first years of existence, in addition to being easy to harvest (SILVA et al., 2012). Despite the use of dwarf cashew clones that are more resistant to powdery mildew, little is known about the chemical mechanisms responsible for this resistance.

Fixed and volatile metabolites obtained from different cashew structures have been reported in the literature for their various biological activities, especially antimicrobial (MAIA S.; ANDRADE A., 2009; MATA, 2018). Volatile organic compounds (VOCs) play an important role in the communication of plants with the surrounding environment so that they become chemical signals and can trigger response mechanisms that can protect plants against biotic and abiotic stresses (NIEDERBACHER; WINKLER; SCHNITZLER, 2015; RICCIARDI et al., 2021; ROSENKRANZ et al., 2021).

Based on the above, four dwarf cashew clones coded as 'CCP 76', 'BRS 226', 'BRS 265' and 'BRS 189' were selected to investigate how VOCs emitted by nuts may be contributing to the defense against the pathogen powdery mildew. The choice of clones was based on their importance for agriculture and trade, as well as on the different levels of response regarding resistance and susceptibility to the disease presented by each type of clone. The literature

reports greater susceptibility to the pathogen on the part of the ‘BRS 189’ clone, whereas the ‘BRS 265’, ‘CCP 76’, and ‘BRS 226’ clones were identified as more resistant.

To carry out this study, the volatile compounds were analyzed using gas chromatography coupled with mass spectrometry, and the data obtained were subjected to chemometric analysis to identify compounds that may be related to the greater defense of resistant clones to the disease. Thus, metabolomics combined with the use of chemometric tools allows for better organization of data in addition to allowing a large amount of data to be analyzed, providing important answers about the compounds present in the samples, which can be identified as candidates for biomarkers of resistance to powdery mildew (VAN DER GREEF; SMILDE, 2005; WIKLUND et al., 2008; PRETORIUS et al., 2021).

Results and Discussion

The pathogen

Regarding the clones investigated, highlight the high susceptibility of the 'BRS 189' clone, while the 'BRS 265' and 'CCP 76' clones are shown to be partially resistant (PINTO et al., 2018). The clone 'BRS 226' had greater resistance to pathogens that cause powdery mildew. In October, it was possible to verify the presence of the pathogen, especially in the cashew nuts of the clone 'BRS 189'.

The collection of samples carried out in October 2019 showed that, about the plants of the 'BRS 189' clone, there were cashew nuts with severe symptoms of the disease as opposed to the cashew nuts of the clones 'BRS 265', 'BRS 226', and 'CCP 76', which were more resistant due to the low or non-occurrence of powdery mildew symptoms in these structures.

Profile of VOCs

Forty VOCs were tentatively identified in the nut samples of the four cashew clones analyzed (Table 4). Most compounds belong to the terpene class; however, alcohols, esters, ketones, aldehydes, and hydrocarbons have also been identified. Based on bibliographic research that takes into account family, genus, and species (BICALHO; REZENDE, 2001; GARRUTI et al., 2003; CEVA-ANTUNES et al., 2006; DZAMIC et al., 2009; JELLER; RÉ; MATIAS, 2010; AGILA; BARRINGER, 2011; GEBARA et al., 2011; LING et al., 2016; SALEHI et al., 2019; LIU et al., 2020), it was observed that the profile of the volatile organic

compounds of the clones is in line within agreement with the compounds already reported in the literature for the genus *Anacardium*.

Table 4 - Volatile organic compounds identified in cashew nuts samples from dwarf cashew clones in October 2019 (*to be continued*).

	COMPOUND	RI LITERATURE	RI FOUND	MATCH	R. MATCH	CHEMICAL CLASS	MOLECULAR FORMULA
C1	3-methyl-1-pentanol	833	840	576	818	alcohol	$C_6H_{14}O$
C2	ethyl isovalerate	849	848	872	885	ester	$C_7H_{14}O_2$
C3	hexanol	863	863	571	718	alcohol	$C_6H_{14}O$
C4	styrene	898	889	973	974	hydrocarbon	C_8H_8
C5	heptanal	901	899	931	942	aldehyde	$C_7H_{14}O$
C6	α-pinene	932	932	854	897	terpene	$C_{10}H_{16}$
C7	ethyl tiglate	929	936	664	790	ester	$C_7H_{12}O_2$
C8	camphene	946	946	770	880	terpene	$C_{10}H_{16}$
C9	pentanoic acid, 3-methyl-, ethyl ester	949	955	795	887	terpene	$C_{10}H_{16}$
C10	benzaldehyde	952	959	879	946	aldeído	C_7H_6O
C11	β-pinene	974	974	913	919	terpene	$C_{10}H_{16}$
C12	3-octanona	979	984	713	781	ketone	$C_8H_{16}O$
C13	β-myrcene	988	988	802	827	terpene	$C_{10}H_{16}$
C14	ethyl hexanoate	997	996	704	915	ester	$C_8H_{16}O_2$
C15	octanal	998	1000	812	963	aldehyde	$C_8H_{16}O$
C16	α-phellandrene	1002	1002	928	938	terpene	$C_{10}H_{16}$
C17	3-carene	1008	1008	843	850	terpene	$C_{10}H_{16}$

Table 4 - Volatile organic compounds identified in cashew nuts samples from dwarf cashew clones in October 2019 (*continuation*).

	COMPOUND	RI LITERATURE	RI FOUND	MATCH	R. MATCH	CHEMICAL CLASS	MOLECULAR FORMULA
C18	α-terpinene	1014	1015	856	864	terpene	$C_{10}H_{16}$
C19	o-cymene	1022	1023	935	949	hydrocarbon	$C_{10}H_{14}$
C20	limonene	1024	1027	888	889	terpene	$C_{10}H_{16}$
C21	β-*cis*-ocimene	1032	1035	709	811	terpene	$C_{10}H_{16}$
C22	β-*trans*-ocimene	1044	1045	901	906	terpene	$C_{10}H_{16}$
C23	γ-terpinene	1054	1056	814	854	terpene	$C_{10}H_{16}$
C24	1-octanol	1063	1067	815	850	terpene	$C_8H_{18}O$
C25	terpinolene	1086	1086	766	783	terpene	$C_{10}H_{16}$
C26	p-cymenene	1089	1089	812	867	hydrocarbon	$C_{10}H_{14}$
C27	heptanoic acid, ethyl ester	1097	1094	767	837	ester	$C_9H_{18}O_2$
C28	perillene	1102	1098	814	854	terpene	$C_{10}H_{14}O$
C29	nonanal	1100	1100	929	934	aldehyde	$C_9H_{18}O$
C30	(4*E*,6*Z*)-*allo*-ocimene	1128	1126	838	887	terpene	$C_{10}H_{16}$
C31	camphor	1141	1144	841	934	terpene	$C_{10}H_{16}O$
C32	menthol	1167	1171	700	757	alcohol	$C_{10}H_{20}O$
C33	butanoic acid, 3-hexenyl ester, (*E*)-	1184	1181	799	867	ester	$C_{10}H_{18}O_2$
C34	dodecane	1200	1195	703	802	hydrocarbon	$C_{12}H_{26}$
C35	decanal	1201	1204	825	864	aldehyde	$C_{10}H_{20}O$
C36	caryophyllene	1417	1422	876	895	terpene	$C_{15}H_{24}$

Table 4 - Volatile organic compounds identified in cashew nuts samples from dwarf cashew clones in October 2019 (*conclusion*).

	COMPOUND	RI LITERATURE	RI FOUND	MATCH	R. MATCH	CHEMICAL CLASS	MOLECULAR FORMULA
C37	α –bergamotene	1432	1435	827	908	terpene	$C_{15}H_{24}$
C38	α-muurolene	1500	1502	827	837	terpene	$C_{15}H_{24}$
C39	δ-cadinene	1522	1524	770	789	terpene	$C_{15}H_{24}$
C40	γ-cadinene	1513	1521	636	656	terpene	$C_{15}H_{24}$

Data analysis

Analysis of the volatile profiles of cashew nuts allowed us to verify that there are differences between healthy samples of resistant and diseased clones of the clone susceptible to powdery mildew, a fact that is illustrated by PLS-DA analysis. PLS-DA models indicate clustering trends between data that share similarities, and this type of analysis is commonly used in metabolomic studies for the classification and identification of biomarkers (SZYMAŃSKA et al., 2012).

The PLS-DA plot (FIGURE 30) shows the formation of four distinct groups, consisting of healthy samples of clones 'BRS 226', 'CCP 76' (which are in the positive part of component 1), and 'BRS 265' (which is in the positive part of component 2, but negative in component 1). As for the samples referring to the clone susceptible to the attack of the pathogen, 'BRS 189', which are in the negative part of both components, it is possible to verify that the two groups formed (referring to the sick and healthy samples of this clone) intersect with each other, a fact that raises similarity in the profile of metabolites of the sick and healthy samples for the 'BRS 189'. This fact allows us suggests that, most likely, this similarity in the metabolite profile contributes to the greater susceptibility of this clone to powdery mildew compared to the other clones under study.

Figure 30. PLS-DA graph constructed with the profile data of volatile metabolites of healthy cashew nuts from clones 'CCP 76', 'BRS 226', 'BRS 265', 'BRS 189' and samples diseased cashew nuts from 'BRS 189'.

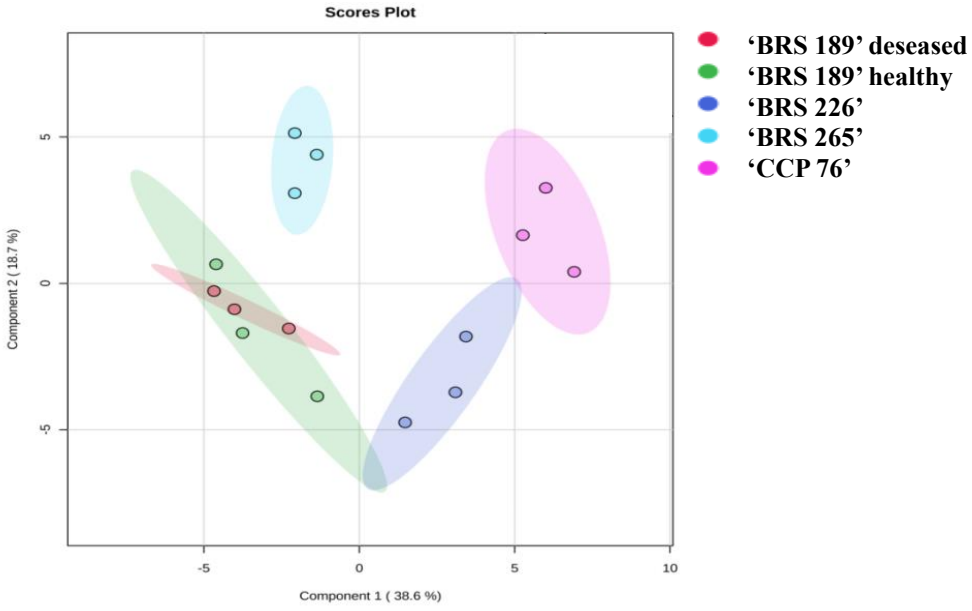

Source: Author (2019).

OPLS-DA models were built and their validity was evaluated based on the parameters R^2Y and Q^2 (Table 5) selected to represent the predictive capacity.

Table 5. Multivariate analysis of PLS-DA and OPLS-DA models of different groups for the metabolomic profile of cashew clones against powdery mildew.

Model	Type	R^2Y	Q^2
'CCP 76', 'BRS 226', 'BRS 265', 'BRS 189' healthy *vs* 'BRS 189' diseased	PLS-DA	0,936	0,597
'BRS 226' healthy *vs* 'BRS 189' diseased	OPLS-DA	0,967	0,912
'CCP 76' healthy *vs* 'BRS 189' diseased	OPLS-DA	0,975	0,885
'BRS 265' healthy *vs* 'BRS 189' diseased	OPLS-DA	0,995	0,661

Next, the results obtained through comparative analysis between samples of healthy resistant ('BRS 226') and moderately resistant ('CCP 76' and 'BRS 265') clones against the samples of the diseased susceptible clone ('BRS 189').

Comparative analysis of the volatile compound profiles of healthy 'BRS 226' clones (resistant to powdery mildew) vs diseased 'BRS 189' (susceptible to powdery mildew)

The HCA plot (FIGURE 31) shows that the profile of volatile metabolites varied according to the resistance and susceptibility of the clones. This was confirmed by the clear separation between the samples in the two clusters.

The OPLS-DA score graph (FIGURE 32a) explains 79.1% of the total variance and makes it possible to verify that two separate groups were formed. The values of the quality parameters for the model were satisfactory: R^2Y= 0.967 and Q^2=0.912 (CHAGAS-PAULA et al., 2015b). Figure 32B shows, through the S-plot, scatter plot, the variables responsible for the separation between the groups, so that the compounds responsible for the discrimination of the diseased samples of the susceptible clone ('BRS 189') are found on the negative axis, while on the positive axis there are the metabolites related to healthy samples of the resistant clone ('BRS 226').

The VIP scores (FIGURE 32C) corroborate the results obtained in the OPLS-DA S-plot, highlighting the most important molecules in the projection of the data, 3-methyl-1-

pentanol (C1), ethyl isovalerate (C2), styrene (C4), ethyl tiglate (C7), ethyl hexanoate (C14), and perillene (C28), which have high concentrations in healthy nuts. In the samples of diseased caashew nuts of the susceptible clone, the compounds heptanal (C5), benzaldehyde (C10), β-myrcene (C13), o-cymene (C19), limonene (C20), camphor (C31), menthol (C32), and α-bergamotene (C37) are highlighted.

Figure 31. HCA graph obtained from comparative analysis data between healthy samples of clone ‘BRS226’ (resistant to powdery mildew) and diseased samples of clone ‘BRS189’ (susceptible to powdery mildew).

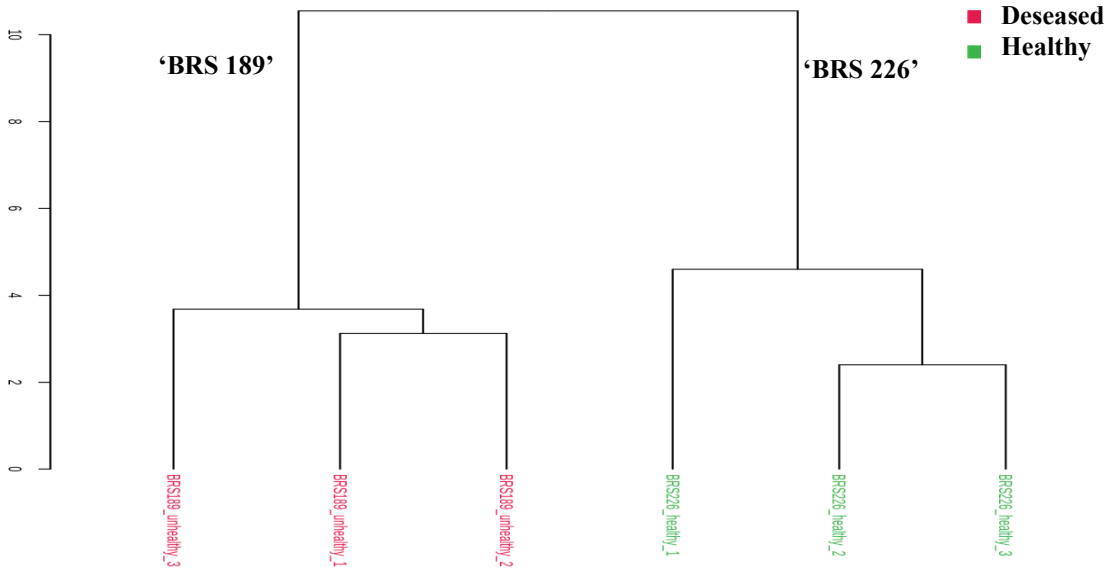

Source: Author (2019).

Figure 32. Graphs (a) OPLS-DA score and (b) S-plot and (c) VIP scores obtained from comparative analysis data between samples of healthy cashew nuts from clone ‘BRS 226’ and diseased from clone ‘BRS 189’ in October 2019.

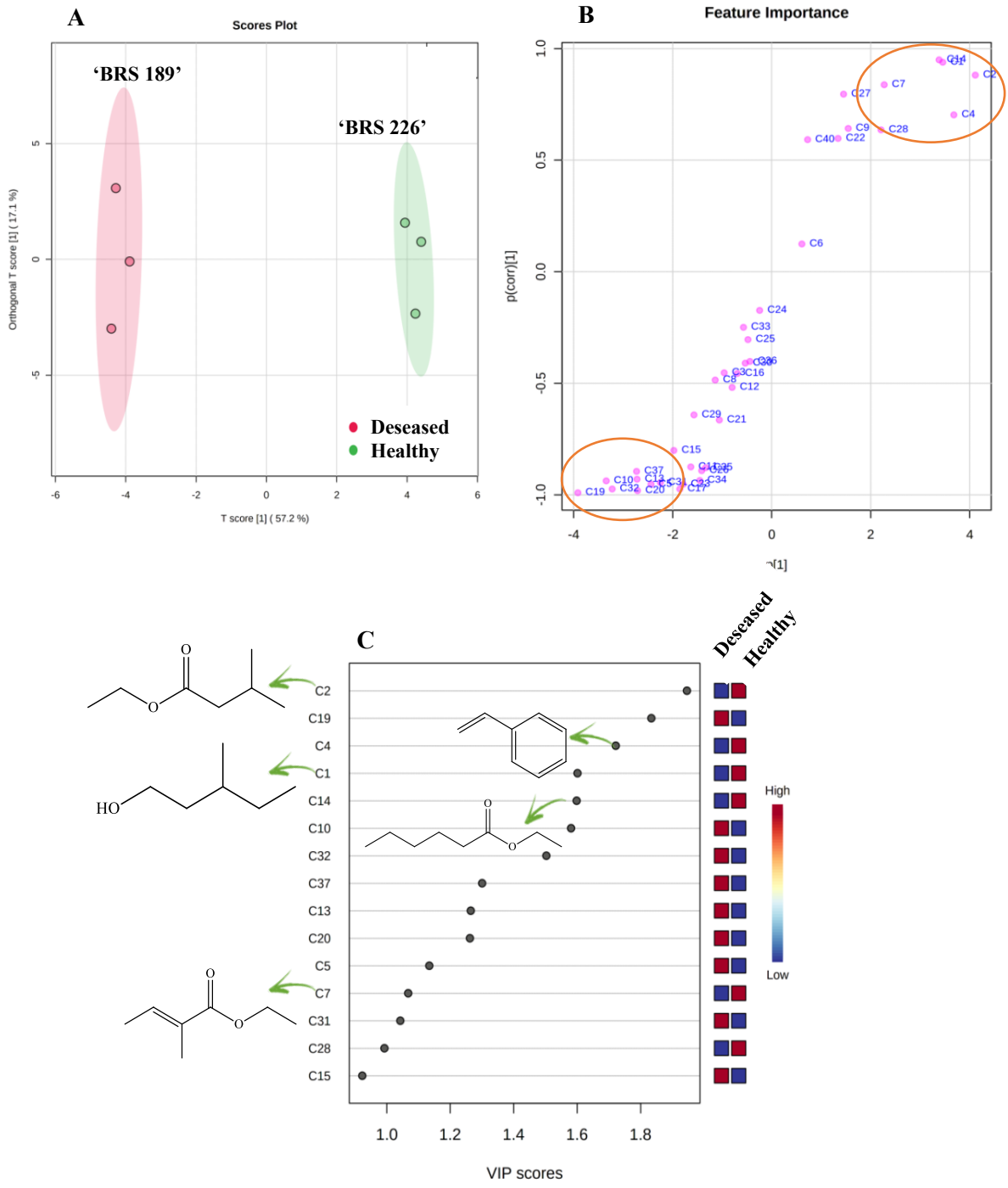

Source: Author (2019).

Comparative analysis of the volatile compound profiles of healthy 'CCP 76' clones (resistant to powdery mildew) vs diseased 'BRS 189' (susceptible to powdery mildew)

The HCA analysis graph (FIGURE 33) shows the formation of two clusters, evidencing the distinction in the profiles of volatile organic compounds of the samples of the healthy and disease-resistant clones.

Figure 33. HCA graph obtained from comparative analysis data between healthy samples from clone 'CCP 76' (resistant to powdery mildew) and diseased samples from clone 'BRS 189' (susceptible to powdery mildew).

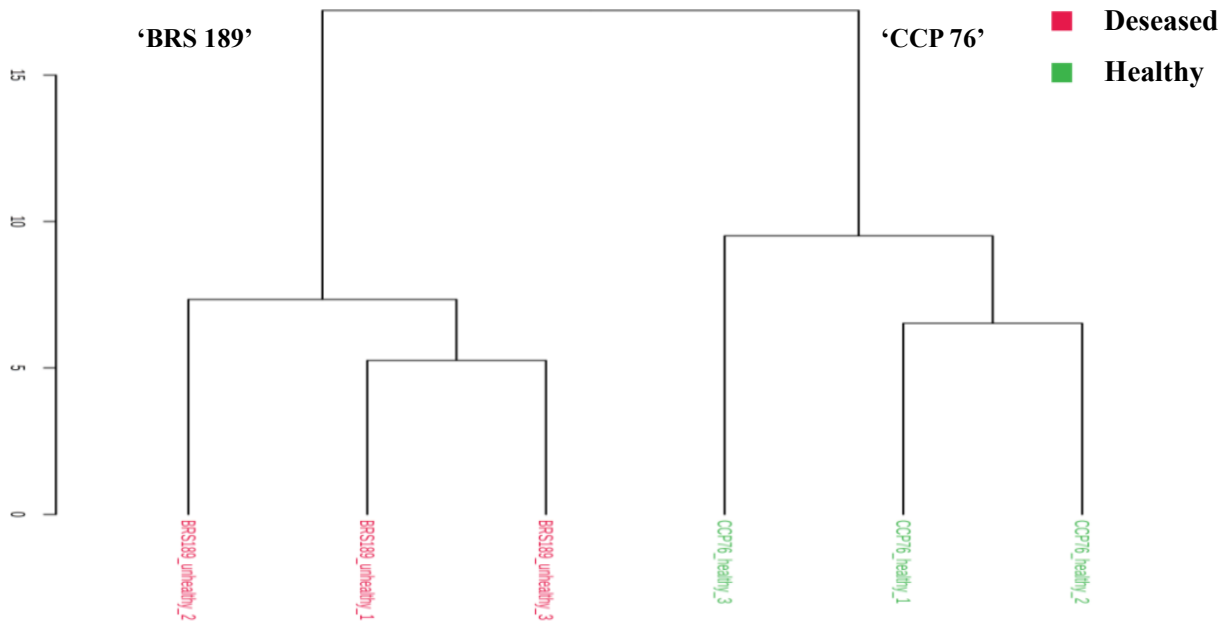

Source: Author (2019).

The OPLS-DA score plot (FIGURE 34a) explained 61.1% of the total variance and confirmed the separation observed in HCA. In the S-plot scatterplot (FIGURE 34b), the discriminating compounds are highlighted by a red circle, so that on the negative axis are the compounds responsible for the discrimination of the diseased cashew nut samples, whereas on the positive axis, the metabolites related to the healthy samples were analyzed. The values of the quality parameters for the model were satisfactory: R^2Y= 0.975 and Q^2=0.885, suggesting statistically significant differences between the analyzed samples (CHAGAS-PAULA et al.,

2015b).

The VIP scores (FIGURE 34c) showed that the metabolites present in healthy samples of the resistant clone included ethyl isovalerate (C2), ethyl tiglate (C7), ethyl 3-methyl-pentanoate (C9), ethyl hexanoate (C14), β-trans-ocimene (C22), ethyl heptanoate (C27), and perillene (C28) (PAPAGEORGIOU; ASSIMOPOULOU; YANNOVITS-ARGIRIADIS, 1999; MAIA; ANDRADE; ZOGHBI, 2000b; DZAMIC et al., 2009; DE OLIVEIRA NOBRE et al., 2015; SALEHI et al., 2019). In the sick samples of the susceptible clone, compounds 3-methyl-1-pentanol (C1), hexanol (C3), heptanal (C5), camphene (C8), benzaldehyde (C10), and β-myrcene (C13) were highlighted by the VIP (MAIA; ANDRADE; ZOGHBI, 2000; DZAMIC et al., 2009; AGILA; BARRINGER, 2011; SAMPAIO et al., 2011; SOSA-MOGUEL et al., 2018b; SALEHI et al., 2019).

Figure 34. Graphs (a) OPLS-DA score and (b) S-plot and (c) VIP score obtained from comparative analysis data between samples of healthy cashew nuts from clone ‘CCP 76’ and diseased from clone ‘BRS 189’ in October 2019.

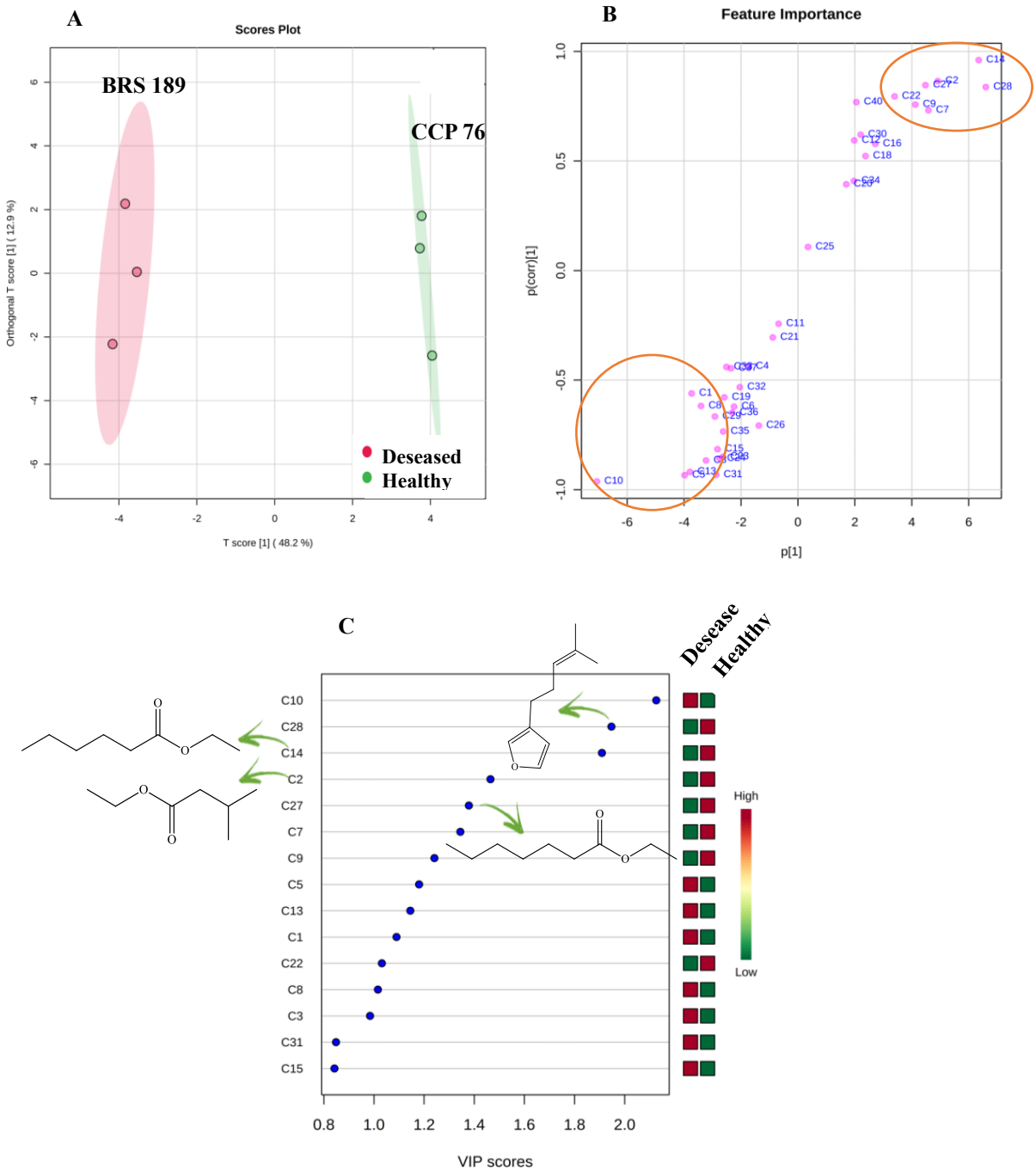

Source: Author (2019).

Comparative analysis of the volatile compound profiles of healthy ‘BRS 265’ clones (resistant to powdery mildew) vs diseased ‘BRS 189’ (susceptible to powdery mildew)

The HCA graph (FIGURE 35) constructed with data referring to healthy samples of clone 'BRS 265' and sick samples of clone 'BRS 189' shows that there are differences in the profiles of volatile metabolites between the two groups.

Figure 35. HCA graph obtained from comparative analysis data between healthy samples from clone ‘BRS 265’ (moderately to powdery mildew) and diseased samples from clone ‘BRS 189’ (susceptible to powdery mildew).

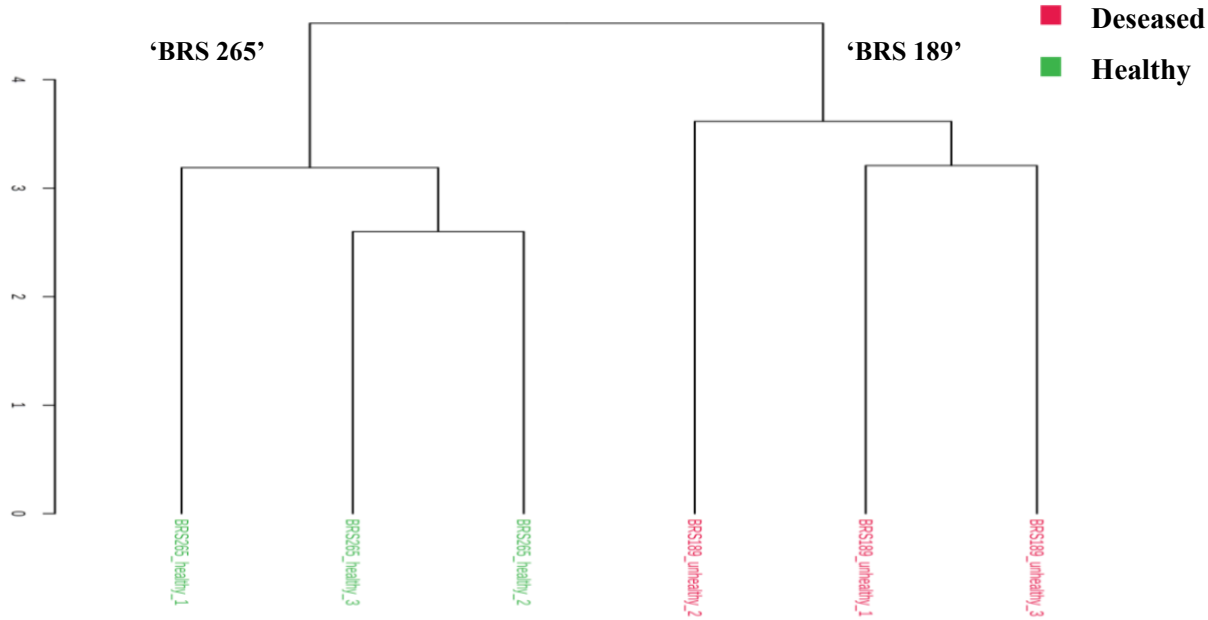

Source: Author (2019).

The OPLS-DA score graph (FIGURE 36a), which explains 53.5% of the total variance, corroborates the separation observed in the HCA, and the S-plot (FIGURE 36b) illustrates the metabolites responsible for this differentiation. On the negative axis of the S-plot, the compounds responsible for the discrimination of samples of diseased cashew nuts, while on the positive axis are the metabolites related to healthy samples. The values of the quality parameters for the model were satisfactory: $R^2Y = 0.995$ and $Q^2 = 0.661$, suggesting statistically significant differences between the analyzed samples (CHAGAS-PAULA et al., 2015b).

The VIP score (FIGURE 36c) highlights that the metabolites present in healthy samples of clone 'BRS 265' include α-pinene (C6), camphene (C8), β-pinene (C11), β-myrcene (C13), α-terpinene (C18), terpinolene (C25) and camphor (C31) (Dzamic et al., 2009; Salehi et al., 2019). For the diseased samples of the 'BRS 189' clone, the metabolites styrene (C4), ethyl

tiglate (C7), benzaldehyde (C10), 1-octanol (C24), dodecane (C34), and γ-cadinene (C40) (MAIA; ANDRADE; ZOGHBI, 2000; AGILA; BARRINGER, 2011; SALEHI et al., 2019).

Figure 36. Graphs (a) OPLS-DA score and (b) S-plot and (c) VIP score obtained from comparative analysis data between samples of healthy cashew nuts from clone ‘BRS 265’ and diseased from clone ‘BRS 189’ in October 2019.

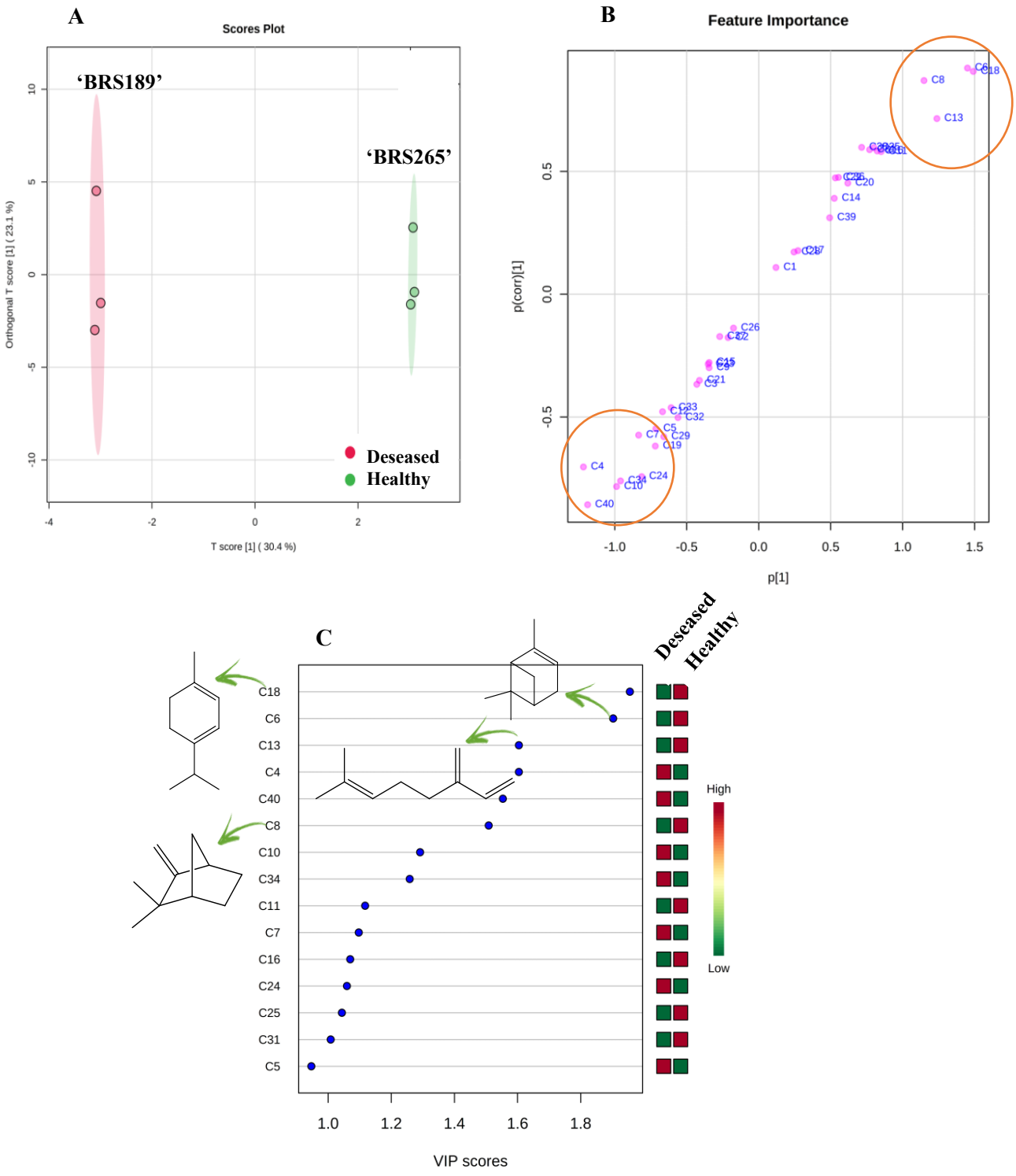

Source: Author (2019).

Comparative analysis of the profiles of volatile compounds from healthy and diseased samples of the 'BRS 189' clone (susceptible to powdery mildew)

As the samples referring to both diseased and healthy cashew nuts of the 'BRS 189' clone were presented in the same group in the PLS-DA graph (FIGURE 30), HCA and OPLS-DA graphs were constructed to verify the metabolites present in the samples of this clone in the absence and presence of powdery mildew symptoms.

HCA (FIGURE 37) showed that there was no efficient separation between samples, suggesting that healthy and diseased nuts share some similarities between their volatile metabolite profiles.

Figure 37. HCA graph obtained from comparative analysis data between healthy and diseased samples of clone 'BRS 189' (susceptible to powdery mildew).

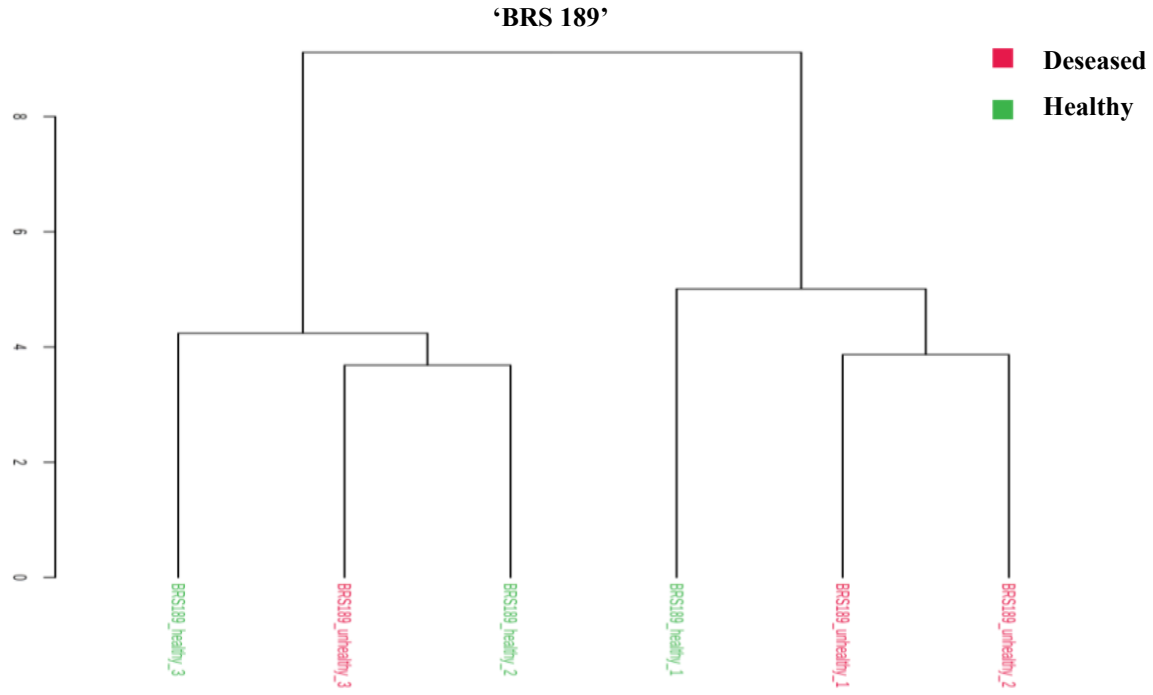

Source: Author (2019).

The OPLS-DA score (FIGURE 38a) explained 70.7% of the total variance and showed the separation between samples of healthy and diseased cashew nuts. The S-plot (FIGURE 38b) illustrates which metabolites are responsible for the observed differentiation, so that, on the negative axis, are the compounds responsible for the discrimination of samples of

diseased cashew nuts, while on the positive axis are the metabolites related to healthy samples of clone 'BRS189'.

The VIP scores (FIGURE 38c) corroborate the data of metabolites responsible for the separation of the samples presented by the S-plot, highlighting, for healthy cashew nuts, the compounds 3-methyl-1-pentanol (C1), ethyl isovalerate (C2), ethyl tiglate (C7), ethyl 3-methyl-pentanoate (C9), 3-octanone (C12) and ethyl hexanoate (C14) as the most important in the projection of the variables. Benzaldehyde (C10) and perillene (C28) were detected in sick cashew nut samples.

Figure 38. Graphs (a) OPLS-DA scores and (b) S-plot and (c) VIP scores obtained from comparative analysis data between samples of healthy and diseased cashew nuts from the 'BRS 189' clone in October 2019.

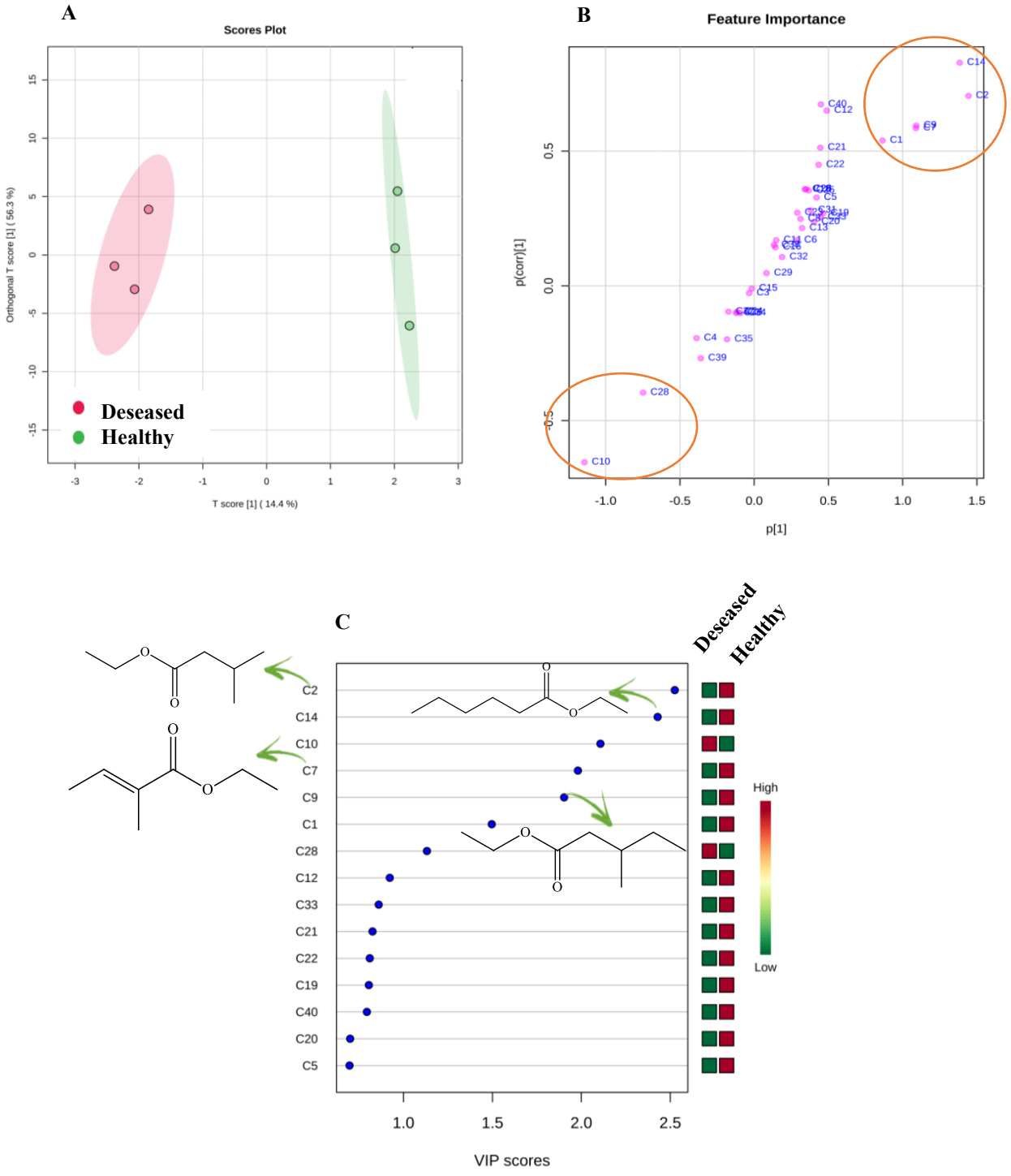

Source: Author (2019).

In volatiles oils, compounds with a high lipophilic character, such as terpenes, terpenoids, esters, and phenolic compounds, predominate. The antimicrobial action of these oils is due to their ease of crossing the cell wall and plasma membrane, causing damage to the cells of microorganisms (ANDRADE et al., 2014). Volatiles oils play an important role in plant defense mechanisms owing to their antifungal, antibacterial, antiviral, and insecticidal activities (CHOUHAN; SHARMA; GULERIA, 2017).

The compound identified as present in most healthy samples was ethyl hexanoate (C14) (MAIA; ANDRADE; ZOGHBI, 2000b). Therefore, it can be pointed out as a possible biomarker of resistance of cashew nuts to powdery mildew, along with the compound ethyl tiglate (C7). The antimicrobial activity of volatile oil rich in these compounds has already been reported in the literature (PASSOS et al., 2003).

In addition, several compounds belonging to the class of terpenes, terpenoids, and esters are highlighted by the VIP score graphs. The proven antimicrobial action of oils rich in these classes of compounds (BASSOLÉ; JULIANI, 2012) may explain the greater resistance to powdery mildew observed in the healthy clones. Thus, the biosynthesis of compounds such as ethyl isovalerate (C2), α-pinene (C6), ethyl tiglate (C7), camphene (C8), ethyl 3-methyl-pentanoate (C9), β-pinene (C11), β-myrcene (C13), ethyl hexanoate (C14), 3-carene (C17), α-terpinene (C18), β-*trans*-ocimene (C22), terpinolene (C25), ethyl heptanoate (C27), perilleno (C28) and camphor (C31), highlighted in the samples of healthy resistant clones, may indicate the greater resistance of clones 'BRS 226', 'CCP 76' and 'BRS 265' when compared to clone 'BRS 189'.

On the other hand, in the healthy cashew nuts of the susceptible clone, compounds belonging to the classes of ketones, alcohols, and esters were found. According to studies by (PUŠKÁROVÁ et al., 2017), volatiles oils containing mostly compounds belonging to these classes are generally not very active against microorganisms. This justifies the fact that this clone, when compared to the others, is the most susceptible to powdery mildew because it is unable to biosynthesize compounds with high antimicrobial potential at high concentrations. In contrast, sick samples contained compounds such as alcohols (3-methyl-1-pentanol (C1), hexanol (C3), 1-octanol (C24)), aldehydes (heptanal (C5), benzaldehyde (C10)), esters (ethyl tiglate (C7)), and hydrocarbons (styrene (C4), o-cymene (C19), and dodecane (C34)). The literature reports that volatiles oils with compounds of these classes as the majority show little activity against microorganisms (KALEMBA; KUNICKA, 2005).

The antimicrobial activity of volatiles oils is due to their rich composition in terms of compounds of different chemical classes, such as phenols, aldehydes, ketones, alcohols,

esters, ethers, and hydrocarbons, whose interactions with each other can result in additive or synergistic effects (BASSOLÉ; JULIANI, 2012). The mechanisms that govern the activity of volatiles oils are complex and involve the inhibition of the synthesis of DNA, RNA, proteins, and polysaccharides from fungi and bacteria, depending on the type of microorganism and the compounds present in the volatile oil (KALEMBA; KUNICKA, 2005).

The activity of a volatile oil is not determined by the amount of its constituents, but by the proportion between them. Many oils that are rich in esters, ketones, and hydrocarbons do not present considerable antimicrobial activity; however, when they contain terpenoids, aldehydes, and even hydrocarbons in high proportions, they may present more appreciable activity (KALEMBA; KUNICKA, 2005; ANDRADE et al., 2014). This is due to interactions between compounds that can lead to different effects, such as antagonistic, additive, or synergistic (BASSOLÉ; JULIANI, 2012).

Different parts of the same plant can contain volatiles oils with different chemical constituents; therefore, they have different antimicrobial activities (KALEMBA; KUNICKA, 2005). Thus, the chemical composition of the volatile compound profiles of the chestnuts may contain compounds that make them more resistant, different from those present in the leaves and flowers of the cashew tree.

Conclusions

Through the analysis of healthy cashew nuts from resistant and diseased clones of the clone susceptible to powdery mildew during the period of infestation of the pathogen in the field, it was possible to verify that the samples presented different profiles of VOCs. With the aid of chemometric tools, the analysis showed that 3-methyl-1-pentanol, ethyl isovalerate, α-pinene, ethyl tiglate, camphene, β-pinene, β-myrcene, ethyl hexanoate, α-terpinene, β-trans-ocimene, terpinolene, heptanoic acid, ethyl ester, perillene, nonanal, and camphor were more abundant in the samples of healthy resistant clones, thus contributing significantly to the differentiation of the samples. It has been proven in the literature that volatiles oils, whose composition includes such compounds, have antifungal activity and are biosynthesized from the plant's defense system when faced with a stressful situation caused by the presence of pathogens. This fact provides support for the identification of these VOCs as possible biomarkers of resistance against *P. anacardii* attack against cashews. Thus, the highlighted compounds are biosynthesized by the cashew nuts of the clones 'BRS 226', 'CCP 76' and 'BRS 265' as one of the forms of plant defense, a fact that was not observed in the diseased samples

of the clone susceptible to the pathogen, 'BRS 189', which did not present such compounds in significant concentrations for them to be highlighted as important in the projections of the data in the chemometric analyses.

The results obtained corroborate the literature data that suggest VOCs as important compounds in plant defense against the presence of phytopathogens and suggest these substances as candidates for resistance biomarkers and, thus, as possible biocontrol agents. These results can help in future studies on the development of pesticides based on natural products, as well as in the understanding of the behavior of early dwarf cashew clones against this phytopathology, a fact that can contribute to research on the selection of individuals in the implantation of orchards less susceptible to *P. anacardii*.

Experimental Section

Plant material

The cashew tree clones from which the nuts were collected are part of the Experimental Field of Embrapa Agroindústria Tropical, planted under rainfed conditions and located in the municipality of Pacajus, in the state of Ceará, Brazil, with geographic coordinates of 4 ° 10 S and 38 ° 27' W and an altitude of 60 m above sea level. In the selected area of the field, there are 16 lines containing, in each one, 30 plants of a type of cashew tree clone from Embrapa coded as 'CCP 76', 'BRS 226', 'BRS 189', and 'BRS 265'. The field lines were divided into four blocks (randomized block design) and, since its implementation in May 2011, the field has received all the treatments recommended by (SERRANO; OLIVEIRA, 2013).

To carry out this work, samples of cashew nuts were collected from five plants previously selected from each of the four types of clone to be studied ('CCP 76', BRS 226', 'BRS 189' and 'BRS 265'). The collection of samples took place in October (incidence of the disease) of 2019 as follows: cashew nuts with an approximate size of 5 centimeters and without symptoms of powdery mildew disease for the four clones were obtained and, in addition to these, they have also collected cashew nuts with symptoms of the disease for the clone 'BRS 189', more susceptible to the pathogen that causes powdery mildew. One nut, apparently without symptoms of powdery mildew, was collected from each plant and placed inside a glass bottle, totaling five nuts for each type of clone. The same procedure was used for the collection of nuts with disease symptoms. All analyses were performed in triplicate, yielding 15 samples, as illustrated in Figure 40.

Figure 39. Scheme of the organization for collecting cashew nuts samples.

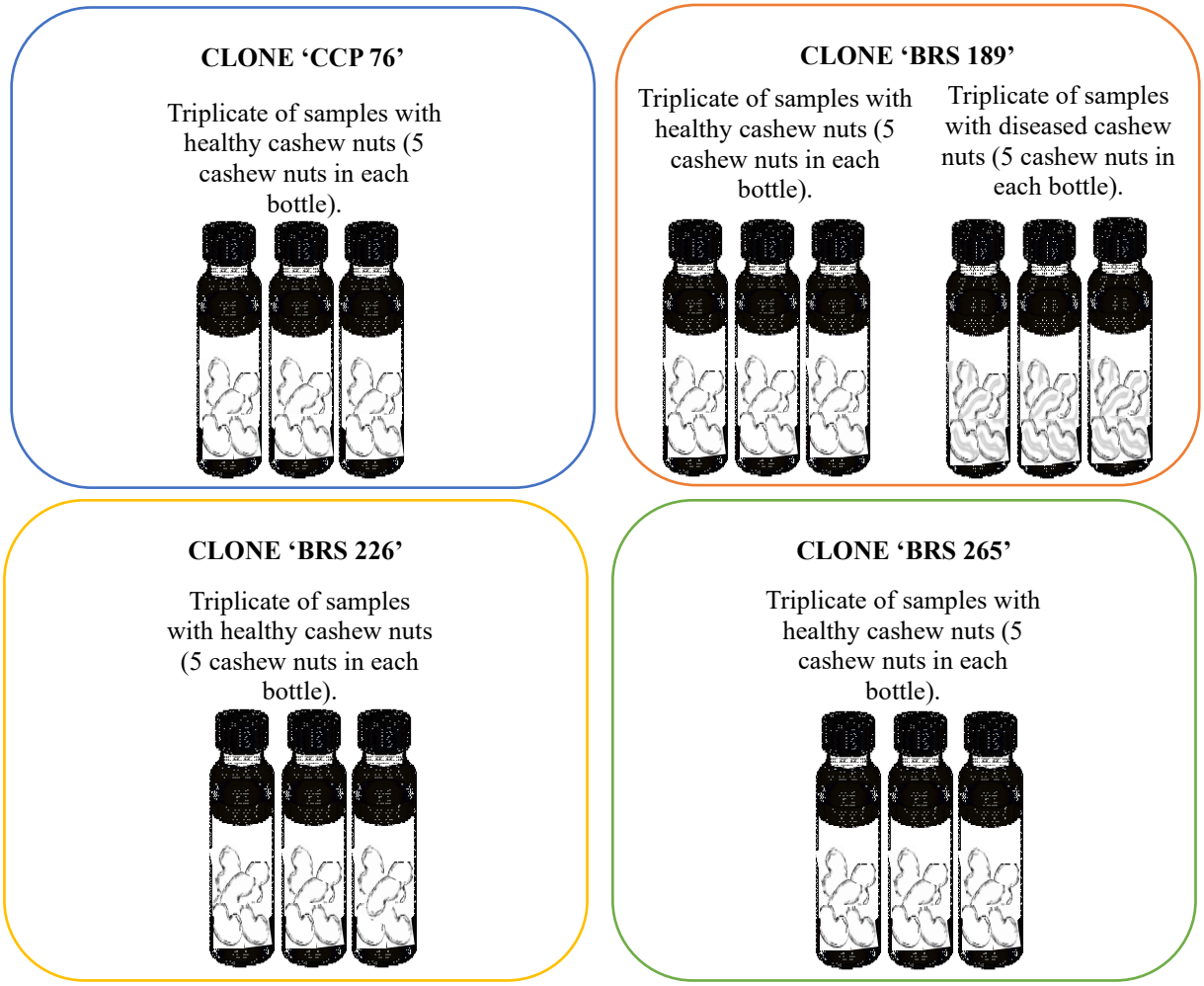

Source: Author (2019).

Extraction and analysis of the volatile organic compounds

For the extraction of volatile organic compounds (VOCs) from cashew nuts, solid-phase microextraction (SPME) via headspace was used, using experimental conditions based on (ROUSEFF et al., 2008).

Because the sample sizes were not compatible with the vials commonly used in GC-MS analysis, glass vials were used to adapt the applied method. The vials (approximately 150 mL) had their lids perforated for the septum/PTFE silicone fitting (Supelco, Bellefonte, PA, USA), specific for GC-MS analysis, aiming to allow the needle containing the fiber to be inserted inside the container, enabling the capture of volatile compounds emitted by the samples. Thus, the analysis was performed by manual injection, and the vials containing the samples

were pre-incubated in a water bath (Cientec, CT-226) at 35 °C for 30 min without agitation. Then, a gray fiber of the divinylbenzene/carboxene/polydimethylsiloxane (DVB/CAR/PDMS) type of 1 cm (Supelco, Bellefonte, PA, USA) was exposed inside the flasks in free space for 15 min for the adsorption of volatile compounds emitted by cashew nuts (FIGURE 41). After the period of capture of the compounds, the fiber was removed from the flasks and sent to the gas chromatograph injector, remaining for 3 min for thermal desorption, at 260 °C, of the captured analytes.

Figure 40. Flask containing samples submitted to heating in a water bath, at 35 ºC, for the extraction and capture of volatile organic compounds emitted by cashew nuts.

Source: Author (2019).

The gas chromatograph used in the analysis was a GC 7890 B system (Agilent Technologies Spain, SL, Madrid) coupled to a mass spectrometer with a quadrupole analyzer (5977A MSD Agilent Technologies Spain, SL, Madrid). An HP5-MS type column ((5% phenyl)-dimethylpolysiloxane) with 30m x 0.25 an of internal diameter and a film thickness of 0.25µm was used in the gas chromatograph to separate the compounds extracted from the cashew nut samples. Analyses were performed in splitless mode using helium gas as the analyte carrier at a flow rate of 1 mL/min.

To obtain the mass spectra, positive-mode electron impact ionization (70 eV) was used to analyze the mass range from 50 to 600 Da. The temperature used in the transfer line was 280 °C and that of the source of ionization 150 °C.

To identify the extracted volatile compounds, the mass spectra acquired were compared with those present in the NIST 2.0 Library, 2012 (National Institute of Standards and

Technology, Gaithersburg, MD, USA) using MassHunter Workstation - Qualitative Analysis version B.06.00 Agilent Technologies. Additionally, a comparison was made between the retention index of the homologous series of C8-C30 n-alkanes (Supelco, 49451-U, Bellefonte, PA, USA) and data reported in the literature (ADAMS, 2017).

Data treatment and chemometric analysis

Using MassHunter Workstation software, which comes with the gas chromatograph, it was possible to obtain the acquisition data of the performed analyses. To perform the deconvolution and alignment of all chromatograms, the MS-Dial software was used, which, in addition to these procedures, also enabled the construction of matrices. The metabolic profile data of the clones already aligned and deconvoluted in the previous step were organized in an Excel spreadsheet, where the names of the samples were organized in lines, and the tentatively identified compounds were organized in columns, thus forming a data matrix.

The information on the areas of the peaks of the VOCs obtained in the chromatograms was subjected to normalization using the Metaboanalyst 4.0 web base (www.metaboanalyst.ca) for this purpose, which also enabled the performance of multivariate chemometric analysis, namely, partial least squares discriminant analysis (PLS-DA), principal component analysis (PCA), and discriminant analysis by orthogonal projections to the latent structure (OLPS-DA), in addition to the construction of heatmaps and hierarchical cluster analysis (HCA) graphs according to the protocol provided (CHONG; WISHART; XIA, 2019).

Acknowledgements

The authors gratefully acknowledge the financial support from the National Council for Scientific and Technological Development (CNPq, Conselho Nacional de Desenvolvimento Científico e Tecnológico), National Institute of Science and Technology - INCT BioNat, grant # 465637/2014-0, Brazil, and the Coordination for the Improvement of Higher Education Personnel (Coordenação de Aperfeiçoamento de Pessoal de Nível Superior – CAPES, Finance Code 001).

Author Contribution Statement

Debora Bezerra de Sousa: Methodology, Formal Analysis, Investigation, Resources, Data curation, Writing – Original Draft. Gisele Silvestre da Silva: Investigation, Writing – Review & Editing. Luiz Augusto Lopes Serrano: Conceptualization, Investigation, Writing – Review & Editing. Marlon Vagner Valentim Martins: Conceptualization, Investigation, Resources, Writing – Review & Editing. Tigressa Helena Soares Rodrigues: Conceptualization, Investigation, Resources, Writing – Review & Editing. Mary Anne Sousa Lima: Conceptualization, Writing – Review & Editing, Supervision. Guilherme Julião Zocolo: Conceptualization, Methodology, Resources, Writing – Review & Editing, Supervision, Project Administration, Funding Acquisition.

8 CONCLUSÕES

O estudo metabolômico dos COVs emitidos por folhas e castanhas de clones de cajueiro tipo anão precoce, mostrou que essas plantas emitem respostas distintas em relação à presença dos patógenos causadores das doenças mofo preto, antracnose e oídio no campo.

A análise dos COVs emitidos pelas folhas do clone 'BRS 265' resistente ao mofo preto (*P. anacardii*), apresentou como maiores destaques os compostos (*E*)-hex-2-enal, α-pineno, pseudolimoneno, silvestreno, β-*cis*-ocimeno, salicilato de metila, α-copaeno, γ-muuroleno, germacreno D, valenceno e germacreno B, associados ao seu mecanismo de defesa. Por outro lado, a análise dos COVs emitidos pelas folhas do clone 'BRS 226', também resistente ao patógeno causador do mofo preto, revelou o (*E*)-hex-2-enal, (*Z*)-hex-3-en-1-ol, (*Z*)-hex-2-en-1-ol, (*Z*)-hex-2-en-1-ol, hexan-1-ol, β-mirceno, α-felandreno, silvestreno e mirtenol associados ao período de incidência do patógeno no campo, permitindo classificá-los como candidatos a biomarcadores de resistência à doença.

Para a antracnose (*C. gloeosporioides*), foi possível identificar que nas folhas dos clones resistentes 'CCP 76', 'BRS 226' e 'BRS 189', houve um aumento significativo na biossíntese de compostos antimicrobianos, fato que não foi observado para o clone 'BRS 265', mais suscetível ao patógeno. No clone resistente 'CCP 76' observou-se nos meses de maior incidência da doença (agosto e setembro), o aumento dos teores dos compostos: hexanal, thuja-2,4 (10)-dieno, *p*-mentha-1 (7), 8-dieno, δ-3-careno, α-terpineno , limoneno, *o*-cimeno, γ-terpineno, terpinoleno, cis-pinocanfona, terpinen-4-ol, aromadendreno e α-himacaleno. Para o clone resistente 'BRS 226', o hexanal, (*Z*)-hex-2-en-1-ol, canfeno, thuja-2,4 (10)-dieno, α-felandreno e p-mentha-1(7),8-dieno, δ-3-careno, hex-3-en-1-ol, propanoato, (*Z*)-, perileno, *p*-menta-1,3,8-trieno, *cis*-3-hexenil isobutirato e dendrolasina foram os COVs associados ao mecanismo de defesa da planta. Por outro lado, o clone 'BRS 189', o hexanal, (*E*)-hex-2-enal, (*E*)- hex-3-en-1-ol, (*Z*)-hex-3-en-1-ol, (*Z*)-hex-2-en-1-ol, tuja-2,4 (10)-dieno e butanoato de (*Z*)-3-hexenila foram os compostos associados ao mecanismo de defesa da planta.

Com relação à doença do oídio, as análises das castanhas de caju dos clones resistentes 'BRS 226', 'CCP 76' e 'BRS 265', permitiram identificar os COVs 3-metil-1-pentanol, isovalerato de etila, α-pineno, tilato de etila, canfeno, β-pineno, β-mirceno, hexanoato de etila, α-terpineno, β-*trans*-ocimeno, terpinoleno, ácido heptanóico, éster etílico, perileno, nonanal e cânfora, como mais abundantes nas amostras sadias de frutos de cajueiro. Estes compostos não foram observados nas amostras de castanhas doentes do clone 'BRS 189 'suscetível, e foram associados ao mecanismo de defesa das plantas.

Os dados obtidos estão em consonância com os apresentados na literatura para biossíntese de compostos voláteis antimicrobianos e reforçam o fato de que os diferentes clones respondem de maneira distinta do ponto de vista químico, quando ocorre a incidência dos patógenos no campo visando à sua proteção e resistência.

Este estudo, inédito na literatura para *A. occidentale*, fornece importantes informações preliminares para estudos futuros de desenvolvimento de defensivos agrícolas naturais, visando a proteção dos pomares de cajueiro às doenças investigadas e aumento do rendimento produtivo das culturas.

REFERÊNCIAS

ABAD, M. J.; ANSUATEGUI, M.; BERMEJO, P. Active antifungal substances from natural sources. **Arkivoc**, [*s. l.*], v. 2007, n. 7, p. 116–145, 2007.

ADAMS, R. P. **Identification of essential oil components by gas chromatography/mass spectroscopy**. 4.1 ed. [*s. l.*]. Carol Stream: Allured Publishing Corporation, 2017.

ADIGA, J. D. *et al*. Phenological growth stages of the cashew tree (*Anacardium occidentale* L.) according to the extended BBCH scale. **Annals of Applied Biology**, [*s. l.*], v. 175, n. 2, p. 246–252, 2019.

AazGILA, A.; BARRINGER, S. A. Volatile profile of cashews (*Anacardium occidentale* L.) from different geographical origins during roasting. **Journal of Food Science**, [*s. l.*], v. 76, n. 5, p. C768–C774, 2011.

AGUDELO-ROMERO, P. *et al*. Transcriptome and metabolome reprogramming in *Vitis vinifera* cv. Trincadeira berries upon infection with *Botrytis cinerea*. **Journal of Experimental Botany**, [*s. l.*], v. 66, n. 7, p. 1769–1785, 2015.

ALGARRA ALARCON, A. *et al*. Emission of volatile sesquiterpenes and monoterpenes in grapevine genotypes following *Plasmopara viticola* inoculation in vitro. **Journal of Mass Spectrometry**, [*s. l.*], v. 50, n. 8, p. 1013–1022, 2015.

ALIFERIS, K. A.; FAUBERT, D.; JABAJI, S. A metabolic profiling strategy for the dissection of plant defense against fungal pathogens. **PLoS ONE**, [*s. l.*], v. 9, n. 11, p. 11-13, 2014.

ALLWOOD, J. W. *et al*. Separating the inseparable: The metabolomic analysis of plant–pathogen interactions. In: HARDY, N. W.; HALL, R. D. (Ed.). **Plant Metabolomics Methods and Protocols**. [*s. l.*], Humana Press, 2011. p. 31–49.

ALMA, M. H. *et al*. Chemical composition and antimicrobial activity of the essential oils from the gum of Turkish Pistachio (*Pistacia vera* L.). **Journal of Agricultural and Food Chemistry**, [*s. l.*], v. 52, n. 12, p. 3911–3914, 2004.

AMEYE, M. *et al*. Green leaf volatile production by plants: A meta-analysis. **New Phytologist**, [*s. l.*], v. 220, n. 3, p. 666–683, 2018.

ANDRADE, B. F. M. T. *et al*. Antimicrobial activity of essential oils. **Journal of Essential Oil Research**, [*s. l.*], v. 26, n. 1, p. 34–40, 2014.

AWODUN, M. A. *et al*. Comparative effects of organic and inorganic soil amendments on the growth of cashew nut (*Anacardium occidentale* L.) seedlings. **Journal of Agricultural Biotechnology and Sustainable Development**, [*s. l.*], v. 7, n. 4, p. 37–42, 2015.

BAJPAI, V. K.; BAEK, K.-H.; KANG, S. C. Control of *Salmonella* in foods by using essential oils: A review. **Food Research International**, [*s. l.*], v. 45, n. 2, p. 722–734, 2012.

BARRERO, A. F. *et al*. New sources and antifungal activity of sesquiterpene lactones. **Fitoterapia**, [*s. l.*], v. 71, n. 1, p. 60–64, 2000.

BARRERO, A. F. *et al*. Antimicrobial activity of sesquiterpenes from the essential oil of *Juniperus thurifera* wood. **Planta Medica**, [*s. l.*], v. 71, n. 1, p. 67–71, 2005.

BARRETTO, L. C. de O. *et al*. *Anacardium occidentale* L.: Prospecção tecnológica aplicada à tecnologia de compostos bioativos em produtos alimentícios. **Revista Geintec**, [*s. l.*], v. 4, p. 1356–1366, 2014.

BARROS, L. de M. **Árvore do conhecimento - caju**. Disponível em: <https://www.agencia.cnptia.embrapa.br/gestor/caju/arvore/CONT000fi8wxjm202wyiv80z4s473zfjkkt9.html>. Acesso em: 24 mai. 2022.

BASSOLÉ, I. H. N.; JULIANI, H. R. Essential oils in combination and their antimicrobial properties. **Molecules**, [*s. l.*], v. 17, n. 4, p. 3989–4006, 2012.

BERRY, A. D.; SARGENT, S. A. Cashew apple and nut (*Anacardium occidentale* L.). In: **Postharvest Biology and Technology of Tropical and Subtropical Fruits**. [*s. l.*]: Elsevier, 2011. p. 414-423.

BICALHO, B.; REZENDE, C. M. Volatile compounds of cashew apple (*Anacardium occidentale* L .). **Z. Naturforsch**, [*s. l.*], v. 56, p. 2–6, 2001.

BORTOLUCCI, W. de C. *et al*. Acaricidal and larvicidal activity of leaves and fractions of rose pepper (*Schinus terebinthifolius* Raddi. (Anacardiaceae) essential oil against *Rhipicephalus* (Boophilus) *microplus*. **Australian Journal of Crop Science**, [*s. l.*], v. 12, n. 10, p. 1645–1652, 2018.

BRAINER, M. S. C. P.; VIDAL, M. de F. Cajucultura. **Caderno Setorial ETENE / Banco Nacional do Nordeste (BNB)**, [*s. l.*], v. 5, n. 114, p. 1–16, 2020.

BRUNO, M. *et al*. Sesquiterpenoids in subtribe Centaureinae (Cass.) Dumort (tribe Cardueae, Asteraceae): Distribution, ^{13}C NMR spectral data and biological properties. **Phytochemistry**, [*s. l.*], v. 95, p. 19–93, 2013.

BÜNGER, R.; MALLET, R. T. Metabolomics and ROC analysis: A promising approach for sepsis diagnosis. **Critical Care Medicine**, [*s. l.*], v. 44, n. 9, p. 1784–1785, 2016.

CALO, J. R. *et al*. Essential oils as antimicrobials in food systems - A review. **Food Control**, [*s. l.*], v. 54, p. 111–119, 2015.

CAMAÑES, G. *et al*. An untargeted global metabolomic analysis reveals the biochemical changes underlying basal resistance and priming in *Solanum lycopersicum*, and identifies 1-methyltryptophan as a metabolite involved in plant responses to *Botrytis cinerea* and *Pseudomonas* sy. **The Plant Journal**, [*s. l.*], v. 84, n. 1, p. 125–139, 2015.

CARDOSO, C. A. L. *et al*. Identification of the volatile compounds of fruit oil of *Anacardium humile* (Anacardiaceae). **Journal of Essential Oil Research**, [*s. l.*], v. 22, n. 5, p. 469–470, 2010.

CARDOSO, J. E. *et al*. Genetic resistance of dwarf cashew (*Anacardium occidentale* L.) to

anthracnose, black mold, and angular leaf spot. **Crop Protection**, [*s. l.*], v. 18, p. 23–27, 1999.

CARDOSO, J. E. *et al*. **Epidemiologia do mofo-preto e danos na produção do cajueiro.** Fortaleza: Embrapa, 2005.

CARDOSO, J. E. *et al*. **Controle Químico do Oídio do Cajueiro.** Fortaleza, Embrapa, 2012.

CARDOSO, J. E. **Principais doenças do cajueiro: Sintomas & controle.** Fortaleza: Embrapa, 2019.

CASTRO-MORETTI *et al*. Metabolomics as an emerging tool for the study of plant–pathogen interactions. **Metabolites**, [*s. l.*], v. 10, n. 2, p. 52, 2020.

CAVALCANTI, J. J. V.; NETO, F. das C. V.; BARROS, L. de M. Avanços, desafios e novas estratégias do melhoramento genético do cajueiro no Brasil. In: **Melhoramento Genético de Plantas no Nordeste,** [*s. l.*]. 2013. p. 151–174.

CAVALCANTI, J. J. V.; RESENDE, M. D. V. de. Seleção precoce intensiva: Uma nova estratégia para o programa de melhoramento genético do cajueiro. **Revista Brasileira de Fruticultura**, [*s. l.*], v. 32, n. 4, p. 1279–1284, 2010.

CEVA-ANTUNES, P. M. N. *et al*. Analysis of volatile composition of siriguela (*Spondias purpurea* L.) by solid phase microextraction (SPME). **LWT - Food Science and Technology**, [*s. l.*], v. 39, n. 4, p. 437–443, 2006.

CISSE, S. *et al*. Assessment of the Natural Landscape Changes Due to Cashew Plantations in the Department of Niakaramandougou (North of Côte d' Ivoire). **Journal of Agricultural Chemistry and Environment**, [*s. l.*], v. 10, n. 2, 2021.

CHAGAS-PAULA, D. A. *et al*. A metabolomic approach to target compounds from the Asteraceae family for dual COX and LOX inhibition. **Metabolites**, [*s. l.*], v. 5, n. 3, p. 404–430, 2015a.

CHAGAS-PAULA, D. A. *et al*. Prediction of anti-inflammatory plants and discovery of their biomarkers by machine learning algorithms and metabolomic studies. **Planta Medica**, [*s. l.*], v. 81, n. 6, p. 450–458, 2015b.

CHAUHAN, N. S.; NATH, R. Effect of moisture content on engineering properties of cashew nut. **International Journal of Current Microbiology and Applied Sciences**, [*s. l.*], v. 10, n. 2, p. 3042–3052, 2021.

CHEN, F.; MA, R.; CHEN, X. L. Advances of metabolomics in fungal pathogen–plant interactions. **Metabolites**, [*s. l.*], v. 9, n. 8, p. 2–19, 2019.

CHENG, S. S.; LIN, H. Y.; CHANG, S. T. Chemical composition and antifungal activity of essential oils from different tissues of Japanese cedar (*Cryptomeria japonica*). **Journal of Agricultural and Food Chemistry**, [*s. l.*], v. 53, n. 3, p. 614–619, 2005.

CHONG, J.; WISHART, D. S.; XIA, J. Using MetaboAnalyst 4.0 for Comprehensive and integrative metabolomics data analysis. **Current Protocols in Bioinformatics**, [*s. l.*], v. 68, n.

1, p. 1–128, 2019.

CHOO, T. M. Breeding barley for resistance to *Fusarium* head blight and mycotoxin accumulation. In: **Plant Breeding Reviews**. Oxford, UK: John Wiley & Sons, Inc., 2010. p. 125–169.

CHOUHAN, S.; SHARMA, K.; GULERIA, S. Antimicrobial activity of some essential oils - present status and future perspectives. **Medicines**, [*s. l.*], v. 4, n. 3, p. 58, 2017.

CONAB. **Análise mensal: castanha de caju**. 61. Disponível em: <https://webcache.googleusercontent.com/search?q=cache:V34mWT5b_SoJ:https://www.conab.gov.br/info-agro/analises-do-mercado-agropecuario-e-extrativista/analises-do-mercado/historico-mensal-de-castanha-de-caju/item/download/37889_d1dcfb853366346219117a35a72b>. Acesso em: 25 mar. 2022.

COURTOIS, E. A. *et al*. Differences in volatile terpene composition between the bark and leaves of tropical tree species. **Phytochemistry**, [*s. l.*], v. 82, p. 81–88, 2012.

DA CRUZ CABRAL, L.; FERNÁNDEZ PINTO, V.; PATRIARCA, A. Application of plant derived compounds to control fungal spoilage and mycotoxin production in foods. **International Journal of Food Microbiology**, [*s. l.*], v. 166, n. 1, p. 1–14, 2013.

DA SILVA, A. C. R. *et al*. Biological activities of α-pinene and β-pinene enantiomers. **Molecules**, [*s. l.*], v. 17, n. 16, p. 6305-6316, 2012.

DE AQUINO, N. C.; ARAÚJO, R. M.; SILVEIRA, E. R. Intraspecific variation of the volatile chemical composition of *Myracrodruon urundeuva* Fr. Allem. (“aroeira-do-sertão”): Characterization of six chemotypes. **Journal of the Brazilian Chemical Society**, [*s. l.*], v. 28, n. 5, p. 907–912, 2017.

DE BRITO, E. S.; DE OLIVEIRA SILVA, E.; RODRIGUES, S. Caju - *Anacardium occidentale*. In: **Exotic Fruits**. [*s.l*]. Elsevier, 2018. p. 85–89.

DE LOURDES CARDEAL, Z.; GUIMARÃES, E. M.; PARREIRA, F. V. Analysis of volatile compounds in some typical Brazilian fruits and juices by SPME-GC method. **Food Additives and Contaminants**, [*s. l.*], v. 22, n. 6, p. 508–513, 2005.

DE OLIVEIRA NOBRE, A. C. *et al*. Volatile profile of cashew apple juice fibers from different production steps. **Molecules**, [*s. l.*], v. 20, n. 6, p. 9803–9815, 2015.

DENDENA, B.; CORSI, S. Cashew, from seed to market: A review. **Agronomy for Sustainable Development**, [*s. l.*], v. 34, p. 753 - 772, 2014.

DERWICH, E.; BENZIANE, Z.; BOUKIR, A. Chemical composition and in vitro antibacterial activity of the essential oil of *Cedrus atlantica*. **International Journal of Agriculture and Biology**, [*s. l.*], v. 12, n. 3, p. 381–385, 2010.

DEVECI, O. *et al*. Chemical composition, repellent and antimicrobial activity of *Schinus molle* L. **Journal of Medicinal Plants Research**, [*s. l.*], v. 4, n. 21, p. 2211–2216, 2010.

DO PRADO, A. C. *et al*. *Schinus molle* essential oil as a potential source of bioactive compounds: Antifungal and antibacterial properties. **Journal of Applied Microbiology**, [*s. l.*], v. 126, n. 2, p. 516–522, 2019.

DOEHLEMANN, G. *et al*. Reprogramming a maize plant: Transcriptional and metabolic changes induced by the fungal biotroph Ustilago maydis. **The Plant Journal**, [*s. l.*], v. 56, n. 2, p. 181–195, 2008.

DORTA, E. *et al*. Screening of phenolic compounds in by-product extracts from mangoes (*Mangifera indica* L.) by HPLC-ESI-QTOF-MS and multivariate analysis for use as a food ingredient. **Food Research International**, [*s. l.*], v. 57, p. 51–60, 2014.

DOS SANTOS, A. *et al*. Analysis of the seasonal variation in chemical profile of *Piper glabratum* Kunth essential oils using GC×GC/qMS and their antioxidant and antifungal activities. **Journal of the Brazilian Chemical Society**, [*s. l.*], v. 30, n. 12, p. 2691–2701, 2019.

DUDAREVA, N. *et al*. Plant volatiles: Recent advances and future perspectives. **Critical Reviews in Plant Sciences**, [*s. l.*], v. 25, n. 5, p. 417–440, 2006.

DZAMIC, A. *et al*. Essential oil composition of *Anacardium occidentale* from Nigeria. **Chemistry of Natural Compounds**, [*s. l.*], v. 45, n. 3, p. 441–442, 2009.

EFFAH, E. *et al*. Mānuka clones differ in their volatile profiles: Potential implications for plant defence, pollinator attraction and bee products. **Agronomy**, [*s. l.*], v. 12, n. 1, p.1-13, 2022.

EGONYU, J. P. *et al*. Cashew volatiles mediate short-range location responses in *Pseudotheraptus wayi* (Heteroptera: Coreidae). **Environmental Entomology**, [*s. l.*], v. 42, n. 6, p. 1400–1407, 2013.

EMMANUELLE, D. *et al*. A review of cashew (*Anacardium occidentale* L.) apple: Effects of processing techniques, properties and quality of juice. **African Journal of Biotechnology**, [*s. l.*], v. 15, n. 47, p. 2637–2648, 2016.

EMPARN. **Cajueiro - Vivendo e aprendendo**. Disponível em: http://adcon.rn.gov.br/ACERVO/EMPARN/DOC/DOC000000000017470.PDF. Acesso em: 23 jun. 2020.

FALAHATI, M. *et al*. Evaluation of the antifungal activities of various extracts from *Pistacia atlantica* Desf. **Current Medical Mycology**, [*s. l.*], v. 1, n. 3, p. 25–32, 2015.

FERREIRA, F. D. *et al*. The inhibitory effects of *Curcuma longa* L. essential oil and curcumin on *Aspergillus flavus* link growth and morphology. **The Scientific World Journal**, [*s. l.*], v. 2013, p. 1-13, 2013.

FIGUEIRÊDO, L. C. *et al*. Genetic and pathogenic diversity of *Colletotrichum gloeosporioides*, the causal agent of cashew anthracnose. **Indian Journal of Fundamental and Applied Life Sciences**, [*s. l.*], v. 2, n. 1, p. 250–259, 2012.

FONSECA, W. L. *et al*. Morphological, molecular phylogenetic and pathogenic analyses of *Erysiphe* spp. causing powdery mildew on cashew plants in Brazil. **Plant Pathology**, [*s. l.*], v. 68, n. 6, p. 1157–1164, 2019.

FORTUNA, A. M. *et al*. Antimicrobial activities of sesquiterpene lactones and inositol derivatives from *Hymenoxys robusta*. **Phytochemistry**, [*s. l.*], v. 72, n. 18, p. 2413–2418, 2011.

FRATERNALE, D. *et al*. Composition and antifungal activity of two essential oils of hyssop (*Hyssopus officinalis* L.). **Journal of Essential Oil Research**, [*s. l.*], v. 16, n. 6, p. 617–622, 2004.

FREIRE, F. C. O. *et al*. Diseases of cashew nut plants (*Anacardium occidentale* L.) in Brazil. **Crop Protection**, [*s. l.*], v. 21, n. 6, p. 489–494, 2002.

FREIRE, F. das C. O. A introdução de fitopatógenos e doenças emergentes na agricultura cearense. **Essentia Sobral**, [*s. l.*], v. 16, n. 2, p. 22–39, 2015.

GA OLATUNJI, O. F. Isolation and characterization of the chemical constituents of *Anacardium occidentale* cracked bark. **Natural Products Chemistry & Research**, [*s. l.*], v. 03, n. 05, p. 2-8, 2015.

GARRISON, T. F. *et al*. Cardanol-Based Supramolecular Gels. In: **Cashew Nut Shell Liquid**. [*s.l.*]. Cham: Springer International Publishing, 2017. p. 129–143.

GARRUTI, D. S. *et al*. Evaluation of volatile flavour compounds from cashew apple (*Anacardium occidentale* L) juice by the osme gas chromatography / olfactometry technique. **Journal of the Science of Food and Agriculture**, [*s. l.*], v. 1462, n. 83, p. 1455–1462, 2003.

GEBARA, S. S. *et al*. Volatile compounds of leaves and fruits of *Mangifera indica* var. coquinho (Anacardiaceae) obtained using solid phase microextraction and hydrodistillation. **Food Chemistry**, [*s. l.*], v. 127, n. 2, p. 689–693, 2011.

GIWELI, A. *et al*. Antimicrobial and antioxidant activities of essential oils of *Satureja thymbra* growing wild in libya. **Molecules**, [*s. l.*], v. 17, n. 5, p. 4836–4850, 2012.

GRECO, M. *et al*. Metabolomics reveals simultaneous influences of plant defence system and fungal growth in *Botrytis cinerea* - infected *Vitis vinifera* cv. Chardonnay berries. **Journal of Experimental Botany**, v. 63, n. 2, p. 695–709, 2012.

GUIMARÃES, A. C. *et al*. Antibacterial activity of terpenes and terpenoids present in essential oils. **Molecules**, [*s. l.*], v. 24, n. 13, p. 1–12, 2019.

GUO, Q. *et al*. The impact of technical cashew nut shell liquid on thermally-induced trans isomers in edible oils. **Journal of Food Science and Technology**, [*s. l.*], v. 53, n. 3, p. 1487–1495, 2016.

GUPTA, R. *et al*. Understanding the plant-pathogen interactions in the context of proteomics - generated apoplastic proteins inventory. **Frontiers in Plant Science**, [*s. l.*], v. 6, n 352, p. 1–7, 2015.

GUPTA, S.; SCHILLACI, M.; ROESSNER, U. Metabolomics as an emerging tool to study plant - microbe interactions. **Emerging Topics in Life Sciences**, [*s. l.*], v. 6, n. 2, p. 175–183, 2022.

GYEDU-AKOTO, E.; AMOAH, F. M.; ODURO, I. Cashew tree (*Anarcadium occidentale* L.) exudate gum. In: **Emerging Natural Hydrocolloids**. Chichester, UK: John Wiley & Sons, Ltd, 2019. p. 327–346.

HAQUE, E. *et al*. Terpenoids with antifungal activity trigger mitochondrial dysfunction in *Saccharomyces cerevisiae*. **Microbiology (Russian Federation)**, [*s. l.*], v. 85, n. 4, p. 436–443, 2016.

HERNANDES, C. *et al*. Chemical composition and antifungal activity of the essential oils of *Schinus weinmannifolius* collected in the spring and winter. **Natural Product Communications**, [*s. l.*], v. 9, n. 9, p. 1383–1386, 2014.

HIMEJIMA, M. *et al*. Antimicrobial terpenes from oleoresin of ponderosa pine tree *Pinus ponderosa*: A defense mechanism against microbial invasion. **Journal of Chemical Ecology**, [*s. l.*], v. 18, n. 10, p. 1809–1818, 1992.

HO, C. L. *et al*. Composition and antimicrobial activity of the leaf and twig oils of *Litsea acutivena* from Taiwan. **Natural Product Communications**, [*s. l.*], v. 6, n. 11, p. 1755–1758, 2011.

HOO, Z. H.; CANDLISH, J.; TEARE, D. What is an ROC curve? **Emergency Medicine Journal**, [*s. l.*], v. 34, n. 6, p. 357–359, 2017.

HRISTOVA, Y. *et al*. Chemical composition and antifungal activity of essential oil of *Hyssopus officinalis* L. from Bulgaria against clinical isolates of *Candida* species. **Biotechnology and Biotechnological Equipment**, [*s. l.*], v. 29, n. 3, p. 592–601, 2015.

HU, Z. *et al*. Metabolic profiling to identify the latent infection of strawberry by *Botrytis cinerea*. **Evolutionary Bioinformatics**, v. 15, p. 1-7, 2019.

IBGE - INSTITUTO BRASILEIRO DE GEOGRAFIA E ESTATÍSTICA. **Levantamento Sistemático da Produção Agrícola**. Rio de Janeiro, 2021. Disponível em: https://sidra.ibge.gov.br/tabela/1618. Acesso em: 30 mar. 2022.

IIJIMA, Y. Recent advances in the application of metabolomics to studies of biogenic volatile organic compounds (BVOC) produced by plant. **Metabolites**, [*s. l.*], v. 4, n. 3, p. 699–721, 2014.

IRITI, M.; FAORO, F. Chemical diversity and defence metabolism: How plants cope with pathogens and ozone pollution. **International Journal of Molecular Sciences**, [*s. l.*], v. 10, n. 8, p. 3371–3399, 2009.

ISMAIL, A. *et al*. Chemical composition and antifungal activity of three Anacardiaceae species grown in Tunisia. **Science International**, [*s. l.*], v. 1, n. 5, p. 148 - 154, 2013.

JANAH, T. *et al*. Chemical profiling and antifungal activity of essential oils of five moroccan threatened populations of *Cupressus atlantica* Gaussen. **Journal of Essential Oil-Bearing Plants**, [*s. l.*], v. 21, n. 6, p. 1694–1705, 2018.

JELLER, A. H.; RÉ, N.; MATIAS, R. Identification of the volatile compounds of fruit oil of *Anacardium humile* (Anacardiaceae). **Journal of Essential Oil Research**, [*s. l.*], v. 22, n. 5, p. 469–470, 2010.

JOGAIAH, S.; ABDELRAHMAN, M. **Bioactive molecules in plant defense**. [*s.l.*]. Cham: Springer International Publishing, 2019.

JONES, O. A. H. *et al*. Using metabolic profiling to assess plant-pathogen interactions: An example using rice (*Oryza sativa*) and the blast pathogen *Magnaporthe grisea*. **European Journal of Plant Pathology**, [*s. l.*], v. 129, n. 4, p. 539–554, 2011.

KALEMBA, D.; KUNICKA, A. Antibacterial and antifungal properties of essential oils. **Current Medicinal Chemistry**, [*s. l.*], v. 10, n. 10, p. 813–829, 2005.

KIRCHNER, K. *et al*. Chemical composition and antimicrobial activity of *Hedyosmum brasiliense* Miq., Chloranthaceae, essential oil. **Brazilian Journal of Pharmacognosy**, [*s. l.*], v. 20, n. 5, p. 692–699, 2010.

KISHIMOTO, K. *et al*. Volatile C6-aldehydes and *allo*-ocimene activate defense genes and induce resistance against *Botrytis cinerea* in *Arabidopsis thaliana*. **Plant and Cell Physiology**, v. 46, n. 7, p. 1093–1102, 2005.

KISHIMOTO, K. *et al*. Direct fungicidal activities of C6-aldehydes are important constituents for defense responses in *Arabidopsis* against *Botrytis cinerea*. **Phytochemistry**, v. 69, n. 11, p. 2127–2132, 2008.

KLEPZIG, K. D.; SMALLEY, E. B.; RAFFA, K. F. Combined chemical defenses against an insect-fungal complex. **Journal of Chemical Ecology**, [*s. l.*], v. 22, n. 8, p. 1367–1388, 1996.

KOEDUKA, T. Functional evolution of biosynthetic enzymes that produce plant volatiles. **Bioscience, Biotechnology, and Biochemistry**, [*s. l.*], v. 82, n. 2, p. 192–199, 2018.

KOSSOUOH, C. *et al*. Essential oil chemical composition of *Anacardium occidentale* L. Leaves from Benin. **Journal of Essential Oil Research**, [*s. l.*], v. 20, n. 1, p. 5–8, 2008.

LAOTHAWORNKITKUL, J. *et al*. Biogenic volatile organic compounds in the Earth system. **New Phytologist**, [*s. l.*], v. 183, n. 1, p. 27–51, 2009.

LAWSON, S. K. *et al*. Volatile compositions and antifungal activities of native american medicinal plants: Focus on the Asteraceae. **Plants**, [*s. l.*], v. 9, n. 1, p. 126, 2020.

LEITE, A. de S. *et al*. Pharmacological properties of cashew (*Anacardium occidentale*). **African Journal of Biotechnology**, [*s. l.*], v. 15, n. 35, p. 1855–1863, 2016.

LIMA, J. S. **Epidemiologia Quantitativa do oídio do cajueiro no clone BRS 189**. 2017. 82 f. Tese (Doutorado em Agronomia) – Pró-Reitoria de Pesquisa e Pós-Graduação,

Universidade Federal do Ceará, Fortaleza, 2017.

LIMA, J. S. *et al*. Reação de clones de cajueiro-anão à antracnose e ao mofo-preto. **Comunicado técnico (Embrapa Agroindústria Tropical)**, Fortaleza, v. 247, p. 1–8, 2019.

LIMA, J. S.; MARTINS, M. V. V.; CARDOSO, J. E. Powdery mildew damage to the production of BRS 189 cashew plants. **Revista Ceres**, [*s. l.*], v. 66, n. 2, p. 132–141, 2019.

LING, B. *et al*. Physicochemical properties, volatile compounds, and oxidative stability of cold pressed kernel oils from raw and roasted pistachio (*Pistacia vera* L. Var Kerman). **European Journal of Lipid Science and Technology**, [*s. l.*], v. 118, n. 9, p. 1368–1379, 2016.

LIU, H. *et al*. Aromatic characterization of mangoes (*Mangifera indica* L.) using solid phase extraction coupled with gas chromatography - mass spectrometry and olfactometry and sensory analyses. **Foods**, [*s. l.*], v. 9, n. 1, p. 75, 2020.

LLOYD, A. J. *et al*. Metabolomic approaches reveal that cell wall modifications play a major role in ethylene-mediated resistance against *Botrytis cinerea*. **The Plant Journal**, [*s. l.*], v. 67, n. 5, p. 852–868, 2011.

LÓPEZ-GRESA, M. P. *et al*. A non-targeted metabolomics approach unravels the VOCs associated with the tomato immune response against *Pseudomonas syringae*. **Frontiers in Plant Science**, [*s. l.*], v. 8, p. 1–15, 2017.

LÓPEZ, A. M. Q.; LUCAS, J. A. Reaction of dwarf cashew clones to *Colletotrichum gloeosporioides* isolates in controlled environment. **Scientia Agricola**, [*s. l.*], v. 67, n. 2, p. 228–235, 2010.

LUBES, G.; GOODARZI, M. Analysis of volatile compounds by advanced analytical techniques and multivariate chemometrics. **Chemical Reviews**, [*s. l.*], v. 117, n. 9, p. 6399–6422, 2017.

LUO, M. *et al*. Effects of citral on *Aspergillus flavus* spores by quasi-elastic light scattering and multiplex microanalysis techniques. **Acta Biochimica et Biophysica Sinica**, [*s. l.*], v. 36, n. 4, p. 277–283, 2004.

MAHIZAN, N. A. *et al*. Terpene derivatives as a potential agent against antimicrobial resistance (AMR) pathogens. **Molecules**, [*s. l.*], v. 24, n. 14, p. 1-21, 2019.

MAIA, J. G. S.; ANDRADE, E. H. A.; ZOGHBI, M. D. G. B. Volatile constituents of the leaves, fruits and flowers of cashew (*Anacardium occidentale* L.). **Journal of Food Composition and Analysis**, [*s. l.*], v. 13, n. 3, p. 227–232, 2000.

MAIA S., J. G.; ANDRADE A., E. H. Data base of the Amazon aromatic plants and ther essential oils. **Quimica Nova**, [*s. l.*], v. 32, n. 3, p. 595–622, 2009.

MAREI, G. I. K.; ABDEL RASOUL, M. A.; ABDELGALEIL, S. A. M. Comparative antifungal activities and biochemical effects of monoterpenes on plant pathogenic fungi. **Pesticide Biochemistry and Physiology**, [*s. l.*], v. 103, n. 1, p. 56–61, 2012.

MARTINS, M. V. V. *et al*. Progresso do oídio em função da fenologia do cajueiro. **Summa Phytopathologica**, [*s. l.*], v. 44, n. 2, p. 178–184, 2018.

MASI, M. *et al*. Farnesane-type sesquiterpenoids with antibiotic activity from *Chiliadenus lopadusanus*. **Antibiotics**, [*s. l.*], v. 10, n. 2, p. 1–12, 2021.

MATA, J. Costa rican cashew (*Anacardium occidentale* L .): Essential oils , carotenoids and bromatological analysis. **American Journal of Essential Oils and Natural Products**, [*s. l.*], v. 6, n. 3, p. 1–9, 2018.

MATSUI, K. *et al*. Differential metabolisms of green leaf volatiles in injured and intact parts of a wounded leaf meet distinct ecophysiological requirements. **PloS one**, [*s. l.*], v. 7, n. 4, p. 1–10, 2012.

MATSUI, K.; KOEDUKA, T. Green leaf volatiles in plant signaling and response. In: NAKAMURA, Y.; LI-BEISSON, Y. (Ed.). **Lipids in plant and algae development**. Subcellular Biochemistry. [*s.l.*]. Cham: Springer International Publishing, 2016. p. 427–443.

MÉRILLON, J. **Natural Antimicrobial Agents**. [*s.l.*]. Cham: Springer International Publishing, 2018. v. 19

MHLONGO, M. I. *et al*. The chemistry of plant - microbe interactions in the rhizosphere and the potential for metabolomics to reveal signaling related to defense priming and induced systemic resistance. **Frontiers in Plant Science**, [*s. l.*], v. 9, n. 9, p. 1–17, 2018.

MICHODJEHOUN-MESTRES, L.; AMRAOUI, W.; BRILLOUET, J. M. Isolation, characterization, and determination of 1-*O*-trans-cinnamoyl- β-*D*-glucopyranose in the epidermis and flesh of developing cashew apple (*Anacardium occidentale* L.) and four of its genotypes. **Journal of Agricultural and Food Chemistry**, [*s. l.*], v. 57, n. 4, p. 1377–1382, 2009.

MICROSOFT. **Microsoft Office Excel** USA, 2021.

MIHAI, A. L.; POPA, M. E. *In vitro* activity of natural antimicrobial compounds against *Aspergillus* strains. **Agriculture and Agricultural Science Procedia**, [*s. l.*], v. 6, p. 585–592, 2015.

MNEIMNE, M. *et al*. Chemical composition and antimicrobial activity of essential oils isolated from aerial parts of *Prangos asperula* Boiss. (Apiaceae) growing wild in Lebanon. **Medicinal & Aromatic Plants**, [*s. l.*], v. 05, n. 03, p. 5–9, 2016.

MONTANARI, R. M. *et al*. Exposure to Anacardiaceae volatile oils and their constituents induces lipid peroxidation within food-borne bacteria cells. **Molecules**, [*s. l.*], v. 17, n. 8, p. 9728–9740, 2012.

MORAIS, S. M. *et al*. Anacardic acid constituents from cashew nut shell liquid: NMR characterization and the effect of unsaturation on its biological activities. **Pharmaceuticals**, [*s. l.*], v. 10, n. 1, p. 1–10, 2017.

MORONKOLA, D. O.; KASALI, A. A.; EKUNDAYO, O. Composition of the limonene dominated leaf essential oil of Nigerian *Anacardium occidentale*. **Journal of Essential Oil Research**, [*s. l.*], v. 19, n. 4, p. 351–353, 2007.

MULYANINGSIH, S. *et al*. Antibacterial activity of essential oils from *Eucalyptus* and of selected components against multidrug-resistant bacterial pathogens. **Pharmaceutical Biology**, [*s. l.*], v. 49, n. 9, p. 893–899, 2011.

MUNTALA, A. *et al*. *Colletotrichum gloeosporioides* species complex: pathogen causing anthracnose, gummosis and die-back diseases of cashew (*Anacardium occidentale* L.) in Ghana. **European Journal of Agriculture and Food Sciences**, [*s. l.*], v. 2, n. 6, p. 1–10, 2020.

Mycobank Database. Disponível em: <http://www.mycobank.org/Biolomics.aspx?Table=Mycobank&Rec=279264&Fields=All>. Acesso em: 21 mai. 2020.

NAKPALO, S. *et al*. Effect of some synthetic fungicides on the in vitro growth of *Colletotrichum gloeosporioides*, causative agent of cashew tree anthracnose in Côte d'ivoire. **Asian Journal of Crop Science**, [*s. l.*], v. 9, n. 4, p. 149–158, 2017.

NAWROT, J. *et al*. Antifungal activity of the sesquiterpene lactones from *Psephellus bellus*. **Plants**, [*s. l.*], v. 10, n. 6, p. 1-13, 2021.

NAWROT, J.; GORNOWICZ-POROWSKA, J.; NOWAK, G. Phytotherapy perspectives for treating fungal infections, migraine, sebhorreic dermatitis and hyperpigmentations with the plants of the *Centaureinae Subtribe* (Asteraceae). **Molecules (Basel, Switzerland)**, [*s. l.*], v. 25, n. 22, p. 1-16, 2020.

NEGRI, S. *et al*. The induction of noble rot (*Botrytis cinerea*) infection during postharvest withering changes the metabolome of grapevine berries (*Vitis vinifera* L., cv. Garganega). **Frontiers in Plant Science**, [*s. l.*], v. 8, n. 21, p. 1–12, 2017.

NIEDERBACHER, B.; WINKLER, J. B.; SCHNITZLER, J. P. Volatile organic compounds as non-invasive markers for plant phenotyping. **Journal of Experimental Botany**, [*s. l.*], v. 66, n. 18, p. 5403–5416, 2015.

OBARA, N.; HASEGAWA, M.; KODAMA, O. Induced volatiles in elicitor-treated and rice blast fungus-inoculated rice leaves. **Bioscience, Biotechnology, and Biochemistry**, [*s. l.*], v. 66, n. 12, p. 2549–2559, 2002.

OLIVEIRA, N. N. *et al*. Cashew nut and cashew apple: A scientific and technological monitoring worldwide review. **Journal of Food Science and Technology**, [*s. l.*], v. 57, n. 1, p. 12–21, 2019.

OLIVEIRA, N. N.; MOTHÉ, C. G.; MOTHÉ, M. G. Sustainable uses of cashew tree rejects: Cashew apple bagasse and cashew gum. **Biomass Conversion and Biorefinery**, [*s. l.*], p. 1-8, 2020.

PAIVA, J. R. de; CRISÓSTOMO, J. R.; BARROS, L. de M. **Recursos Genéticos do**

Cajueiro: Coleta, Conservação, Caracterização e Utilização. Fortaleza. Embrapa Agroindústria Tropical, 2003.

PAPAGEORGIOU, V. P.; ASSIMOPOULOU, A. N.; YANNOVITS-ARGIRIADIS, N. Chemical composition of the essential oil of *Chios turpentine*. **Journal of Essential Oil Research**, [*s. l.*], v. 11, n. 3, p. 367–368, 1999.

PARANIDHARAN, V. *et al*. Resistance-related metabolites in wheat against *Fusarium graminearum* and the virulence factor deoxynivalenol (DON). **Botany**, [*s. l.*], v. 86, n. 10, p. 1168–1179, 2008.

PASSOS, X. S. *et al*. Composition and antifungal activity of the essential oils of *Caryocar brasiliensis*. **Pharmaceutical Biology**, [*s. l.*], v. 41, n. 5, p. 319–324, 2003.

PATADE, M. A. *et al*. Utilization of cashew nut waste: Cashew apple and shell. **International Journal of Chemical Studies**, [*s. l.*], v. 8, n. 1, p. 2076–2078, 2020.

PATEL, R. N.; BANDYOPADHYAY, S.; GANESH, A. Extraction of cashew (*Anacardium occidentale*) nut shell liquid using supercritical carbon dioxide. **Bioresource Technology**, v. 97, n. 6, p. 847–853, 2006.

PEREIRA, F. G. *et al*. Antifungal activities of the essential oil and its fractions rich in sesquiterpenes from leaves of *Casearia sylvestris* Sw. **Anais da Academia Brasileira de Ciencias**, [*s. l.*], v. 89, n. 4, p. 2817–2824, 2017.

PERIGO, C. V. *et al*. The chemical composition and antibacterial activity of eleven *Piper* species from distinct rainforest areas in Southeastern Brazil. **Industrial Crops and Products**, [*s. l.*], v. 94, p. 528–539, 2016.

PIESIK, D. *et al*. Cereal crop volatile organic compound induction after mechanical injury, beetle herbivory (*Oulema* spp.), or fungal infection (*Fusarium* spp.). **Journal of Plant Physiology**, [*s. l.*], v. 168, n. 9, p. 878–886, 2011.

PINTO, O. R. D. O. *et al*. Importância do oídio em plantas cultivadas: Abordagem em frutíferas e olerícolas. **Enciclopédia Biosfera - Centro Científico Conhecer**, [*s. l.*], v. 10, n. 18, p. 19–29, 2014.

PINTO, O. R. de O. **Reação de clones comerciais de cajueiro ao oídio**. 2016a. 119 f. Tese (Doutorado em Agronomia) – Pró-Reitoria de Pesquisa e Pós-Graduação, Universidade Federal do Ceará, Fortaleza, 2016a.

PINTO, O. R. de O. *et al*. Morphological analyses of *Pseudoidium anacardii* infecting Brazilian cashew plants. **Summa Phytopathologica**, [*s. l.*], v. 42, n. 3, p. 257–260, 2016b.

PINTO, O. R. O. *et al*. Reaction of commercial clones of cashew to powdery mildew in northeastern Brazil. **Crop Protection**, [*s. l.*], v. 112, p. 282–287, 2018.

PIUS, G.; MGANI, Q. A. Synthesis of Semiochemicals and Related Fine Chemicals from Cashew Nut Shell Liquid. **Tanzania Journal of Science**, [*s. l.*], v. 45, n. 3, p. 297–306, 2019.

PONZIO, C. *et al*. Ecological and phytohormonal aspects of plant volatile emission in response to single and dual infestations with herbivores and phytopathogens. **Functional Ecology**, [*s. l.*], v. 27, n. 3, p. 587–598, 2013.

POWERS, C. N. *et al*. Antifungal and cytotoxic activities of sixty commercially-available essential oils. **Molecules**, [*s. l.*], v. 23, p. 13, 2018.

PRETORIUS, C. J. *et al*. Metabolomics for biomarker discovery: Key signatory metabolic profiles for the identification and discrimination of oat cultivars. **Metabolites**, [*s. l.*], v. 11, n. 3, p. 1-23, 2021.

PUŠKÁROVÁ, A. *et al*. The antibacterial and antifungal activity of six essential oils and their cyto/genotoxicity to human HEL 12469 cells. **Scientific Reports**, [*s. l.*], v. 7, n. 1, p. 1-11, 2017.

QUINTANA-RODRIGUEZ, E. *et al*. Plant volatiles cause direct, induced and associational resistance in common bean to the fungal pathogen *Colletotrichum lindemuthianum*. **Journal of Ecology**, [*s. l.*], v. 103, n. 1, p. 250–260, 2015.

RAMAK, P. *et al*. Biosynthesis , regulation and properties of plant monoterpenoids. **Journal of Medicinal Plant Research**, [*s. l.*], v. 8, n. 2015, p. 983–989, 2014.

RICCIARDI, V. *et al*. From plant resistance response to the discovery of antimicrobial compounds: The role of volatile organic compounds (VOCs) in grapevine downy mildew infection. **Plant Physiology and Biochemistry**, [*s. l.*], v. 160, n. 2020, p. 294–305, 2021.

RICO, R.; BULLÓ, M.; SALAS-SALVADÓ, J. Nutritional composition of raw fresh cashew (*Anacardium occidentale* L.) kernels from different origin. **Food Science and Nutrition**, [*s. l.*], v. 4, n. 2, p. 329–338, 2016.

ROSENKRANZ, M. *et al*. Volatile terpenes – Mediators of plant-to-plant communication. **The Plant Journal**, [*s. l.*], v. 108, n. 3, p. 617–631, 2021.

ROUSEFF, R. L. *et al*. Sulfur volatiles in guava (*Psidium guajava* L.) leaves: Possible defense mechanism. **Journal of Agricultural and Food Chemistry**, [*s. l.*], v. 56, n. 19, p. 8905–8910, 2008.

RUSSO, R. *et al*. Exploitation of cytotoxicity of some essential oils for translation in cancer therapy. **Evidence-based Complementary and Alternative Medicine**, [*s. l.*], v. 2015, n. 2015, p. 1–9, 2015.

SÁ, F. T. de; PAIVA, F. F. de A.; MARINHO, F. de A. **Plantando Caju**. Fortaleza, 2000. 33p. Disponível em: https://www.agencia.cnptia.embrapa.br/Repositorio/Plantando_caju_000g0591zi302wx5ok0q43a0rzjrqez3.pdf. Acesso em: 23 abr. 2020.

SÁ, S. *et al*. Phytochemistry and antimicrobial activity of *Campomanesia adamantium.* **Brazilian Journal of Pharmacognosy**, [*s. l.*], v. 28, n. 3, p. 303–311, 2018.

SALAS, J. J.; GARCÍA-GONZÁLEZ, D. L.; APARICIO, R. Volatile compound biosynthesis

by green leaves from an *Arabidopsis thaliana* hydroperoxide lyase knockout mutant. **Journal of Agricultural and Food Chemistry**, [*s. l.*], v. 54, n. 21, p. 8199–8205, 2006.

SALEHI, B. *et al*. *Anacardium* plants: Chemical, nutritional composition and biotechnological applications. **Biomolecules**, [*s. l.*], v. 9, n. 9, p. 1–34, 2019.

SAMPAIO, K. L. *et al*. Aroma volatiles recovered in the water phase of cashew apple (*Anacardium occidentale* L.) juice during concentration. **Journal of the Science of Food and Agriculture**, [*s. l.*], v. 91, n. 10, p. 1801–1809, 2011.

SARANG, K.; RUDZIŃSKI, K. J.; SZMIGIELSKI, R. Green leaf volatiles in the atmosphere -properties, transformation, and significance. **Atmosphere**, [*s. l.*], v. 12, n. 12, p. 1655, 2021.

SCALA, A. *et al*. Green leaf volatiles: A plant's multifunctional weapon against herbivores and pathogens. **International Journal of Molecular Sciences**, [*s. l.*], v. 14, n. 9, p. 17781–17811, 2013.

SERRANO, L. A. L. *et al*. **Influência do Oídio nas Castanhas de Diferentes Genótipos de Cajueiro,** 2013. Disponível em: https://ainfo.cnptia.embrapa.br/digital/bitstream/item/98566/1/BPD13005.pdf. Accesso em: 12 jan. 2020.

SERRANO, L. A. L.; OLIVEIRA, V. H. de. Aspectos botânicos, fenologia e manejo da cultura do cajueiro. In: EMBRAPA (Ed.). **Agronegócio Caju: práticas e inovações**. 1ª ed. Fortaleza: 16p. 1–38. 2016

SERRANO, L. A. L.; PESSOA, P. F. A. de P. Sistema de Produção do Caju. In: **Sistema de Produção Embrapa**, 2ª ed., Fortaleza. 2016.

SHARIFI-RAD, J. *et al*. Biological activities of essential oils: From plant chemoecology to traditional healing systems. **Molecules**, [*s. l.*], v. 22, n. 70, p. 1 - 55, 2017.

SHARMA, M.; KULSHRESTHA, S. *Colletotrichum gloeosporioides*: an anthracnose causing pathogen of fruits and vegetables. **Biosciences Biotechnology Research Asia**, [*s. l.*], v. 12, n. 2, p. 1233–1246, 2015.

SHIMADA, T. *et al*. Characterization of three linalool synthase genes from *Citrus unshiu* Marc. and analysis of linalool-mediated resistance against *Xanthomonas citri* subsp. citri and *Penicilium italicum* in citrus leaves and fruits. **Plant Science**, [*s. l.*], v. 229, p. 154–166, dez. 2014.

SHIOJIRI, K. *et al*. Changing green leaf volatile biosynthesis in plants: An approach for improving plant resistance against both herbivores and pathogens. **Proceedings of the National Academy of Sciences of the United States of America**, [*s. l.*], v. 103, n. 45, p. 16672–16676, 2006.

SILVA, A. V. C. *et al*. Diversidade genética entre cajueiros comerciais. **Scientia Plena**, [*s. l.*], v. 8, n. 6, p. 1-9, 2012.

SINGH, R. *et al*. Antifungal and phytotoxic activity of essential oil from root of *Senecio*

amplexicaulis Kunth. (Asteraceae) growing wild in high altitude-Himalayan region. **Natural Product Research**, [*s. l.*], v. 30, n. 16, p. 1875–1879, 2016.

SITAREK, P. *et al*. Antibacterial, anti-inflammatory, antioxidant, and antiproliferative properties of essential oils from hairy and normal roots of *Leonurus sibiricus* L. and their chemical composition. **Oxidative Medicine and Cellular Longevity**, [*s. l.*], v. 2017, p. 1-13, 2017.

SMERIGLIO, A. *et al*. Characterization and phytotoxicity assessment of essential oils from plant by products. **Molecules**, [*s. l.*], v. 24, n. 16, p. 1–16, 2019.

SOSA-MOGUEL, O. *et al*. Characterization of odor-active compounds in three varieties of ciruela (*Spondias purpurea* L.) fruit. **International Journal of Food Properties**, [*s. l.*], v. 21, n. 1, p. 1008–1016, 2018.

SOYLU, E. M.; KURT, Ş.; SOYLU, S. In vitro and in vivo antifungal activities of the essential oils of various plants against tomato grey mould disease agent *Botrytis cinerea*. **International Journal of Food Microbiology**, [*s. l.*], v. 143, n. 3, p. 183–189, 2010.

SOYLU, E. M.; SOYLU, S.; KURT, S. Antimicrobial activities of the essential oils of various plants against tomato late blight disease agent *Phytophthora* infestans. **Mycopathologia**, [*s. l.*], v. 161, n. 2, p. 119–128, 2006.

SUGIMOTO, K. *et al*. Processing of airborne green leaf volatiles for their glycosylation in the exposed plants. **Frontiers in Plant Science**, [*s. l.*], v. 12, p. 1–9, 2021.

SZYMAŃSKA, E. *et al*. Double-check: Validation of diagnostic statistics for PLS-DA models in metabolomics studies. **Metabolomics**, [*s. l.*], v. 8, p. 3–16, 2012.

TANAKA, T. *et al*. Identification of a hexenal reductase that modulates the composition of green leaf volatiles. **Plant Physiology**, [*s. l.*], v. 178, n. 2, p. 552–564, 2018.

TIKU, A. R. Antimicrobial compounds and their role in plant defense. In: **Molecular Aspects of Plant-Pathogen Interaction**. Singapore: Springer Singapore, 2018. p. 283–307.

TOLOUEE, M. *et al*. Effect of *Matricaria chamomilla* L. flower essential oil on the growth and ultrastructure of *Aspergillus niger* van Tieghem. **International Journal of Food Microbiology**, [*s. l.*], v. 139, n. 3, p. 127–133, 2010.

UACIQUETE, A.; KORSTEN, L.; VAN DER WAALS, J. E. Epidemiology of cashew anthracnose (*Colletotrichum gloeosporioides* Penz.) in Mozambique. **Crop Protection**, [*s. l.*], v. 49, p. 66–72, 2013.

UL HASSAN, M. N.; ZAINAL, Z.; ISMAIL, I. Green leaf volatiles: Biosynthesis, biological functions and their applications in biotechnology. **Plant Biotechnology Journal**, [*s. l.*], v. 13, n. 6, p. 727–739, 2015.

ULUKANLI, Z. *et al*. Chemical composition, antibacterial and insecticidal activities of the essential oil from the *Pistacia terebinthus* L. Spp. Palaestina (Boiss.) (Anacardiaceae). **Journal of Food Processing and Preservation**, [*s. l.*], v. 38, n. 3, p. 815–822, 2014.

VAN DER GREEF, J.; SMILDE, A. K. Symbiosis of chemometrics and metabolomics: Past, present, and future. **Journal of Chemometrics**, [*s. l.*], v. 19, n. 5–7, p. 376–386, 2005.

VELAGAPUDI, R. *et al*. Agathisflavone isolated from *Anacardium occidentale* suppresses SIRT1-mediated neuroinflammation in BV2 microglia and neurotoxicity in APPSwe-transfected SH-SY5Y cells. **Phytotherapy Research**, [*s. l.*], v. 32, n. 10, p. 1957–1966, 2018.

VELOSO, J. S. *et al*. Factors influencing biological traits and aggressiveness of *Colletotrichum* species associated with cashew anthracnose in Brazil. **Plant Pathology**, [*s. l.*], v. 70, n. 1, p. 167–180, 2021.

VIANA, F. M. P. *et al*. Control of cashew black mould by acibenzolar-S-methyl. **Tropical Plant Pathology**, [*s. l.*], v. 37, n. 5, p. 354–357, 2012.

VINCENTI, S. *et al*. Biocatalytic synthesis of natural green leaf volatiles using the lipoxygenase metabolic pathway. **Catalysts**, [*s. l.*], v. 9, n. 10, p. 1–35, 2019.

VIVALDO, G. *et al*. The network of plants volatile organic compounds. **Scientific Reports**, [*s. l.*], v. 7, n. 1, p. 1–18, 2017.

WAKAI, J. *et al*. Effects of *trans*-2-hexenal and *cis*-3-hexenal on post-harvest strawberry. **Scientific Reports**, [*s. l.*], v. 9, n. 1, p. 1-10, 2019.

WALTERS, D.; DANIELL, T. Microbial induction of resistance to pathogens. In: **Induced Resistance for Plant Defence**. Oxford, UK: Blackwell Publishing, 2007. p. 143–156.

WIKLUND, S. *et al*. Visualization of GC/TOF-MS-based metabolomics data for identification of biochemically interesting compounds using OPLS class models. **Analytical Chemistry**, [*s. l.*], v. 80, n. 1, p. 115–122, 2008.

WILLIAM ALLWOOD, J. *et al*. Dual metabolomics: A novel approach to understanding plant-pathogen interactions. **Phytochemistry**, [*s. l.*], v. 71, n. 5–6, p. 590–597, 2010.

WONNI, I. Diseases of cashew nut plants (*Anacardium occidentale* L.) in Burkina Faso. **Advances in Plants & Agriculture Research**, [*s. l.*], v. 6, n. 3, p. 78–83, 2017.

XIA, J. *et al*. Translational biomarker discovery in clinical metabolomics: An introductory tutorial. **Metabolomics**, [*s. l.*], v. 9, n. 2, p. 280–299, 2013.

YAMASAKI, Y. *et al*. Biological roles of monoterpene volatiles derived from rough lemon (*Citrus jambhiri* Lush) in citrus defense. **Journal of General Plant Pathology**, [*s. l.*], v. 73, n. 3, p. 168–179, 2007.

YU, D. *et al*. Antifungal modes of action of tea tree oil and its two characteristic components against *Botrytis cinerea*. **Journal of Applied Microbiology**, [*s. l.*], v. 119, n. 5, p. 1253–1262, 2015.

YU, Q. *et al*. Mass spectrometry-based metabolomics for irritable bowel syndrome biomarkers. **Therapeutic Advances in Gastroenterology**, [*s. l.*], v. 12, p. 1-12, 2019.

ZOGHBI, M. das G. B. *et al*. Variation of essential oil composition of *Tapirira guianensis* Aubl. (Anacardiaceae) from two sandbank forests, North of Brazil. **Química Nova**, [*s. l.*], v. 37, n. 7, p. 1188–1192, 2014.

ZUZARTE, M. *et al*. Antifungal activity of phenolic-rich *Lavandula multifida* L. essential oil. **European Journal of Clinical Microbiology and Infectious Diseases**, [*s. l.*], v. 31, n. 7, p. 1359–1366, 2012.